Oncogenic signalling in BRAF/RAS wild type melanoma

ZIZHEN MING

A thesis submitted to Macquarie University in fulfilment of the requirements for the degree of Doctor of Philosophy

Department of Biomedical Sciences

Faculty of Medicine and Health Sciences

Macquarie University

February 2019

Declaration of originality

This work has not previously been submitted for a degree or diploma in any university. To the best of my knowledge and belief, the thesis contains no material previously published or written by another person except where due reference is made in the thesis itself.

_____ Date: 11/02/2019

Zizhen Ming

Supervisor: Professor Helen Rizos

Co-supervisors: Doctor Esther (Su Yin) Lim & Professor Richard F. Kefford

Precision Cancer Therapy

Department of Biomedical Sciences

Faculty of Medicine and Health Sciences

Macquarie University

Date of submission: 11/02/2019

Acknowledgements

First and foremost, I would like to express my deepest thanks to my dear supervisor Prof. Helen Rizos, not only for her patience, motivation, enthusiasm, incredibly immense knowledge and tremendous academic support, but also for her trust, providing me so many wonderful opportunities to present my research outcomes and training me to be a qualified researcher. She is the best supervisor, an outstanding scientist with stringent academic attitude and great contributions to the field of melanoma research. Without her help, this thesis would not have been possible.

I would also like to express my sincere gratitude to my co-supervisor Dr Esther (Su Yin) Lim, not only for her continuous support, incredible insight and encyclopaedic knowledge, but also for her humble personality and great empathy. I have never lost hope whatever difficulties I was facing over the last three years because of her firm support. Without her encouragement, I would not have made it this far. Profound grace also goes to my co-supervisor Prof. Rick Kefford, for his valuable clinical insight and his generosity.

I would also like to thank everyone else in the Precision Cancer Therapy (PCT) Group, Elena Shklovskaya, Russell Diefenbach, Mariana Brocardo, Andreia Vaqueirinho de Pinho, Mal Irvine, Bernadette Pedersen, Ashleigh Stewart, Carina Fung, Suzanah Boyd, Jenny Lee, Sara Alavi, John Park, for their professional suggestions and assistances, to make our lab such an enjoyable place to work. Particularly thank to Mal, Ashleigh and Bernadette for training me with laboratory techniques and helping me solve lab related issues, thank to Mariana for all support in chapter 3.

I would also like to thank Dr. Honghua (Helen) Hu, for her unconditional help and all wise advises. Without her support, I would not have started my PhD journey since the very beginning.

Special mention goes to all lovely friends I've met in Sydney, Sheran li, Yulong Sun, Xiaomin Zhang, Yan Wang, Xin Xu, Libing Fu, Minna Fang, Jing Li, Zhengnan Shan, Mingzi Zhang, Yujie Li, Yibing Wei, Anindya, and David, thanks for their friendship and sharing great moments with me.

Finally, but not least, I would like to thank my family and my boyfriend Shilun, for their constant love and support. I have much respect for my grandpa, who has huge caring for nature and has volunteered to promote environmental protection for years, he teaches me kindness. My grandma has made an enormous contribution to our family and sacrificed a lot for us, she never stops learning and teaches me selflessness. My dad has been working so hard to support our family, he is strict but never keeps me in chains, he gives me the freedom to pursue whom I want to be. My younger sister has been my best friend all my life, she is so smart and teaches me to think differently and always be myself. I also thank my admired uncle, for his wisdom, foresight and all valuable suggestions when it comes to the important moments in my life. My beloved aunt, who is not only my family but also my best friend, thank her for sharing the ups and downs in my life. Particular gratitude goes to my boyfriend, who is the best person out there for me. He has been an incredible supporter and has unconditionally loved me during my highs and lows. Without their support and love, I would never have made this happen.

.

Publications

Journal publications

Ming Z, Lim SY, Kefford RF, Rizos H. Mitogen-activated protein kinase dependency in *BRAF*/*RAS* wild type melanoma: a rationale for combination inhibitors. Submitted to Molecular Cancer in February 2019.

Conference abstracts for poster or oral presentations

Ming Z, Lim SY, Kefford RF, Rizos H. Multiple signalling pathways are active in *BRAF*/*NRAS* wild type melanomas. American Association for Cancer Research Annual Meeting (AACR) 2018; 2018 Apr 14-18; Chicago, IL.

Ming Z, Lim SY, Kefford RF, Rizos H. Identification of survival signalling pathways in *BRAF*/*NRAS* wild type melanoma. Society for Melanoma Research 2017 Congress. 2017 Oct 18-21; Brisbane, Australia.

Ming Z, Lim SY, Irvine M, Kefford RF, Rizos H. Identification of survival signalling pathways in *BRAF*/*NRAS* wild type melanoma. BioFocus Research Conference 2016. 2016 Dec 15; Sydney, Australia.

Ming Z, Lim SY, Irvine M, Kefford RF, Rizos H. Identification of survival signalling pathways in *BRAF*/*NRAS* wild type melanoma. The Australian Melanoma Conference 2016. 2016 Oct 28-29; Sydney, Australia.

Ming Z, Lim SY, Irvine M, Kefford RF, Rizos H. Identification of survival signalling pathways in *BRAF*/*NRAS* wild type melanoma. The Sydney Cancer Conference 2016. 2016 Sept 22-23; Sydney, Australia.

Abstract

Selective inhibition of the mitogen-activated protein kinase (MAPK) pathway has significantly improved the survival of patients with *BRAF*^{V600}-mutant advanced melanoma. However, *BRAF*/*RAS* wild type (WT) melanomas have no known actionable mutations, and immune checkpoint inhibitors remain the only effective therapy for patients with this melanoma subtype. In this PhD project, we explored the signalling activity and response of *BRAF*/*RAS* WT melanomas to combination small molecule inhibitors.

In Chapter 2, we investigated MAPK dependency in 23 melanoma cell lines, including 10 *BRAF*^{V600}-mutant and 13 *BRAF*/*RAS* WT (seven *NF1*-mutant and six triple WT) melanomas. Melanoma cell lines were treated with the MEK inhibitor trametinib, and the impact of MEK inhibition on cell survival and proliferation were examined. We showed that *BRAF*/*RAS* WT melanomas had variable responses to MEK inhibition; 23% were highly sensitive, indicating dependency on MAPK signalling for survival and proliferation, whereas 38% were resistant, and this was commonly associated with high mutation burden and loss-of-function mutations in *NF1*. We demonstrated that NF1 loss conferred MEK inhibitor resistance in *BRAF*^{V600}-mutant cells but not in *BRAF*/*RAS* WT melanomas.

The mutational profiles of *BRAF*/*RAS* WT melanomas revealed concurrent mutations in RASopathy genes, and enrichment of *TP53* mutations. In Chapter 3, we explored the precise contribution of p53 loss to MEK inhibitor resistance in our panel of melanoma cells. We also examined the efficacy of a p53 activator in combination with MEK inhibition on suppressing melanoma proliferation. Finally, in Chapter 4, the activity of oncogenic signalling pathways in *BRAF/RAS* WT melanoma cell lines was examined and the activity of combination inhibitors targeting activated cascades was tested.

Table of Contents

List of Figures

List of Tables

List of Abbreviations

ALM	Acral-lentiginous malignant melanoma
AMS	Atypical mole syndrome
ARID2	AT-Rich interaction domain 2
ASK1	Apoptosis signal-regulating kinase 1
ATM	Ataxia telangiectasia-mutated
AUC	Area under the curve
BAP1	BRCA-1 associated protein 1
BCL-2	B-cell lymphoma 2
BCL2L12	Bcl-2-like protein 12
BH3	Bcl-2 homology domain 3
BLCAP	Bladder cancer-associated protein
BRAF	V-Raf murine sarcoma viral oncogene homolog B
CD279	Cluster of differentiation 279
CDKN2A	Cyclin-dependent kinase inhibitor 2A
CDK4/6	Cyclin-dependent kinases 4 and 6
CRAF	V-Raf-1 murine leukemia viral oncogene homolog 1
CTLA-4	Cytotoxic T lymphocyte-associated protein-4
CTNNB1	Catenin beta 1
CYSLTR2	Cysteinyl leukotriene receptor 2
DCC	Deleted in colorectal carcinoma
DDX3X	DEAD-box helicase 3 X-linked
DMEM	Dulbecco’s Modified Eagle Medium

DGKB	Diacylglycerol kinase beta
EGFR	Epidermal growth factor receptors
EIF1AX	Eukaryotic translation initiation factor 1A
ERK	Extracellular signal-regulated kinases
EZH2	Enhancer of zeste homolog 2
GNAQ/11	Guanine nucleotide-binding protein G(q) subunit alpha and 11
HDAC	Histone deacetylases
IDH1	Isocitrate dehydrogenase (NADP (+)) 1
IGF-1R	Insulin-like growth factor 1 receptor
JNK	c-Jun N-terminal kinases
KBTBD8	Kelch repeat and BTB domain containing 8
KDR	Kinase insert domain receptor
KIT	KIT proto-oncogene receptor tyrosine kinase
LMM	Lentigo malignant melanoma
MAPK	Mitogen-activated protein kinase
MAP2K (MEK)	Mitogen-activated protein kinase kinase
MAP2K1	Mitogen-activated protein kinase kinase 1
MDM2	Mouse double minute 2 homolog
MNK2	MAPK-interacting kinases 2
MITF	Microphthalmia-associated transcription factor
MSK1/2	Mitogen- and stress-activated kinases 1 and 2
mTORC2	Mammalian target of rapamycin complex 2
NF1	Neurofibromatosis type 1
NF-κB	Nuclear factor-κB

NM	Nodular melanoma
NRAS	Neuroblastoma RAS viral oncogene homolog
OS	Overall survival
PAK1	p21 (RAC1) activated kinase 1
PAX8	Paired box gene 8
PBS	Phosphate-buffered saline
PDGFR	Platelet-derived growth factor receptor
PD-1	Programmed cell death protein-1
PFS	Progression-free survival
PI3K/AKT	Phosphoinositide 3-kinase/protein kinase B
PI	propidium iodide
PIP2	Phosphatidylinositol-4,5-bisphosphate
PIP3	Phosphatidylinositol-3,4,5-trisphosphate
PKC	Protein kinase C
PPP6C	Protein phosphatase 6 catalytic subunit
PTEN	Phosphatase and tensin homolog
PTPN11	Tyrosine-protein phosphatase non-receptor type 11
PTPRK	Protein tyrosine phosphatase, receptor type K
p90RSK	P90 ribosomal S6 kinase
RAC1	Ras-related C3 botulinum toxin substrate 1
RALY	RALY heterogeneous nuclear ribonucleoprotein
RASA2	RAS p21 protein activator 2
RASSF2	Ras Association Domain Family Member 2
RB1	RB transcription corepressor 1

RNF185	Ring finger protein 185
ROS	Reactive oxygen species
RPMI	Roswell Park Memorial Institute-1640 medium
RTK	Receptor tyrosine kinases
SDS	Sodium dodecyl sulfate
SF3B1	Splicing factor 3b, subunit
SMAD4	Mothers against decapentaplegic homolog 4
SNX31	Sorting nexin 31
SOS1	SOS Ras/Rac Guanine Nucleotide Exchange Factor 1
SPRY	Sprouty homolog
SPRED1	Sprouty related EVH1 domain containing 1
SRSF2	Serine and arginine rich splicing factor 2
SSM	Superficial spreading melanoma
STK19	Serine/threonine-protein kinase 19
TBS	Tris-buffered saline
TERT	Telomerase reverse transcriptase
TP53	Tumour protein 53
TRegs	Regulatory T-cells
TTBS	Tween-TBS
UV	Ultraviolet
WES	Whole exome sequencing
ZNF778	Zinc finger protein 778
5’UTR	The 5’ untranslated region

Chapter 1

Introduction

1.1 Melanoma etiology and biology

Melanoma is an aggressive form of skin cancer that originates from melanocytes, a neural crest-derived cell type. Melanocytes are positioned mostly at the basal layer of the skin's epidermis, but are also present in the eye, oral cavity, and in other tissues throughout the body. Melanocytes produce melanin pigments upon exposure to ultraviolet (UV) radiation, and this provides protection to neighbouring keratinocytes (1). Due to the UV radiation absorption and scattering capacity of melanin, epidermal keratinocytes use melanin to protect their nucleus from UV radiation-induced DNA damage (2).

The progress from melanocytes to melanoma, termed melanomagenesis, involves multiple steps that include the sequential acquisition of genomic alterations that promote proliferation, invasion and immune escape, as reviewed in (3). The microenvironment also influences melanoma development and progression. For instance, melanoma interactions with fibroblasts and the changing concentrations of growth factors, cytokines and nutrients all contribute to melanoma transformation, proliferation and invasion (4).

1.1.1 Melanoma incidence

Melanoma is a deadly form of skin cancer, occupying 4% of all skin cancer but causing 75% of skin cancer deaths. Incidence of Melanoma has continued increasing over many decades, and Australia is one of those regions in the world with the highest rates of melanoma, second only to New Zealand (5). According to the latest report by the Australia Institute of Health and Welfare (AIHW), 13,941 new cases of melanoma were diagnosed in Australia in 2017, accounting for 10% of all cancers diagnosed, making melanoma the fourth most commonly diagnosed cancer in both males and females (Figure 1.1) (6). Males tend to have higher incidence (59%) of melanoma relative to females with the highest incidence (24%) in people aged from 60 to 69 (7). Melanoma is the most common

cancer diagnosed in young Australians (20% of all cancer types from 15 to 39 years old) and causes more deaths in young adults (aged 20 to 39 years old) compared to other cancer types (6, 8).

Melanoma is highly metastatic, and patients with advanced melanoma have a poor prognosis. In Australia alone, the number of deaths from melanoma increased from 596 in 1982 to 1,770 in 2016. Deaths in male melanoma patients saw a larger rise from 380 to 1,230 compared to in female patients, from 216 to 545 in 1982 and 2016, respectively. From the period of 1982 to 2016, the age-standardised mortality rate elevated from 4.7 deaths to 6.2 deaths per 100,000 people in Australia (7).

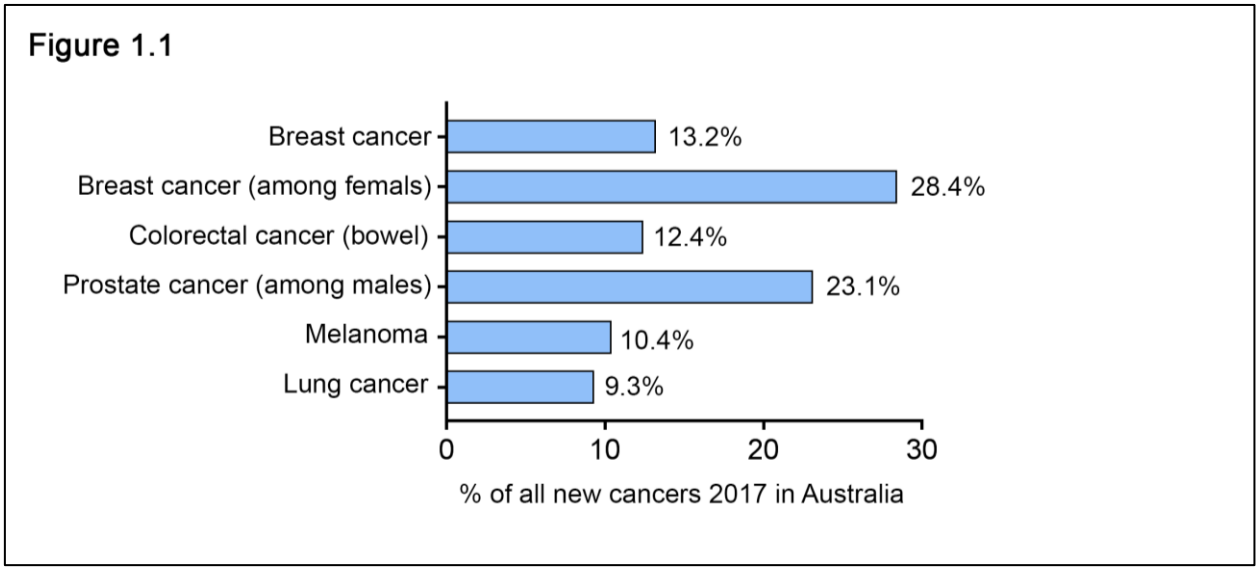

Figure 1.1: New cases of the most common cancers diagnosed in 2017 in Australia
Melanoma is the fourth most commonly diagnosed cancer accounting for 10.4% of all cancer types in Australia (6).

1.1.2 Melanoma risk factors

Several risk factors predispose to melanoma development, including environmental (UV radiation) and genetic (family history, hair and eye colour, number of melanocytic nevi) risk factors (9, 10).

UV radiation (UVA and UVB) from sunlight or artificial tanning (tanning beds) is a dominant environmental risk factor for cutaneous melanoma. UVA (315 nm-400 nm) is more abundant than UVB (280 nm-315 nm), accounting for 95% of solar UV radiation (11-13) and UVA is mostly produced by tanning beds, although at 12 times the dose derived from the sun (14). The short-wavelength UVC (<280 nm) is the most damaging type of UV radiation, but is effectively absorbed by ozone and does not reach the earth's surface to cause much harmful effects (15). An estimated 60-70% of cutaneous malignant melanoma is caused by intermittent, intense UV exposure, or chronic and cumulative sun exposure (16). Exposure to UV radiation leads to genetic changes, and cytosine to thymine or guanine to adenine transitions at pyrimidine dinucleotide sites are characteristic of UV-induced damage (17). For instance, hot spot melanoma-associated mutations in the *STK19* (serine/threonine-protein kinase 19), *RAC1* (Ras-related C3 botulinum toxin substrate 1), and *PPP6C* (serine/threonine-protein phosphatase 6 catalytic subunit) genes, and loss-of-function mutations in *NF1* (neurofibromatosis type I) and *CDKN2A* (cyclin-dependent kinase Inhibitor 2A) are enriched for cytosine to thymine transitions, presumably by reason of UV-induced DNA damage (17, 18).

Family history is another major risk factor for melanoma and includes two or more close relatives with melanoma (19). Individuals with many benign, dysplastic nevi or atypical mole syndrome and individuals with red or blond hair, blue eyes, fair skin, and aged over 65 also have a greater susceptibility of developing melanoma (13). Germline mutations in the *CDKN2A* gene have been identified in approximately 46% of melanoma-prone

families (20), while mutations in other genes such as *BAP1* (*BRCA-1* associated protein 1), *TERT* (telomerase reverse transcriptase), *MITF* (microphthalmia-associated transcription factor) have also been reported (21). All of these gene mutations are associated with increased incidence of melanoma (22-25). Recently, novel deleterious mutations were also determined in non-coding regulatory regions of *PAX8* (paired box gene 8) and *SMAD4* (mothers against decapentaplegic homolog 4) genes in patients with familial melanoma (26).

1.2 Subtypes of melanoma

Melanoma can be divided into four clinical-histopathological subtypes including SSM (superficial spreading melanoma), ALM (acral-lentiginous malignant melanoma), LMM (lentigo malignant melanoma) and NM (nodular melanoma).

SSM spreads along the surface of the skin before invasion, and is the most common subtype, representing approximately 65-70% of all melanoma cases (Table 1.1). Compared to other subtypes, SSM occurs more often in younger individuals (median age 50), is particularly common on the trunk in males and the lower extremities in females, as reviewed in (27), and is strongly associated with intermittent sun exposure and sunburn (28). SSM normally presents as a dark, flat lesion on the skin with variegated colours and irregular borders. Unequable epidermal thickening, circumscription, and prominent intracytoplasmic melanisation are other common features of SSM, as reviewed in (27). Genetically, SSM is characterised by having frequent *BRAF* or *NRAS* mutations (29).

LMM is an invasive melanoma associated with lentigo maligna, first described by Hutchinson in 1890 (30). LMM is usually referred to as an "*in situ*" melanoma and accounts for 4-15% of all invasive melanomas. LMM is mostly caused by accumulative sun exposure and appears more common in the regions of the head, neck, forearm, face, and particularly on the nose and cheek of older patients (median age 80). Histologically, LMM is characterised by lentiginous proliferation of melanocytes in severely sun damaged skin, as reviewed in (27, 31). Unlike in SSM, *BRAF* (v-Raf murine sarcoma viral oncogene homolog B) mutations in LMM are rare (32).

NM in one of the most invasive melanoma subtypes and contributes to at least 10-15% of total invasive melanomas (33). The NM tumours are normally brown, black or blue-black in colour and present as a smooth-surface cutaneous nodule, mostly caused by

intermittent sun exposure. These tumours are normally found on lower limbs or the head and neck of males over 50 (34). NM cells proliferate downwards through the skin (vertical growth) and tend to invade the dermis very quickly without an obvious horizontal growth phase (12, 35, 36), and are thus characterized by a rapid growth rate (0.49 mm/month) and poor prognosis (37). Several studies have reported high *NRAS* mutation rates in NM (38, 39).

ALM is a type of non-UV associated melanoma, frequently occurring on soles, palms, and nail beds, and was first described in 1976 (40). ALM represents the most common melanoma subtype in Asian or African individuals (41, 42), however, it is rare in the Caucasian population (only 2-3% of all diagnosed melanomas) (43). Poor prognosis due to delayed detection and diagnosis tend to be a feature for patients with ALM, resulting in more advanced disease at the time of diagnosis (42, 44). ALM occurs more frequently in elderly individuals who have a lower incidence of familial melanoma and sunburn, but these patients tend to have a family history of non-cutaneous tumours, as reviewed in (27). Compared to SSM, *BRAF*, *NRAS* (neuroblastoma RAS viral oncogene homolog) and *NF1* mutations rarely occur in ALM, but *KIT* (KIT proto-oncogene receptor tyrosine kinase) mutations, loss-of-function mutations in *CDKN2A*, *TP53* (tumor protein p53) and *ARID2* (AT-Rich interaction domain 2), and activating hotspot mutations in *GNAQ* (guanine nucleotide-binding protein G(q) subunit alpha) and *SF3B1* (splicing factor 3b, subunit 1) occur more frequently in ALM. ALM also tends to have higher somatic structural variants (e.g. deletions, duplications, tandem duplications and foldback inversions) (45). Desmoplastic melanoma (DM) is another rare melanoma subtype, accounted for less than 1% of total melanoma and 4% of cutaneous melanoma cases (46, 47).

Apart from the most common cutaneous melanoma subtypes, other rarer forms of melanoma have been identified and include mucosal melanoma and uveal melanoma. Mucosal melanoma accounts for less than 1.4% of all melanomas and occurs on many

mucosal surfaces of the body (48). Over 50% of cases are detected on the region of neck and head, such as oral, nasal, and sinus mucosa, and the other 50% originate in the anal/genital mucosal surfaces (49). Mucosae of the pharynx, larynx, esophagus and gallbladder can also be affected but are less common. Patients with mucosal melanomas tend to be older (median age 70). Compared to cutaneous melanoma, mucosal melanoma has lower mutation loads and shares common features with acral melanoma, such as having a higher rate of copy number and structural variants and lacking common driver mutations. For example, *BRAF* mutations occur in only 3-8%, and *NRAS* mutations in 4-14%, of mucosal melanoma (45). A recent study showed that *GNAQ* and *GNA11* (guanine nucleotide-binding protein subunit alpha-11) mutations occur in 9.5% of mucosal melanoma in the Chinese population and are associated with poor prognosis (50). Uveal melanoma is another rare melanoma subtype, representing <5% of melanomas (48), and mainly occurs in Caucasians (51). Uveal melanoma arises from melanocytes in the eye. Approximately 90% of cases involve the choroid, 7% affect the ciliary body, and 3% affect the iris (29, 52). Uveal melanoma tends to present in older aged males and has large tumour basal diameter and thickness. Uveal melanoma typically metastasise to the liver, lung and bone, contributing to poor prognosis and high mortality rate (53). Genetically, uveal melanoma lack mutations in *BRAF*, *NRAS* or *KIT*, but have frequent mutations in *GNAQ* and *GNA11*, found in 33% and 39% of uveal melanoma, respectively, and both encode an alpha subunit of the heterotrimeric G proteins (54, 55). Mutant *GNAQ* and *GNA11* contribute to the constitutive activation of G-protein signalling to promote melanomagenesis. Other genes commonly mutated in uveal melanoma include *SF3B1*, *BAP1*, *SRSF2* (serine and arginine rich splicing factor 2), *CYSLTR2* (cysteinyl leukotriene receptor 2) and *EIF1AX* (eukaryotic translation initiation factor 1A), as reviewed in (45, 56, 57).

Table 1.1: Features of melanoma subtypes

Melanoma subtype	Superficial spreading melanoma	Lentigo malignant melanoma	Nodular melanoma	Acral-lentiginous malignant melanoma	Desmoplastic melanoma	Mucosal melanoma	Uveal melanoma
Age distribution	30 to 50 years old	Median age = 80	> 50 years old	> 60 years old	Median age = 60	Median age = 70	Wide age range
Incidence[1]	65-70%	4-15%	10-15%	2-3%	<1%	1.4%	<5%
Location	Trunk and lower limbs	Head, neck, forearm, face	Lower limbs, head and neck	Palms, soles and nail beds	Head and neck	Oral, nasal, sinus and anal/genital mucosa	Choroid, ciliary body, iris
Aetiology	Intermittent, intense sun exposure	Accumulative sun exposure	Intermittent sun exposure	Unknown	Accumulative sun exposure	Unknown	Unknown
Genetics	*BRAF*^{V600E} or *NRAS* mutations, *PTEN* and *NF1* loss	*BRAF*^{V600K} mutations, *TP53* loss, *KIT* mutations	*BRAF*^{V600E} or *NRAS* mutations, *PTEN* loss	*CDKN2A, TP53 and ARID2* loss, *KIT, GNAQ* or *SF3B1* mutations	*NF1, TP53 and ARID2* loss-of-function mutations	*GNAQ* or *GNA11* mutations	*GNAQ, GNA11 BAP1, SF3B1, SRSF2, CYSLTR2 and EIF1AX* mutations

[1]Incidence indicates the frequency of all melanoma cases in Caucasians.

1.3 Genetic classification of cutaneous melanoma

Cutaneous melanomas carry a significantly higher number of genetic alterations compared to other types of solid cancers (58). Over the last few years, several large-scale sequencing studies have identified frequently mutated genes such as *BRAF* (47%-52%) and *NRAS* (30%) in cutaneous melanoma (17, 45, 59, 60). Other commonly mutated genes have also been identified including *RAC1*, *PPP6C*, *ARID2*, *STK19*, *SNX31* (sorting nexin 31), *TACC1* (transforming acidic coiled-coil containing protein 1), *DCC* (deleted in colorectal carcinoma) and *PTPRK* (protein tyrosine phosphatase, receptor type K) (17, 60). More recently, the Cancer Genome Atlas (TCGA) whole exome sequencing project revealed additional commonly altered genes in cutaneous melanoma, including *CDKN2A*, *TP53*, *IDH1* (isocitrate dehydrogenase (NADP (+)) 1), *PTEN* (phosphatase and tensin homolog), DDX3X (dead-box helicase 3 X-linked), *MAP2K1* (mitogen-activated protein kinase kinase 1), *NF1* and *RB1* (RB transcription corepressor 1). This study established a genomic classification system for cutaneous melanoma based on their predominant genotype: *BRAF*-mutant, *RAS*-mutant, *NF1*-mutant and triple wild type (WT) melanoma (59).

1.3.1 *BRAF*-mutant melanomas

The *BRAF* gene encodes the BRAF serine/threonine kinase BRAF, a member of the RAF kinase family, which transduces regulatory signals from the RAS GTPase to the mitogen-activated protein kinase kinase proteins MEK1 and MEK2 within the mitogen-activated protein kinase (MAPK) signalling pathway. Activating *BRAF* mutations have been detected in several types of cancers including colorectal cancers, lung cancers, sarcomas, breast cancers, liver cancers and ovarian carcinomas (61, 62). In cutaneous melanoma, *BRAF* is the most commonly mutated gene, detected in 47%-52% of cutaneous melanoma cases (17, 45, 59). *BRAF* mutations predominantly affect valine at

codon 600, which is substituted for glutamic acid (E; 85% of *BRAF*^{V600} mutations), lysine (K; 8% of *BRAF*^{V600} mutations), arginine (R; 1-2% of *BRAF*^{V600} mutations) or aspartic acid (D; 0.5% of *BRAF*^{V600} mutations) (63). *BRAF*^{K601} is the second most frequently occurring *BRAF* mutation (59). A recent report by Hayward *et al*. (2017) identified *BRAF*^{K601E} mutation in 2 of 183 (1%) melanoma samples using whole-genome sequencing (45).

Hot-spot mutations in *BRAF* are mutually exclusive of *NRAS* activating mutations (64), whereas *BRAF* non-hot-spot mutations commonly co-occur with *RAS* mutations(59). *BRAF*-mutant melanomas also show focal amplification of the *BRAF* gene (65). *TERT* promoter mutations and *PTEN* mutations or deletions also commonly co-occur with *BRAF* mutations in melanoma (66, 67).

The frequency of *BRAF* mutations differs across different subtypes of melanomas. For instance, *BRAF* mutations are rare in LMM and ALM, but more common in SMM (68). Furthermore, approximately 90% of melanomas with a *BRAF* hot-spot mutation also express a UV-mutation signature (59, 69).

1.3.2 *RAS*-mutant melanomas

The second most frequently mutated gene in melanoma is *NRAS*, which encodes the NRAS GTPase protein. The RAS protein superfamily includes NRAS, KRAS and HRAS, all of which share structural and functional similarities. *RAS* mutations constitutively activate the MAPK pathway and the PI3K/AKT (phosphoinositide 3-kinase/protein kinase B) pathway.

NRAS mutations have been identified in 30% of cutaneous melanomas, and most of these mutations (i.e. 82-96%) are hotspot mutations affecting codon Q61 (Q61R/K/L/H), G12 (G12R/D/A) or G13 (G13R/D). Mutations in *HRAS* and *KRAS* have also been determined in melanoma patient samples, but these occur at low frequencies (1% and

3%, respectively). Focal amplification of *NRAS* was shown to co-occur with *NRAS* mutations in melanoma from the TCGA study (59). *TERT* promoter mutation was also identified in 72% of *NRAS*-mutant melanoma (17, 39, 45, 59, 70).

The majority of melanoma patients with *NRAS* hot-spot mutations have a history of UV exposure and tend to be older compared to patients without *NRAS* mutations (59). *NRAS* mutations are most commonly found in SSM and NM (71, 72) and these often show elevated rates of mitotic activity, indicative of enhanced proliferation (73).

Histologically, *NRAS*-mutant melanomas are more aggressive compared to other subtypes. Moreover, *NRAS*-mutant melanoma patients normally have thicker lesions and higher chance of lymph node metastases (73). Compared to non-*NRAS*-mutant tumours, melanoma patients with *NRAS* mutations have lower median overall survival (OS), suggesting that *NRAS*-mutant status may predict poorer outcomes (74). There are currently no specific targeted therapeutic agents for *NRAS*-mutant melanomas, as reviewed in (71).

1.3.3 *NF1*-mutant melanomas

The third most commonly mutated gene in melanoma is *NF1*, a tumour suppressor gene that encodes a GTPase-activating protein, known to negatively regulate RAS activity through its intrinsic GTPase activity (75).

NF1 has been implicated as an important melanoma-associated gene in several studies. Mutations in *NF1* were found in 13% of cutaneous melanoma, and 90% of these mutations are inactivating or predicted loss-of-function mutations (i.e. nonsense, splice-site variant or insertion-deletion mutations) (59). NF1 loss concurrently activates MAPK and PI3K/AKT signalling, via RAS activation (76). *NF1*-mutant melanomas appear to have the highest median level of CRAF (v-raf-1 murine leukemia viral oncogene homolog

1) expression, suggesting heterogeneity in the degree of MAPK pathway activation (59, 77).

NF1 mutations are mutually exclusive of *BRAF* and *NRAS* mutations. One study reported *NF1* mutations were present in only 4% of *BRAF*-mutant melanoma and 0.9% of *NRAS*-mutant melanoma. In contrast, *NF1* mutations are more frequently found in melanomas without *BRAF* or *RAS* mutations (77). Specifically, the *NF1* gene was mutated more frequently in melanomas with WT *BRAF* or *RAS* (38.7- 46%). Approximately 70% of *BRAF/RAS* WT melanomas show a UV DNA damage signature with concurrent mutations in *NF1* (59, 78), but this genomic profile is only present in 8% of *BRAF*- and *NRAS*-mutant melanomas.

Melanoma patients with *NF1* mutations are typically older, tend to be males and nearly 93% of *NF1*-mutant melanomas display a characteristic UV signature. Although the OS of melanoma patients with *NF1* mutations was reportedly similar to other melanoma genetic subtypes (59), a recent study found that NF1 loss confers poorer OS across all the four genomic subtypes (78). Melanomas with *NF1* mutations are associated with markedly higher number of somatic mutations (45, 77, 78), and structural variants contribute heavily to this high mutation burden (45). *TERT* promoter mutations are common in *NF1*-mutant melanoma, and *NF1* mutations commonly co-occur with mutations in other RASopathy genes, including *PTPN11* (tyrosine-protein phosphatase non-receptor type 11), *SOS1* (SOS Ras/Rac Guanine Nucleotide Exchange Factor 1), *RAF1* and *RASA2* (45, 77). Moreover, mutations in *SPRY* (sprouty homolog) and sprouty-related genes, such as *SPRED1* (sprouty related EVH1 domain containing 1*)*, which encode proteins that negatively regulate the MAPK signalling pathway, were identified in *NF1*-mutant melanomas (77). Mutations in *RASSF2* (Ras Association Domain Family Member 2), a RAS-domain-containing gene (77), *TP53* and *CDKN2A*, were also enriched in *NF1*-mutant melanomas (78).

1.3.4 Triple wild-type (WT) melanomas

The fourth genetic melanoma subtype is the triple WT melanomas, which lack hot-spot *BRAF*, *RAS* and *NF1* mutations. Triple WT melanomas account for about 20-30% of cutaneous melanoma and around 51% of mucosal and acral melanomas (17, 45, 59, 70, 77, 79). Compared to the other genetic subtypes, triple WT melanomas harbour the lowest UV mutation signature but carry many complex structural rearrangements (59).

A series of rare, low-frequency driver mutations have been detected in the triple WT subgroup, including activating mutations in *CTNNB1* (catenin beta 1), *EZH2* (enhancer of zeste homolog 2) and *MAP2K1* genes, loss-of-function or inactivating mutations in *CDKN2A*, *TP53*, *ARID2* and the X-chromosome gene *FAM58A* (cyclin M), which negatively regulates CRAF expression. Mutations in uveal melanoma driver genes such as *GNAQ*, *GNA11* and activating hotspot mutations in *SF3B1* have also been identified in triple WT melanomas (45, 59). Compared to other subtypes, triple WT melanomas have enriched focal amplification of *CCND1*, *MDM2* (mouse double minute 2 homolog), *KRAS* and *KIT genes*, the latter being commonly co-amplified with *PDGFRA* (platelet-derived growth factor receptor alpha) and *KDR* (kinase insert domain receptor) genes. High copy-number alterations of *CDK4* (cyclin-dependent kinases 4), *TERT*, *KIT* and *BCL-2* (B-cell lymphoma 2) (45, 59, 80) and gene fusions of *PAK1* (p21 (RAC1) activated kinase 1), *DGKB* (diacylglycerol kinase beta) and *RAF1* have also been reported in triple WT melanomas (45, 59).

1.4 Frequent mutations contributing to melanomagenesis

In addition to the most common driver melanoma genes described above, large-scale sequencing studies have uncovered other significantly mutated genes in melanoma (Table 1.2). These include alterations in *KIT*, *TP53*, *PTEN*, *CDKN2A*, *MAP2K1*, *RAC1*, *PPP6C*, *STK19*, *SNX31*, *TACC1*, *ARID2*, *IDH1*, *DDX3X* and *RB1* (17, 60, 81-83). Promoter mutations in *NDUFB9* (NADH: ubiquinone oxidoreductase subunit B9), *BLCAP* (bladder cancer-associated protein), *KBTBD8* (kelch repeat and BTB domain containing 8), *NSUN6* (NOP2/Sun RNA methyltransferase family member 6), *RALY* (RALY heterogeneous nuclear ribonucleoprotein), *RNF185* (ring finger protein 185), *RPL29* (ribosomal protein L29), *RPS27* (ribosomal protein S27) and *ZNF778* (zinc finger protein 778), 5' UTR (the 5' untranslated region) mutation in *RPS27*, (45, 84-86), and synonymous mutations in *BCL2L12* (BCL2 like 12), which increase transcript and protein levels (87), were also reported in melanoma by several other research groups (88, 89). We describe the function and contribution of a few genes relevant to this thesis below.

1.4.1 PTEN

PTEN (Phosphatase and tensin homolog) is a tumour suppressor gene, encoding a phosphatidyl-inositol-3,4,5-triphosphate 3-phosphatase. Deletion, loss-of-function mutations or reduced expression of *PTEN* have been identified in many cancer types, including breast, prostate, glioblastomas, endometrial and thyroid cancers (90, 91). Mutations in *PTEN* are more common in the coding region, such as in exon 5 (40%), which encodes the phosphatase domain, and mutations in the *PTEN* promoter or in splice donor and acceptor sites have also been identified (92).

PTEN is a critical tumour suppressor in melanoma and its loss is significantly associated with increased thickness of primary melanomas (79), and more aggressive cutaneous

melanoma (93). In the TCGA melanoma cohort, *PTEN* alterations were detected in 15% of melanoma samples (94, 95). A more recent study showed genetic alterations in *PTEN* in around 46% of melanomas, all of which were cutaneous melanoma, including 31% gene deletions, 8% substitution/insertion/deletions and 7% structural variants (45). Absence of *PTEN* is more common in *BRAF*-mutant and *BRAF*/*RAS* WT melanomas, suggesting that *PTEN* loss may lead to activation of the *PI3K*/*AKT* signalling pathway independent of *NRAS* mutation in primary melanomas (17).

1.4.2 TP53

Tumour protein 53 (*TP53*) is a tumour suppressor gene encoding a transcription factor. The p53 protein is involved in regulating cell cycle progression, cellular senescence, apoptosis, and is activated by cellular stress signals including UV radiation. *TP53* is one of the most frequently mutated genes in human cancer (96), and these mutations usually abolish its tumour suppressor activity (97).

In cutaneous melanoma, *TP53* mutations are present in around 5-19% of patients, mostly concurrent with *NF1* mutations, and less frequently with *NRAS* or *BRAF* mutations (17, 45, 59). Melanoma samples with *TP53* mutations tend to have markedly high mutation load. Furthermore, about 94% of *TP53* mutated melanomas showed evidence of UV mutation signatures (17, 59). In a recent study, *TP53* loss-of-function mutations were detected in mucosal and acral melanomas, suggesting a crucial role for this protein in these melanoma subgroups (45).

Although *TP53* mutations are relatively rare in melanoma compared to other cancer types, inactivation of p53 has been reported in about 90% of melanoma cases (98). p53 activity is negatively regulated by MDM2 and MDM4, which promote p53 ubiquitin-dependent degradation and inhibit p53 transcriptional activation, respectively (99).

Amplification of MDM2 occurs more frequently in triple WT melanomas, suggesting that this melanoma subtype may respond to MDM2 inhibitors such as nutlin-3 and AMG 232, which have been shown to have anti-tumour effects in melanoma (59, 100, 101). Moreover, inactivating mutations in *CDKN2A* (38% of melanoma cases), a complex gene locus that encodes the $p14^{ARF}$ tumour suppressor, which acts to negatively regulate MDM2, can also inhibit p53 function (97).

1.4.3 CDKN2A

CDKN2A (Cyclin-dependent kinase inhibitor 2A) is located on the frequently deleted human chromosome band 9p21, and it is also a tumour suppressor gene, as reviewed in (102). *CDKN2A* encodes two distinct proteins $p16^{INK4a}$ and $p14^{ARF}$ (103). The $p16^{INK4a}$ protein is a negative regulator of cell cycle through binding to cyclin-dependent kinases 4 and 6 (CDK4/6), and activating retinoblastoma (RB) protein (104), whereas $p14^{ARF}$ interacts with MDM2 to stabilise p53 (105, 106).

CDKN2A mutations have been detected in several types of human cancers, such as head and lung cancer, neck squamous cell carcinomas, pancreatic cancer, and breast cancer (107, 108). In melanoma, *CDKN2A* mutations were identified in 13-19% of patients, and deletion of *CDKN2A* was further identified in 38-46% of primary melanoma samples (17, 45, 59).

Table 1.2: Significantly mutated genes in melanoma

Gene	Description	Function	Mutation Type	Frequency
ARID2	AT-rich interacting domain 2	Subunit of the polybromo- and BRG1-associated chromatin remodelling complex which facilitates activation by nuclear receptors.	Loss-of-function	14%
BRAF	BRAF proto-oncogene, serine/threonine kinase	Kinase regulating the MAPK signalling pathway	Activating hotspot	51%
CDKN2A	Cyclin-dependent kinase inhibitor 2A	Encodes two tumour suppressors, the cyclin-dependent kinase inhibitor $p16^{INK4a}$ and the p53 activator $p14^{ARF}$	Loss-of-function	41%
DDX3X	DEAD-box helicase 3 X-linked	ATP-dependent RNA helicase activity.	Loss-of-function	7%
GNAQ	G protein subunit alpha Q	Guanine nucleotide-binding protein, α subunit in the G_q class. Couples receptor to activation of phospholipase C. Activates diverse signalling cascades including MAPK, PKC, YAP and PI3K/AKT signalling	Activating hotspot	2.1%
GNA11	G protein subunit alpha 11		Activating hotspot	3%
IDH1	Isocitrate dehydrogenase 1	Catalyses the oxidative decarboxylation of isocitrate to 2-oxoglutarate. Cancer mutations result in neomorphic enzyme activity.	Activating hotspot	6%
KIT	KIT proto-oncogene receptor tyrosine kinase	Tyrosine receptor protein kinase for the cytokine stem cell factor. Promotes MAPK and PI3K/AKT signalling	Activating hotspot	7%
MAP2K1	Mitogen-activated protein kinase kinase 1	Dual specificity protein kinase in the MAPK cascade. Downstream effector of RAF proteins.	Activating hotspot	7%
MAP2K2	Mitogen-activated protein kinase kinase 2	Dual specificity protein kinase in the MAPK cascade. Downstream effector of RAF proteins.	Activating hotspot	2.8%
N-RAS	NRAS proto-oncogene, GTPase	Intrinsic GTPase activity. Activated by guanine nucleotide exhange factors and inactivated by GTPase activating proteins. Promote MAPK and PI3K/AKT signalling.	Activating hotspot	30%
H-RAS	HRAS proto-oncogene, GTPase		Activating hotspot	1%
K-RAS	KRAS proto-oncogene, GTPase		Activating hotspot	3%
NF1	Neurofibromin 1	Stimulates GTPase activity of RAS to inhibit RAS signalling	Loss-of-function	13%
PPP6C	Protein phosphatase 6 catalytic subunit	Catalytic subunit of protein phosphatase, involved in cell cycle progression	Loss-of-function	8%

PTEN	Phosphatase and tensin homogue	Tumour suppressor with a phosphatidylinositol-3,4,5-triphosphate (PIP3) 3-phosphatase activity. Negatively regulates levels of PIP3 and inhibits the PI3K/AKT signalling pathway.	Loss-of-function	15%
RAC1	Rac family small GTPase 1	GTPase belonging to the RAS family of GTP-binding proteins. Promotes MAPK and PI3K/AKT signalling.	Activating hotspot	10%
RASA2	RAS p21 protein activator 2	Member of the GAP1 family of GTPase activating proteins. Enhances the weak intrinsic GTPase activity of RAS resulting in the inactive GDP-bound form of RAS.	Loss-of-function	6%
RB1	RB transcription corepressor 1 (retinoblastoma 1)	Negative regulator of cell cycle progression, binds and inhibits the E2F1 transcription factor	Loss-of-function	5%
SF3B1	Splicing factor 3b subunit 1	Subunit 1 of the splicing factor 3b complex. Regulates mRNA splicing	Activating hotspot	5%
TP53	Tumour protein p53	Tumour suppressor encoding transcription factor activity, DNA binding and oligomerisation domains. Stabilised in response to cellular stress to regulate target genes involved cell cycle arrest, apoptosis, DNA repair and metabolism	Loss-of-function	17%

Frequencies of genetic alterations (mutations and copy number alterations) were derived from the Skin Cutaneous Melanoma data set (TCGA, PanCancer Atlas) using cBioPortal (94, 95)

1.5 Major signalling pathways in cutaneous melanoma

The acquisition of mutations in melanoma lead to complex alteration and deregulation of molecular signalling pathways. These pathways regulate melanoma cell proliferation, survival, differentiation, and pigmentation, and generally involve the transfer of extracellular signals from receptor tyrosine kinases to multiple downstream effectors (Figure 1.2). In this section, we review several key signalling pathways important for melanoma development and progression, including the MAPK (ERK, extracellular signal-regulated kinases), the JNK (c-Jun N-terminal kinases), p38, PI3K/AKT, the RTK (receptor tyrosine kinase), the WNT/ß-catenin, and the NF-κB (nuclear factor-Kb) signalling pathways.

1.5.1 The mitogen-activated protein kinase signalling pathways

The MAPK signalling cascade is essential in regulating cellular processes such as cell proliferation, metabolism, and survival. MAPK-dependent signalling pathways are initiated by a wide range of extracellular stimuli (i.e. growth factors, hormones, stress and inflammation) binding to cell membrane receptors such as RTKs or G protein-coupled receptors. RTKs consist of extracellular ligand binding sites, transmembrane-spanning region, and intracellular catalytic tyrosine kinase domains, as reviewed in (109). The extracellular ligand binding domain is variable and induces receptor dimerization upon ligand binding, which then leads to tyrosine phosphorylation at the intracellular domains, providing specific binding sites for docking proteins, such as Grb2 (growth factor receptor-bound protein 2), Src, or phospholipase C γ. Binding of Grb2 recruits SOS (son of sevenless) to stimulate exchange of GDP, bound to RAS, for GTP, resulting in activation of RAS, as reviewed in (110-112).

The MAPK signalling pathway is comprised of three major cascades: the ERK (referred to as the MAPK pathway throughout this thesis), the JNK pathway, and the p38 pathway (isoforms α, ß, γ, δ). These three MAPK cascades have distinct subgroups of sequential-activated protein kinases: MAPK kinase kinases (MAPKKKs), MAPK kinases (MAPKKs), and MAPKs. MAPKKKs are activated upon interaction of the kinase with a small GTP-binding protein of the RAS/Rho family, leading to phosphorylation and activation of MAPKKs, which further phosphorylates MAPKs on threonine and tyrosine residues, as reviewed in (113) (Figure 1.3).

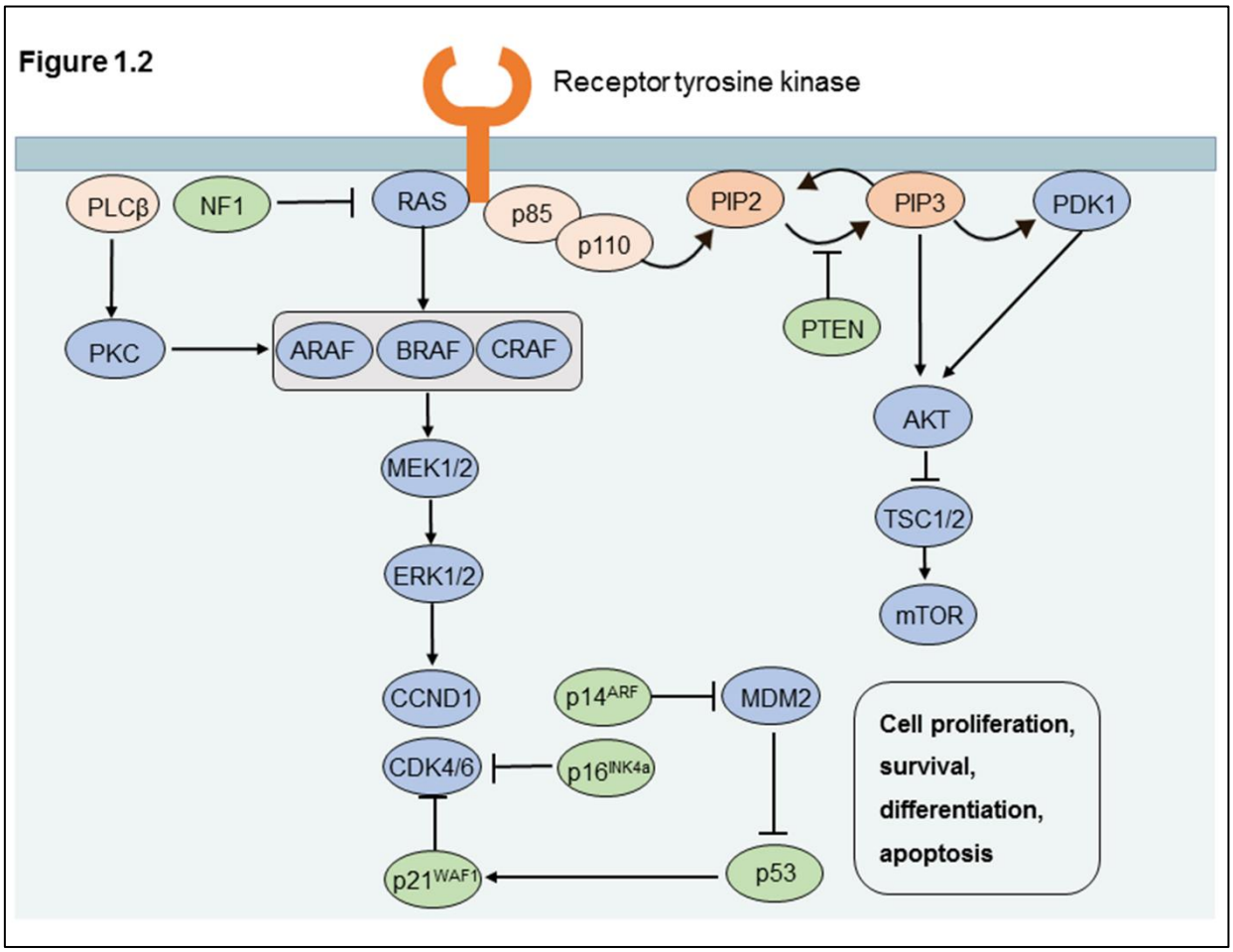

Figure 1.2: Major oncogenic signalling pathways in cutaneous melanoma

Several signalling pathways in cutaneous melanoma are initiated by activation of receptor tyrosine kinase (RTK). Phospholipase C (PLC) stimulates protein kinase C (PKC) to active downstream MAPK (RAF-MEK-ERK) cascade, via activation of three RAF isoforms (ARAF, BRAF, and CRAF). Activating mutations in BRAF and/or RAS also promote activation of the MAPK pathway, which stimulate downstream CCND1 (cyclin D1) and CDK4/6 activity. Activation of RTK also leads to plasma membrane recruitment of PI3Ks. Activated PI3Ks (p85/p110) are capable of converting the plasma membrane lipid phosphatidylinositol-4,5-bisphosphate (PIP2) to phosphatidylinositol-3,4,5-trisphosphate (PIP3), which can activate phosphoinositide-dependent kinase 1 (PDK1) and downstream AKT. Loss of PTEN promotes the accumulation of PIP3, resulting in AKT activation. Overexpression of RTKs and loss of NF1 also stimulate the MAPK and PI3K/AKT signalling networks, leading to cell proliferation and survival. The *CDKN2A* locus encodes the $p14^{ARF}$ and $p16^{INK4a}$ tumour suppressors. $p14^{ARF}$ suppresses MDM2 expression, which negatively regulates p53. In turn, p53 induces expression of $p21^{Waf1}$, which negatively regulates CDK4/6 activity. CDK4/6 is also negatively regulated by $p16^{INK4a}$.

MAPK signalling

The MAPK signalling pathway consists of RAF (ARAF, BRAF and CRAF), MEK1/2 and ERK1/2 kinases (Figure 1.3). A significant proportion of ERK1/2 accumulates in the nucleus following MAPK pathway activation. Activated ERK1/2 phosphorylate over 150 different known substrates, including membrane proteins, cytoskeletal elements, nuclear targets (c-jun, Elk1, NF-AT, STAT3 and c-Myc), and several MAPK-activated protein kinases. The main substrates of ERK1/2 are p90 ribosomal S6 kinase (p90RSK), MAPK-interacting kinases 2 (MNK2) and mitogen- and stress-activated kinases 1 and 2 (MSK1/2), as reviewed in (113, 114). Sustained activation of ERK1/2 promotes G1/S phase transition, by phosphorylating and activating nuclear transcription factor Elk-1, which leads to the formation of functional c-Fos/c-Jun AP-1 complex, and promoting expression of cyclin D1(115).

Constitutive activation of the MAPK signalling pathway plays a major role in driving melanomagenesis and more than 90% of melanoma cases show hyper-activation of MAPK signalling (116). Sustained activation of the MAPK pathway occurs mostly through activating mutations in *BRAF*, *RAS*, and amplification of other RAS family members such as *KRAS* and *HRAS* (17, 45, 59, 117).

Apart from *BRAF* or *RAS* mutations, other genetic or epigenetic changes in effectors within the MAPK pathway can also cause uncontrolled activation (45, 118). For example, genetic alterations (activating mutations, gene rearrangements or amplifications) of RTK family members, including *EGFR* (epidermal growth factor receptors), *PDGFR*, *IGF-1R* (insulin-like growth factor receptor), *FGFR* (fibroblast growth factor receptor), *VEGFR* (vascular endothelial growth factor receptor), *HGFR* (hepatocyte growth factor receptor), and proto-oncogene *c-KIT* (119, 120), activating mutations in *MEK1* and *MEK2* (*MAP2K1* or *MAP2K2*), or loss of tumour suppressors (*NF1*, *PTEN*) have all been shown to cause

MAPK pathway activation (45, 76, 81, 121-123). Additional autocrine mechanisms implicated in triggering MAPK signalling include c-Met overexpression, a receptor for hepatocyte growth factor, and down regulation of MAPK pathway inhibitory proteins such as SPRY2 (a CRAF inhibitor) (124, 125).

In *BRAF*/*RAS* WT melanoma, BRAF can activate MEK by forming a complex with CRAF in a RAS dependent manner (126). Moreover, *BRAF*/*RAS* WT melanomas with *NF1* mutations have the highest level of CRAF expression, indicating activation of MAPK signalling in this subtype (59). *RAC1* alterations (10% of melanomas), can cause subsequent PAK1 activation, can also lead to phosphorylation of CRAF and MEK1 (127), although *CRAF* mutations are rare in melanoma, accounting for about 4% of all melanomas(59). $CRAF^{R391W}$ missense mutation was identified as an oncogenic driver mutation, and it was commonly found in *NF1*-mutant or triple WT melanomas(128). Cell lines derived from these melanomas were highly dependent on $CRAF^{R391W}$ expression for MAPK activity, demonstrating mutated *CRAF* as a potent oncogene in melanoma (128, 129). Hence, MAPK signalling can be constitutively activated in the absence of *BRAF* and *RAS* mutations, and this suggests that the MAPK pathway may be equally important in melanoma genotypes other than *BRAF*-mutant and *RAS*-mutant melanomas (130).

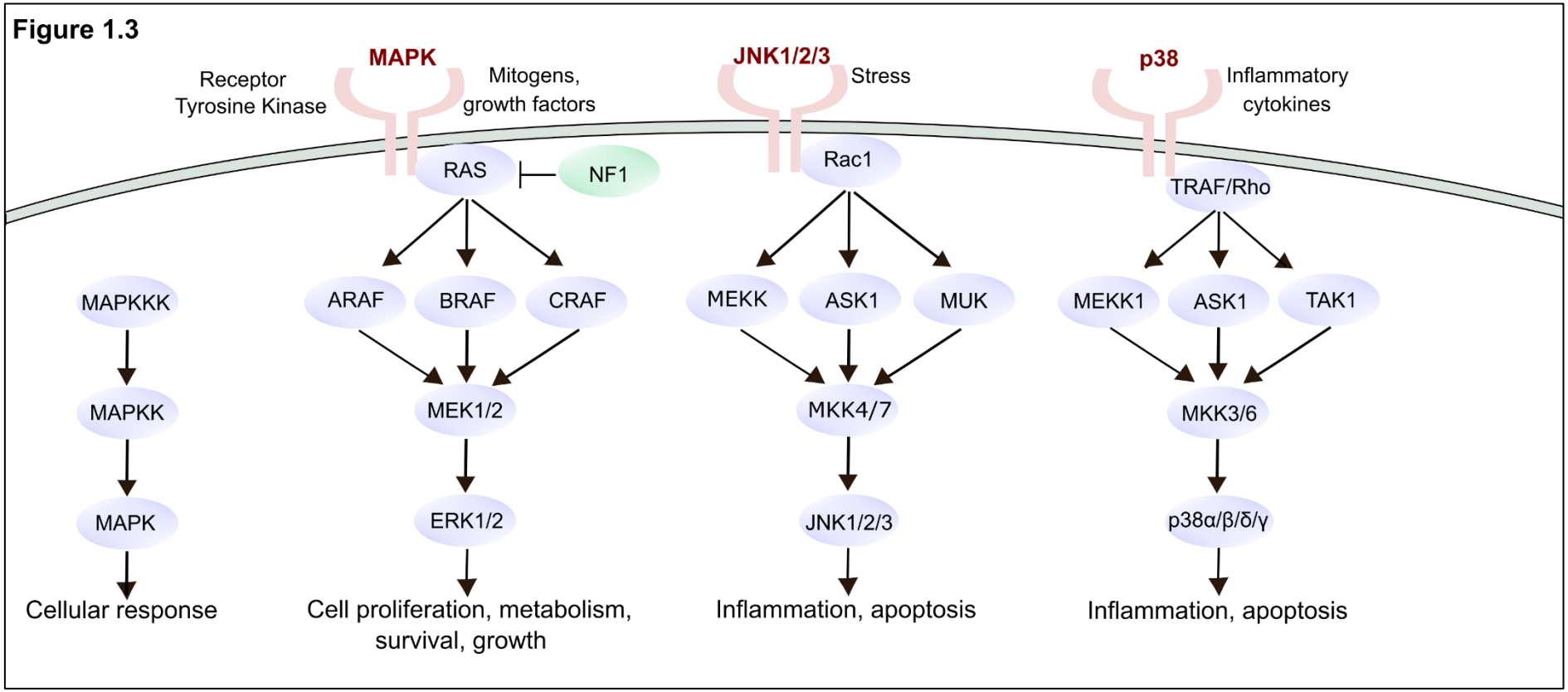

Figure 1.3: MAPK signalling cascades

Each MAPK signalling cascade comprises distinct MAPKKK, MAPKK and MAPK effectors. The three main cascades include i) MAPK pathway, activated by mitogens or growth factors, and functions in promoting cell proliferation and survival; ii) JNK pathway, activated by stress, and involved in inflammation and cell apoptosis; and iii) p38 pathway, activated by inflammatory cytokines, and regulates inflammation and apoptosis.

p38 signalling

The p38 family of proteins is a series of serine/threonine kinases known as “stress-activated” kinases, consisting of four isoforms p38α, p38ß, p38γ, p38δ, which are encoded by *MAPK14*, *MAPK11*, *MAPK12*, and *MAPK13*, respectively. p38α and p38ß are universally expressed in different tissues. However, p38γ and p38δ tend to have a more tissue-specific expression pattern. For instance, p38γ is predominantly expressed in muscle while p38δ is more frequently expressed in skin and kidney, as reviewed in (131-133). In melanoma, all p38 isoforms are expressed with the exception of p38δ, as reviewed in (134).

Several stressors are capable of activating p38 signalling, including pro-inflammatory cytokines, heat shock proteins, UV, hypoxia and ischemia (Figure 1.3), as reviewed in (113). For example, p38 signalling is activated by the cytokines tumour necrosis factor and interleukin-1, resulting in the recruitment of TRAF proteins, and this process is mediated by the Rho family GTPases Rac and Cdc42, as reviewed in (134). The p38 pathway was originally demonstrated to regulate inflammatory responses and modulate cytokine expression (135), as well as regulate tumorigenesis by activating G1/S and G2/M checkpoints (135). Enhanced levels of phosphorylated p38α have been shown to correlate with malignancy in different cancer types, indicating its oncogenic role in human cancer (136). In contrast, p38 signalling has also been described to have tumour suppressor roles, by downregulating cyclin D1 expression to inhibit cell proliferation as well as by activating the p53 apoptosis pathway (137, 138).

Two main upstream MAPKKs (MKK3 and MKK6), which are activated by several MAPKKKs including the apoptosis signal-regulating kinase 1 (ASK1), MEKK4, Tpl2, TAK1, and TAO1/2, rapidly phosphorylate p38 isoforms at the threonine-glycine-tyrosine (TGY) phosphorylation motif, as reviewed in (113, 132, 133) (Figure 1.3). p38 isoforms can be

additionally activated by autophosphorylation mechanisms (139). Activation of p38 leads to activation of kinases (MNK1, MNK2, MSK1, MAPKAPK2, and MAPKAPK3), and transcription factors (Elk-1, p53, MEF-2, CHOP-1, and ATF-2), contributing to cytoplasmic/nuclear signalling and cellular response to growth factors, cytokines, or pharmacological agents (133, 140).

In melanoma, activation of the p38 pathway has been reported to result in distinctly varied effects, either promoting melanoma cell growth and migration, or having anti-tumour activity (141-143). For example, p38 signalling was associated with melanoma differentiation, and was correlated with decreased phosphorylation of retinoblastoma protein and cell cycle arrest (144). Increased levels of phosphorylated p38 were shown to upregulate both tyrosinase activity and melanogenic enzymes such as MITF through binding phosphorylated CREB (134, 145). Another report showed that p38 signalling regulates VE-cadherin junction disassembly, stimulating melanoma migration across endothelial cells (146). In contrast, p38 signalling induces expression of a series of cytokines including interferon-α, tumour necrosis factor-α, IL-1 and IL-24, which have anti-proliferative effects on melanoma development (134, 147, 148). Two other effectors, MC1R (melanocortin 1 receptor) and α-MSH (after cleavage of pro-opiomelanocortin), are also regulated by p38-activated upstream stimulating factor-1 (149).

JNK signalling

The JNK (c-Jun N-terminal kinases) family of proteins include three members JNK1, JNK2, and JNK3, which are encoded by the *MAPK8*, *MAPK9*, and *MAPK10* genes, respectively, as reviewed in (150). JNK1 and JNK2 are universally expressed, but JNK3 has a more restricted expression pattern, found mostly in the brain, heart, and testis. Ten different isoforms of JNK can be generated and spliced from these three genes (151). JNK signalling is activated predominantly by inflammatory cytokines (tumour necrosis

factor-α and IL-1ß) and environmental stress (152, 153), and less frequently by cellular stresses including oxidative stress or genotoxic (154). Two MAPKKs, MKK4 and MKK7, were identified to phosphorylate JNK at Thr183 and Tyr185 residues and several other MAPKKs including MEKK family proteins MLK, ASK1, TPL-2 and TAK1 were also shown to contribute to JNK activation, as reviewed in (134, 150) (Figure 1.3). PKC (protein kinase C) can also activate JNK, which further activates its downstream effector cyclin D1 to positively regulate G1/S cell cycle transition in melanomagenesis (155).

JNK has various downstream effectors, among which is the transcription factor c-Jun whose activity and expression is also regulated by MAPK signalling (156). Phosphorylated c-jun together with c-Fos and ATF2 form a complex to constitutively activate effectors that regulate cell cycle, cell proliferation, cell differentiation and death (157, 158). Other transcription factors such as c-Myc, and the STAT family of proteins are also phosphorylated by JNK, as reviewed in (134).

The importance of the JNK pathway in melanoma was first demonstrated by the elevated expression of jun-B and c-fos RNA transcripts in metastatic melanoma compared to melanocytes (159). Since then, numerous studies have uncovered a role for JNK signalling in promoting melanomagenesis. For instance, JNK signalling was critical for melanoma cell proliferation, and its inhibition in a large panel of melanoma cell lines caused significant cell cycle arrest (160). Another report showed that MALT1 (Mucosa associated lymphoma antigen 1), which is elevated in melanoma, promoted melanoma proliferation through JNK/c-Jun activation (161).

1.5.2 PI3K/AKT signalling

The PI3K/AKT pathway is another core signalling cascade contributing to tumorigenesis in human cancers. In melanoma, this pathway modulates essential functions in tumour initiation, progression, invasion, and drug resistance (162).

PI3Ks belong to a conserved protein kinase family, which bind serine/threonine residues of substrates or lipid messengers such as phosphatidylinositol. Among multiple forms of PI3Ks, the class IA enzymes, which includes the p110 catalytic subunit and a p85 regulatory subunit, contribute to PI3K/AKT pathway activation, as reviewed in (163) (Figure 1.2). Activation of PI3K isoforms is due to the stimulation of RTKs or G-protein-coupled receptors, thus leading to plasma membrane recruitment of PI3Ks. Activated PI3Ks are capable of converting the PIP2 to PIP3, which can then recruit signalling proteins serine-threonine kinase AKT and PDK1 via the plekstrin-homology domains to the membrane. PDK1, after localizing on the membrane, can phosphorylate AKT at a residue in the kinase domain (Thr308) while the mammalian target of rapamycin complex 2 (mTORC2) is recruited to phosphorylate the other residue in the hydrophobic motif (Ser473) of AKT; phosphorylation of AKT at both residues stimulate its catalytic activity , as reviewed in (164). AKT has many downstream targets, one example being mTORC1, which upon phosphorylation by AKT, activate p70S6 kinase to promote cell proliferation (165) (Figure 1.2).

Constitutive activation of the PI3K/AKT signalling cascade can be induced by amplifications or activating mutations in RTKs (i.e. *KIT*, *EGFR*) or *NRAS*, mutations in *PIK3CA* that encodes the p110a catalytic subunit, or loss of NF1 or PTEN (166-168). The pathway can also be negatively regulated; AKT activity and mTORC1 signalling are suppressed by p70S6K-mediated phosphorylation of IRS and RICTOR (169).

Several studies have shown that the PI3K/AKT pathway cooperates with MAPK signalling during melanomagenesis, to control cell proliferation through co-regulating cyclin D1 expression, suggesting that combination targeting of these two pathways may have beneficial effects in inhibiting melanoma growth (170).

1.5.3 Wnt/ß-catenin signalling

The Wnt signalling pathway is a crucial intracellular signal transduction pathway involved in cell growth, proliferation, migration and behaviour (171). The Wnt pathway comprises the canonical pathway, which includes the intracellular transcriptional co-activator ß-catenin as a central component, and the non-canonical pathway that involve alternative cascades that lack the participation of ß-catenin, as reviewed in (172).

Absence of Wnt ligands in the canonical Wnt pathway results in the formation of a degradation complex that recruits cytoplasmic ß-catenin. ß-catenin is subsequently phosphorylated at threonine and serine residues by GSK3ß and CK1; this process promotes ß-catenin ubiquitination and proteasomal degradation (173). In contrast, binding of Wnt ligands to the Frizzled and low-density lipoprotein receptor-related protein 5 or 6 co-receptor causes dissociation of the degradation complex, thus releasing ß-catenin. This then allows ß-catenin to translocate to the nucleus where it binds TCF/LEF transcription factors to promote transcription of genes regulating cell development and differentiation (174).

Alterations in genes encoding effectors within the Wnt signalling pathway are common in different types of cancers, including hepatocellular carcinoma, hepatoblastoma, and colorectal carcinoma, as reviewed in (175). Oncogenic activation of ß-catenin via amino acid deletions or substitutions was identified in 23% of melanoma cell lines, but is rarely detected in primary melanoma (176). Constitutive activation of Wnt/ß-catenin signalling

was associated with increased melanoma cell growth, likely via regulation of downstream transcription factor Brn-2 (177). Moreover, Wnt/ß-catenin-mediated metabolic reprogramming of cancer cells can directly affect vessel density and expression of pro-tumourigenic growth factors (178). In addition to direct effects on cancer cells, a recent study comparing non-T-cell-inflamed and T-cell-inflamed metastatic melanoma samples revealed a correlation between activation of Wnt/ß-catenin signalling and absence of T-cell infiltration (179), suggesting additional effects of this pathway on mediating immune response.

1.6 Current therapies in melanoma

Before 2011, survival rates for patients with advanced metastatic melanoma were poor, and standard-of-care included chemotherapy in the form of dacarbazine (180), or less commonly, immunotherapy with the cytokine IL-2 (181). However, with new insights into the genomic landscape of melanoma (17, 45, 59) and the regulation of anti-cancer immunity (182), several new therapeutic agents have been approved by the FDA (The US Food and Drug Administration) for the treatment of patients with advanced melanoma. These new therapies include selective kinase inhibitors targeting the MAPK signalling pathway (183-186), and immunotherapies that re-invigorate the immune system against melanoma cells. Melanoma patients have benefited substantially from these therapies, with better overall survival (OS) and dramatically improved response rates (187-189).

1.6.1 Targeted therapies

BRAF inhibitors

BRAF inhibitors, vemurafenib and dabrafenib, are currently approved in the US and Australia as treatment for patients with advanced *BRAF*^{V600}-mutant melanoma. These inhibitors are ATP-competitive selective inhibitors of the V600E/K mutant form of *BRAF* (Table 1.3). In a phase III randomized clinical trial comparing vemurafenib with dacarbazine chemotherapy in 675 patients with metastatic melanoma, the response rates were 57% for vemurafenib compared to 9% for dacarbazine, and median progression-free survival (PFS) was 6.9 months for vemurafenib compared to 1.6 months for dacarbazine (hazard ratio (HR) 0.38; $p<0.0001$) (190). Dabrafenib, the second FDA-approved selective BRAF inhibitor, showed similar potency. In the BREAK-3 phase III trial, dabrafenib demonstrated higher response rates compared to dacarbazine, 50% compared to 6%, and improved median PFS (5.1 months vs 2.7 months; HR 0.30; p

<0.0001) (183). Recently in 2018, another BRAF inhibitor encorafenib was approved for combination treatment with a MEK inhibitor in a phase III trial for patients with unresectable or metastatic *BRAF*^{V600}-mutant melanoma (191). Furthermore, BRAF inhibitor has shown efficacy in patients with metastatic brain melanoma (192).

The most common adverse events induced by BRAF inhibitors are rash (41%), arthralgia (56%), fatigue (46%), photosensitivity (41%) (for vemurafenib) (193), rash (30%), alopecia (27%), arthralgia (19%), fatigue (18%), hyperkeratosis (36%), pyrexia, fatigue and headaches (for dabrafenib) (194), and palmar-plantar erythrodysaesthesia syndrome (14%), myalgia (10%), and arthralgia (9%) (for encorafenib). Squamous cell carcinomas were common grade 3 and 4 toxicities for both vemurafenib and dabrafenib (190, 195).

Allosteric MEK inhibitors

Given the importance of MAPK signalling in *BRAF*^{V600}-mutant melanoma, inhibition of MEK1/2 has also shown clinical efficacy in patients with *BRAF*^{V600}-mutant melanoma. Several allosteric inhibitors of MEK1/2 are currently FDA-approved for melanoma, including trametinib, binimetinib, and cobimetinib (Table 1.3). In a phase III trial, patients with *BRAF*$^{V600E/K}$-mutant metastatic melanoma who received trametinib showed an overall response rate of 22%, and median PFS of 4.8 months compared to 1.5 months for patients who received standard chemotherapy (HR 0.45, p<0.001). At 6 months, OS was 81% in the trametinib group compared to 67% in the chemotherapy group (p=0.01) (196). Based on this phase III trial, trametinib was first approved by the FDA as a single agent for the treatment of *BRAF*^{V600}-mutant melanoma (196). Metastatic melanoma patients with rare activating *BRAF* mutations (non-V600) treated with trametinib also showed a better response rate of 40% compared to when patients were treated with a BRAF inhibitor (7%); the median PFS was 4.8 months in the trametinib group compared to the BRAF inhibitor group with PFS of 1.6 months (197). The most common toxicities

associated with trametinib include dermatitis acneiform (82%), diarrhoea (45%) and ocular events (9%), most of which were grade 1 or 2, decreased ejection fraction or ventricular dysfunction (7%) and grade 3 or 4 rash (8%) (196, 198).

MEK1/2 inhibition has also been evaluated in *NRAS*-mutant and *BRAF/NRAS* WT melanomas. In a phase II clinical trial, the MEK inhibitor binimetinib showed promising clinical activity with a response rate of 20% in both *BRAF*-mutant and *NRAS*-mutant patients (199). Another phase II study that included 117 patients with *NRAS*-mutant melanoma treated with binimetinib showed an overall response rate of 14.5% and median PFS of 3.6 months (200). Furthermore, a phase III trial showed improved PFS in *NRAS*-mutant melanoma patients who received binimetinib compared to those who received dacarbazine (2.8 months vs 1.5 months; HR 0.62; $p<0.001$) (201). In a recent report, *NRAS*-mutant melanoma patients who received MEK inhibitors (binimetinib, pimasertib or trametinib) before or after immunotherapy had 5 months longer median OS (25 months vs 20 months, $p=0.57$) compared to those without MEK inhibitor treatment (202).

Several preclinical studies have also confirmed that *BRAF*/*NRAS* WT melanoma cell lines are exquisitely sensitive to trametinib irrespective of *NF1* status (76, 203, 204). In a phase I clinical trial that included 20 *BRAF/NRAS* WT melanoma patients treated with trametinib, the objective response rate was 20% (198). Although the clinical benefit of MEK inhibitor monotherapy is modest, combination of MEK inhibitor with other selective inhibitors has shown greater clinical efficacy and will be discussed in subsequent sections.

Combination BRAF and MEK inhibitors

Combination of BRAF and MEK inhibitors has demonstrated better efficacy than the use of either inhibitor alone (Table 1.3). In a multicentre phase III randomised controlled trial (COMBI-d) comparing combination dabrafenib and trametinib to dabrafenib and placebo in 423 advanced melanoma patients, the dabrafenib and trametinib combination

significantly improved overall response rate (69% vs 53%, p=0.0014), median OS (25.1 vs 18.7 months; HR 0.71; p=0.0107) and median PFS (11.0 vs 8.8 months; HR 0.67; p=0.0004) (185). Another phase III study (COMBI-v) comparing combination BRAF and MEK inhibitors to vemurafenib monotherapy in 704 melanoma patients showed markedly improved overall response rate (64% vs 51%; p<0.001), median PFS (11.4 vs 7.3 months; HR 0.56; p<0.001) and median OS (26.1 vs 17.8 months; HR 0.68) (205, 206). Similarly, melanoma clinical trials of vemurafenib in combination with the MEK1/2 inhibitor cobimetinib showed improved anti-tumour efficacy and better clinical outcomes compared to vemurafenib monotherapy (186, 207, 208). Combination of encorafenib with binimetinib compared to vemurafenib or encorafenib monotherapy were also examined in a phase III trial. Longer median PFS was achieved in the combination group (14.9 months) compared to vemurafenib (7.3 months, HR 0.54; p<0.001) or encorafenib (9.6 months, HR 0.75) alone (191). Combination of BRAF and MEK inhibitors are now the standard-of-care targeted therapy for *BRAF*^{V600}-mutant melanoma.

Table 1.3: Phase III clinical trial data for BRAF and MEK inhibitors in patients with advanced *BRAF*^{V600}-mutant melanoma

Drug	Vemurafenib	Dabrafenib	Trametinib	Vemurafenib + Cobimetinib	Dabrafenib + Trametinib	Encorafenib + Binimetinib
Trial	BRIM-3	BREAK-3	METRIC	CoBRIM	COMBI-d	COLUMBUS
Comparator	Dacarbazine	Dacarbazine	Dacarbazine	Vemurafenib	Dabrafenib	Encorafenib or Vemurafenib
No. of patients	675	250	322	495	423	577
Median follow up (months)	12	17	20.3	18.5	20	16.6
Median PFS (months)	6.9	6.9	4.8	12.3	11.1	14.9
Progression HR (CI)	0.38 (0.32-0.46)	0.37 (0.24-0.58)	0.45 (0.33-0.63)	0.56 (0.46-0.71)	0.67 (0.53-0.84)	0·54 (11·0–18·5)
Overall response %	57%	59%	81%	70%	69%	63%
Median OS (months)	13.6	20	NR	22.3	25.1	33.6
Death HR (CI)	0.7 (0.57-0.87)	0.77 (0.52-1.13)	0.54 (0.32-0.92)	0.70 (0.55-0.90)	0.71 (0.55-0.92)	0.54 (0·41-0·71)
OS at 1 year (%)	55.4	NA	NA	74.5%	74.6%	75·5%

PFS, progression free survival; OS, overall survival; NR, not reached; HR, hazard ratio; CI, 95% confidence interval; NA, not applicable.

Table adapted from (209).

Alternative targeted therapies in melanoma

The anti-tumour efficacy of inhibitors targeting PI3K/AKT signalling have been investigated in preclinical models and in clinical trials, including inhibitors of isoform-specific PI3K (PI3Kα, PI3Kß, PI3Kγ, or PI3Kδ) and pan-isoform PI3K inhibitors, AKT inhibitors, mTOR inhibitors, and dual PI3K/mTOR inhibitors. Several inhibitors of the PI3K/AKT pathway are in ongoing clinical trials for different tumours and include AZD5363 and MK2206 (AKT inhibitors), Rapamycin (mTORC1 inhibitor), ZSTK474 and BKM120 (pan PI3K inhibitors), BEZ235 and GSK2126458 (dual PI3K/mTOR inhibitors), as reviewed in (210, 211).

The pan-PI3K inhibitor BKM120 (buparlisib) showed promising effects in inducing melanoma cell cycle arrest and cell death, and potent inhibition of melanoma brain metastasis growth in mouse models (212, 213). The safety and efficacy of buparlisib are currently being assessed in an open-label phase II trial, involving *BRAF*^{V600E}-mutant (patients who previously failed BRAF and MEK inhibitor treatment) and *BRAF* WT (patients who previously failed immunotherapy) melanoma patients with brain metastases (214). Another novel pan-PI3K inhibitor, BAY 80-6946, also induced cell cycle arrest and apoptosis in melanoma cell lines, and inhibited tumour growth in transplanted mouse models (215).

AKT inhibitors have also shown anti-tumour efficacy in preclinical studies. For instance, the ATP-competitive AKT inhibitor AZD5363 inhibited cell growth in a large subset of cancer cell lines and mouse models, and response to AZD5363 was more pronounced in cells with *PTEN* deletion, activating *PIK3CA* mutations, and *HER2* amplification (216, 217). Despite this, treatment with AKT inhibitors has not produced favourable clinical results; MK-2206, a potent allosteric pan-AKT inhibitor, showed marginal anti-tumour activity in an early clinical trial (218). Similarly, rapamycin, a mTORC1 inhibitor, showed

modest melanoma growth inhibition in preclinical models but was not effective as a single agent in clinical trials (219).

Co-targeting of PI3K/AKT and MAPK pathway may have beneficial anti-tumour effects. Combination of PI3K and MEK inhibitors induced robust apoptosis and markedly inhibited tumour growth of *BRAF*-mutant (220) and *NRAS*-mutant melanomas (221). Treatment of a panel of *BRAF*-mutant metastatic melanoma cell lines with a pan-PI3K or a pan-PI3K/mTOR inhibitor enhanced sensitivity to BRAF and MEK inhibition (222). Similarly, blockade of the PI3K/AKT pathway in conjunction with BRAF inhibition enhanced apoptosis in *BRAF*-mutant melanoma cell lines (223). Moreover, resistance to vemurafenib and MEK inhibitors in melanoma can be reversed with treatment using combination RAF or MEK inhibitor with an AKT or mTOR inhibitor (224). A phase I trial of 24 patients with advanced $BRAF^{V600}$-mutant tumours treated with vemurafenib and PX-866 (a PI3Kα inhibitor) reported partial response in seven patients and stable disease in 10 patients (225).

CDKs are constitutively activated in melanoma, due to mutation or amplification of *CDK4* or loss of $p16^{INK4a}$, a suppressor of CDK4/6 (17). Focal amplifications of *CDK4* have been identified in *BRAF*/*RAS* WT melanomas (17), leading to deregulation of cell cycle and uncontrolled cell proliferation. CDK4/6 inhibitors showed promising anti-tumour activities in various tumour types (226, 227), including melanoma (228, 229). In *BRAF*-mutant melanoma, the selective dual-CDK4/6 inhibitor LY2835219 induced apoptotic cell death in BRAF inhibitor resistant cell lines, and significant tumour growth regression in mouse models (230). Approximately 83% of primary acral melanoma patients show frequent copy number variations in CDK4 pathway-related genes, including *CDK4*, *CCND1*, and *CDKN2A*, and treatment with a pan-CDK inhibitor AT7519 and a selective CDK4/6 inhibitor PD0332991 reduced melanoma cell viability *in vitro* and *in vivo* (231). In metastatic melanoma patients who failed immunotherapy, treatment with a CDK4/6

inhibitor resulted in tumour control lasting over six months in tumours with copy number variations in *CDK4, CCND1* and/or *CDKN2A* (232).

Combined pharmacological inhibition of MEK and CDK4 suppressed tumour growth *in vivo* in a mouse model of *NRAS*-mutant melanoma, whereas MEK inhibitor monotherapy failed to induce cell cycle arrest (233). Due to the success of targeting CDK activity in these preclinical studies, several clinical trials have been established. A phase I/II study of 14 patients with *NRAS*-mutant melanoma treated with the CDK4/6 inhibitor ribociclib and binimetinib reported partial responses in 43% of patients, with six patients showing stable disease (four with tumour shrinkage > 20%) (234). Similarly, another phase I/II study of combination ribociclib and binimetinib in patients with *NRAS*-mutant melanoma showed 23% partial response rate, and median PFS of 6.2 months (235).

The tyrosine kinase inhibitor imatinib has shown activity in *KIT*-mutant melanoma. In an early phase II trial that included 28/295 advanced melanoma patients with *KIT* alterations, treatment with imatinib produced an overall response rate of 16%, with durable responses lasting over a year (236). Subsequently, a phase II study involving 43 metastatic melanoma patients with *KIT* aberrations reported an overall response rate of 23% (10/43); nine of the ten responding patients had *KIT* mutations in exons 11 or 13 (237). Another multicentre phase II trial consisting of 25 metastatic melanomas with *KIT* mutations or amplifications treated with imatinib reported an overall response rate of 29%, and more than 50% of *KIT*-mutated melanoma responded (238). However, though amplification of the *KIT* gene is common in *BRAF*/*RAS* WT melanomas (17, 59), activity of imatinib in melanoma with *KIT* amplification, but not *KIT* mutation, is very limited (238).

Downstream effectors of the MAPK pathway have also been targeted for therapy. The ERK inhibitor SCH772984 was shown to overcome BRAF or MEK inhibitor resistance in *BRAF*- or *NRAS*-mutant melanoma (239, 240). A proportion of *BRAF*/*RAS* WT melanoma

cell lines also showed high sensitivity to SCH772984 treatment, with potent cell cycle arrest and cell death (241). Selective PAK1 inhibition with a PAK inhibitor PF-3758309 decreased tumour growth in *BRAF* WT melanoma xenografts (242).

Apart from signalling pathways, inhibitors targeting other regulatory proteins have also been tested in melanoma. For instance, HDAC (histone deacetylase) inhibition showed potent anti-tumour activity, reflected by G1 cell cycle arrest, cell apoptosis and induction of immune response (243). HDAC inhibition may also overcome BRAF inhibitor resistance in *BRAF*-mutant melanoma cells (244). Some HDAC inhibitors, including vorinostat and entinostat have been tested in clinical trials and showed anti-tumour activity in melanoma (245, 246). Moreover, pan-HDAC inhibitors AR42 and sodium valproate were recently reported to increase MHC Class I expression on melanoma cells, and enhance response to immunotherapy, suggesting these inhibitors as potential combination strategies for melanoma treatment (247).

1.6.2 Immunotherapy with immune checkpoint inhibitors

The immune system plays an essential role in recognizing and defending the host against microbial infections and other foreign injuries or pathogens (248). However, cancer cells can escape from immune attack by expressing inhibitory receptors or ligands, known as immune checkpoints that function to disable the activation of T-cells (249). The development of immune checkpoint inhibitors that block these inhibitory receptors to enhance T-cell mediated anti-tumour immune responses have significantly improved response duration and OS of patients with advanced metastatic melanoma. Immune checkpoint inhibitors that target the cytotoxic T lymphocyte-associated protein-4 (CTLA-4) and the programmed cell death protein-1 (PD-1) receptors are the most extensively studied in melanoma (187, 250-252).

CTLA-4 inhibition

Cytotoxic T lymphocyte-associated protein-4 (CTLA-4), also known as CD152, is expressed on activated T-cells and TRegs (regulatory T-cells) (253). CTLA-4 is homologous to the T-cell stimulatory receptor protein CD28, and the CTLA-4 and CD28 ligands, B7-1 (CD80) and B7-2 (CD86), are expressed on antigen presenting cells (254). CTLA-4 inhibits immune cell activation by competing with the homologous T-cell stimulatory protein CD28 for binding to the B7-1 and B7-2 ligands (255). Moreover, CTLA-4 is also able to remove the ligands from antigen presenting cells via trans-endocytosis, to prevent them from binding to the co-stimulatory CD28 (256). Therefore, CTLA-4 expression is important for tumours to escape the host immune surveillance (257).

Ipilimumab is a monoclonal antibody (IgG1) that binds CTLA-4 on effector T and TReg cells and inhibits the interaction of CTLA-4 with the B7 ligands to promote anti-tumour immunity (258). In a phase III trial (CA184-002), patients with unresectable stage III or IV

melanoma who received ipilimumab demonstrated improved OS of 10.1 months and the best overall response rate of 10.9%, compared to treatment with glycoprotein 100 (gp100) peptide vaccine (6.4 months, 1.9%) (HR 0.66; P=0.003) (187) (Table 1.4). Additionally, in another phase III clinical trial, melanoma patients treated with ipilimumab plus dacarbazine showed longer OS compared to dacarbazine alone (11.2 months versus 9.1 months, HR 0.72; P<0.001) (259). Evaluation of long-term survival of advanced melanoma patients treated with ipilimumab in these phase II/III clinical trials reported 22% of patients alive three years after treatment (260). Immune-related adverse events, such as dermatitis, diarrhoea and colitis, are common toxicities associated with ipilimumab treatment (261).

PD-1 inhibition

Programmed cell death protein-1 (PD-1), also known as CD279 (cluster of differentiation 279), is another immune checkpoint molecule which is predominantly expressed on activated CD4+ T-cells and activated CD8+ T-cells. PD-1 is also expressed on a small percentage of B lymphocytes, natural killer T-cells, and myeloid cells (262). Unlike CTLA-4 which is involved in early activation of T-cells, PD-1 is operational during the effector phase of T-cell activation with distinct mechanism regulating immunosuppression (263). Binding of PD-1 to its ligands, PD-L1 (B7-H1) and PD-L2 (B7-DC), can result in apoptosis of lymphocytes and downregulation of T-cell function (264, 265). Upregulation of PD-L1 was identified in metastatic melanoma, and it was associated with tumour-infiltrating lymphocytes and IFN-γ production (266). Elevated levels of PD-1 expression on CD8+ and CD4+ T-cells have also been reported in melanoma patients (267), indicating that overexpression of PD-1 and its ligands may be a common mechanism of T-cell suppression in melanoma.

Inhibiting PD-1 on T-cells using anti-PD-1 antibodies such as nivolumab and pembrolizumab have shown impressive clinical outcomes in melanoma patients (263) (Table 1.4). Compared to ipilimumab, anti-PD-1 showed better anti-tumour efficacy with longer OS (36.9 vs 19.9 months, HR 0.54; $p<0.0001$) and PFS (6.9 vs 2.9 months, HR 0.42; $p<0.0001$), and higher objective response rate (45% vs 19%) (268). Both nivolumab and pembrolizumab show comparable clinical activity (269).

Combination of CTLA-4 and PD-1 inhibitors

Although CTLA-4 and PD-1 inhibitors produce durable responses and improve survival outcomes, only 20%-40% of melanoma patients will respond to treatment (187, 270, 271) and approximately 43% of responding patients will eventually acquire resistance and progress within three years (272, 273).

Recent clinical trials have shown that the combination of the two inhibitors improves response rate and patient survival (274-277). A phase III trial of 314 patients with previously untreated, unresectable stage III or IV *BRAF*^{V600}-mutant melanoma treated with nivolumab and ipilimumab showed median PFS of 11.5 months, a complete response rate of 19% at three years, and median duration of response of 50.1 months (268). Combination of ipilimumab and nivolumab has also been tested in 94 patients with metastatic brain melanoma and showed a partial response rate of 30%, and complete response rate of 26%, with 2% of patients showing stable disease lasting at least six months (274). The major clinical trials using CTLA-4 and PD-1 inhibitors, either alone or in combination, in metastatic melanoma are summarized in Table 1.4.

Combination immune checkpoint inhibitors is also associated with increased toxicity with more than 50% of patients experiencing grade 3–4 adverse events, including diarrhoea and increased lipase. Monotherapy treatment with either inhibitor is less toxic; grade 3–4

adverse events were observed in 22% of patients treated with nivolumab and in 28% of patients treated with ipilimumab (268).

Table 1.4: List of FDA-approved immune checkpoint inhibitors used in ongoing clinical trials for the treatment of metastatic melanoma

Drug	Ipilimumab	Pembrolizumab	Nivolumab	Ipilimumab+ Nivolumab
Trial	CA184-002 (187)	KEYNOTE-006 (278)	CheckMate 066 (250)	CheckMate 067 (275)
Comparator	Glycoprotein 100	Ipilimumab	Dacarbazine	Ipilimumab
No. of patients	676	834	418	314
Median follow up (months)	27.8	22.9	NR	36
Median PFS (months)	2.9	5.6	5.1	11.5
Progression HR (CI)	0.64	0.61 (0·5-0.75)	0.43 (0.34-0.56)	0.43 (0.35 to 0.52)
Overall response %	60%	37%	40.0%	58%
Median OS (months)	10.1	NR	NR	NR
Death HR (CI)	0.66 (0.51 to 0.87)	0.68 (0.53-0.87)	0.42 (0.25-0.73)	0.55 (0.45-0.69)
OS at 1 year (%)	46%	74%	73%	NR

PFS, progression free survival; OS, overall survival; NR, not reached; HR, hazard ratio; CI, 95% confidence interval.

1.6.3 Combination of targeted therapy and immunotherapy

Although 70% of *BRAF*-mutant melanoma patients respond to MAPK pathway inhibitors, half of these patients will acquire resistance within one year, while only 40% of patients will respond to immune checkpoint inhibitors (252, 260). Therefore, there is increasing interest in combining molecularly targeted and immunotherapies for melanoma. Pre-clinical studies have shown that these combinations could be synergistic. For example, BRAF or MEK inhibition stimulate T-cell proliferation and activation in co-culture models of melanoma cells with T-cells (279). Moreover, MAPK inhibition induced marked T-cell infiltration in melanoma tumours (280). Clinical trials of PDL1/PD1 inhibitors combined with MAPK (BRAF/MEK) inhibitors are currently ongoing (NCT02130466, NCT02027961, NCT02967692, NCT02908672) (281, 282). However, dose-limiting hepatotoxicity remains a major issue for these combinations (283-285).

1.7 Resistance mechanisms to MAPK inhibition in melanoma treatment

More than 50% of patients with *BRAF*^{V600E}-mutant melanoma treated with BRAF and/or MEK inhibitors develop drug resistance and disease progression within the first year of treatment (286, 287). Resistance mechanisms differ between individuals and may involve genomic and/or non-genomic alterations (Table 1.5).

Table 1.5: Summary of acquired MAPK resistance mechanisms

Acquired resistance mechanisms	
MAPK reactivation	**Alternative pathways activation**
BRAF^{V600} alternate splicing	PI3K/AKT pathway activation
BRAF^{V600} amplification	RTK up-regulation (PDGFRß, EGFR, ERBB3, IGF-1R)
CRAF overexpression	Loss of *PTEN*
COT (MAP3K8) overexpression	HGF/MET signalling activation
RAS activating mutation	*CCND1*/*cyclinD1* amplification
MEK1 and *MEK2* activating mutation	STAT3-PAX3 overexpression
RAC1 mutation	*AKT* mutation

1.7.1 MAPK reactivation

BRAF alterations

A secondary mutation in *BRAF*^{L514V} was identified as a mechanism of acquired resistance to BRAF inhibition in a *BRAF*^{V600E}-mutant brain tumour (288). However, no other secondary *BRAF* mutations have been uncovered in melanomas resistant to MAPK inhibition. Amplification of *BRAF*, which is a copy number gain of the mutant allele of *BRAF*, contributes to hyperactivation of ERK (289) and leads to resistance to MAPK inhibition (65). Amplification of *BRAF* was identified in 8% to 30% of BRAF inhibitor-resistant melanoma patients (290, 291), and may be circumvented by increasing the dosage of BRAF inhibitor or using combination BRAF and MEK inhibitors (65).

BRAF splice variants are found in 32% of melanoma cases, several of which are associated with resistance to BRAF inhibitors (291-293). These aberrant *BRAF* variants lack the RAS-binding domain and mediate BRAF inhibitor resistance through dimerisation (289, 292, 294). BRAF inhibitor stimulates MAPK hyperactivation in *BRAF* WT melanomas via BRAF-CRAF, BRAF-ARAF, and CRAF-CRAF dimer complex formation (294, 295).

MAPKs overexpression

MAPK reactivation can also occur due to elevated expression of other RAF isoforms, such as CRAF and ARAF. Increased expression of CRAF and ARAF are associated with resistance to BRAF inhibitor in melanoma cell lines (296, 297), and co-targeting MEK and IGF-1R/PI3K signalling can overcome resistance (297). COT (Cancer Osaka Thyroid), encoded by *MAP3K8*, is overexpressed in *BRAF*^{V600E}-mutant cell lines resistant to the BRAF inhibitor vemurafenib (298). Increased levels of COT activate MAPK signalling via phosphorylation of MEK and ERK in an RAF-independent manner (298). Clinically,

MAP3K8 mRNA overexpression has been confirmed in BRAF inhibitor-resistant melanoma cases (292, 294, 298).

Activating mutations

Reactivation of MAPK signalling can occur as a consequence of activating gene mutations. Activating mutations in *MEK1* and *MEK2* have been shown to contribute to resistance to BRAF inhibitor or combination of BRAF and MEK inhibitors in melanoma (290, 292, 299). For example, *MEK2*^{C125S}-mutant melanoma has sustained ERK activation and melanoma proliferation even in the presence of BRAF and MEK inhibitors (299). *NRAS* mutations also promote MAPK reactivation and resistance to BRAF inhibitor (290, 300, 301).

1.7.2 Activation of alternative signalling pathways

PI3K reactivation has been detected in 20% of melanoma patients resistant to BRAF and MEK inhibitors (290, 294). Overexpression of RTKs, such as PDGFRß, IGF-1R or EGFR induces RAS activity and lead to reactivation of the PI3K/AKT pathway in melanoma patients treated with BRAF and MEK inhibitors (79, 300, 302, 303). PI3K/AKT pathway reactivation can also be caused by loss of PTEN and mutations in *PI3K* or *AKT* genes.

1.8 Scope of this thesis

Despite the success of targeted kinase inhibitors in improving OS of patients with *BRAF*- or *NRAS*-mutant melanomas, treatment options for patients with advanced-stage unresectable *BRAF*/*RAS* WT melanoma remain limited, even though this melanoma subset accounts for appropriately 25% of all melanoma cases. Early results from the CheckMate-066 clinical trial demonstrated improved OS rate of 73% with the PD-1 inhibitor nivolumab compared to 42% with chemotherapy in patients with *BRAF* WT metastatic melanoma. Moreover, patients treated with nivolumab showed objective response rate of 40% compared to 13.9% when treated with chemotherapy (250). The CheckMate-067 and CheckMate-069 studies further demonstrated that nivolumab in combination with the CTLA-4 inhibitor ipilimumab improved objective response rate and anti-tumour efficacy compared to ipilimumab alone in *BRAF* WT melanoma patients (268, 275, 304). Based on these findings, combination nivolumab and ipilimumab has now been approved for treatment of metastatic *BRAF* WT melanomas (277).

Although immune checkpoint inhibitors have shown promising results in *BRAF/RAS* WT melanoma, 40%-60% of patients do not respond to treatment, and a proportion develop acquired resistance after initial response. Therefore, there is an urgent need to identify more effective treatment strategies for patients with *BRAF*/*RAS* WT melanoma.

In this thesis, the hypothesis and aims for each chapter are as follows:

Chapter 2:

Hypothesis: *BRAF*/*RAS* WT melanomas remain dependent on MAPK signalling for survival and/or proliferation, and inhibition of this pathway may require multiple kinase inhibitors in the *NF1*-mutant subtype. Aims: To investigate the dependency of MAPK

signalling in *BRAF*/*RAS* WT melanomas, and to explore the efficacy of targeted therapies in this subtype.

Chapter 3:

Hypothesis: MEK inhibitor resistance in *BRAF*/*RAS* WT melanoma is associated with *TP53* mutation and p53 loss of function. Aims: To investigate the precise contribution of p53 to *BRAF*/*RAS* WT melanoma signalling and MAPK dependency, and to explore the therapeutic implications of p53 reactivation in melanoma.

Chapter 4:

Hypothesis: Activation of alternative survival signalling pathways drive MEK inhibitor resistance in *BRAF*/*RAS* WT melanoma, and combination therapies that inhibit these alternate pathways will improve anti-tumour activity in patients with *BRAF*/*RAS* WT melanoma. Aims: To investigate alternative survival signalling pathways in *BRAF*/*RAS* WT melanoma, and to explore the anti-tumour efficacy of combination therapies of multiple kinase inhibitors in *BRAF*/*RAS* WT melanoma.

Our results characterised the precise contribution of MAPK signalling to the proliferation and survival of *BRAF/RAS* WT melanomas, by assessing the impact of the MEK inhibitor trametinib in a panel of *BRAF*-mutant and *BRAF/RAS* WT melanoma cell lines (Chapter 2). We report that *NF1* and *TP53* are frequently mutated in *BRAF*/*RAS* WT melanoma, and that loss-of-function *NF1* (Chapter 2) and *TP53* mutations (Chapter 3) are significantly associated with resistance to trametinib in *BRAF*/*NRAS* WT melanomas. However, when we assessed the impact of NF1 and p53 using shRNA knockdown, we found that suppression of NF1 and p53 expression had minimal effects on trametinib resistance (Chapters 2 and 3).

BRAF/*RAS* WT melanomas have a higher mutation burden than *BRAF*- and *NRAS*-mutant melanomas (305), and the high mutational load may contribute to activation of multiple oncogenic signalling pathways. Thus, we sought to identify alternative survival signalling pathways in *BRAF/RAS* WT melanomas (Chapter 4), and more importantly, evaluated strategies of co-targeting multiple signalling pathways. Collectively our data suggest that melanoma with high mutation burden are less likely to respond to molecular therapies, because of the complex patterns of pathway activity in these cancer cells. Importantly, *NF1* mutations appear to be useful surrogates for predicting mutation burden and may be helpful in selecting the patients most likely to benefit from first-line immunotherapies.

Chapter 2

Mitogen-activated protein kinase dependency in BRAF/RAS wild type melanoma: a rationale for combination inhibitors

---

2.1 Introduction

Cutaneous melanomas can be classified into four distinct genetic subtypes based on the mutation status of driver oncogenes *BRAF*, *RAS* (*NRAS*, *KRAS* and *HRAS*) and *NF1*. The *BRAF*-mutant, *RAS*-mutant, *NF1*-mutant and triple wild type (*BRAF*/*RAS*/*NF1* WT) subtypes account for 51%, 30%, 13% and 6% of cutaneous melanomas, respectively, and these genotypes predict signalling dependency and inform clinical management (45, 59). For instance, $BRAF^{V600}$-mutant melanomas rely on MAPK activity for survival and inhibition of this pathway with combination BRAF and MEK inhibitors provides rapid disease control in almost 70% of patients and improves patient survival (184, 185, 299, 306). In contrast, although triple WT and *RAS*-mutant melanoma display elevated MAPK signalling (59, 80, 307), treatment with MEK inhibitor alone or in combination with other molecular inhibitors (e.g. AKT inhibitors) produced only limited clinical benefit with PFS of less than 4 months (199, 308, 309).

For *BRAF* WT melanoma patients, immune checkpoint inhibitors remain the only effective therapeutic option with three-year survival rates of 50% in response to PD-1 inhibition (188, 250, 275). Recently, the combination of immunotherapy and MEK inhibitors has shown promising results in early phase trials of *BRAF* WT melanoma (310, 311), and more data are being collected in an ongoing phase 3 clinical trial (NCT03273153). The rationale supporting this treatment combination is based on the immune stimulatory effects of MEK inhibitors, which induce melanocyte-lineage antigen and MHC protein expression and promote the infiltration of CD8+ and CD4+ T-cells into the tumour (279, 312, 313). Immune cell infiltration is presumably stimulated by the release of tumour antigens upon drug-induced tumour cell death, and in *BRAF*-mutant melanoma, intra-tumoural T-cell infiltration reflects treatment response (280).

In this study, we hypothesized that *BRAF*/*RAS* WT melanomas remain dependent on MAPK signalling for survival and/or proliferation, but effective inhibition of this pathway may require multiple kinase inhibitors depending on the *NF1* gene. In order to examine MAPK dependency in *BRAF*/*RAS* WT melanomas, we analysed the impact of the MEK inhibitor trametinib in a large panel of 10 $BRAF^{V600}$-mutant and 13 *BRAF*/*RAS* WT melanoma cell lines.

Trametinib is an allosteric, non-ATP-competitive inhibitor of MEK1/2 that directly combines to MEK1/2 and inhibits RAF-dependent phosphorylation of MEK1/2 (314). As described in detail in Chapter 1 (Section 1.6.1), trametinib is currently FDA-approved as monotherapy or used in combination with BRAF inhibitors for patients with advanced *BRAF*-mutant melanoma (185, 196, 197). Furthermore, MEK1/2 inhibitors have shown clinical efficacy in *NRAS*-mutant melanomas (199-201) and have demonstrated anti-tumour activities in preclinical models of *BRAF*/*RAS* WT melanoma (76, 204). Dermatitis acneiform (82%), diarrhoea (45%) and ocular events (9%), decreased ejection fraction or ventricular dysfunction (7%) and grade 3 or 4 rash (8%), are the most common side effects in patients receiving trametinib(196, 198).

The efficiency of combination inhibitors (trametinib, ERK inhibitor (SCH772984) and/or RAF inhibitor (AZ628)) in inhibiting the MAPK pathway was also examined in a subset of *NF1*-mutant melanoma cell lines. SCH772984, an ATP-competitive, highly selective inhibitor for MAPK downstream effector ERK1/2 (240), can affect the intrinsic kinase activity of ERK1/2 through binding to its unphosphorylated form and inhibit the MEK-dependent phosphorylation of ERK1/2 (315). In pre-clinical studies, SCH772987 has shown promising anti-tumour activity in *BRAF*-mutant melanoma cell lines and medicated potent ERK inhibition *BRAF* WT melanoma cell lines (241). Additionally, as described previously in Chapter 1 (Section 1.6.1), SCH772984 was effective in *BRAF*- or *NRAS*-mutant melanoma resistant to BRAF or MEK inhibitor (239, 240). Also, SCH772984

induced potent cell cycle arrest and cell death in a proportion of *BRAF*/*RAS* WT melanoma cell lines with potent ERK inhibition (241).

The AZ628 is a type II, ATP-competitive pan-RAF kinase inhibitor, which binds to the inactive conformation of the protein outside the ATP pocket to stabilize RAF activity (316). Recent research confirmed that pan-RAF inhibitors effectively inhibit proliferation of *BRAF*- or *NRAS*-mutant melanomas resistant to BRAF/MEK inhibitors, by not inducing the paradoxical activation of MAPK signalling (317). Furthermore, AZ628 in combination with MEK inhibitor, has shown significant tumour growth inhibition in non-*BRAF*-mutant melanomas, both *in vitro* and *in vivo* (318). Based on these data, we aimed to provide a rationale for combining molecular inhibitors that effectively suppress MAPK signalling, potentially with immune therapies for *BRAF*/*RAS* WT melanoma.

2.2 Methods

2.2.1 Cell culture and reagents

The majority of melanoma cell lines were provided by Prof Nicholas Hayward and Prof Peter Parsons at QIMR Berghofer Medical Research Institute, Prof Bruce Ksander at Harvard Medical School, Prof Peter Hersey at the Centenary Institute Sydney and Prof Xu Dong Zhang at the University of Newcastle, Australia. Two melanoma cell models, SCC14-0257 and SMU15-0217, were generated as described previously (319). Cell authentication was confirmed using the Stem Elite ID system from Promega. This study was carried out in accordance with the recommendations of the Human Research Ethics Committee protocols from Royal Prince Alfred Hospital (Protocol X15-0454 and HREC/11/RPAH/444).

Cell lines were cultured in Dulbecco's Modified Eagle Medium (DMEM) or Roswell Park Memorial Institute-1640 (RPMI) media supplemented with 10% heat-inactivated fetal bovine serum (FBS; Sigma-Aldrich, MO, USA), 4 mM glutamine (Gibco, Thermo Fisher Scientific, MA, USA) and 20 mM HEPES (Gibco) and were maintained at 37°C in 5% CO_2. All inhibitors were purchased from Selleck Chemicals (Houston, TX, USA) and prepared in dimethyl sulfoxide (DMSO). The MEK1/2 inhibitor trametinib (GSK1120212) and BRAF inhibitor dabrafenib (GSK2118436) were prepared as 1 mM stocks. The pan-RAF inhibitor AZ628 and ERK1/2 inhibitor SCH772984 were prepared as 10 mM stocks.

2.2.2 DNA extraction and Whole Exome Sequencing

DNA was extracted from early-passage melanoma cells using the G-spin™ Total DNA Extraction Kit as per manufacturer's protocol (Intron Biotechnology, Seongnam, South Korea) and DNA quantified using the SmartSpec Plus Spectrophotometer (Bio-Rad, CA,

USA). Integrity of genomic DNA was further confirmed by gel electrophoresis. Exome sequencing of melanoma cell lines was performed as previously described (320). Exonic DNA was enriched using the Illumina TrueSeq technology, targeting the 62 Mb encompassing protein-coding regions, and sequenced on an Illumina HiSeq2000. Read pairs were aligned to the reference human genome (hg19) using Burrows-Wheeler Aligner (BWA). Duplicates were removed with Picard and applied GATK indel realignment and base quality recalibration. Single-nucleotide variants and small insertion/deletions (INDELS) were detected by SAMTools. To generate a list of high-quality variants, low-coverage variants (single-nucleotide polymorphism quality ≤30, read depth ≤10) and variants in the top 5% of exonically variable regions, annotated as common polymorphisms, or in the 1000 Genomes Project, were removed using Ingenuity Variant Analysis (http://www.ingenuity.com; Qiagen, Venlo, Netherlands).

2.2.3 MTT Cell viability assay

Melanoma cells were seeded into 96-well plates (1-2×10^3 cells per well) in DMEM or RPMI-1640 media and allowed to adhere for 24 h before treatment. Media was removed and varying doses of the MEK inhibitor trametinib (0, 0.5, 1, 2, 5, 10, 50, 100, 500, 5000 nM) were added. Cells were also treated with 0.1% DMSO as control. Cells were incubated for 72 h before measuring cell viability using the Luminescent CellTiter-Glo® 2.0 Assay reagent (Promega, WI, USA). Luminescence readings were acquired on a PHERASTAR FS microplate reader (BMG LABTECH, Ortenberg, Germany). Cell viability was calculated as a percentage normalised to controls after background subtraction. A minimum of three independent viability assays were performed for each cell line in triplicate. The IC_{50} (half maximal inhibitory of drug) value was generated from dose-response curves fitted using a comparison of three-parameter regression fit or four-parameter regression fit in GraphPad PRISM 7 software (GraphPad, CA, USA).

2.2.4 Cell cycle analysis

Adherent and floating melanoma cells were collected for cell cycle and apoptosis analysis as previously described (321). Melanoma cells were treated with 10 nM trametinib or 100 nM dabrafenib or 0.1% DMSO, incubated for 72 h before performing cell cycle analysis by flow cytometry using propidium iodide (PI). DNA content from 10,000 cells was analysed using the ModFIT software (Verity Software House, ME, USA) and numbers of apoptotic cells (sub G1 phase) were determined using the FACSDiVa software (Becton Dickinson, NJ, USA). The percentage of S phase inhibition was calculated as (percentage of DMSO-treated cells in S phase – percentage of trametinib-treated cells in S phase)/ (percentage of DMSO-treated cells in S phase) x 100. Change in percentage of sub G1 is relative to the DMSO-treated cells.

2.2.5 Western Blotting

Melanoma cells were treated with 0.1% DMSO, or 10 nM trametinib, 2 µM AZ628, 500 nM SCH772984, alone or in combination, for 24 h before extracting total cellular proteins by incubating cells in RIPA lysis buffer (1x PBS, 1% (v/v) NP40, 0.5% (w/v) sodium deoxycholate, 0.1% (w/v) SDS) containing protease inhibitors and phosphate phosphatase inhibitors (Roche, Basel, Switzerland) for 30 min on ice. Cell lysates were centrifuged at 4°C for 5 min at 13,000 rpm before collecting supernatant. Protein concentration was measured using the DC protein assay kit (Bio-Rad). Total proteins (20-40 µg) were resolved on 10% SDS-polyacrylamide gels and transferred to Immobilon-FL PVDF membranes (Millipore, MA, USA).

Membranes were incubated with REVERT total protein stain (LI-COR, NE, USA) for 15 min after transfer, rinsed 2x with wash solution (6.7% (v/v) glacial acetic acid, 30% (v/v) methanol in water), and imaged immediately in the 700 nm channel using the Odyssey

imaging system. The REVERT fluorescent signal (700nm) in each lane and each target protein (700/800nm) was quantified using ImageStudioTM Software (Li-COR). In particular, the fluorescence signal for REVERT total protein was captured using the Draw Rectangle tool by drawing a thin rectangle in the centre of each lane without background subtraction to avoid background shapes overlapping other lanes. The fluorescence signal for each target protein was detected by adding the rectangles individually for each band and using the median normalised background subtraction method available in the software. The REVERT total values were used as a loading control and for data normalisation (protein of interest/REVERT total values). Membranes were then washed with reversal solution (0.1% (w/v) sodium hydroxide, 30% (v/v) methanol, in water) for 7 min to remove the stain, rinsed with water and blocked using LI-COR Odyssey blocking buffer (LI-COR) for 1h at room temperature.

Western blots were probed with the following primary antibodies targeting: total p90RSK (1:1000, 6B9D6F8, Abcam, Cambridge, UK), phosphorylated p90RSK (Ser363, 1:3000, Santa Cruz, TX, USA), total ERK (1:2000, 137F5, Cell Signalling, MA, USA), phosphorylated ERK (Tyr204, 1:500, E4, Santa Cruz), DUSP6 (1:1000, EPR129Y, Abcam), phosphorylated S6 ribosomal protein (Ser235/236, 1:2000, 2F9, Cell Signalling), NF1 (1:1000, Bethyl Laboratories, TX, USA), total CRAF (1:1000, Cell Signalling), and phosphorylated CRAF (Ser 338, 1:1000, Merck, NJ, USA) overnight at 4°C. Membranes were washed with Tris-buffered saline with 0.05% (v/v) Tween 20, then incubated with secondary antibodies IRDye® 800CW Donkey anti-Mouse, IRDye® 800CW Donkey anti-Rabbit, IRDye® 680LT Donkey anti-Mouse or IRDye® 680LT Donkey anti-Rabbit (LI-COR). Membranes were detected on the Odyssey imaging system (LI-COR). Each western blot was performed using at least two biological replicates.

Activated GTP-bound RAS was examined using an active RAS detection kit (#8821, Cell Signalling), which employs a protein pull-down assay using GST-CRAF-RBD fusion that

binds the activated form of GTP-bound RAS and the level of RAS activity was examined as described in the manufacturer's instructions.

To quantify MAPK activity, the MAPK activity score for each cell line was derived from the normalised protein expression data for p-ERK, p-p90RSK, DUSP6 and p-S6. p-ERK and p-p90RSK were normalised to their respective total protein levels, and DUSP6 and p-S6 were normalised to the REVERT (LI-COR) total protein stain. Normalised protein data were log2 transformed from which z-scores were calculated. The MAPK activity score was computed as the mean of z-score of the normalised protein data.

2.2.6 Lentivirus transduction

Lentivirus particles were produced in HEK293T cells using the shRNA expression vector (Sigma-Aldrich, MO, USA) encased in viral capsid encoded by three packaging plasmids as described previously (322). Viral supernatant was harvested 72 h post-transfection. Melanoma cells were infected using a multiplicity of infection of 5 to provide an efficiency of infection above 90%. All transduced cells were selected by puromycin for at least two weeks prior to experiments. Western blotting was utilized to assess efficacy of knockdown. The shRNA constructs used in this study were each cloned into the *pSIH-HI-PURO* vector (System Biosciences, CA, USA) and included a control shRNA that did not show complete homology to any known human transcript and had the following sequence: 5'-TTAGAGGCGAGCAAGACTA-3'. The *NF1* shRNA1 (TRCN0000039717, NM_000267.18627s1c1) and *NF1* shRNA2 (TRCN0000238778, NM_000267.2954s21c1) were purchased from Sigma-Aldrich.

2.2.7 Statistical analysis

Data presented were mean of at least three independent experiments, unless otherwise specified. Statistical analysis was performed in GraphPad Prism (Version 7). Multiple

comparisons were assessed using the Kruskal-Wallis test for non-parametric data with Dunn's multiple comparison test using family-wise significance and confidence level of 0.05. Comparison of drug activity was performed using one-way ANOVA with Holm-Sidak's multiple comparison test, with a single pooled variance. P-values of less than 0.05 were considered statistically significant.

2.3 Results

2.3.1 *BRAF/RAS* WT melanoma cells show variable responses to MEK inhibition

The dependence of melanoma cells on MAPK signalling for proliferation and survival was assessed using MTT metabolic assays and flow cytometry-based cell cycle analysis following treatment with MEK inhibitor trametinib. A panel of 23 human melanoma cell lines was examined, including 10 *BRAF*$^{V600E/K}$-mutant melanoma cells, seven *NF1*-mutant and six triple WT cell lines (Table 2.1).

Table 2.1: Gene mutation and trametinib response status of melanoma cell lines used in this study

	Cell line	Response[1]	*BRAF* mutations	*NF1* mutations	RASopathy mutation
***BRAF*^{V600}-mutant**	SKMel28	HS	V600E	-	-
	MM200	HS	V600E	-	-
	C088M1	HS	V600K	-	-
	HT144	HS	V600E	-	-
	SCC14-0257	HS	V600K	-	-
	C060M1	HS	V600E	-	-
	A375	IS	V600E	-	-
	A0M4	IS	V600E	-	-
	C016M1	IS	V600E	-	-
	NM39	IS	V600E	-	-
***NF1*-mutant**	C084M	IS	-	R2517*; R249*	SOS1^{S297L}, PTPN11^{F71L}, CBL^{P417S}, SPRED^{R395W}
	C025M1	IS	-	P2094L; P211L	-
	C086M	IS	-	Q2595*; Q261*; Q282*	SOS1^{R310C,H308Y}, SPRED2^{S294L,F99L}
	MeWo	R	-	Q1336*	RASA2^{P475L}
	SMU15-0217	R	-	R1362*; Q1574*; Q1595*	RASA2^{R35*,Q686*}, CBL^{P433L}, RASA1^{T87A}
	D24M	R	-	R1958C; R1937C	CBL^{P582S}, RASA1^{P140S}
	D22M1	R	-	R440*	PTPN11^{L560F}, RAF1^{E478K}, MAP2K1^{P124L}, RASA1^{E632fs*}
Triple WT	C037M1	HS	-	-	-
	D10M1	HS	-	-	RASSF2^{M141T}
	A04-GEH	HS	-	-	-
	C022M1	IS	-	-	RASGEF1A^{G44E}
	D35	IS	-	-	SHOC2^{N527S}
	SCC08-0008	R	-	-	SHOC2^{I119V}

[1]Response to trametinib: HS, highly sensitive; IS, intermediate sensitive; R, resistant. Mutation status as shown; -, wild type sequence

Melanoma cells were classified into three distinct subgroups based on their responses to MEK inhibition. Highly sensitive melanoma cells responded to trametinib by undergoing potent S phase inhibition that was associated with an increase in the sub G1 phase and displayed IC_{50} values of less than 8 nM, indicating MAPK signalling dependency for proliferation and survival (Figure 2.1 and 2.2). Melanoma cells showing intermediate sensitivity to MEK inhibition had a relatively low, albeit broader range of IC_{50} values (1.4-14 nM), underwent significant cell cycle arrest, but showed limited evidence of cell death in response to trametinib. These cells required MAPK signalling for proliferation, but not survival (Figure 2.1 and 2.2). Cells displaying high or intermediate sensitivity to trametinib displayed indistinguishable levels of S phase inhibition and IC_{50} values, whereas they differed significantly in the degree of trametinib-induced cell death (Figure 2.2A). Highly resistant melanoma cells showed minimal changes in cell cycle distribution and displayed trametinib IC_{50} concentrations above 17 nM, and these were significantly higher than the IC_{50} values observed in the sensitive melanoma cells (Figure 2.1 and 2.2).

In our panel of 23 melanoma cell lines, the nine highly sensitive cell lines included 6/10 (60%) *BRAF*$^{V600E/K}$-mutant and 3/6 (50%) triple WT cell lines. Another nine melanoma cell lines displayed intermediate sensitivity to MEK inhibition and included 4/10 (40%) *BRAF*$^{V600E/K}$-mutant, 3/7 (43%) *NF1*-mutant and 2/6 (33%) triple WT cell lines (Figure 2.2). The remaining five melanoma cell lines, including 4/7 (57%) *NF1*-mutant, and 1/6 (17%) triple WT, were classified as highly resistant to MEK inhibition (Figure 2.2). Overall, our data showed that 5/6 triple WT melanoma cell lines displayed some sensitivity to MEK inhibition and indicated that loss-of-function *NF1* mutation was strongly associated with MEK inhibitor resistance (Table 2.2). In particular, *NF1*-mutant cells displayed significantly higher IC_{50} values and reduced cell cycle inhibition compared to triple WT and *BRAF*^{V600E}-mutant cells (Figure 2.2).

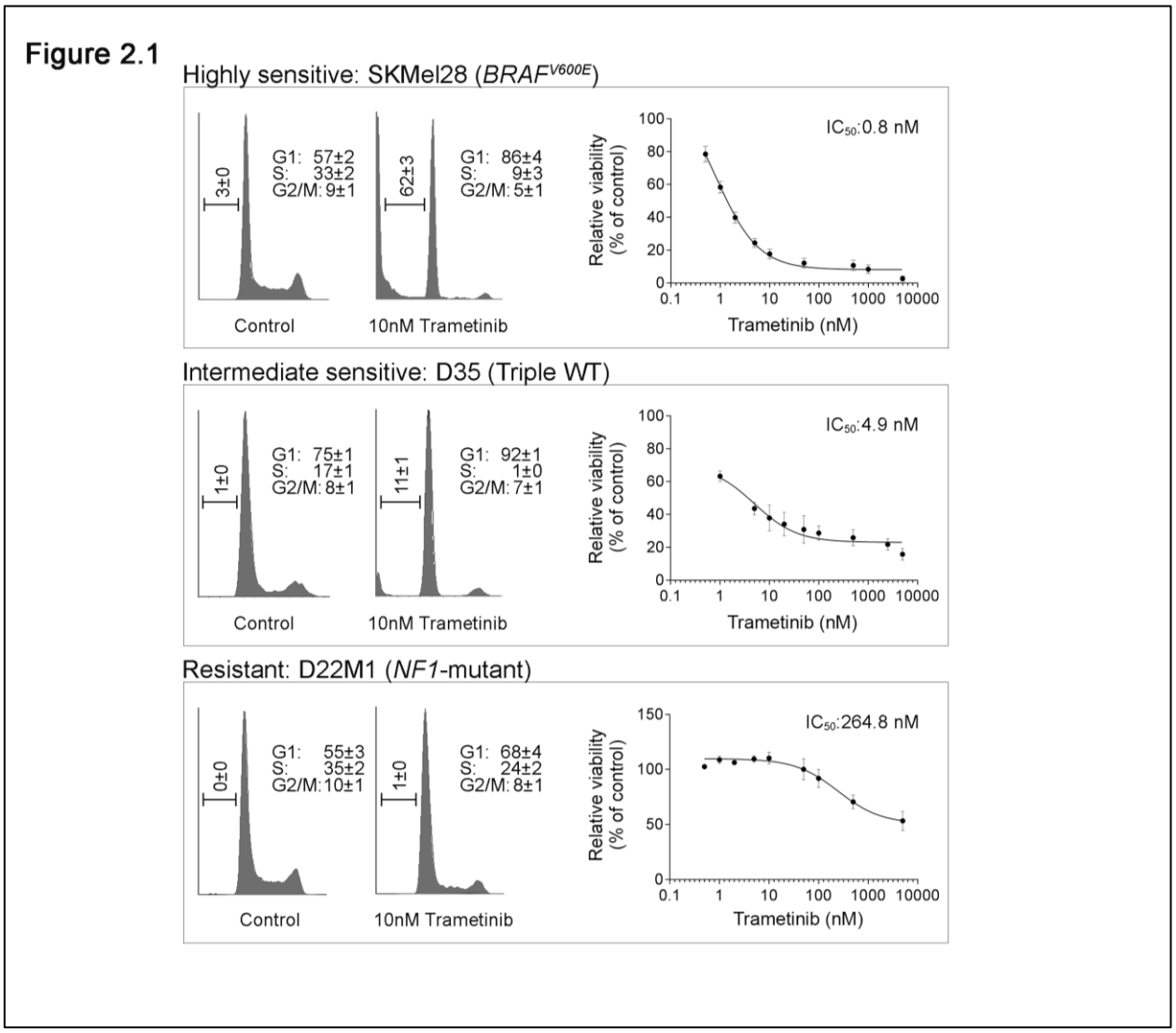

Figure 2.1: Diverse MEK dependency in melanoma cell line

Melanoma cell lines were treated with 10 nM trametinib for 72 h to assess cell cycle and apoptotic responses, and at varying doses to determine relative cell viability (% of control). Graphs show three distinct trametinib response types, represented by three melanoma cell lines. Cell cycle profile of control (DMSO-treated) and trametinib-treated cells are shown for the three cell lines. Dose-response curves showed the relative viability (% of control) of melanoma cell lines treated with varying doses of trametinib. Data represent mean of at least three independent experiments, and error bars represent standard deviation. SKMel28 is highly sensitive, with potent S phase inhibition and cell death (sub G1, relative to control), and displayed a low trametinib IC_{50} value. D35 showed intermediate sensitivity, with potent S phase inhibition but no cell death, and displayed an intermediate IC_{50} value. D22M1 is highly resistant, with minimal S phase inhibition and cell death, and displayed very high IC_{50} value.

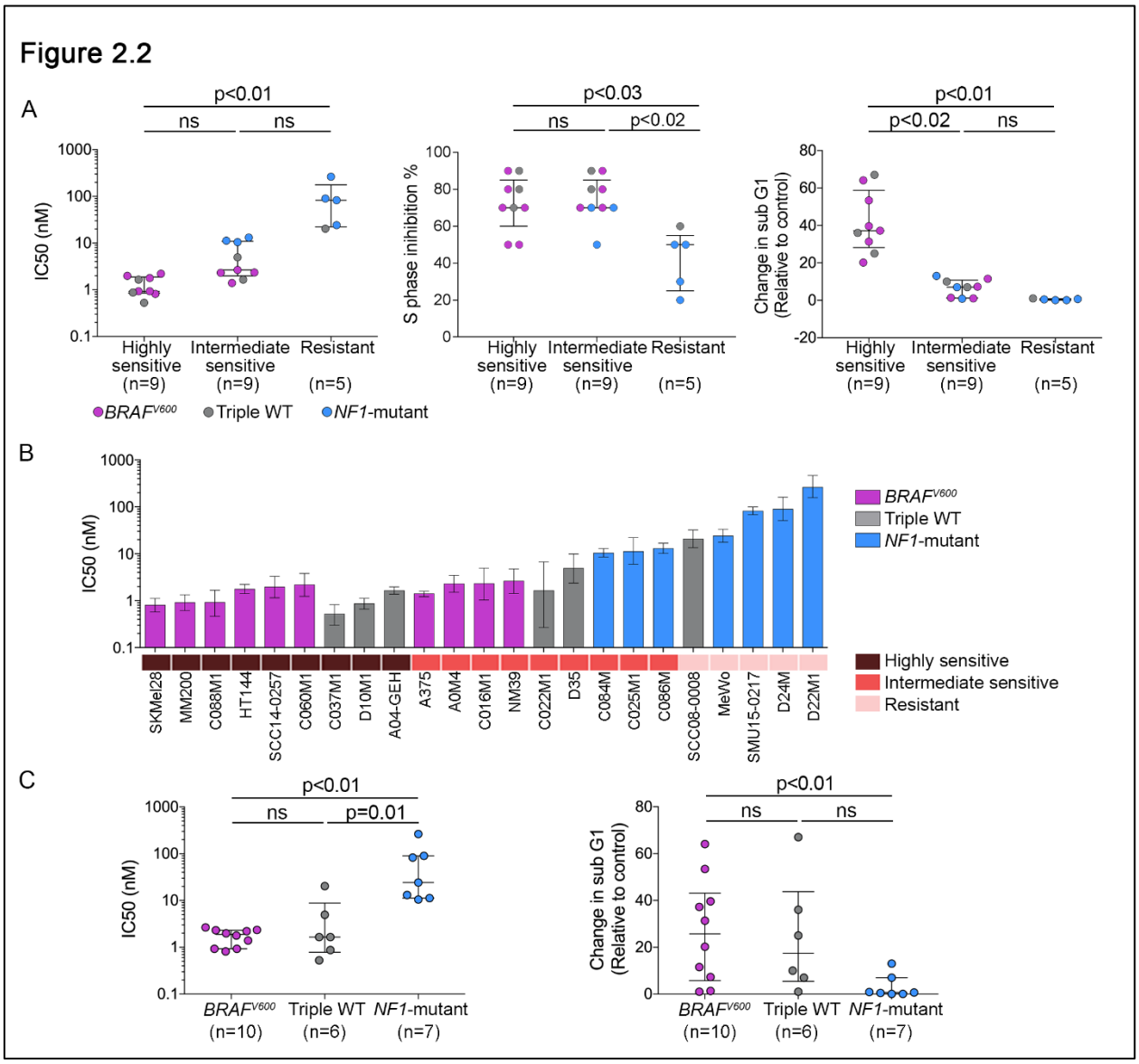

Figure 2.2: Melanoma responses to trametinib

Melanoma cell lines were treated with trametinib for 72 h at varying doses to determine IC_{50} values and with 10 nM trametinib to assess cell cycle and apoptotic responses. (A) Graphs show the IC_{50} values (left), percentage of S phase inhibition (middle) and change in sub G1 (relative to control, right) according to trametinib response groups: highly sensitive (n=9), intermediate sensitive (n=9) and resistant (n=5) melanoma cell lines. Median and interquartile ranges are shown on the scatter plots. (B) Melanoma cell line IC_{50} values arranged according to trametinib response groups. Bar graphs show mean IC_{50} values with 95% confidence intervals from at least three independent experiments. (C) Graphs show the IC_{50} values (left) and change in sub G1 (relative to control, right) according to melanoma genotypes: *BRAF*^{V600} (n=10), Triple WT (n=6) and *NF1*-mutant (n=7) melanoma cell lines. Statistical comparison between three groups was performed using Kruskal-Wallis with Dunn's multiple comparison test. Adjusted p-values are shown, ns is not significant. Median and interquartile ranges are shown on the scatter plots.

Table 2.2: Association between *NF1* status and trametinib response in melanoma cell lines

Trametinib response	*NF1* mutation		Fisher's exact test P-value
	WT	Mutant	
Highly/intermediate sensitive	15	3	p=0.0173
Resistant	1	4	

Statistical association was performed using Fisher's exact test.

2.3.2 MEK inhibitor-induced proliferative arrest reflects the degree of MAPK pathway inhibition

To examine whether MEK inhibitor responses directly reflected MAPK activity, we analysed the expression of several MAPK downstream effector proteins (p-ERK, p-p90RSK, DUSP6, p-S6) at baseline and after trametinib treatment (Figure 2.3). We combined the normalised protein expression values of these four MAPK effector proteins and defined a single score of MAPK activity (Section 2.2.5). Although the baseline MAPK activity score was indistinguishable in the three trametinib response groups (Figure 2.4), the degree of MAPK inhibition (i.e. MAPK score post trametinib/MAPK score pre trametinib) reflected the response to trametinib. In particular, the highly sensitive cells showed a substantial reduction in MAPK signalling post MEK inhibition compared to resistant cells (Figure 2.4). Of the nine melanoma cell lines displaying intermediate trametinib sensitivity, two distinct cell populations were evident based on the degree of MAPK inhibition: six cell lines showed MAPK inhibition similar to highly sensitive melanoma cells whereas three cell lines, all *NF1*-mutant, displayed a reduced degree of MAPK inhibition.

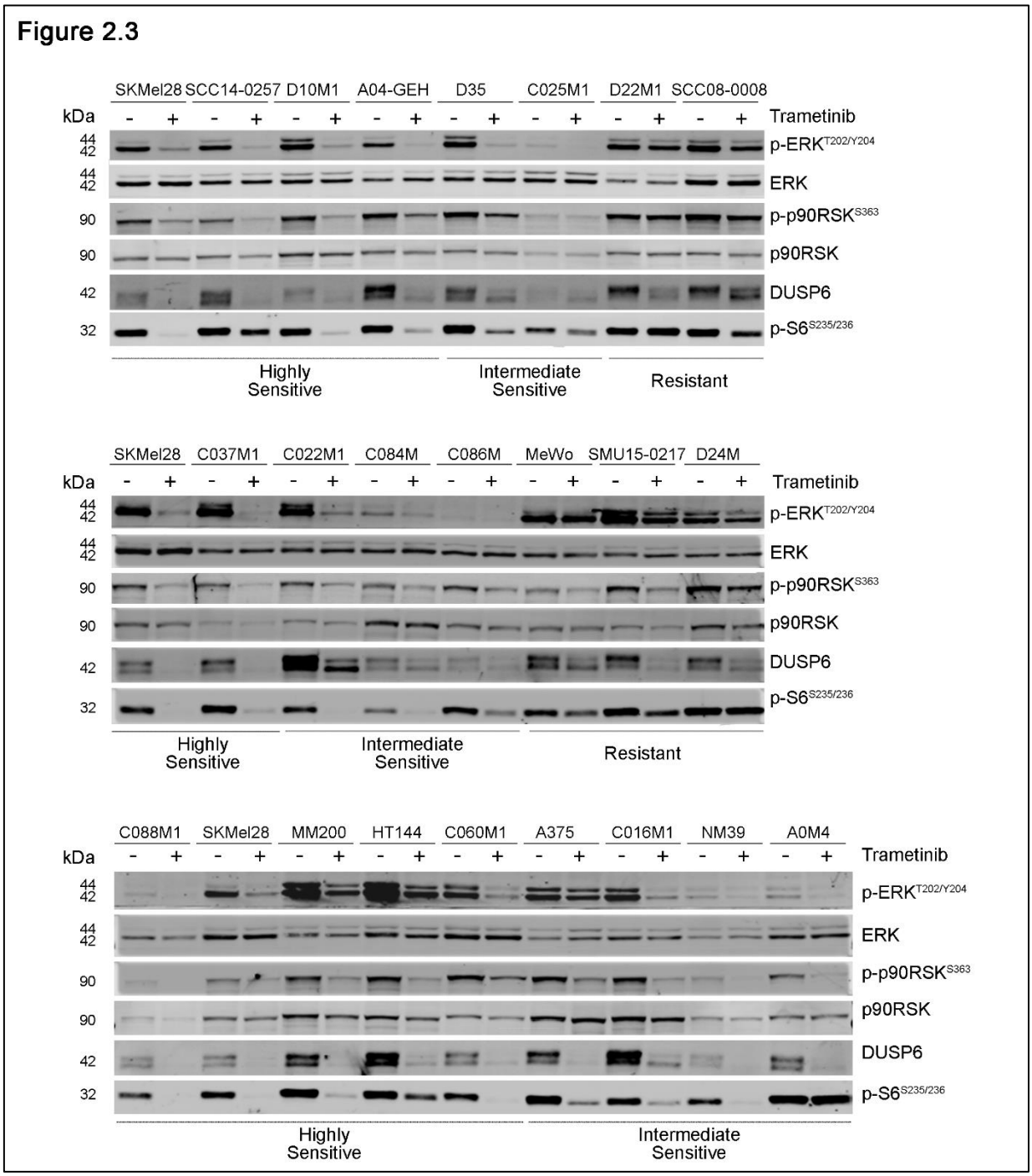

Figure 2.3: Western blots showing the degree of MAPK inhibition in response to MEK inhibitor

Western blot analysis of melanoma cell lysates for protein markers (p-ERK, ERK, p-p90RSK, p90RSK, DUSP6, and p-S6) of MAPK activity 24 h after treatment with DMSO (-) or 10 nM trametinib (+). REVERT total protein stain was performed as loading control (Figure S2.1). Three biological replicates were performed, and the results showed derived from one representative experiment.

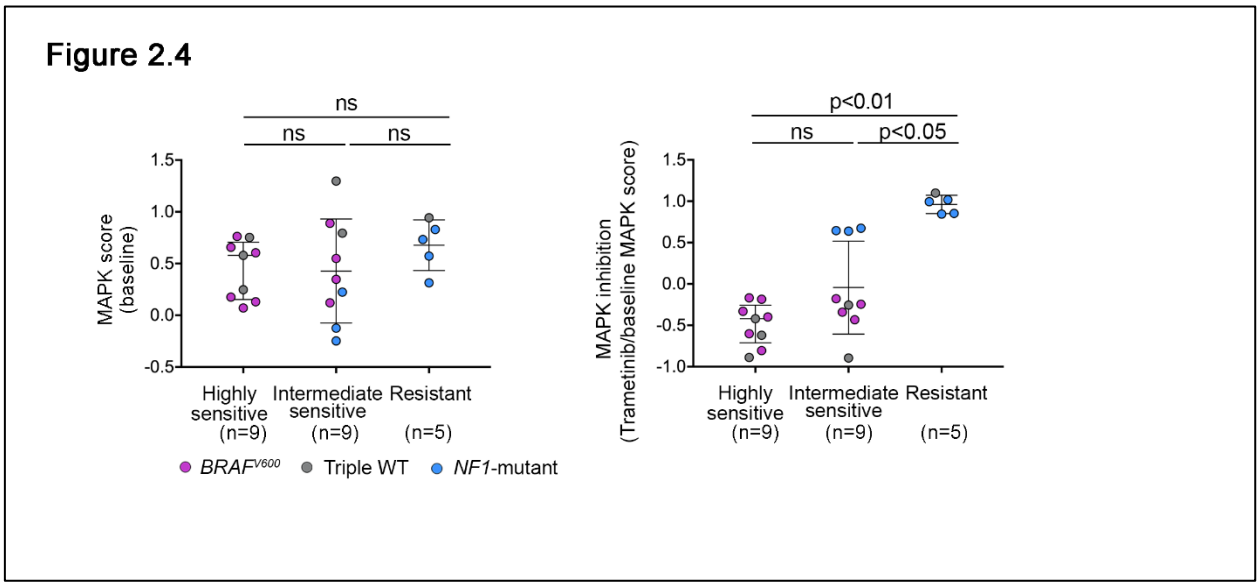

Figure 2.4: MEK inhibitor responses reflect the degree of MAPK inhibition

The baseline MAPK activity score (left panel) and the degree of MAPK inhibition (MAPK score post-trametinib/pre-trametinib, right panel) is shown across the panel of 23 melanoma cell lines according to trametinib response groups: highly sensitive (n=9), intermediate sensitive (n=9) and resistant (n=5) melanoma cell lines. The MAPK activity score for each cell line was calculated as detailed in Section 2.2.5. Data were derived from three independent experiments and median and interquartile ranges are shown on the scatter plots. Statistical comparison between three groups was performed using Kruskal-Wallis test, with Dunn's multiple comparison test. Adjusted p-values are shown, ns is not significant.

2.3.3 Loss of NF1 does not confer MEK inhibitor resistance in triple WT melanoma

Considering that 4 of 5 trametinib resistant melanoma cells had loss-of-function *NF1* mutations we explored the precise influence of NF1 in triple WT melanoma. As expected, *NF1* nonsense mutations were associated with loss of NF1 protein expression (Figure 2.5A), and this was associated with increased phosphorylation of CRAF at serine 338 (Figure 2.5B and 2.6) and elevated RAS activation, based on RAS-GTP pulldown assays (Figure 2.6).

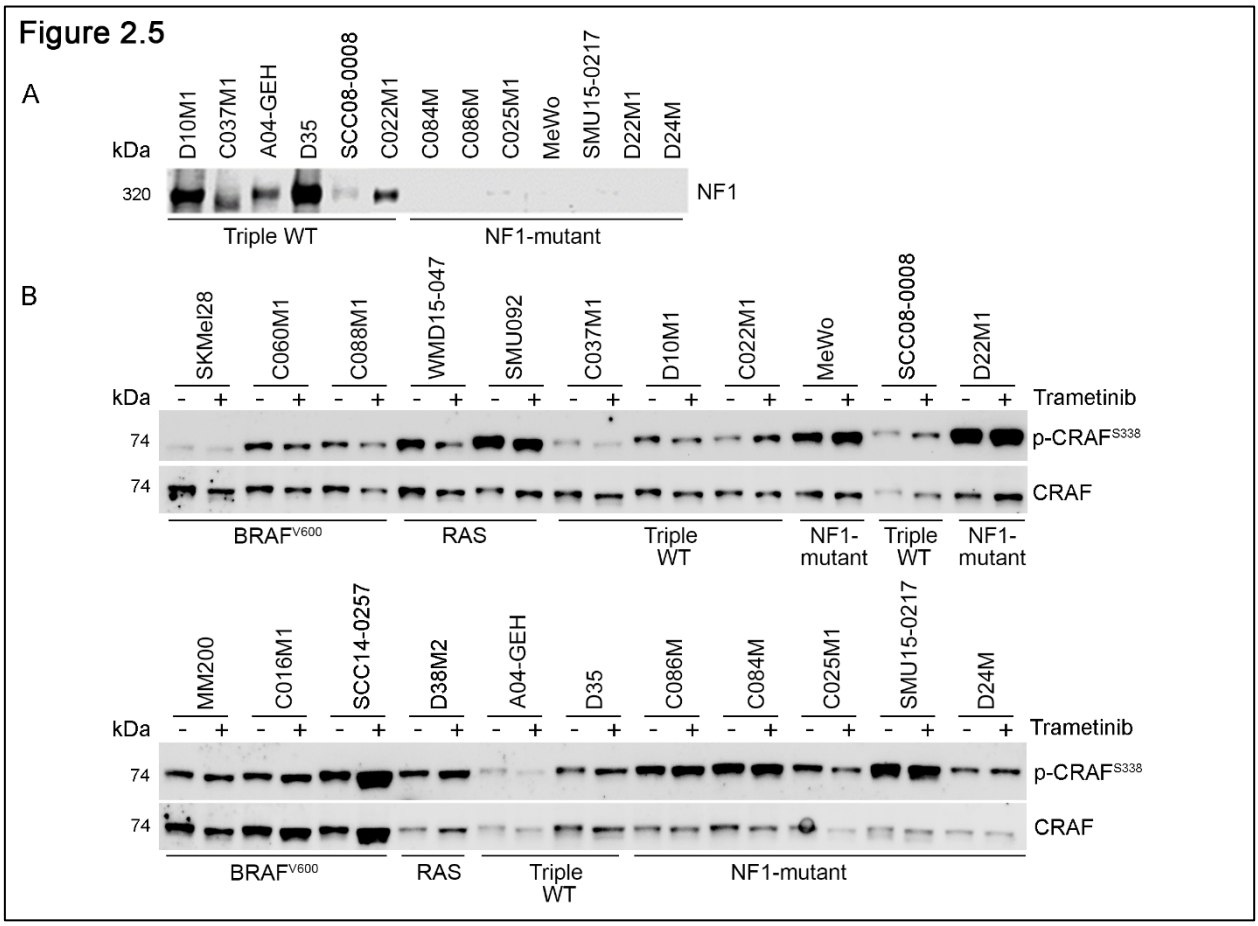

Figure 2.5: Expression of NF1 and phosphorylation of CRAF at serine 338 in melanoma cell lines with different genotypes

Western blots of cell lysates showing (A) NF1 protein expression in triple WT and *NF1*-mutant melanoma cell lines and (B) Phosphorylation of CRAF at serine 338 in melanoma cell lines with different genotypes: *BRAF*^{V600} (n=6), *RAS*-mutant (Rat sarcoma viral oncogene, n= 3), Triple WT (n=6) and *NF1*-mutant (n=7) melanoma cell lines. REVERT total protein stain was used as loading control (Figure S2.2).

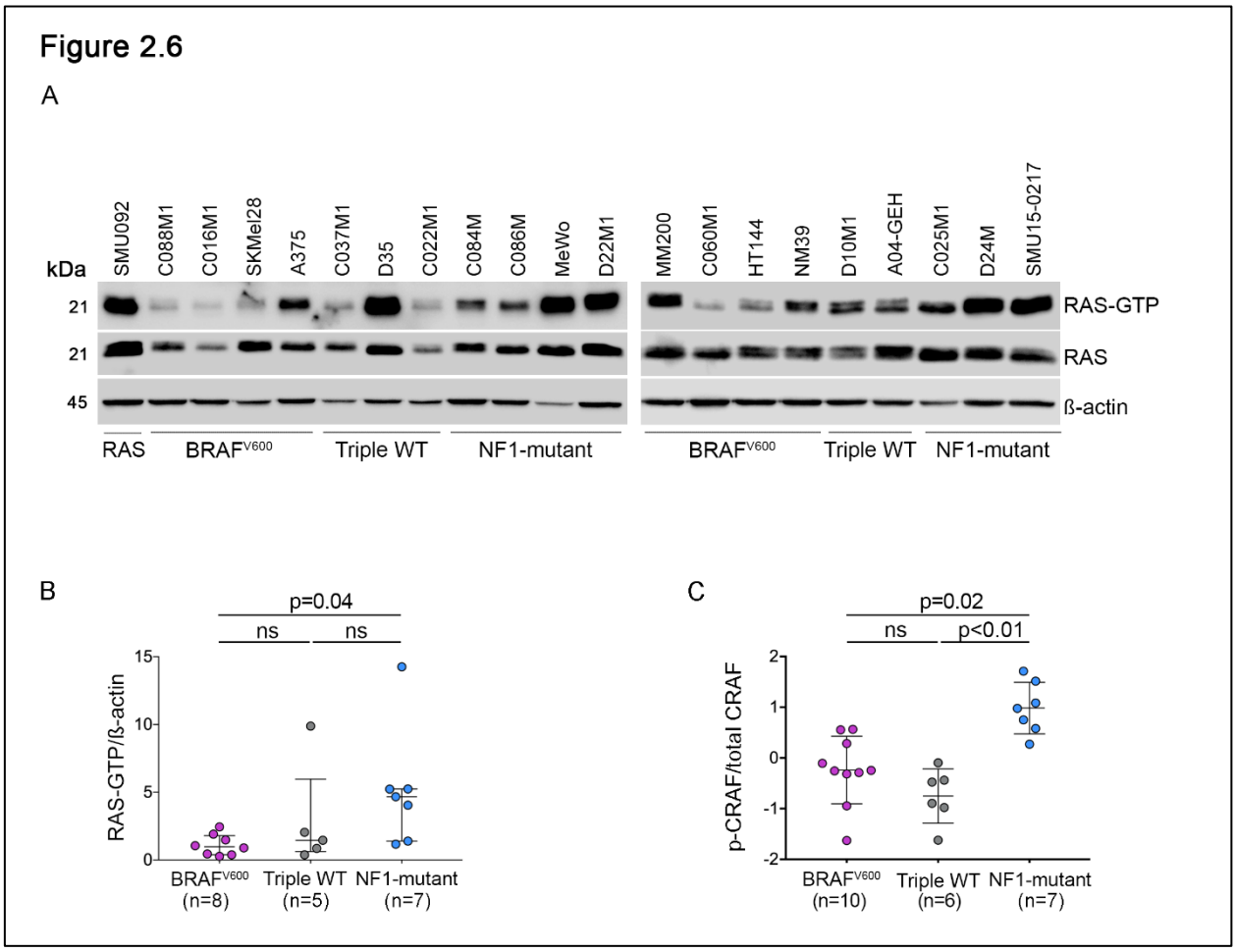

Figure 2.6: *NF1*-mutant melanomas have elevated Ras and CRAF activity

(A) The indicated melanoma cells were subjected to pull-down assays using GST-bound CRAF Ras-binding domain for active Ras (rat sarcoma viral oncogene). The Ras pull down (RAS-GTP), and total lysates were analysed by western blot analysis. ß-actin stain was used as loading control. (B) Ras activity (calculated as RAS-GTP normalised to ß-actin) is shown according to melanoma cell genotype: *BRAF*^{V600} (n=8), Triple WT (n=5) and *NF1*-mutant (n=7) melanoma cell lines. Statistical comparison between three groups was performed using Kruskal-Wallis, with Dunn's multiple comparison test. Adjusted p-values are shown. Median and interquartile ranges are shown on the scatter plots, ns is not significant. (C) Phosphorylated CRAF^{S338} normalised to total CRAF (converted to z-scores to enable analysis of two independent western experiments) is shown according to melanoma cell genotype. Statistical comparison between three groups was performed using Kruskal-Wallis, with Dunn's multiple comparison test. Adjusted p-values are shown. Median and interquartile ranges are shown on the scatter plots, ns is not significant.

The impact of NF1 on trametinib sensitivity was examined by suppressing NF1 expression in four trametinib sensitive melanoma cell lines, including one *BRAF*^{V600E}-mutant cell line (A375) and three triple WT cell lines (A04-GEH, C037M1, and D35). Melanoma cells were transduced with two NF1-specific silencing constructs or a negative control shRNA construct without homology to any human gene. Both NF1 shRNA molecules effectively downregulated NF1 protein accumulation in all cell lines (Figure 2.7A) and MAPK dependency was determined using MTT assays and cell cycle analysis 72 h after trametinib treatment.

As expected, suppression of NF1 diminished sensitivity of *BRAF*^{V600E}-mutant A375 to MEK inhibition (Figure 2.7). In contrast, all three NF1-shRNA-transduced triple WT cell lines showed no significant alterations in IC_{50} values or sub G1 accumulation compared to control transduced cells (Figure 2.7). These data are consistent with immunoblot analysis of MAPK signalling effectors; NF1-silenced A375 cells showed elevated baseline p-S6 and weaker suppression of p-ERK and p-S6 in response to trametinib compared to control transduced cells (Figure 2.8). In contrast, triple WT cells showed equivalent baseline p-S6 accumulation and responded to trametinib with potent suppression of S6 and ERK phosphorylation, regardless of *NF1* status (Figure 2.8). We also noted that MEK inhibition increased levels of p-CRAF^{S338} in the *BRAF*-mutant A375 cells, but not in triple WT cells, following NF1 silencing (Figure 2.8). Thus, loss of NF1 is sufficient to confer resistance to MEK inhibition in *BRAF*^{V600}-mutant but not triple WT melanoma cells.

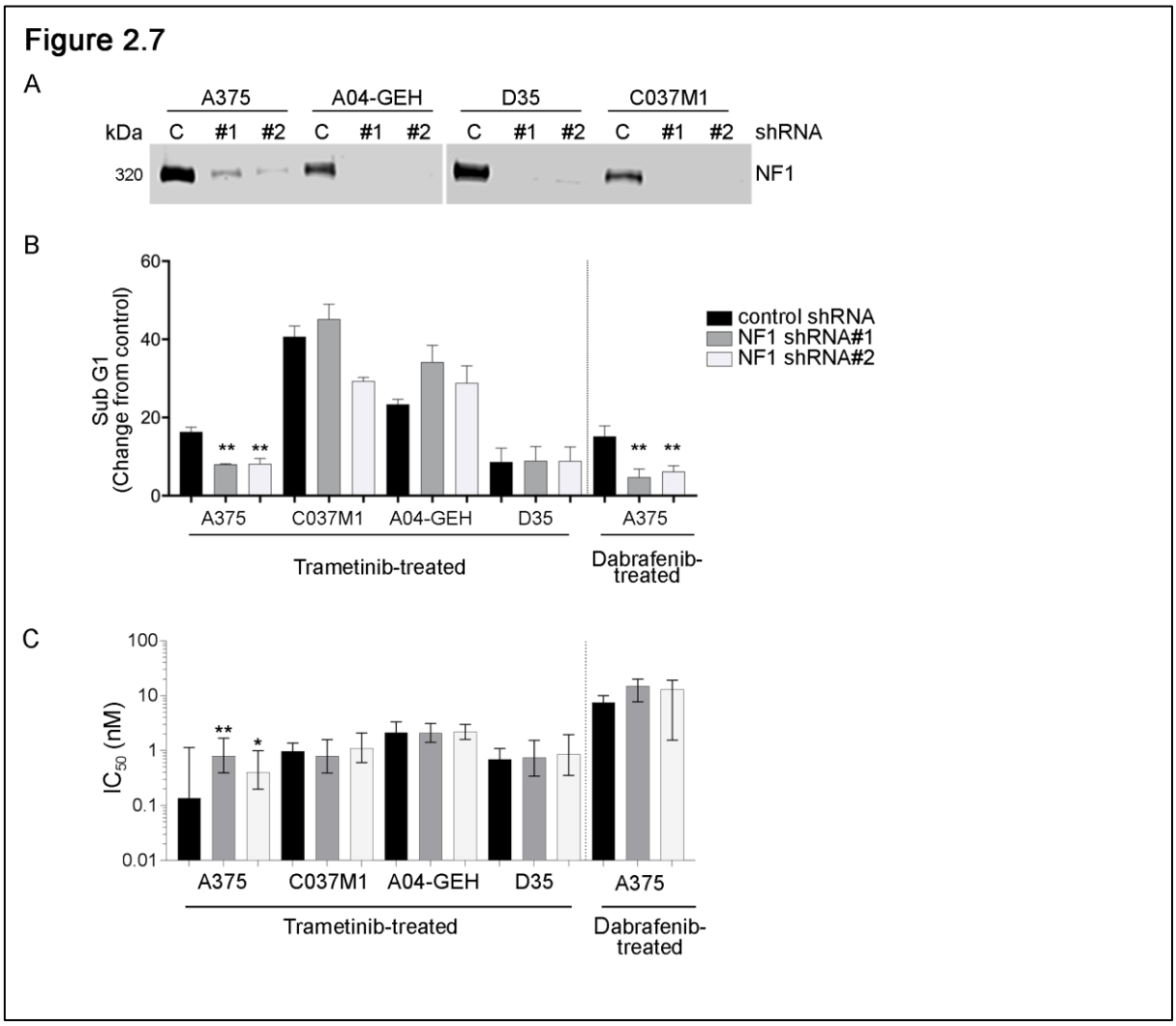

Figure 2.7: Loss of NF1 does not confer MEK inhibitor resistance in triple WT melanoma

(A) Western blotting analysis of NF1 protein expression in melanoma cell lines after transduction with NF1 shRNA molecules #1 and #2 compared to transduction with C, a non-targeting shRNA. REVERT total protein stain was performed as loading control (Figure S2.3). (B) Change in percentage of sub G1 (relative to DMSO-treated control) in control (black bars) or NF1 shRNA-transduced (grey bars) melanoma cell lines after trametinib or dabrafenib treatment. Data represent mean from at least three independent experiments and error bars represent standard deviation. Statistical comparison between control and NF1-silenced cells was performed using one-way ANOVA, with Holm's-Sidak multiple comparison test. *adjusted p-value<0.05, **adjusted p-value <0.01 compared to control. (C) Trametinib or dabrafenib IC_{50} values of control (black bars) or NF1 shRNA-transduced (grey bars) melanoma cell lines. Bar graphs show mean IC_{50} values with 95% confidence intervals from at least three independent experiments. Y axis is shown as log scale.

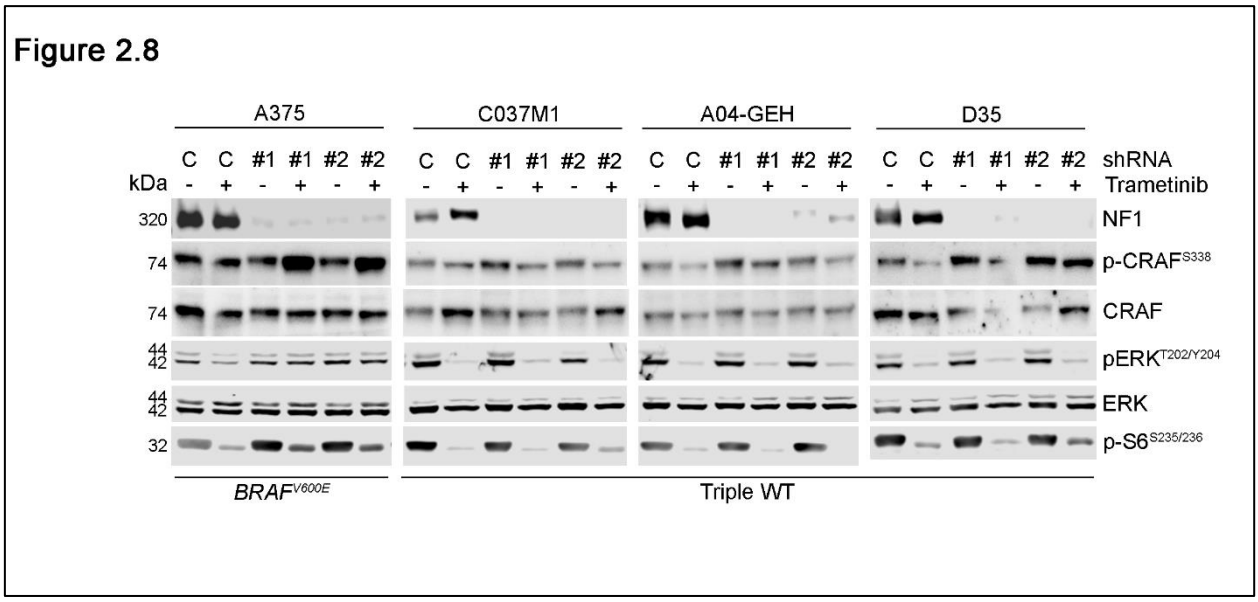

Figure 2.8: Effects of NF1 silencing on trametinib-induced signalling changes in melanoma

Western blots for protein markers of NF1, and MAPK (p-CRAF, CRAF, p-ERK, ERK, p-S6) activity in control or NF1 shRNA-transduced cells 24 h after treatment with DMSO (-) or 10 nM trametinib (+). C, control; #1, NF1 shRNA#1; #2, NF1 shRNA#2. REVERT total protein stain was performed as loading control. Results detailed in Section 2.3.3. REVERT total protein stain was performed as loading control (Figure S2.4).

2.3.4 Specific RASopathy gene variants do not predict MEK inhibitor resistance

The fact that NF1 loss did not confer resistance to MEK inhibition in *BRAF*/*RAS* WT melanoma suggested that NF1 may not act as a dominant regulator of MAPK signalling in this melanoma subtype. This is consistent with data showing that *NF1*-mutant melanomas that are *BRAF*/*NRAS* WT display a strong UV-mutation signature and high mutation load that alters RASopathy genes such as *RASA2*, *PTPN11*, *SOS1*, *RASSF2* and *RAF1* (77, 78, 305). We analysed the tumour mutation load (G1000=0, missense mutations only and read depth>20) and mutation frequencies in selected melanoma driver genes in our panel of 23 melanoma cell lines. We confirmed that mutations in *RASA2*, *SOS1* and *PTPN11* were enriched in our panel of *NF1*-mutant melanoma cells, which showed the highest mutation load compared to triple WT or *BRAF*^{V600}-mutant melanoma cells (Figure 2.9, Table 2.1), although no single mutated gene accurately predicted MEK inhibitor resistance. For instance, *PTPN11* and *SHOC2* mutations were each found in two *NF1*-mutant cell lines with variable responses to trametinib (Table 2.1).

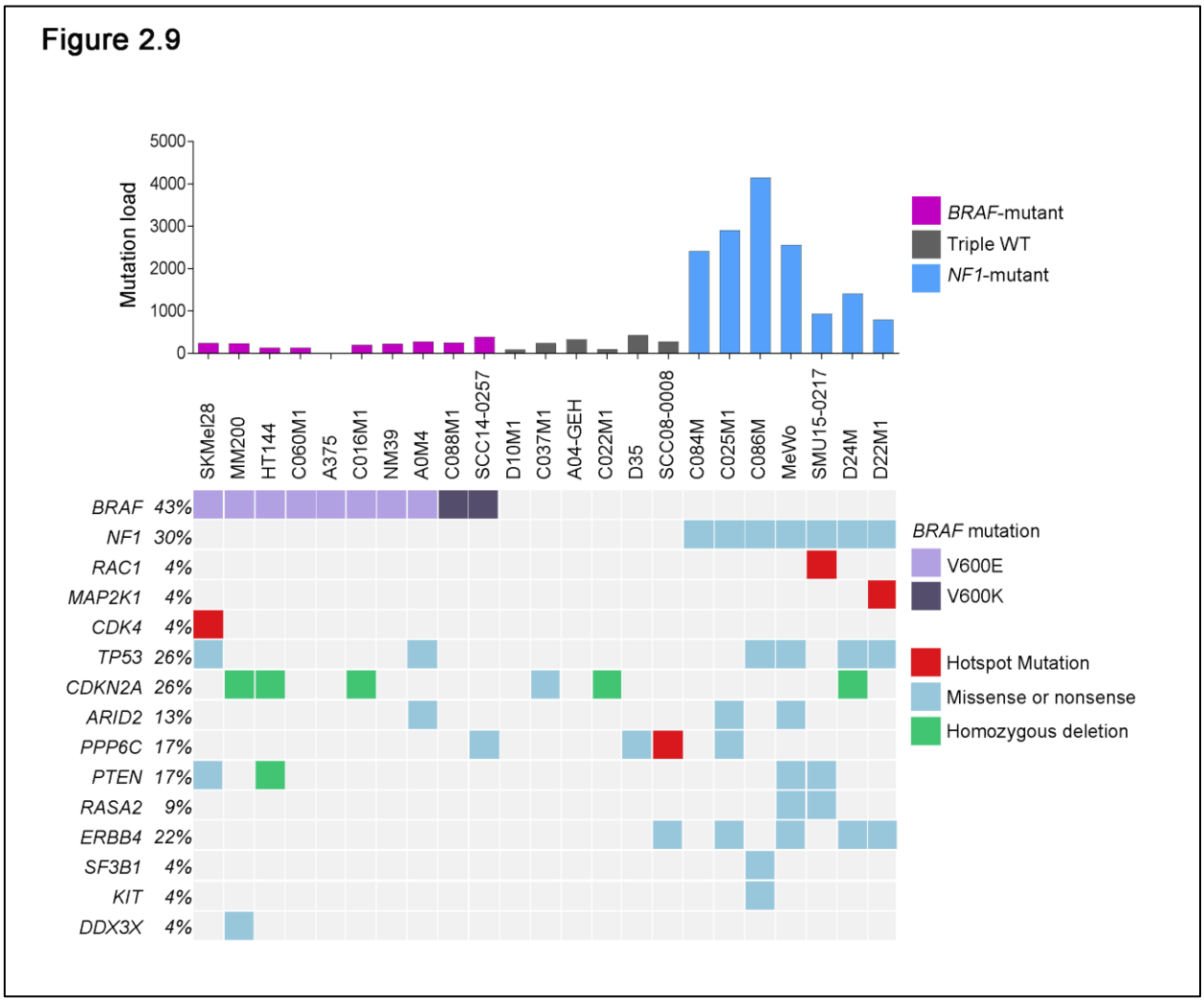

Figure 2.9: Mutation profile in selected melanoma driver genes

(A) Total missense mutations and (B) mutations in selected melanoma driver genes with mutation frequencies. No *RAS* mutations were detected in our panel of melanoma cell lines (n=23). Low read depth (<20) for *TP53* and *PTEN* mutations detected in cell line SKMel28.

2.3.5 Combination inhibition of MAPK signalling overcomes trametinib resistance in *NF1*-mutant melanoma

Although *NF1*-mutant melanoma cells were resistant to MEK inhibition, we hypothesized that the co-occurrence of multiple MAPK activating mutations in this melanoma subtype may require combination inhibitors to effectively block MAPK activity. To test this, we selected five *NF1*-mutant melanoma cell lines that displayed resistance or intermediate sensitivity to trametinib, and one triple WT melanoma cell line C022M1 with intermediate sensitivity. Cell cycle responses were examined after treatment with multiple MAPK inhibitors, including the pan-RAF inhibitor AZ628 (2 µM), the ERK inhibitor SCH772984 (500 nM) and MEK inhibitor trametinib (10 nM), either alone or in combination. In four of these six melanoma cell lines, we noted greater sensitivity to combination MAPK inhibition. In particular, SMU15-0217, C084M and MeWo cells showed significant induction of cell death in response to combination MAPK inhibition (Figure 2.10). This was most evident for the trametinib resistant SMU15-0217 cell line (NF1- and RASA2-null) that showed no cell death in response to single agent MEK, ERK or RAF inhibitor, but displayed over 50% sub G1 accumulation when two or more MAPK inhibitors were used in combination. Furthermore, the resistant D22M1, MeWo and SMU15-0217 cell lines responded to ERK inhibitor monotherapy by undergoing S phase inhibition, which was further enhanced when cells were exposed to two MAPK inhibitors (Figure 2.11). Finally, the C025M1 and C022M1 cell lines, which displayed intermediate sensitivity to trametinib, continued to show intermediate sensitivity (i.e. S phase inhibition) in response to single agent or combination MAPK inhibitors (Figure 2.11). Thus, all five *NF1*-mutant cell lines tested, including the three displaying resistance to trametinib, remained dependent on MAPK signalling for proliferation and/or survival. The increased sensitivity to combination MAPK inhibition was also associated with more potent inhibition of MAPK signalling. As shown in Figure 2.12, single agent treatment had little effect in suppressing

MAPK signalling in nearly all six cell lines, whereas combination treatment was more efficient at inhibiting MAPK signalling.

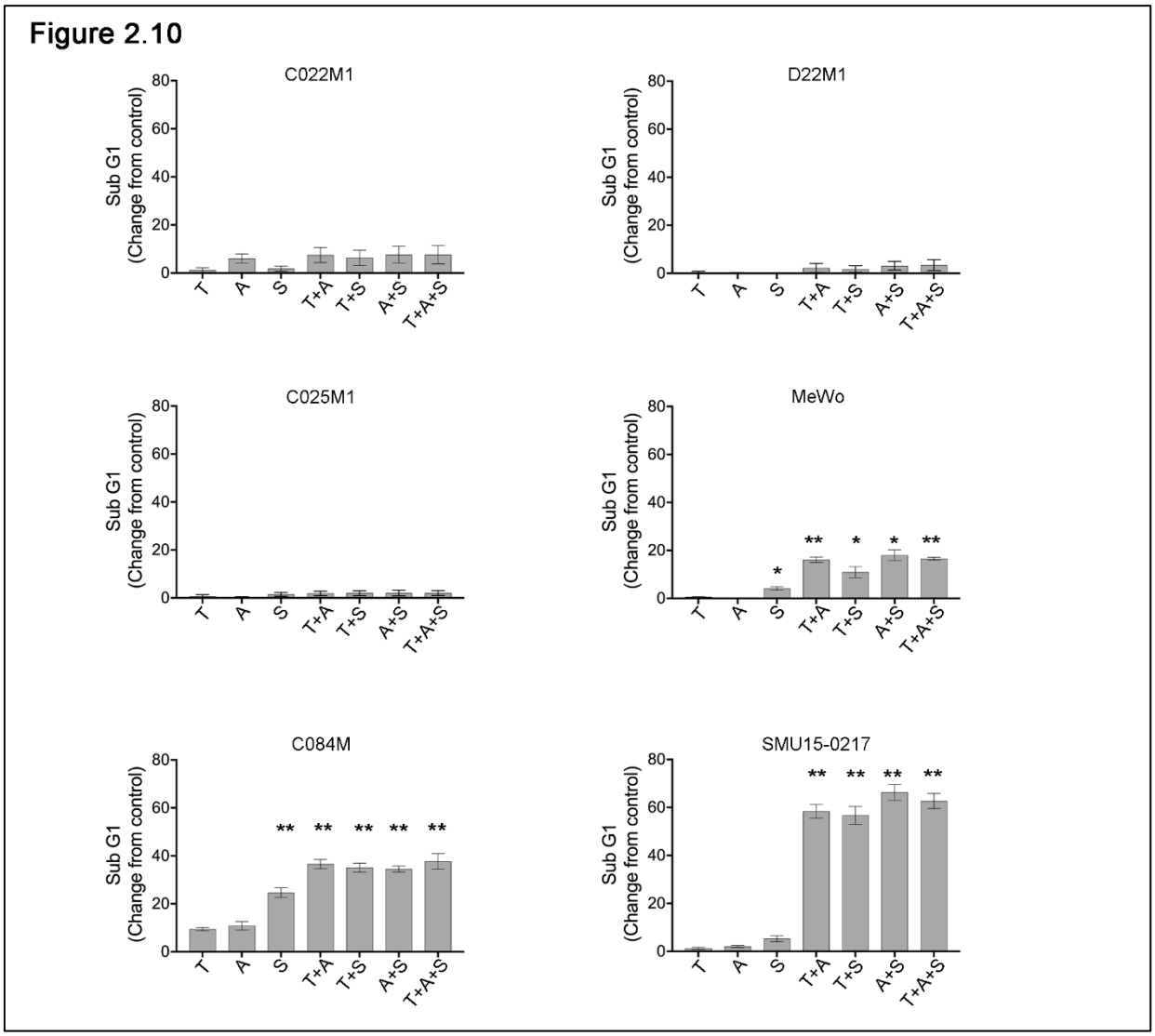

Figure 2.10: Concurrent inhibition of multiple MAP kinases enhances cell death in some *NF1*-mutant melanomas

Graphs show change in percentage of sub G1 (relative to the DMSO-treated cells). Indicated melanoma cell lines were treated with single or multiple MAPK inhibitors, including the pan-RAF inhibitor AZ628 (A) at 2 µM, the ERK inhibitor SCH772984 (S) at 500 nM and trametinib (T) at 10 nM for 72 h. Data represent mean from at least three independent experiments and error bars represent standard deviation. Statistical comparison between trametinib and other kinase inhibitor-treated cells was performed using one-way ANOVA, with Holm's-Sidak multiple comparison test. *adjusted p-value<0.05, ** adjusted p-value <0.01.

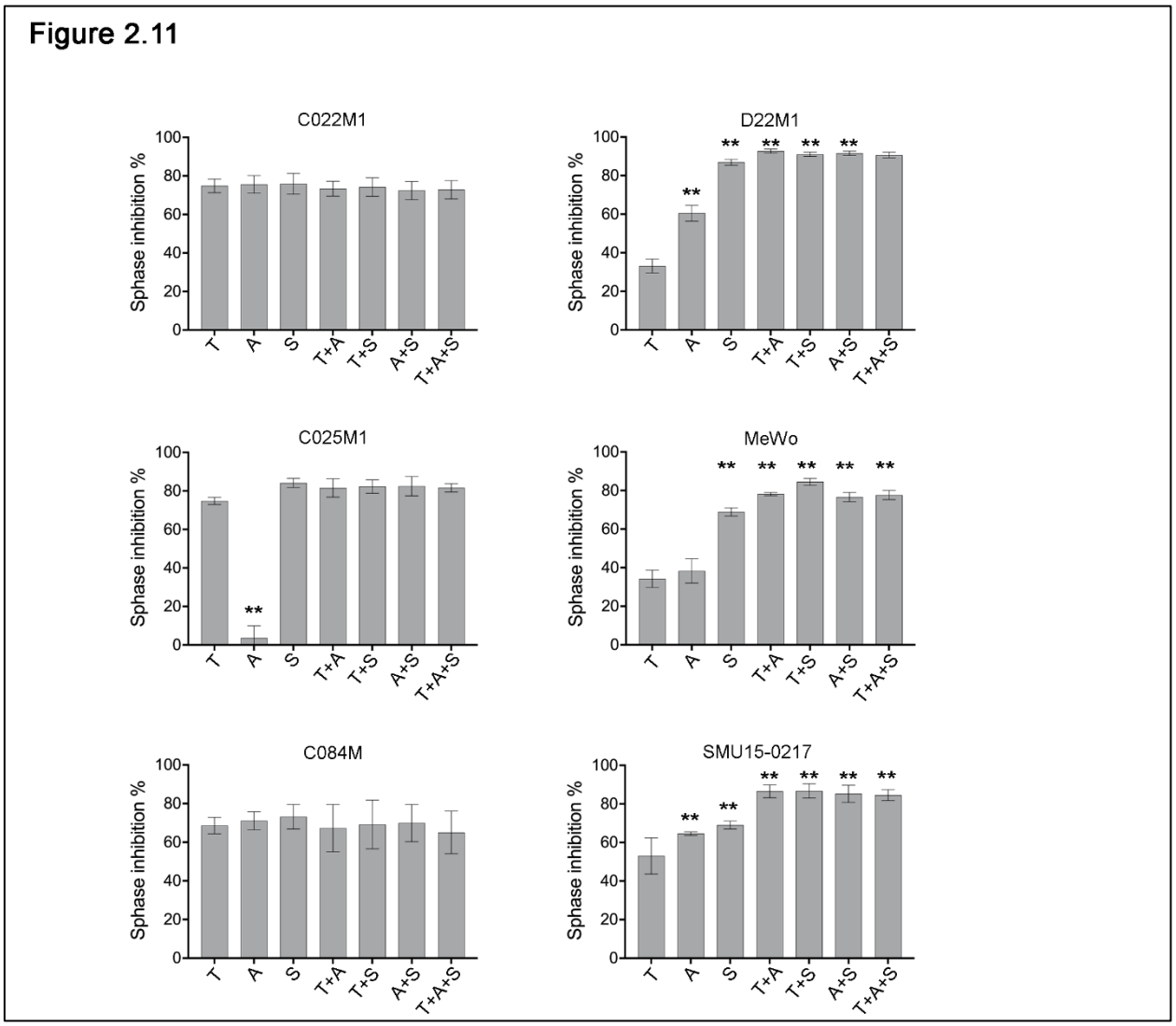

Figure 2.11: Concurrent inhibition of multiple MAP kinases can enhance cell cycle arrest in *NF1*-mutant melanomas

Graphs show percentage of S phase inhibition. Indicated melanoma cell lines were treated with single or multiple MAPK inhibitors, including the pan-RAF inhibitor AZ628 (A) at 2 µM, the ERK inhibitor SCH772984 (S) at 500 nM and trametinib (T) at 10 nM for 72 h. Results detailed in Section 2.3.5. Data represent mean from at least three independent experiments and error bars represent standard deviation. Statistical comparison between trametinib and other kinase inhibitor treated cells was performed using one-way ANOVA, with Holm's-Sidak multiple comparison test. *adjusted p-value<0.05, **adjusted p-value <0.01.

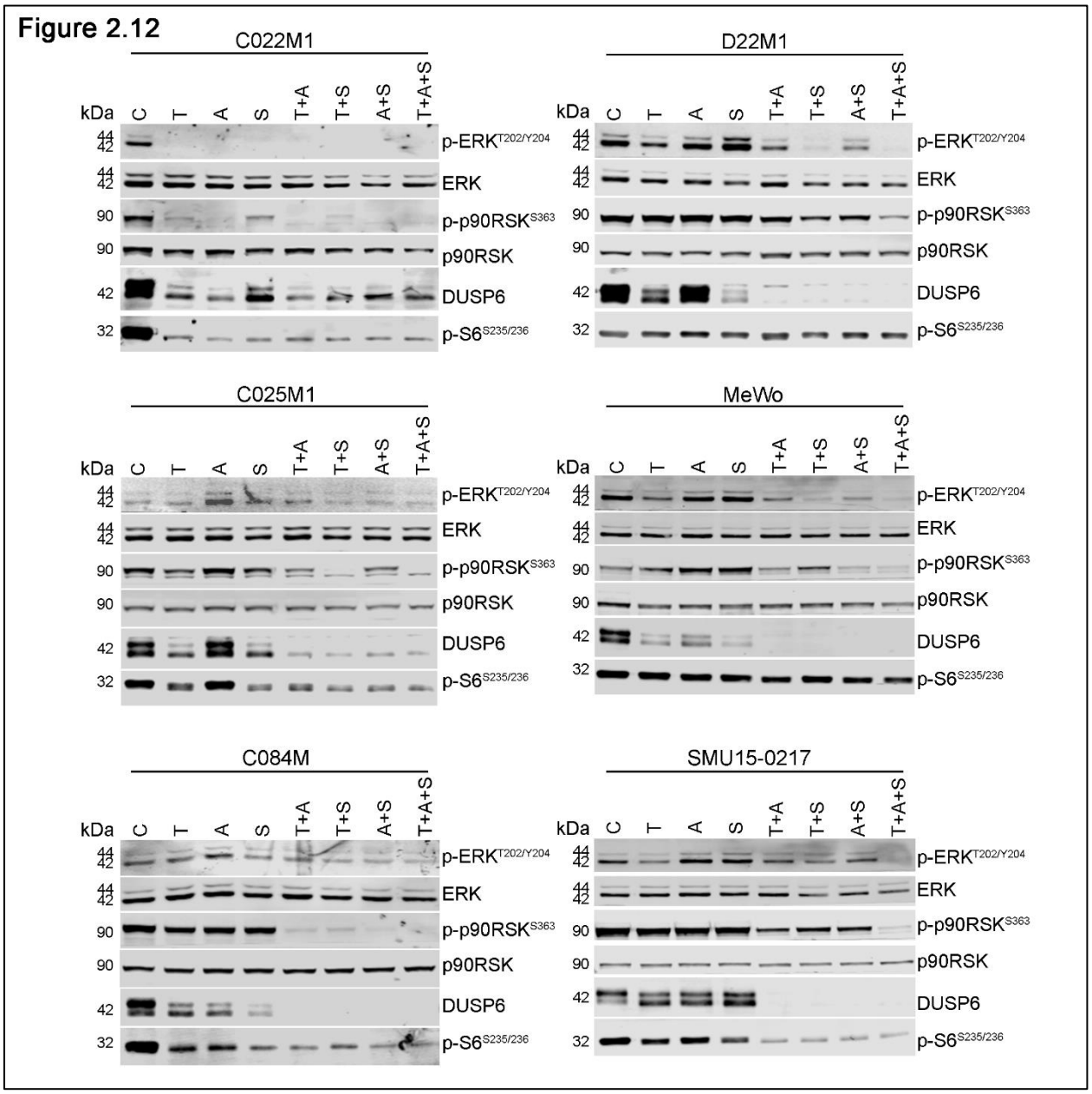

Figure 2.12: Effects of concurrent inhibition of multiple MAP kinases on signalling changes in melanoma

Western blots of indicated melanoma cells show MAPK activity protein markers 24 h after treatment with DMSO (C), various single agent or combinations of trametinib (T), RAF inhibitor AZ628 (A), and ERK inhibitor SCH772984 (S). REVERT total protein stain was used as loading control (Figure S2.5).

2.4 Discussion

Selective inhibition of the MAPK pathway using combination BRAF (vemurafenib, dabrafenib) and MEK inhibitors (trametinib) has significantly improved the survival of patients with *BRAF*^{V600}-mutant melanoma (299, 323, 324), and combination MEK (binimetinib) and CDK4 inhibitors (palbociclib) has produced encouraging early clinical trial results in patients with *NRAS*-mutant melanoma (234). For patients with *BRAF*/*RAS* WT melanoma, however, immune checkpoint inhibitors remain the only effective treatment in the 40% of responding patients (250, 251, 276). Defining the precise role of MAPK signalling in this subset of melanoma patients has important therapeutic implications as response to MEK inhibition can co-operate with immunotherapies to improve patient outcomes.

In this chapter, we analysed the impact of the MEK inhibitor trametinib in a panel of 23 melanoma cell lines, including 10 *BRAF*^{V600}-mutant and 13 *BRAF*/*RAS* WT cell lines, to examine MAPK dependency in *BRAF*/*RAS* WT melanomas. We showed that only 3/13 (23%) *BRAF*/*RAS* WT melanoma cell lines, all with intact NF1, showed a level of sensitivity to MEK inhibition that was equivalent to *BRAF*^{V600}-mutant melanoma cells. In contrast, 5/13 (38%) *BRAF*/*RAS* WT melanomas were highly resistant to MEK inhibition, and four of these had loss-of-function *NF1* mutations. Importantly, we confirm that these *NF1*-mutant melanoma cell lines retained MAPK dependency for survival or proliferation but displayed elevated RAS and CRAF activation that required concurrent inhibition of several kinases (including ERK, RAF and MEK) to effectively block MAPK signalling.

MEK inhibitor monotherapy alone is unable to induce cell death in *BRAF*/*RAS* WT melanomas with NF1 loss. These data contrast with previous reports showing MEK inhibitor sensitivity in *BRAF*/*RAS* WT melanomas that is comparable to *BRAF*^{V600E}-mutant melanoma (76, 77, 204). Importantly, these studies relied only on MTT metabolic assays

for sensitivity analyses and using these assays we found that 4/7 (57%) *NF1*-mutant melanomas show IC_{50} values comparable to sensitive *BRAF*-mutant melanoma cells.

The requirement for combinatorial MAPK inhibition in *NF1*-mutant melanomas may reflect their high mutational load, which is associated with alterations in RASopathy genes such as *RASA2*, *SOS1* and *PTPN11* (305). The distinct genetic profiles of the *BRAF*-mutant, triple WT and *NF1*-mutant melanomas may also modulate the contribution of NF1 in MAPK signalling regulation. In particular, NF1 loss was sufficient to promote MEK inhibitor resistance in $BRAF^{V600E}$-mutant melanoma (325), but not in *BRAF*/*RAS* WT melanoma cell models. In response to trametinib treatment, p-ERK was inhibited more potently in the presence of NF1 in $BRAF^{V600E}$-mutant melanoma whereas p-ERK inhibition was comparable in NF1-intact and NF1-null *BRAF*/*RAS* WT cells.

Collectively our data indicate that all melanoma subtypes rely on MAPK signalling for survival and/or proliferation, but inhibition of this pathway requires multiple kinase inhibitors in the *BRAF*/*RAS* WT subtype. In particular, we show that *NF1* gene status is an accurate predictor of MEK inhibitor monotherapy resistance, and resistance reflects the inability of trametinib to effectively inhibit the MAPK signalling cascade. Inhibition of MAPK signalling was achieved in all *NF1*-mutant cells with combination MEK and ERK inhibitors and this promoted enhanced cell death or proliferative arrest in 4 out of 5 *NF1*-mutant cell models tested.

Our data support the treatment strategy that combines molecular targeted and immune therapies in melanoma and several ongoing clinical trials, with various drug combinations, are being evaluated. For instance, in a phase I study, pembrolizumab plus dabrafenib and trametinib demonstrated promising anti-tumour activity in $BRAF^{V600}$-positive patients (326). In a phase II study of $BRAF^{V600E/K}$-mutant patients with treatment-naïve advanced melanoma, treatment with pembrolizumab plus dabrafenib and trametinib produced

longer PFS and objective response rates (327). Although treatment strategies combining these therapies are often associated with high burden of toxicity (328-331), clinical trials are exploring the safety of combinatorial therapy. For instance, a phase I study of an anti-PD-L1 antibody in combination with dabrafenib and trametinib in *BRAF* mutation-positive melanoma, or in combination with trametinib in *BRAF* WT melanoma, showed clinical activity and a manageable safety profile (310). Ongoing research and clinical trial need to refine the dosing and timing schedule of combination therapies as well as the optimal mix of drugs to use in combination. The molecular and signalling profile of the tumour subtype, in particular the *NF1* mutation status, may also guide treatment selection.

Supplementary Figures

Figure S2.1

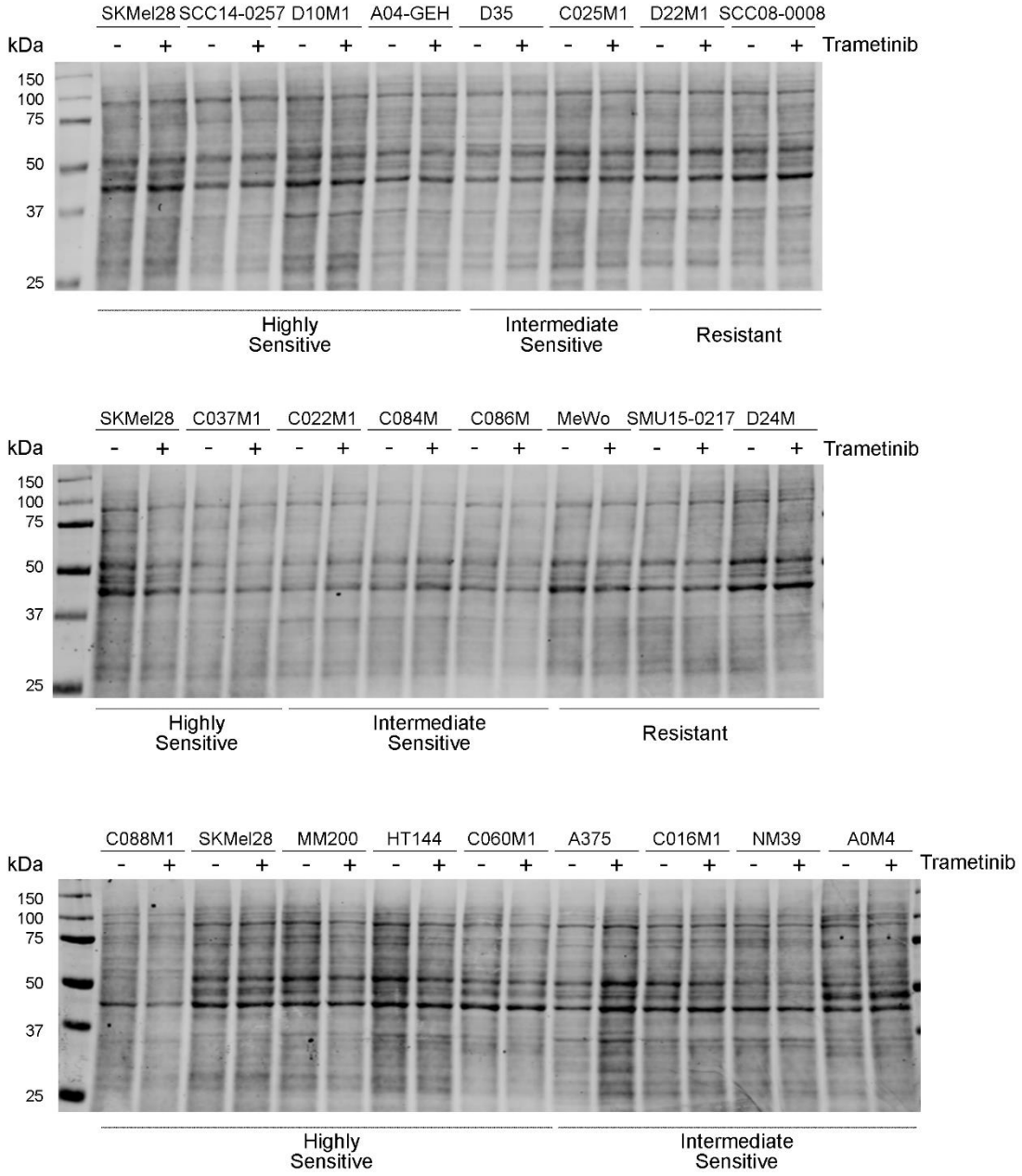

Figure S2.1: Detection of the REVERT total protein stain

Western blots for the REVERT total protein stain, performed as loading control for Figure 2.3. Indicated melanoma cell lines were treated with DMSO (-) or 10 nM trametinib (+) for 24h.

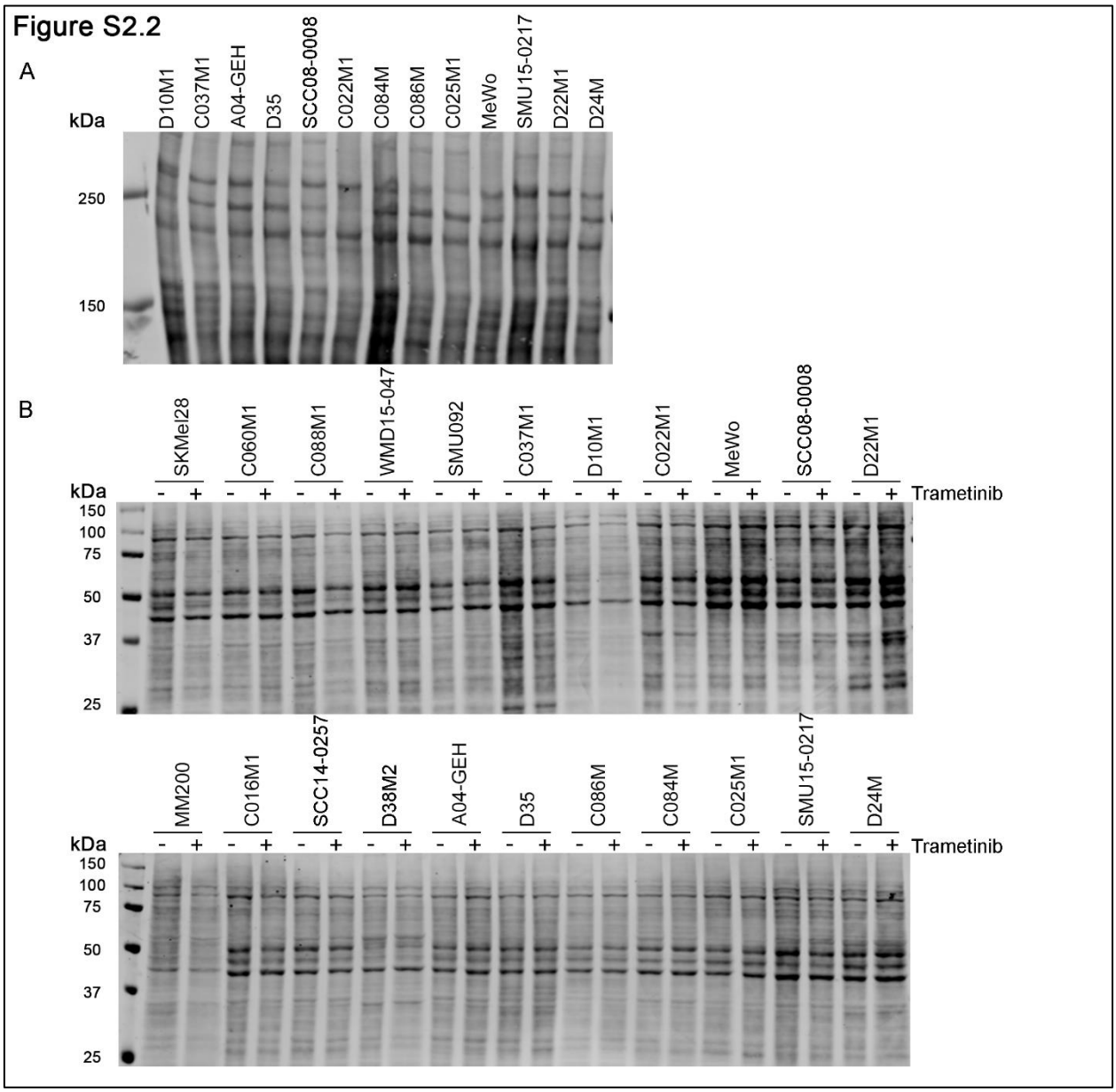

Figure S2.2: Detection of the REVERT total protein stain

Western blots for the REVERT total protein stain, performed as loading control for Figure 2.5.

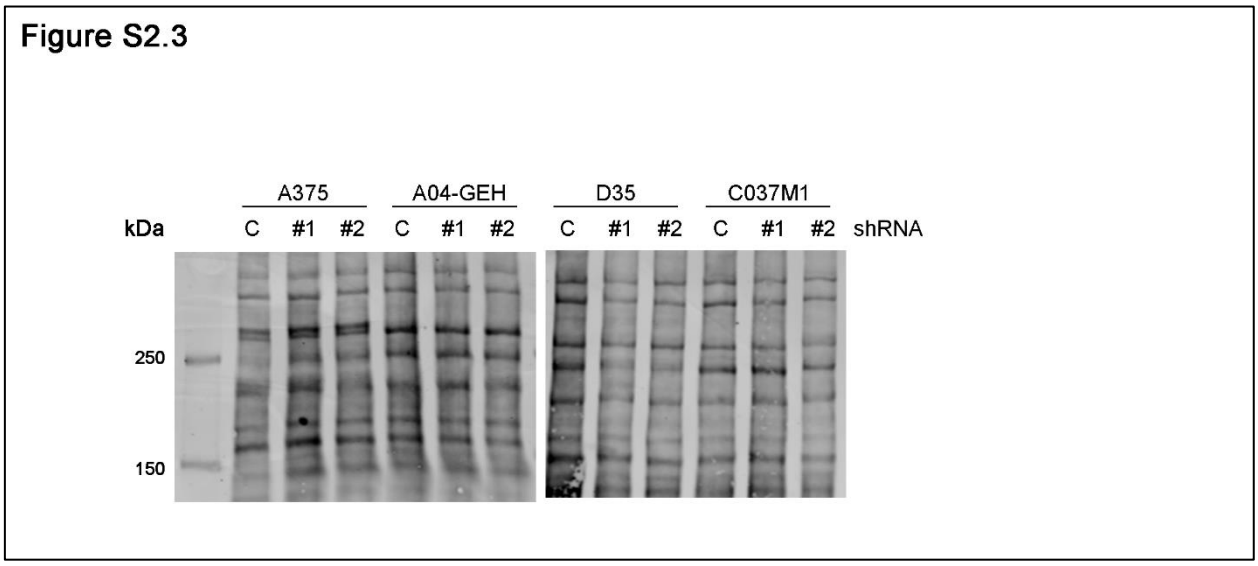

Figure S2.3: Detection of the REVERT total protein stain

Western blots for the REVERT total protein stain, performed as loading control for Figure 2.7 (A).

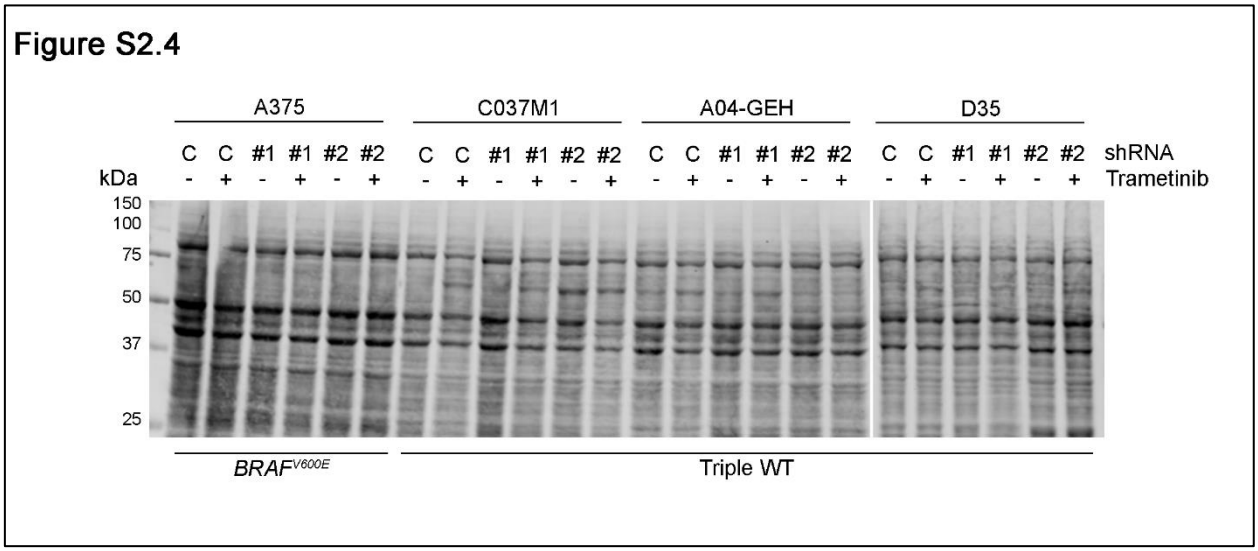

Figure S2.4: Detection of the REVERT total protein stain

Western blots for the REVERT total protein stain, performed as loading control for Figure 2.8.

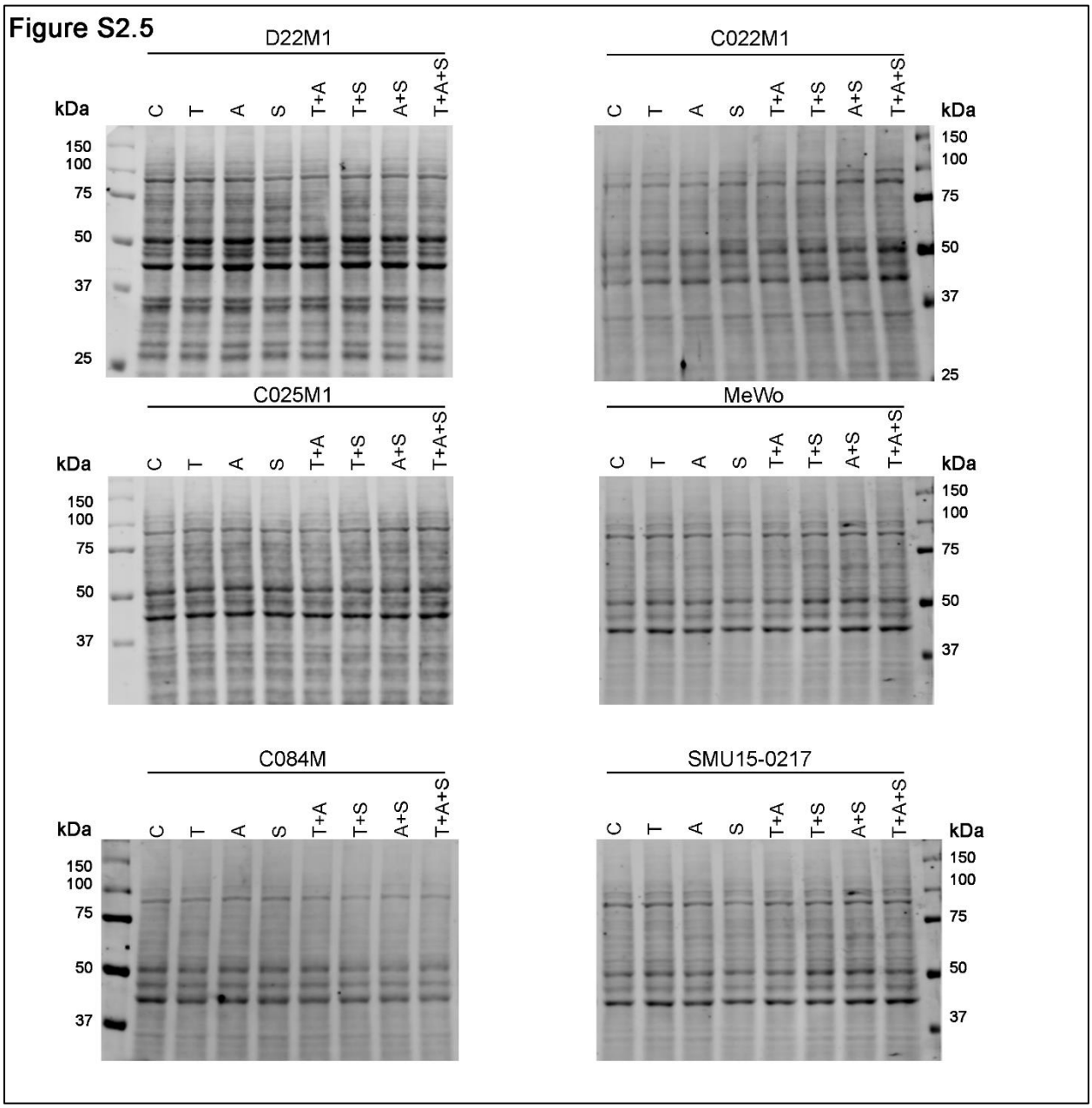

Figure S2.5: Detection of the REVERT total protein stain

Western blots for the REVERT total protein stain, performed as loading control for Figure 2.12.

Chapter 3

Influence of p53 on melanoma responses to trametinib

3.1 Introduction

In the previous chapter we confirmed that trametinib-resistant *BRAF*/*RAS* WT melanomas were enriched for gene mutations. In particular, mutations in *TP53*, and RASopathy genes, including *NF1*, were common in trametinib-resistant *BRAF*/*RAS* WT melanoma. In this chapter the contribution of p53 to *BRAF*/*RAS* WT melanoma signaling and MAPK dependency was explored.

p53 is a sequence-specific transcriptional factor that is activated in response to cellular stress signals such as DNA damage, aberrant oncogene activation, hypoxia and ribosome stress, and promotes cell cycle arrest or cell death, as reviewed in (332). The *TP53* gene is the most frequently mutated gene in human cancer and is altered in almost 50% of human tumours (333). Nonsense or frameshift mutations normally result in loss of p53 protein expression, whereas missense mutations in the DNA binding region of p53 predominantly lead to loss of WT p53 activity (334). Typically, p53 binds as a tetramer to p53 response elements which usually reside within the promoter region of many genes involved in DNA repair, cell cycle regulation, metabolism, feedback regulation, apoptosis and autophagy (Table 3.1).

Table 3.1: Summary of p53 functions and transcriptional targets

Function	Proteins encoded by p53 transcription targets
Cell cycle regulation	$p21^{Waf1}$, Gadd45A, 14-3-3α, FBXW7ß, PGF, TGFA, KITLG
DNA repair	PCNA, XPC, DDB2, POLH, RRM2B
Feedback regulation	MDM2, CCNG1
Apoptosis	BAX, PUMA, NOXA, FAS, APAF1, SUSD6
Metabolism	GLAS2, FDXR, TIGAR
Autophagy	PRKAB1, DRAM1

Table adapted from (335)

TP53 mutations are less frequent in melanoma compared to other tumour types and occur in approximately 5-19% of melanoma cases (17, 45, 59). The frequency of *TP53* mutations can vary according to the melanoma subtype; cutaneous melanomas with mutation signatures indicative of UV-induced damage tend to show increased mutation burden and more frequent *TP53* mutations (59).

p53 function can also be inactivated in melanoma via alternate mechanisms. For instance, 50% of melanomas overexpress MDM2, an E3 ubiquitin-protein ligase that regulates p53 degradation, and *MDM2* gene amplification is associated with melanoma thickness and invasion level (336-338). MDM2 activity can also be induced in melanoma via the loss of the MDM2 inhibitor $p14^{ARF}$, which is caused by loss-of-function mutations in the *CDKN2A* chromosome 9p locus and occurs in approximately 50% of melanomas (17, 45, 59, 339). Increased expression of the MDM2 homologue, MDMX (MDM4), also inhibits p53 through binding to MDM2, and has been detected in around 60% of malignant melanoma (340, 341). Similarly, the iASPP (inhibitor of apoptosis stimulating protein of p53) protein interacts with and inhibits the proapoptotic activity of p53. Phosphorylation of iASPP, which promotes the nuclear accumulation of monomeric iASPP, occurs in 91% of *TP53* WT melanomas, and promotes p53 inhibition. Phosphorylation of iASPP is associated with poor survival in melanoma patients (342). There is also substantial evidence that inactivation of p53 is associated with melanoma development and aggressiveness. For instance, *TP53* is not mutated in melanocytic nevi (343, 344) and p53 protein accumulation is evident in metastatic melanoma, but not in benign melanocytic lesions (345).

Collectively these data demonstrate that p53 function, rather than the *TP53* gene, is commonly altered in melanoma and contributes to disease development and progression. Consequently, the reactivation of p53 has been considered a potential therapy in many cancers, including melanoma. For instance, small molecule MDM2 or iASPP antagonists

promoted p53-mediated melanoma cell cycle arrest and apoptosis, and in combination with BRAF inhibitors, they promoted enhanced melanoma cell cycle inhibition and apoptosis *in vitro* and *in vivo* (342).

From the studies presented in Chapter 2, we confirmed that *TP53* mutations were enriched in *BRAF*/*RAS* WT cell lines (Chapter 2, Figure 2.9). In this chapter, we hypothesized that MEK inhibitor resistance in *BRAF*/*RAS* WT melanoma is associated with *TP53* mutation and p53 loss of function. We aimed to investigate the precise contribution of p53 to *BRAF*/*RAS* WT melanoma signalling and MAPK dependency, and to explore the therapeutic implications of p53 reactivation in melanoma.

3.2 Methods

3.2.1 Cell culture and reagents

Cell lines and cell culture conditions used in this study are described in Chapter 2 (Section 2.2.1). Short term melanoma cell models including WMD15-047, SMU-084, SMU-092, SCC14-0257 and SMU15-0217 were generated as described previously (319). All inhibitors were purchased from Selleck Chemicals (Houston, TX, USA) and prepared in dimethyl sulfoxide (DMSO). The MEK1/2 inhibitor trametinib (GSK1120212) was prepared as 1 mM stocks. The MDM2 antagonist nutlin-3 was prepared as 10 mM stocks.

3.2.2 DNA extraction and Whole Exome Sequencing

Details of DNA extraction and whole exome sequencing (WES) are as described in Chapter 2 (Section 2.2.2). 29 melanoma cell lines were screened by whole exome sequencing.

3.2.3 MTT Cell viability and cell cycle assays

MTT Cell viability and cell cycle distribution analyses were performed are as described in Chapter 2 (Sections 2.2.3 and 2.2.4).

3.2.4 Western blotting

Melanoma cells were treated with 10 nM trametinib, 20 µM nutlin-3 or 0.1% DMSO for 24 h before extracting total cellular proteins. The methods of protein extraction, protein assay and western blotting are as described previously in Chapter 2 (Section 2.2.5). Western blots were probed with the following primary antibodies targeting: total p53 (1:500, DO-1, Santa Cruz, TX, USA), $p21^{Waf1}$ (1:500, SX118, BD Pharmingen, MA, USA), total p90RSK

(1:1000, 6B9D6F8, Abcam, Cambridge, UK), phosphorylated p90RSK (Ser363, 1:3000, Santa Cruz), total ERK (1:2000, 137F5, Cell Signalling, MA, USA), phosphorylated ERK (Tyr204, 1:500, E4, Santa Cruz), DUSP6 (1:1000, EPR129Y, Abcam), p-S6 (Ser235/236, 1:2000, 2F9, Cell Signalling), total AKT (1:500, 40D4, Cell Signalling), phosphorylated AKT (Ser473, 1:1000, 736E11, Cell Signalling), and phosphorylated p70S6K (Ser411, 1:2000, A-6, Santa Cruz) overnight at 4ºC. Membranes were washed with Tris-buffered saline with 0.05% (v/v) Tween 20 then incubated with secondary antibodies IRDye® 800CW Donkey anti-Mouse, IRDye® 800CW Donkey anti-Rabbit, IRDye® 680LT Donkey anti-Mouse or IRDye® 680LT Donkey anti-Rabbit (LI-COR). Membranes were detected on the Odyssey imaging system (LI-COR). Each western blot was performed using two biological replicates.

3.2.5 Lentivirus transduction

Lentivirus particles were produced as described previously (322) and melanoma cells infected using a multiplicity of infection of 5 (Chapter 2, Section 2.2.6). Western blotting was utilized to assess efficacy of knockdown 72 h after transduction. The p53-directed shRNA sequences correspond to nucleotides 956-974 and 1026-1044 (Genbank accession number NM_000546), and the non-targeting negative control shRNA did not show complete homology to any known human transcript. These constructs were used in a previous study (346).

3.2.6 IncuCyte real-time proliferation assay

Melanoma cells were seeded into 12-well (5-8 x 10^4 cells per well) or 24-well plates (1-4 x 10^4 cells per well) in DMEM or RPMI-1640 media and allowed to adhere for 24 h before treatment. Media was removed and 20 µM nutlin-3, 10 nM trametinib, either alone or in combination, were added. Cells were also treated with 0.1% DMSO as control. Cells were

immediately incubated in IncuCyte ZOOM live cell imaging system (Essen BioScience, MI, USA) for 72 h. Four to nine images in different fields of view were taken for each well by the IncuCyte scanning system and phase confluence was measured every 4 h. The percentage of cell confluence after treatment was reported relative to the DMSO-treated controls, with time of drug addition set at 100%.

3.2.7 Statistical analysis

Data represent at least three independent experiments, unless otherwise specified. Statistical analysis was performed in GraphPad Prism (Version 7). All statistical methods applied are detailed in each figure legend. P-values of less than 0.05 were considered statistically significant.

3.3 Results

3.3.1 *TP53* mutations are associated with trametinib resistance in melanomas

A panel of 29 melanoma cell lines was exome sequenced to examine their mutation profiles. The cell lines included the 23 melanoma cell lines described in Chapter 2 and an additional six cell lines including three *RAS*-mutant cell lines, WMD15-047 ($HRAS^{Q61R}$), SMU-092 ($NRAS^{Q61L}$), and D38M2 ($NRAS^{Q61R}$), two melanoma cells with unusual *BRAF* mutations, ME1007 ($BRAF^{G466R}$) and C077M1 ($BRAF^{S457L}$), and one *BRAF*/*RAS* double-mutant cell line SMU-084 ($BRAF^{D594E}$/$HRAS^{G13R}$) (Table 3.2). We examined the mutation profile of *TP53* and 14 other genes commonly mutated in melanoma (45, 59). *TP53* was the third most commonly mutated gene detected in our panel of cells and mutations affecting the *TP53* gene were identified in 7/29 (24%) melanoma cell lines (Table 3.2). In the seven *TP53*-mutant melanoma cell lines, four showed *NF1* mutations, one had a $BRAF^{V600E}$ mutation, one had a $BRAF^{S457L}$ mutation, and another had an $HRAS^{Q61R}$ mutation. $TP53^{L145R}$ mutation was detected in SKMel28, but the read depth was considerably low (<20), thus we classified SKMel28 as *TP53*-WT cell line in our analysis.

We assessed the association between *TP53* mutation status and trametinib response in this panel of melanoma cells. Of the 11 cell lines that showed high sensitivity to trametinib, ten had WT *TP53* and only the WMD15-047 cell line had a loss-of-function $TP53^{E286K}$ missense mutation (347). Similarly, of the 11 melanoma cell lines that showed intermediate sensitivity to trametinib, nine were *TP53* WT cell lines while two had nonsense *TP53* mutations (Q192* and E247* in the A0M4 and C086M cells, respectively). The remaining seven cell lines were resistant to trametinib, and of these, four were *TP53*-mutant while three were *TP53* WT (Table 3.2).

Table 3.2: *TP53* mutations and functional status in 29 melanoma cell lines

	Cell Line	Response[a]	*TP53* mutation[b]	p53 function[c]
***BRAF*^{V600E}**	SKMel28 [342, 348, 349]	HS	WT	nd
	MM200 [350]	HS	WT	+
	C088M1	HS	WT	nd
	C060M1	HS	WT	+
	HT144 [351]	HS	WT	nd
	SCC14-0257	HS	WT	nd
	A375[352, 353]	IS	WT	+
	A0M4	IS	Q192*	nd
	C016M1	IS	WT	nd
	NM39	IS	WT	+
NF1	C084M	IS	WT	-
	C025M1	IS	WT	nd
	C086M	IS	E247*	nd
	MeWo [354]	R	Q278*	-
	SMU15-0217	R	WT	-
	D24M	R	F113V	-
	D22M1	R	E248K	-
Triple WT	C037M1	HS	WT	+
	D10M1	HS	WT	nd
	A04-GEH	HS	WT	+
	C022M1	IS	WT	+
	D35	IS	WT	+
	SCC08-0008	R	WT	nd
***BRAF* other**	SMU-084	IS	WT	nd
	ME1007	R	WT	nd
	C077M1	R	Q292H	-
***RAS* mutant**	WMD15-047	HS	E286K	nd
	SMU-092	HS	WT	nd
	D38M2	IS	WT	nd

[a]Response to trametinib was assessed using MTT and cell cycle assays. HS, highly sensitive; IS, intermediate sensitive; R, resistant; [b]*TP53* mutation status was determined using whole exome sequencing; [c]p53 function was determined using the IncuCyte real-time proliferation assay following treatment with nutlin-3. nd, not determined, +, functional p53, -, non-functional p53, *BRAF* other denotes non-*V600E/K BRAF* mutations. Previous studies reporting TP53 status or p53 function in melanoma cell lines have been referenced.

Importantly, *TP53*-mutant melanoma cell lines had significantly higher trametinib IC_{50} values and less cell death (change in sub G1) following trametinib treatment (10nM, 72h) compared to *TP53* WT cell lines (Figure 3.1). Overall, *TP53* mutation was significantly associated with resistance to trametinib treatment (see Table 3.2) (Fisher's exact test, p=0.037) (Table 3.3).

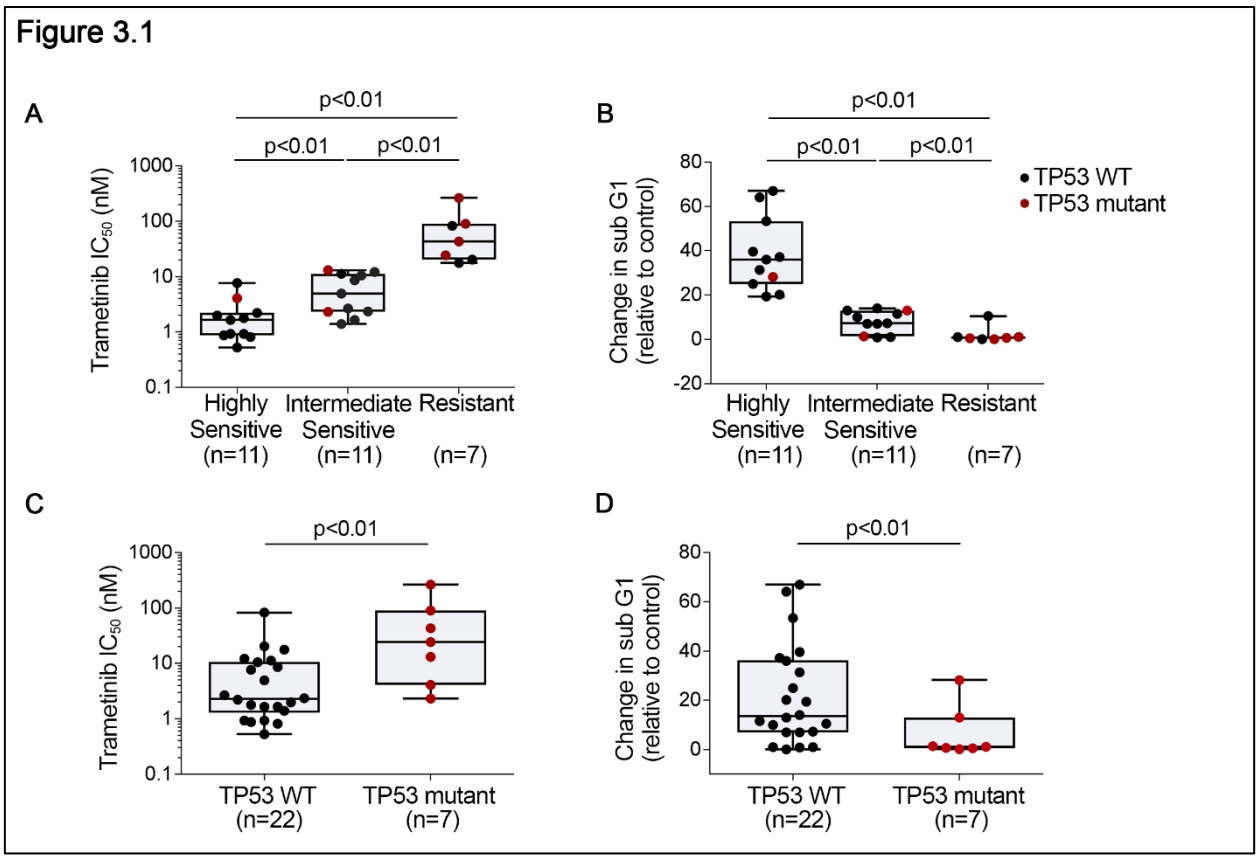

Figure 3.1: Melanoma sensitivity to trametinib is associated with *TP53* mutation status

Box plots show (A) trametinib IC_{50} values and (B) trametinib (10nM, 72h)-induced change in percentage of sub G1 (relative to DMSO-treated control) of melanoma cells classified as highly sensitive, intermediate sensitive and resistant to trametinib. Cell lines with mutant *TP53* are shown in red. Statistical comparison between groups was performed using Kruskal-Wallis with Dunn's multiple comparison test. Adjusted p-values are shown. (C) Trametinib IC_{50} values and (D) change in percentage of sub G1 (relative to DMSO-treated control) of melanoma cells shown according to p53 status. Statistical comparison between groups was performed using Mann-Whitney test. Each dot represents one cell line (mean of at least three independent experiments), box plots indicate the median and the interquartile range and the whiskers indicate the range.

Table 3.3: Association between *TP53* status and trametinib response in melanoma cell lines

Trametinib response	*TP53* mutation		Fisher's exact test P-value
	WT	Mutant	
Highly/intermediate sensitive	19	3	p=0.0377
Resistant	3	4	

Statistical association was performed using Fisher's exact test.

3.3.2 Defective p53 function is associated with trametinib resistance in melanomas

Given that inactivation of the p53 pathway may be caused by mechanisms other than mutations within the *TP53* gene, we examined the functional status of p53 in our cell lines using the MDM2 antagonist nutlin-3. Nutlin-3 inhibits the interaction between MDM2 and p53, resulting in stabilisation and activation of p53 (355). Fourteen melanoma cell lines, including ten *TP53* WT and four *TP53*-mutant cell lines were treated with 20 µM nutlin-3 or 0.1% DMSO for 72 h before assessing changes in cell proliferation. As shown in Table 3.2 and Figure 3.2, eight melanoma cell lines showed significant cell cycle arrest in response to nutlin-3, and all eight cell lines were WT for *TP53*. The remaining six cell lines showed minimal or no cell growth inhibition, and of these, two were *TP53* WT while four were *TP53*-mutant (Table 3.2, Figure 3.2). Thus, as expected, all *TP53*-mutant cell lines had non-functional p53, while 2/10 (20%) *TP53* WT cells (C084M and SMU15-0217) also showed no p53 response after MDM2 inhibition (Table 3.2).

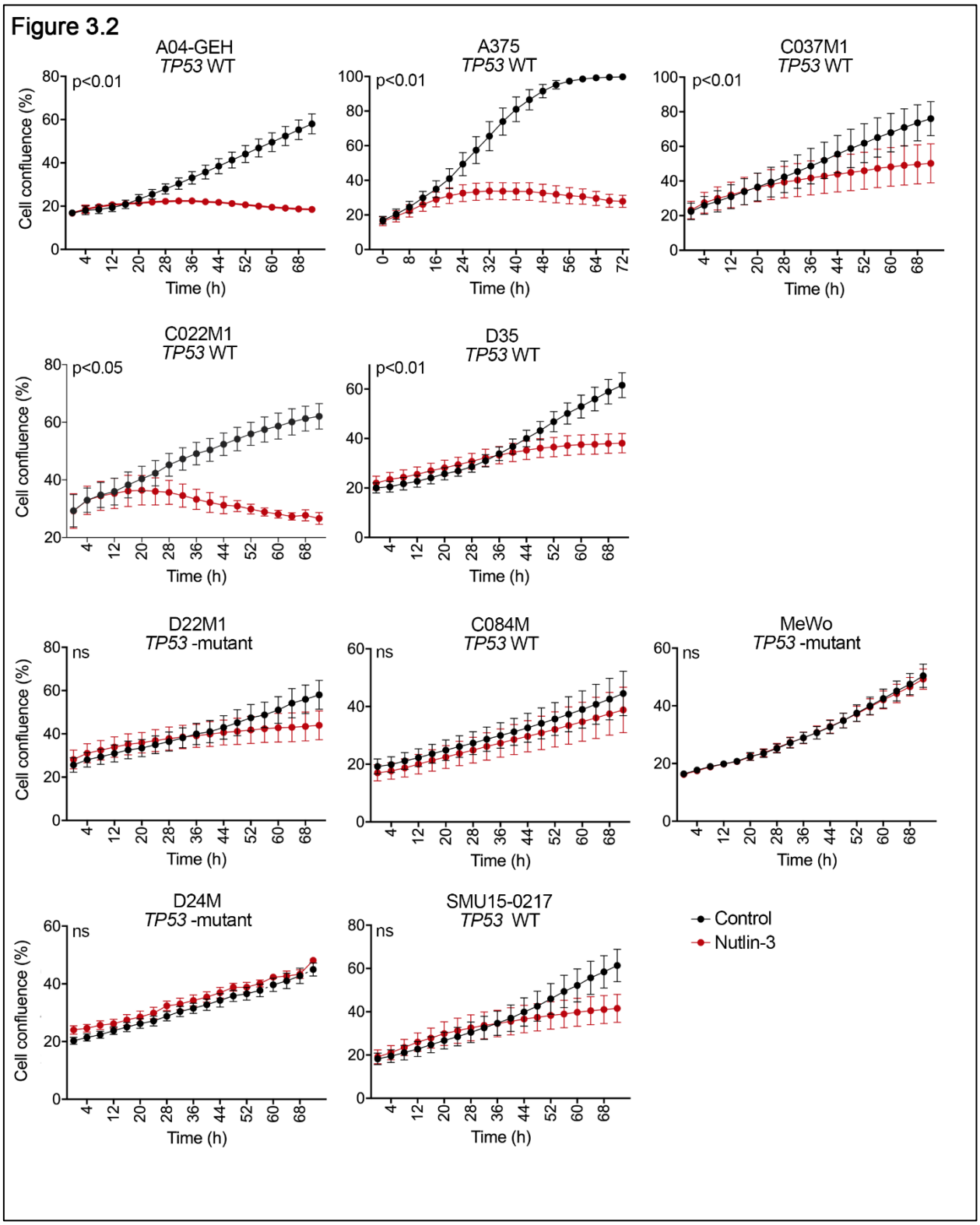

Figure 3.2: p53 functional status in melanoma cell lines

Melanoma cells were treated with DMSO or 20 µM nutlin-3 for 72 h and cell proliferation examined using the Incucyte real-time proliferation assay. Graphs show percentage cell confluence and data represent mean of at least three independent experiments and error bars represent the standard error of the mean. Area under the curve (AUC) was calculated for each cell line and difference in AUC between treated and control groups were compared using paired t-test. ns, not significant.

To confirm that nutlin-3 treatment restored p53 function, expression of p53 protein was examined in five melanoma cell lines following treatment with nutlin-3 or DMSO at 24 h. As shown in Figure 3.3, expression of p53 and its downstream target p21^{Waf1} were elevated following treatment with nutlin-3 compared to DMSO-treated controls, but only in *TP53* WT cell lines, and not in the *TP53*-mutant cell line MeWo.

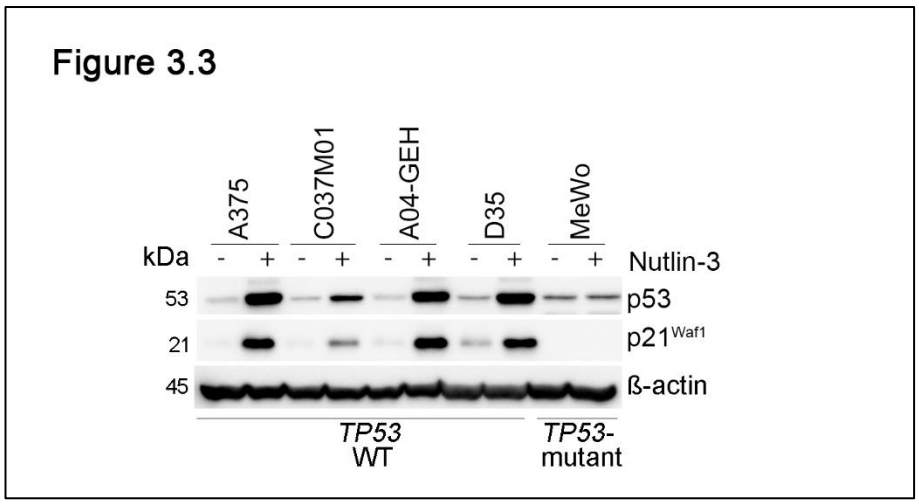

Figure 3.3: Nutlin-3 promotes p53 stabilization and p21^{Waf1} accumulation in *TP53* WT melanoma cells

Western blot showing p53 and p21^{Waf1} expression in melanoma cells 24 h after treatment with DMSO (-) or 20 µM nutlin-3 (+). ß-actin stain was used as loading control.

We re-examined the association of p53 and trametinib sensitivity in melanoma cells, adding p53 functional data (based on nutlin-3 response) rather than *TP53* genotype only as shown in Table 3.2. *TP53*-mutant cells were considered with non-functional p53. Of the 17 melanoma cell lines with established p53 functional status, five were highly sensitive to trametinib (one with non-functional p53 and four with functional p53) and seven had intermediate sensitivity (three with non-functional p53 and four with functional p53). All five cell lines resistant to trametinib had non-functional p53 (Figure 3.4). These data confirm that loss of p53 function does not preclude sensitivity to trametinib, but is

significantly associated with trametinib resistance, as measured by MTT viability and cell cycle distribution assays (Figure 3.4).

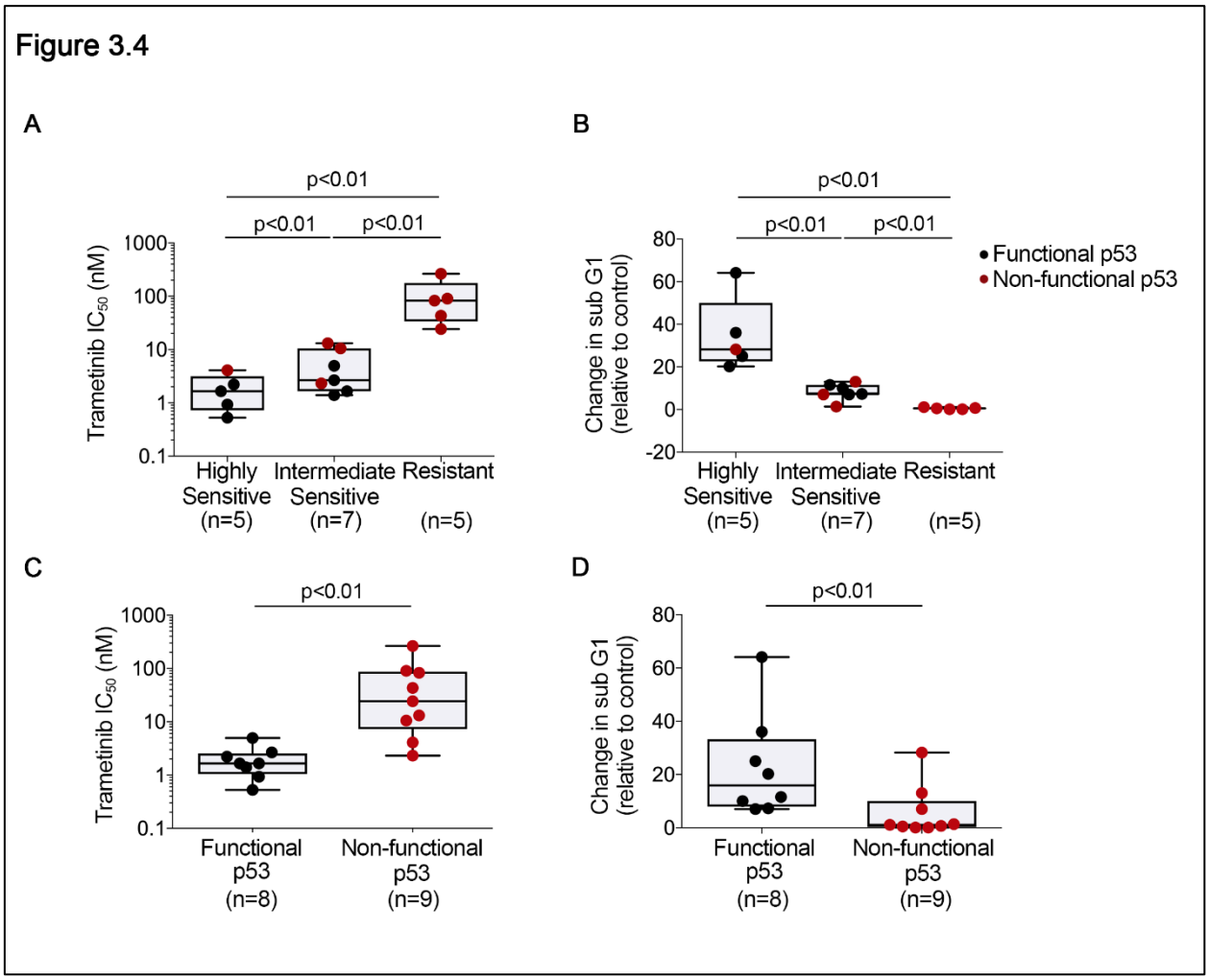

Figure 3.4: Melanoma sensitivity to trametinib is associated with p53 functional status

Box plots show (A) trametinib IC_{50} values and (B) change in sub G1 (relative to DMSO-treated control) of melanoma cells grouped according to trametinib sensitivity. Cell lines with non-functional p53 are shown in red. Statistical comparison between groups was performed using Kruskal-Wallis with Dunn's multiple comparison test. Adjusted p-values are shown. (C) Trametinib IC_{50} values and (D) change in sub G1 (relative to DMSO-treated control) is shown according to p53 functional status. Statistical comparison between groups was performed using a Mann-Whitney test. Each dot represents one cell line (mean of at least three independent experiments), box plots indicate the median and the interquartile range and the whiskers indicate the range.

3.3.3 Knockdown of p53 expression had minimal effects on trametinib resistance

To identify the precise contribution of p53 function on melanoma responses to MEK inhibition, we examined the effects of p53 knockdown in four melanoma cell lines. These cell lines included the *BRAF*^{V600E}-mutant A375 cells and the three sensitive triple WT cell lines (C037M1, D35, A04-GEH), all with WT *TP53* and functional p53 (Table 3.2). Melanoma cell lines were lentivirally-transduced with one of two independent p53 shRNA constructs or a negative control shRNA construct without homology to any known human gene. Downregulated p53 expression was confirmed 72 h post transduction in the p53-silenced cell lines by western blotting (Figure 3.5).

Figure 3.5

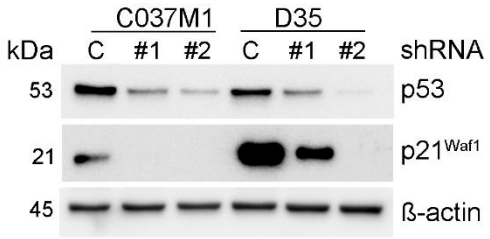

Figure 3.5: p53 silencing in melanoma

Western blot for p53 and p21^{Waf1} in melanoma cells 72h post transduction with lentivirus expressing p53 shRNA molecules #1 and #2 compared to transduction with lentivirus expressing control (C) non-targeting shRNA ([MOI]=5). ß-actin stain was used as loading control.

The p53 function was also examined in the control and p53-silenced cell lines following nutlin-3 treatment. Predictably, nutlin-3 treatment induced less cell growth inhibition in two p53-silenced cell lines compared to control (Figure 3.6), although this was not evident in the C037M1 or D35 cells which show no significant or minimal nutlin-3-induced arrest.

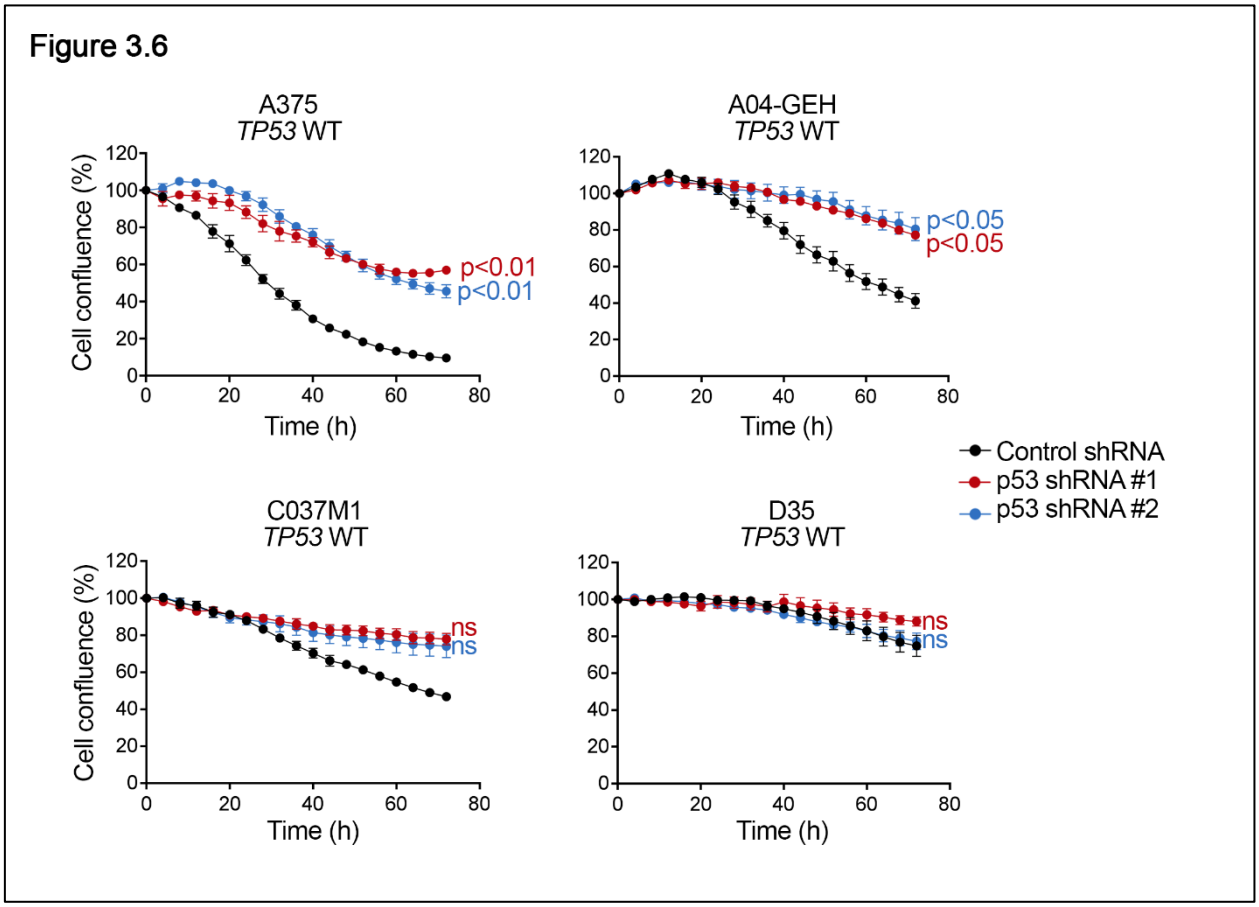

Figure 3.6: Nutlin-3 response in melanoma cell lines with or without p53 suppression

Control-transduced and p53-silenced melanoma cell lines (A375, C037M1, A04-GEH, and D35) were treated with DMSO or 20 µM nutlin-3 for 72 h, and cell proliferation examined every 4 h using the Incucyte real-time proliferation assay. Graphs show percentage cell confluence and data represent mean of at least three independent experiments and error bars represent the standard error of the mean. AUC was calculated for each cell line and difference in AUC between control shRNA and p53-silenced cells were compared using paired t-test. ns, not significant.

Response to trametinib was examined in the control and p53-silenced melanoma cell lines using MTT assays and cell cycle analysis (Figure 3.7). We found that p53 silencing had no impact on trametinib sensitivity in the *BRAF*^{V600}-mutant cell line A375 (Figure 3.7). Compared to control A375 (IC_{50} 1 nM), the p53-silenced A375 cells had equivalent trametinib IC_{50} values (IC_{50} 1.2 and 0.8 nM). Similarly, p53 suppression in the triple WT D35 and A04-GEH cell lines did not change trametinib IC_{50} values (Figure 3.7). The downregulation of p53 did not alter the level of trametinib-induced cell death or S phase inhibition in three of the four melanoma cell lines tested (Figure 3.8). Interestingly, the triple WT cell line C037M1 showed a dramatic decrease in cell death following trametinib treatment in the p53-silenced cells compared to control, although IC_{50} values remained comparable (Figure 3.7 and 3.8).

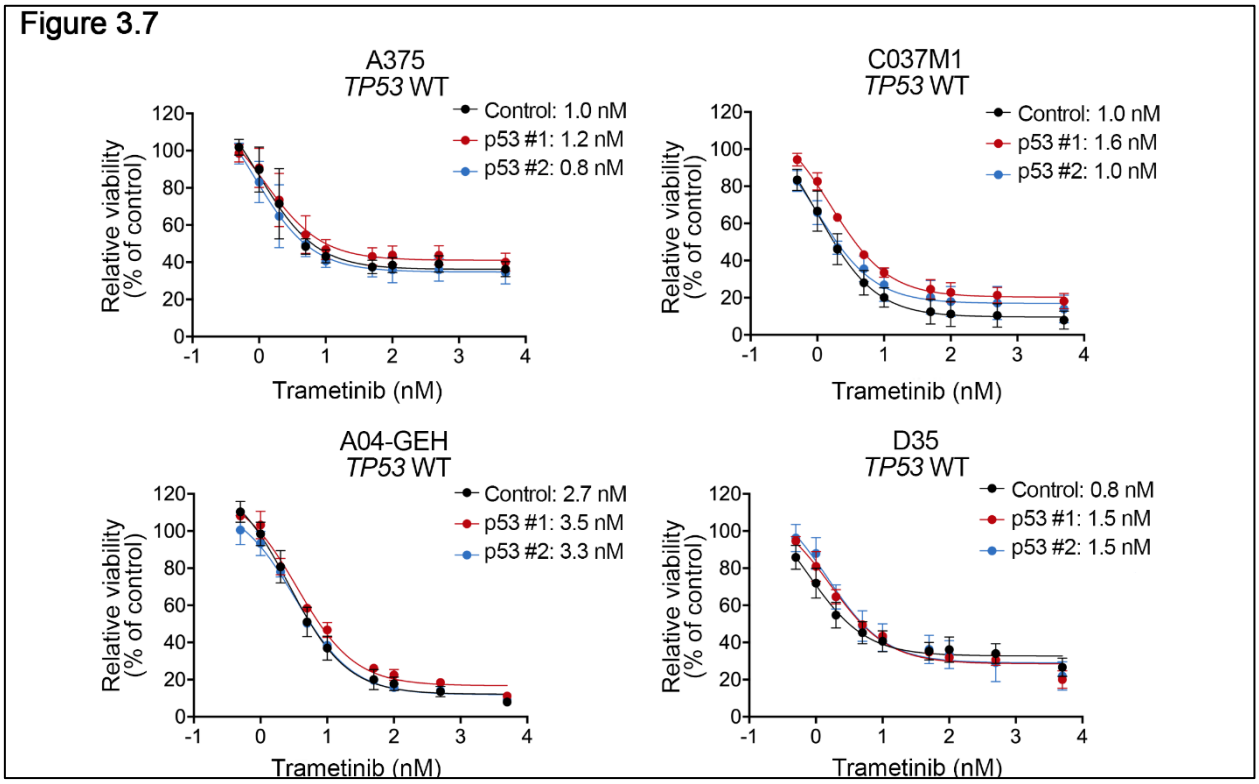

Figure 3.7: Loss of p53 does not confer MEK inhibitor resistance in melanoma
Melanoma cells were transduced with control shRNA, p53 shRNA #1 or p53 shRNA #2 for 72 h, and dose response curves were obtained after treatment with trametinib at varying doses for 72 h for each cell line. Trametinib IC_{50} values for each cell line are shown. Data represent mean and standard deviation of at least three independent experiments.

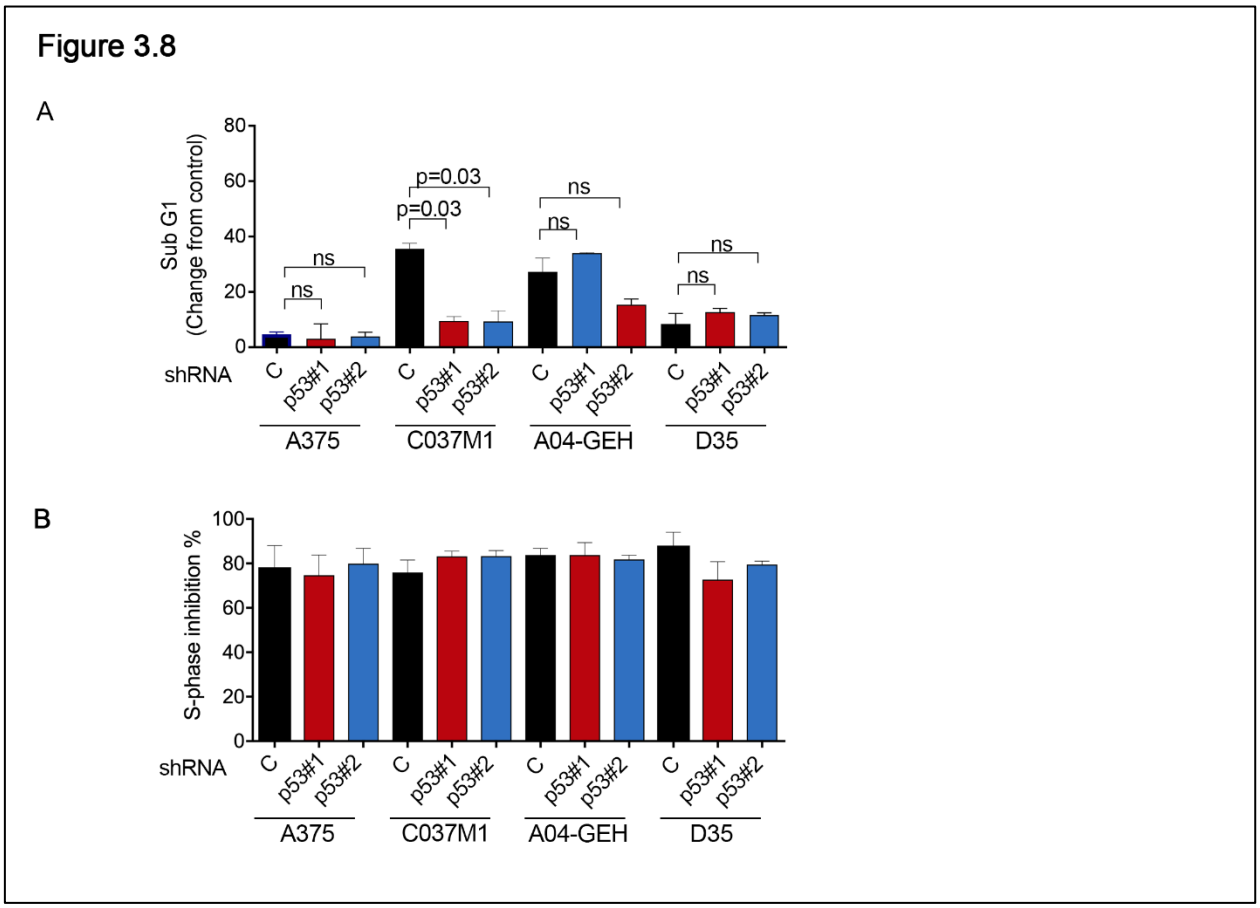

Figure 3.8: Loss of p53 does not alter cell cycle effects induced by MEK inhibition in melanoma

(A) Change in percentage of sub G1 and (B) S phase inhibition in control shRNA, p53 shRNA #1 or p53 shRNA #2-transduced melanoma cell lines after trametinib treatment (10 nM) for 72 h. Data represent median and interquartile range of at least three independent experiments. Statistical comparison between control and p53-silenced cells was performed using Mann-Whitney test. ns, not significant. No significant differences were detected in the percentage of S-phase inhibition.

To understand how trametinib treatment altered pathway activity in these p53-silenced melanoma cells (A375, C037M1, A04-GEH and D35), we examined the expression of p53 pathway downstream effector $p21^{Waf1}$, MAPK downstream effectors (p-ERK, p-p90RSK, DUSP6, p-S6), and PI3K/AKT downstream effectors (p-AKT, p-p70S6K). As expected, all four p53-silenced cell lines showed downregulated $p21^{Waf1}$ expression compared to their respective controls (Figure 3.9A). Interestingly, MEK inhibition by trametinib decreased $p21^{Waf1}$ expression in triple WT melanoma cell lines, but not in the *BRAF*^{V600}-mutant cell line A375 (Figure 3.9B), suggesting different mechanisms regulating cell cycle arrest or apoptosis in *BRAF*^{V600}-mutant compared to triple WT melanoma cell lines. p53-silenced C037M1 cells showed weaker suppression of p-S6 in response to trametinib compared to control transduced cells (Figure 3.9B). In contrast, the other three cell lines showed potent suppression of S6 phosphorylation in response to trametinib, regardless of p53 status (Figure 3.9C). p53 suppression did not alter PI3K/AKT signalling at baseline or in response to trametinib in all four cell lines (Figure 3.9).

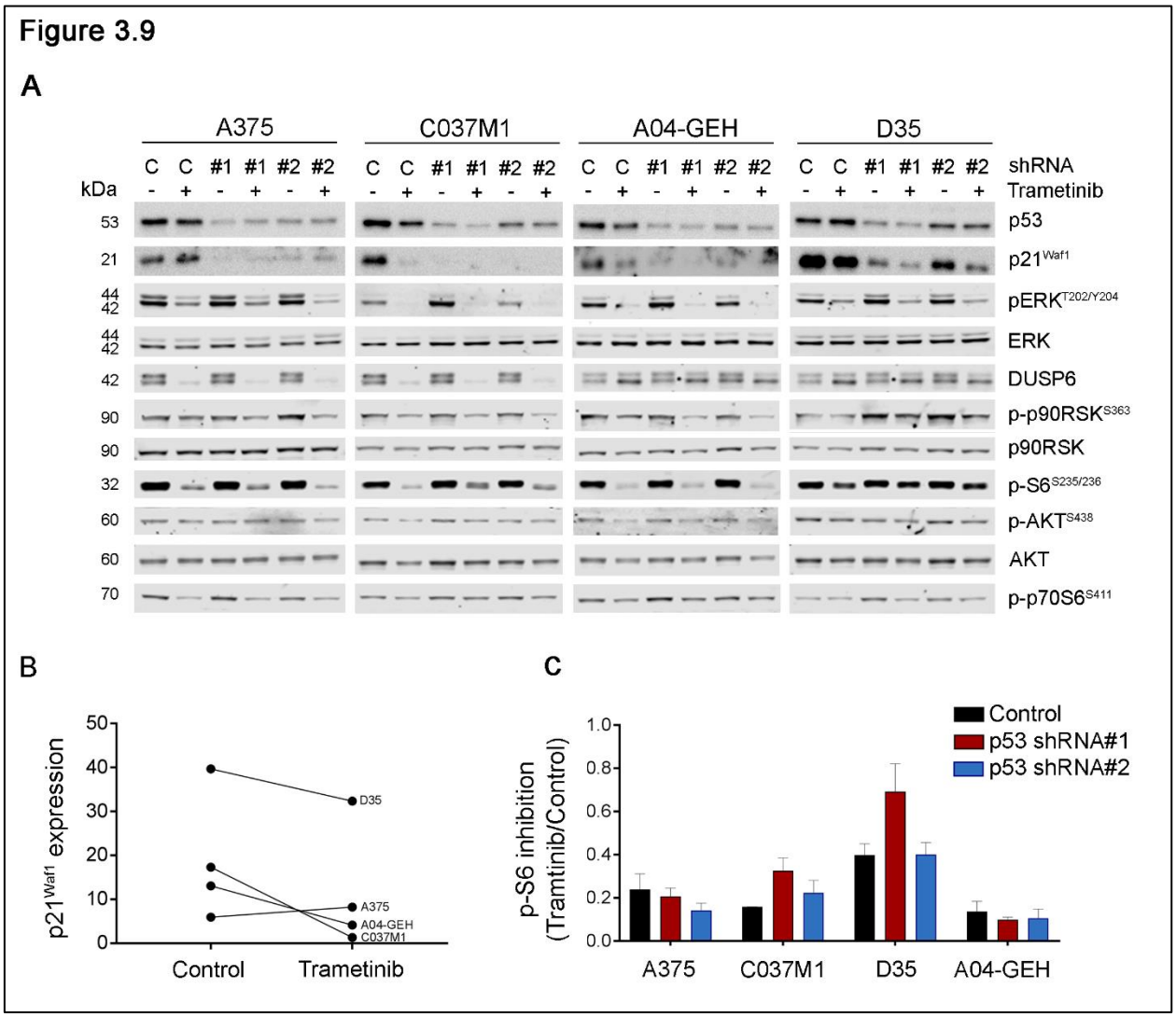

Figure 3.9: Effects of p53 silencing on trametinib-induced signalling changes in melanoma

(A) Western blots for protein markers of p53 (p53, p21^{Waf1}), MAPK (p-ERK, ERK, DUSP6, p-p90RSK, p90RSK, p-S6) and PI3K (p-AKT, AKT, p-p70S6K) activity in control or p53 shRNA-transduced cells 24 h after treatment with DMSO (-) or 10 nM trametinib (+). C, control; #1, p53 shRNA#1; #2, p53 shRNA#2. REVERT total protein stain was performed as loading control. (B) Quantitative analysis of p21^{Waf1} in p53 shRNA-transduced melanoma cells before (control) and 24 h after trametinib treatment (10 nM). Data shown are from a representative western blot, and the densitometric values of p21^{Waf1} were measured using LICOR Image Studio™ software. (C) Change in densitometric values of phosphorylated S6 (trametinib/DMSO control) in melanoma cell lines transduced with control shRNA (black) compared to p53 shRNA-transduced cells (red and blue). Data represent median and range of two independent experiments. Statistical comparison between control and p53-silenced cells was performed using the Mann-Whitney test, no significance detected.

3.3.4 Reactivation of p53 did not enhance melanoma response to trametinib

Considering that non-functional p53 was associated with trametinib resistance, we hypothesised that restoration of p53 function may increase sensitivity of these cells to trametinib. We selected five cell lines with functional p53 (A375, C037M1, A04-GEH, D35, and C022M1), and treated them with nutlin-3 (20 µM), trametinib (10 nM), or the combination. Another five cell lines with non-functional p53 (C084M, MeWo, SMU15-0217, D24M and D22M1) were also included for comparison. As expected, cell lines with non-functional p53 showed no change in cell proliferation with nutlin-3 treatment, and these cell lines also showed no proliferative change in response to trametinib alone, or the combination (Figure 3.10). However, in two of the five cell lines with functional p53 (A375 and A04-GEH), nutlin-3 treatment resulted in more potent cell growth inhibition compared to trametinib treatment alone, although the combination of nutlin-3 and trametinib did not further increase growth inhibition. In the other two cell lines (C037M1 and D35), trametinib, rather than nutlin-3, was the more potent cell cycle inhibitor, and inhibition was not enhanced when the two were combined, though no significance determined in D35 (Figure 3.10). Interestingly, we found one *TP53* WT cell line C084M, which had intermediate sensitivity to trametinib, showed slight reduction in cell growth with nutlin-3 or trametinib treatment. However, when nutlin-3 was combined with trametinib, this cell line showed more pronounced growth inhibition when compared to controls (Figure 3.10).

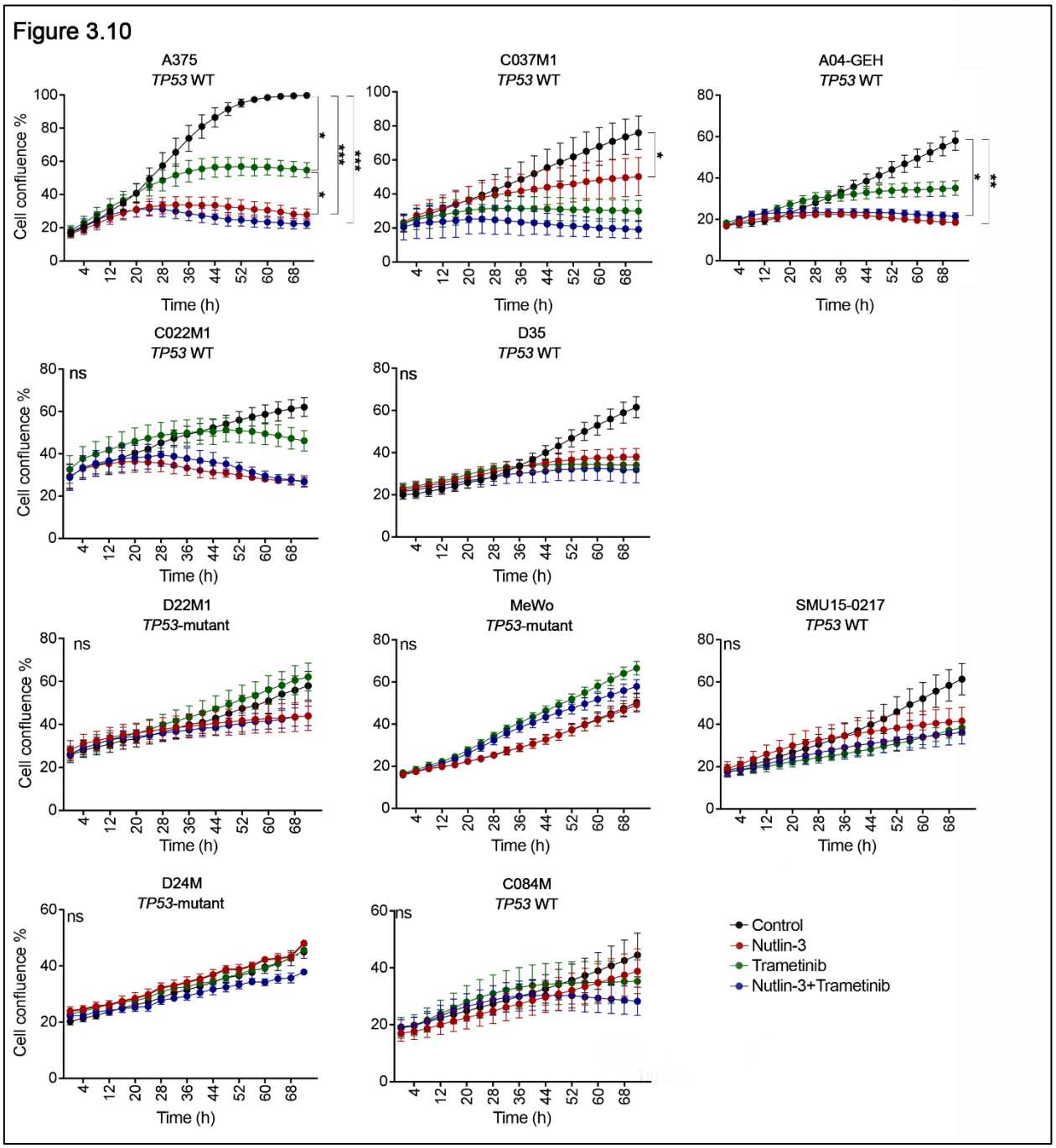

Figure 3.10: Treatment of melanoma cells with trametinib alone or in combination with nutlin-3

Melanoma cell lines were treated with DMSO, trametinib (10 nM) and nutlin-3 (20 µM), either alone or in combination, for 72 h and cell proliferation examined every 4 h using the IncuCyte real-time proliferation assay. Graphs show percentage cell confluence and data represent mean of at least three independent experiments and error bars represent the standard error of the mean. AUC was calculated for each cell line and differences in AUC between groups compared using paired one-way ANOVA with Holm-Sidak's multiple comparison test. ns, not significant. *adjusted p-value<0.05, ** adjusted p-value <0.01, ***adjusted p-value<0.001.

3.4 Discussion

The majority of melanoma patients treated with BRAF and MEK inhibitors develop resistance within the first year of treatment, and the lack of durable responses remains a major barrier to improving patient survival (320, 356). Hence, there has been significant interest in exploring novel combination therapies as a means of overcoming or circumventing resistance to BRAF/MEK inhibitors in melanoma.

The p53 tumour suppressor is often referred to as the guardian of the genome due to its central role in regulating cell cycle arrest and apoptosis in response to various cellular stressors, including DNA damage, aberrant oncogene activity and ribosome stress. The role of p53 in melanomagenesis has been controversial. *TP53* is not commonly mutated in melanoma, although its regulation appears to be frequently altered due to loss of the $p14^{ARF}$ or overexpression of the negative regulators MDM2/MDM4 (59, 97, 357, 358). Further, p53 expression can limit the progression of metastatic melanoma from nevi via the activation of the $p21^{Waf1}$ cell cycle regulatory cascade. Transgenic animal models also support the contribution of p53 in melanomagenesis; TP-RasV12G transgenic mice on the Mdm4+/− background showed reduced melanoma growth, less metastasis and increased survival compared to TP-RasV12G transgenic mice (359), and p53 deficiency enhanced the incidence of melanoma development and metastasis in *BRAF*-mutant transgenic mouse and zebrafish models (348, 360-362). However, the role of p53 in response and resistance to MAPK pathway inhibition, particularly in *BRAF*/*RAS* WT melanoma cells, has not been well studied.

In the present study, we demonstrated that resistance to MEK inhibition was associated with *TP53* mutation and p53 loss-of-function in melanoma (Figure 3.1 and 3.4). However, suppression of p53 expression did not confer resistance to trametinib treatment, in both *BRAF*-mutant and triple WT melanoma cell lines. Only one triple WT melanoma cell line

C037M1 showed significantly reduced trametinib-induced cell death upon p53 silencing compared to control silenced cells, suggesting that this cell line may be reliant on the p53 pathway for apoptosis in response to MEK inhibition, whereas this effect was not observed in the other cell lines tested (Figure 3.7). This was also reflected by the western blotting data showing that p53-silenced C037M1 cells had less inhibition of phosphorylated S6 following trametinib treatment compared to control-transduced cells. (Figure 3.9). Apoptosis of melanoma cells following treatment with MEK inhibitors has been shown to depend on the upregulation of pro-apoptotic proteins PUMA and Bim, and the down-regulation of the anti-apoptotic Bcl-2 family member Mcl-1 (363), all of which are regulated by p53 (364). Moreover, the Bcl-2 homology domain 3 (BH3) mimetic induces activation of p53 via accumulation of reactive oxygen species (ROS), and together with MEK inhibitor, can synergistically promote tumour cell killing (365). Therefore, apoptosis of the triple WT cell line C037M1 in response to MEK inhibition may involve the regulation of pro-apoptotic and anti-apoptotic proteins in a p53-dependent manner. However, the other three cell lines (A375, D35, A04-GEH) did not appear to rely on p53 for cell survival, and a recent study showed that MEK inhibitor treatment promoted PUMA expression via the ERK/Foxo3a signalling pathway, suggesting that cell death may be regulated by alternative signalling mechanisms in some melanoma cells (366). For future work, we aim to examine the pro-apoptotic and anti-apoptotic targets of p53 by western blotting to confirm the effects and mechanisms of cell death induced by MEK inhibition.

Because p53 loss-of-function is associated with resistance to trametinib, we examined if p53 reactivation, either alone or in combination with trametinib, can enhance melanoma cell cycle arrest or cell death. Several small molecular activators of p53 are available such as nutlin-3, which inhibits MDM2, SAH-p53-8 which inhibits MDM4, and PRIMA-1, which converts p53 to an active conformation to restore its DNA binding and transcriptional

activity. Use of these activators has been shown to have synergistic effects with MAPK inhibition in suppressing cell cycle progression or enhancing apoptosis in melanoma (100, 340, 367-369). However, our study shows that trametinib treatment in combination with p53 reactivation using nutlin-3 enhanced cell growth inhibition in only one triple WT cell line (*TP53* WT) C037M compared to single agent treatment, although some *TP53* WT cell lines, including *BRAF*^{V600E}-mutant cell line A375 and triple WT cell lines A04-GEH, showed more potent cell growth inhibition with nutlin-3 treatment compared to trametinib (Figure 3.10).

Some studies have attempted to delineate the mechanism underlying p53 deregulation and resistance to MAPK pathway inhibition in *BRAF*-mutant or *NRAS*-mutant melanomas. Najem *et al.* (2017) showed that activation of the anti-apoptotic p53 downstream effector Bcl2 was strongly associated with MEK inhibitor resistance in *NRAS*-mutant melanoma, and p53 reactivation synergised with MEK inhibition to promote apoptosis (370). Another study revealed that the MAPK effector DUSP6 is regulated by the p53 pathway through its upstream ATM (ataxia telangiectasia-mutated) protein, and trametinib synergised with MDM2 inhibitors through a DUSP6-dependent mechanism to enhance melanoma cell death (371). However, in our study, we observed cell growth inhibition with the MDM2 inhibitor nutlin-3 but no cell death. Five cell lines that were resistant to trametinib were *TP53*-mutant or had non-functional p53, and not surprisingly, nutlin-3 treatment had no impact on trametinib response in these cells. Another eight cell lines were p53 functional, and p53 reactivation induced potent cell cycle arrest in these cell lines, indicating that these cell lines depended on the p53 pathway for cell growth (Table 3.2, Figure 3.2).

Several clinical trials are currently assessing the efficacy of combination MAPK inhibitors and p53 activators in melanoma. For instance, a phase I clinical trial using the MDM2 inhibitor AMG 232 combined with trametinib and/or dabrafenib showed promising anti-

tumour activity in *TP53* WT cutaneous melanoma patients (NCT02110355) (372). Use of an MDM2 inhibitor in combination with MEK inhibition is also being studied in other cancer types, and the combination of trametinib with the MDM2 inhibitor RG7388 enhanced anti-tumour effects in glioblastoma cells (373).

In the present study, we showed that p53 reactivation can inhibit tumour cell growth in some *TP53* WT melanoma cell lines, indicating its potential efficacy as a combinatorial therapy in melanoma. However, increased anti-tumour effects combining p53 reactivation and MEK inhibition was detected only in one cell line, suggesting that more complicated combination treatment strategies will be needed, such as the targeting of anti-apoptotic proteins in combination with MEK inhibition and p53 reactivation.

Supplementary Figures

Figure S3.1

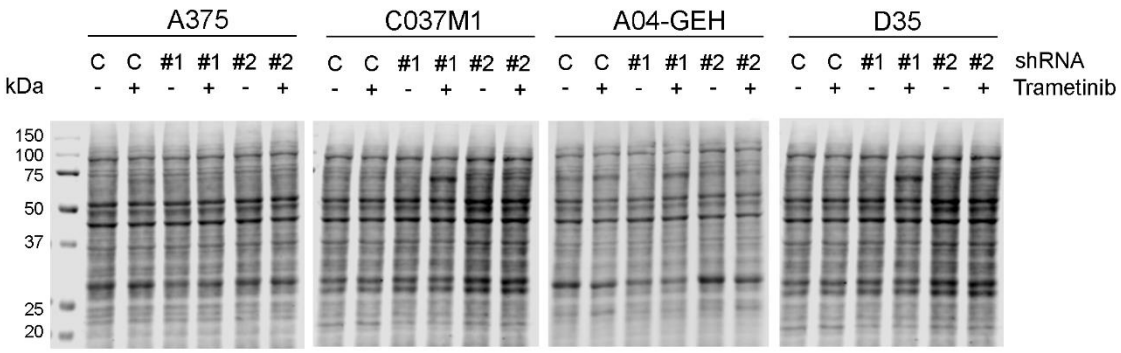

Figure S3.1: Detection of the REVERT total protein stain

Western blots for the REVERT total protein stain, performed as loading control for Figure 3.9. Indicated control or p53 shRNA-transduced melanoma cell lines were treated with DMSO (-) or 10 nM trametinib (+) for 24h. C, control; #1, p53 shRNA#1; #2, p53 shRNA#2.

Chapter 4

Multiple signaling pathways are active in BRAF/RAS wild type melanoma

4.1 Introduction

Cutaneous melanoma has a mutation burden of 16.8 mutations/Mb, the highest reported for any cancer type (374). These mutations are predominantly driven by UV exposure (375), and although the majority are passenger mutations that confer little or no growth advantage, several common driver alterations, affecting the *BRAF*, *NRAS* and *NF1* genes, have been identified. Approximately 51% of cutaneous melanomas have activating *BRAF* mutations, and almost 90% of these mutations alter the valine (V) at codon 600 (Cancer Genome Atlas, 2015); 85% of these *BRAF* V600 mutations change valine (V) for glutamic acid (E) (V600E), 8-20% substitute valine (V) for lysine (K) (V600K) and 1-2% change valine (V) for arginine (R) (V600R) (17, 61, 63, 64, 339, 376).

Hot-spot activating mutations in the upstream NRAS GTPase occur in 30% of cutaneous melanoma and commonly alter glycine (G) at position 12, glycine at position 13 or glutamine (Q) at position 61 (17, 45, 59). The *NF1* gene encodes a negative regulator of RAS and is the third most frequently mutated gene, altered in approximately 13% of melanomas (59). Predictably, these three driver genes are usually altered in melanoma in a mutually exclusive manner (77). Many other genes, which are less frequently altered, also contribute to the development and treatment response of cutaneous melanoma (Table 4.1).

Activating *BRAF* and *RAS* mutations induce the constitutive activation of the MAPK cascade. This signalling pathway plays a central role in regulating melanoma proliferation, migration and survival (377, 378). Consequently, inhibition of MAPK signalling with selective BRAF and MEK inhibitors has demonstrated significant anti-tumour activity in patients with advanced $BRAF^{V600}$-mutant melanoma (184, 185, 299, 324). MAPK signalling activation has also been identified in *BRAF*/*RAS* WT melanomas as a result of *NF1* loss, *KIT* activation and amplification, copy number and mutations

affecting *MAP2K1* (MEK1) and *MAPK3* (ERK1) genes (59, 80). However, the activity of alternate signalling pathways in *BRAF*/*RAS* WT melanoma are less well characterized, and potentially heterogenous considering the high mutation burden in *BRAF*/*RAS* WT melanoma (305). In one sequencing study of *BRAF*/*NRAS* WT melanoma samples, a number of activated signalling pathways, in addition to MAPK, were identified including GNAQ/GNA11, cell cycle progression, the p53/BCL survival network, MITF differentiation, NRAS, c-KIT and PI3K/AKT (305).

In Chapter 2 we confirmed that a subset of *BRAF*/*RAS* WT melanoma cell lines (8/13; 62%) was dependent on the MAPK pathway for survival and/or proliferation. However, 38% (5/13) of *BRAF*/*RAS* WT melanoma cell lines showed no or minimal response to MEK inhibition, which suggests activation of compensatory alternate survival signals. Moreover, these MEK inhibitor-resistant cells showed higher mutation load and presence of frequent driver mutations, suggesting that other oncogenic signalling pathways may contribute to survival.

In this study, we compared the activity of 43 kinases and proteins using the Human Phospho-Kinase Antibody Array (R&D Systems) in a panel of 13 *BRAF*/*RAS* WT (six triple WT and seven *NF1*-mutant) and seven $BRAF^{V600}$-mutant (five $BRAF^{V600E}$ and two $BRAF^{V600K}$) melanoma cell lines. The kinase data were used to examine the activity of signalling pathways, and the potential contribution of these pathways to MEK response and resistance in melanoma. The efficacy of combination therapies simultaneously inhibiting multiple signalling pathways was also examined in *BRAF*/*RAS* WT melanoma.

Table 4.1: Commonly altered genes that influence melanoma development, progression and treatment response

Gene	Description	Frequency	Role in melanoma
ARID2	AT-rich interaction domain 2	14%	Associated with better response to immunotherapy (379).
BRAF	BRAF Proto-oncogene, Serine/Threonine kinase	51%	Driver oncogene, associated with better prognosis. Targeted therapy available (380).
CDKN2A	Cyclin dependent kinase inhibitor 2A	41%	Loss associated with poor prognosis (381) and resistance to immunotherapy and BRAF inhibitors (356, 382). Germline mutations predispose to melanoma (383).
KIT	KIT Proto-Oncogene Receptor tyrosine kinase	7%	Altered mostly in mucosal and acral melanoma, associated with poor prognosis (384)
MAP2K1	Mitogen-activated protein kinase kinase 1	7%	Driver oncogene, and associated with poor prognosis (385) and resistance to BRAF and MEK inhibitors (386, 387).
NRAS	NRAS Proto-Oncogene, GTPase	30%	Driver oncogene, associated with high frequency of metastasis and poor prognosis (380), and resistance to BRAF inhibitors (290, 300).
NF1	Neurofibromin 1	13%	Loss associated with high mutation burden, poor prognosis (78) and resistance to BRAF inhibitor (76).
PPP6C	Protein phosphatase 6 catalytic subunit	8%	Driver oncogene, early event in melanoma progression, stop mutations associated with metastases (388).
PTEN	Phosphatase and tensin homolog	15%	Loss associated with metastasis and poor prognosis (93) and resistance to immunotherapy and BRAF inhibitors (389, 390).
RASA2	Ras P21 protein activator 2	6%	Associated with poor prognosis (391).
RAC1	Rac Family Small GTPase	10%	Driver oncogene, associated with metastasis and poor prognosis (392).
TP53	Tumour protein P53	17%	Associated with poor prognosis (393).

Frequency of genetic alterations (mutations and copy number alterations) were derived from the Skin Cutaneous Melanoma data set (TCGA, PanCancer Atlas) using cBioPortal (94, 95)

4.2 Methods

4.2.1 Cell culture and reagents

The details of cell lines and culture conditions included in this study are described in Chapter 2 (Section 2.2.1). All inhibitors were purchased from Selleck Chemicals (Houston, TX, USA) and prepared in dimethyl sulfoxide (DMSO). The MEK1/2 inhibitor trametinib (GSK1120212) and the inhibitor imatinib (GSK2118436) (a multi-target inhibitor of v-Abl, c-Kit and PDGFR) were prepared as 1 mM stocks. The EGFR inhibitor erlotinib and SRC inhibitor dasatinib were prepared as 10 mM stocks.

4.2.2 Cell cycle analysis

Adherent and floating melanoma cells were collected for cell cycle and apoptosis analysis as previously described (321). Melanoma cells were treated with 10 nM trametinib, 2 µM erlotinib, 10 nM imatinib, 1 µM dasatinib, either alone or in combination, or with 0.1% DMSO for 72 h before performing cell cycle analysis by flow cytometry using propidium iodide. The detailed method for cell cycle and data analysis are described in Chapter 2 (Section 2.2.4).

4.2.3 Western blotting

Melanoma cells were treated with 10 nM trametinib, 2 µM erlotinib, 10 nM imatinib, 1 µM dasatinib, either alone or in combination, or with 0.1% DMSO for 24 h before extracting total cellular proteins. Western blotting was carried out as described in Chapter 2 (Section 2.2.5). Western blots were probed with the following primary antibodies targeting: total ERK (1:2000, 137F5, Cell Signalling, MA, USA), phosphorylated ERK (Tyr204, 1:500, E4, Santa Cruz, TX, USA), phosphorylated EGFR (Tyr1068, 1:500, Cell Signalling), total

EGFR (1:2000, D38B1 (XP), Cell Signalling), phosphorylated SRC (Tyr416, 1:500, Cell Signalling), and total SRC (1:50, Clone 327, Abcam, Cambridge, UK).

4.2.4 Human Phospho-Kinase Array

The Human Phospho-Kinase Array Kit (R&D Systems, MN, USA) was used to detect the relative level of tyrosine phosphorylation of 43 distinct phospho-kinases. Melanoma cells were treated with 10 nM trametinib or 0.1% DMSO for 24 h before extracting total cellular proteins using the lysis buffer provided, and according to the manufacturer's protocol. Briefly, membrane arrays were blocked with blocking buffer for 1 h, then incubated with 540 µg of total cell lysate (total protein obtained by combining three independent experiments) overnight at 4°C. The arrays were washed and incubated with biotinylated antibodies for 2 h. The arrays were washed again, incubated with streptavidin–horseradish-peroxidase-conjugated detection antibodies, treated with Clarity™ Western ECL (enhanced chemiluminescence) solution (Bio-Rad, CA, USA), and exposed using the ChemiDoc™ Imaging System (Bio-Rad). The outline of these kinase arrays, including protein identity and coordinates, are shown in Figure 4.1

Densitometry values of each cell line were selected from similar exposure times which showed equivalent values for the reference spots (positive signals to confirm the assay performance) and the mean of the duplicate values, coefficient of variation of which was less than 10%, were calculated as the expression data for each phosphorylated kinase or total protein.

Figure 4.1

Human Phospho-Kinase Array

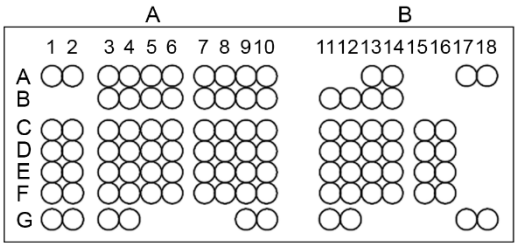

Membrane/Coordinate	Target
A-A1, A2	Reference Spot
A-A3, A4	p38α$^{T180/Y182}$
A-A5, A6	ERK1/2$^{T202/Y204, T185/Y187}$
A-A7, A8	JNK 1/2/3$^{T183/Y185, T221/Y223}$
A-A9, A10	GSK-3α/ß$^{S21/S9}$
B-A13, A14	p53^{S392}
B-A17, A18	Reference Spot
A-B3, B4	EGFR^{Y1086}
A-B5, B6	MSK1/2$^{S376/S360}$
A-B7, B8	AMPKα1^{T183}
A-B9, B10	Akt 1/2/3^{S473}
B-B11, B12	Akt 1/2/3^{T308}
B-B13, B14	p53^{S46}
A-C1, C2	TOR^{S2448}
A-C3, C4	CREB^{S133}
A-C5, C6	HSP27$^{S78/S82}$
A-C7, C8	AMPKα2^{T172}
A-C9, C10	ß-Catenin
B-C11, C12	p70 S6 Kinase^{T389}
B-C13, C14	p53^{S15}
B-C15, C16	c-Jun^{S63}
A-D1, D2	Src^{Y419}
A-D3, D4	Lyn^{Y397}
A-D5, D6	Lck^{Y394}
A-D7, D8	STAT2^{Y689}
A-D9, D10	STAT5a^{Y694}

Membrane/Coordinate	Target
B-D11, D12	p70 S6 Kinase$^{T421/S424}$
B-D13, D14	RSK1/2/3$^{S380/S386/S377}$
B-D15, D16	eNOS^{S1177}
A-E1, E2	Fyn^{Y420}
A-E3, E4	Yes^{Y426}
A-E5, E6	Fgr^{Y412}
A-E7, E8	STAT6^{Y641}
A-E9, E10	STAT5b^{Y699}
B-E11, E12	STAT3^{Y705}
B-E13, E14	p27^{T198}
B-E15, E16	PLC-γ1^{Y783}
A-F1, F2	Hck^{Y411}
A-F3, F4	Chk-2^{T68}
A-F5, F6	FAK^{Y397}
A-F7, F8	PDGF Rß^{Y751}
A-F9, F10	STAT5a/b$^{Y694/Y699}$
B-F11, F12	STAT3^{S727}
B-F13, F14	WNK1^{T60}
B-F15, F16	PYK2^{Y402}
A-G1, G2	Reference Spot
A-G3, G4	PRAS40^{T246}
A-G9, G10	PBS (Negative Control)
B-G11, G12	HSP60
B-G17, G18	PBS (Negative Control)

Figure 4.1: Coordinates and identity of kinases and proteins on the Human Phospho-Kinase Array

A total number of 43 phosphorylated kinases and proteins, two total proteins (ß-catenin and HSP60), three reference spots, and two PBS negative control, spotted in duplicates, were included in the Human Phospho-Kinase Array. The coordinates and table adapted from the Human Phospho-Kinase Array Kit (R&D systems).

The expression data were $\log_2$ transformed and median normalised using R (Version 3.2.2) (394), and z-scores were calculated using the Morpheus online tool (https://software.broadinstitute.org/morpheus/). To identify differentially expressed phosphorylated kinases, normalised expression data between two groups was compared using a moderated t-test in Morpheus.

To explore the signalling pathway activity, kinases and proteins were grouped according to their associated pathways, as shown in Table 4.2. A total of 38 phospho-kinases and proteins were grouped into ten signalling pathways. The mean of z-scores for kinases implicated in each signalling pathway was calculated as the pathway activity score. Heatmap of the pathway activity score was generated using Morpheus (Broad Institute, MA, USA).

Table 4.2: Kinases and proteins included in each signalling pathway

Pathway		Kinases included in pathway score
MAPK	Mitogen-activated protein kinase pathway	p-ERK, p-RSK1/2/3
PI3K/AKT	Phosphatidylinositol 3-kinase/protein kinase B pathway	p-AKT, p-p70RSK, p-PRAS40, mTOR
P38	P38 pathway	p-p38, p-MSK1/2
JNK	c-Jun N-terminal kinase pathway	p-JNK1/2/3, p-c-Jun
RTK	Receptor tyrosine kinase pathway	p-EGFR, p-PDGFRß
AMPK	AMP-activated protein kinase pathway	p-AMPK, CREB
WNT	Wnt pathway	ß-catenin
SRC	Src family kinases pathway	p-Src, p-Lyn, p-Lck, p-Fyn, p-Yes, p-Fgr, p-Hck, and p-FAK
STAT	Signal transducer of activation pathway	STAT6, STAT5b, STAT2, STAT5a, STAT5a/b, STAT3
P53	P53 pathway	p-p53, p-Chk-2

4.2.5 Statistical analysis

Statistical analysis was performed in GraphPad Prism (Version 7) or Morpheus software. All statistical methods applied are detailed in each figure legend. Differences were considered to be statistically significant when $P < 0.05$.

4.3 Results

4.3.1 Heterogenous activation of kinases reflects melanoma genotype and response to trametinib

We previously demonstrated that *BRAF*/*RAS* WT melanoma cell lines have variable responses to single or combination inhibitors of RAF, ERK and MEK inhibitors (Figure 2.1 and 2.2). We hypothesised that the *BRAF*/*RAS* WT cell lines that were resistant to these inhibitors may depend on alternative signalling pathways for survival. Therefore, we explored the signalling activity of 20 melanoma cell lines including seven $BRAF^{V600}$-mutant, six triple WT and seven *NF1*-mutant cells using the Human Phospho-Kinase Arrays. Examples of probed phospho-arrays derived from three melanoma cells showing variable responses to trametinib are shown in Figure 4.2.

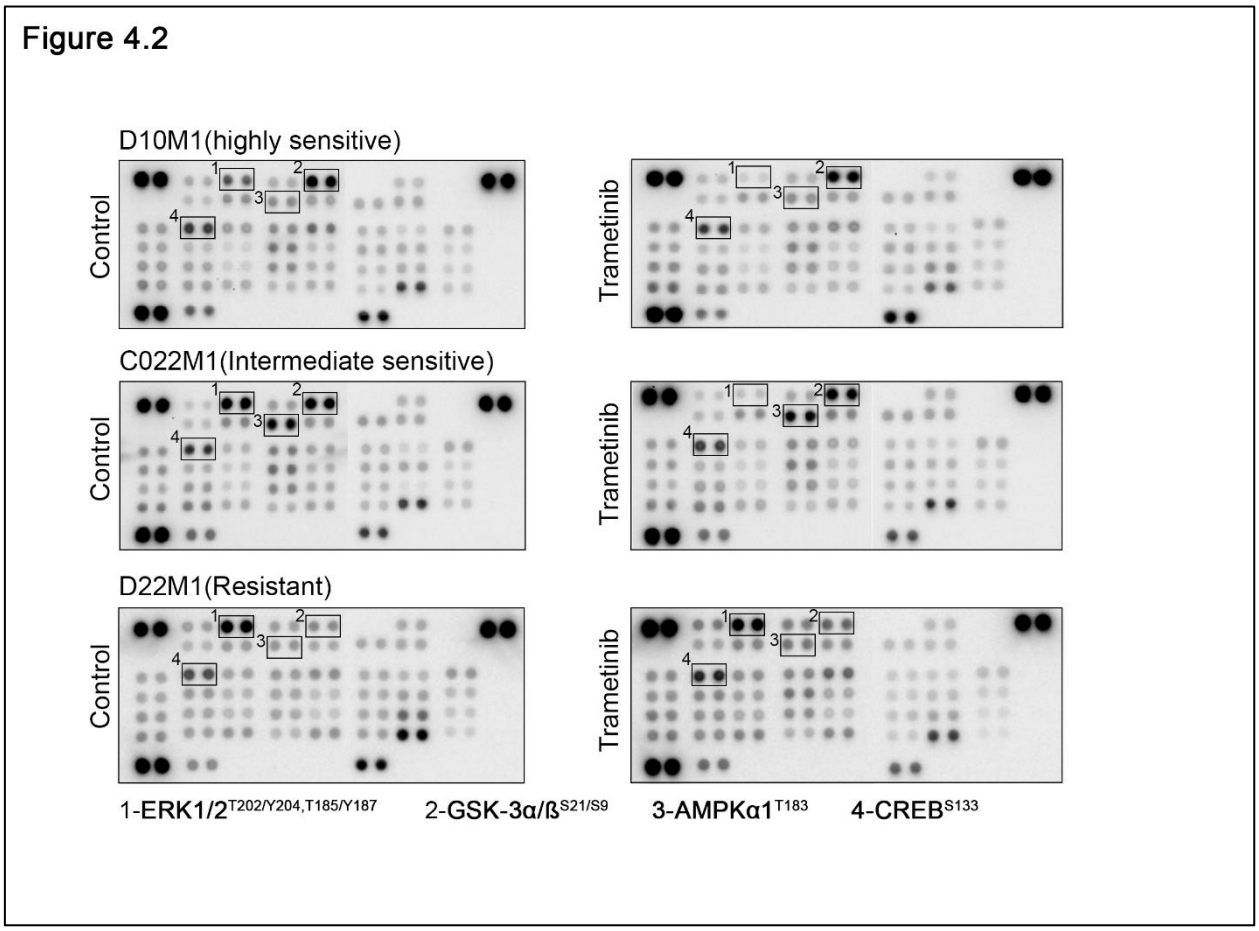

Figure 4.2: Phospho-kinase array membrane blots of melanoma cell lines before and after trametinib treatment

Representative images of the phospho-kinase array membrane blots from three *BRAF*/*RAS* WT melanoma cell lines after treating cells with 0.1% DMSO (Control) or 10 nM trametinib at 24 h. Coordinates for each membrane were provided in Figure 4.1, and a few example proteins are indicated for reference.

Trametinib response and kinase phosphorylation

Densitometric analysis of the kinase arrays revealed several important features of response and resistant to trametinib.

1. Phosphorylated ERK (pERK) levels were comparable across all 20 cell lines at baseline (DMSO-treated), regardless of whether the cells were sensitive (highly and intermediate sensitive) or resistant to trametinib (Figure 4.3A).

2. The change in pERK levels (i.e. pERK in trametinib-treated cells/pERK in DMSO-treated cells) was significantly greater in melanoma cells showing some sensitivity to trametinib compared to resistant melanoma cells (Figure 4.3B). This corresponded to pERK levels after trametinib treatment being significantly lower in melanoma cells displaying sensitivity to trametinib (Figure 4.3C).

3. Phosphorylation of other kinases was highly variable in our melanoma cell lines, and no other kinase was differentially phosphorylated at baseline (Table S4.1), after trametinib (Table S4.2) or when fold change (trametinib-treated cells/DMSO-treated cells; Table S4.3) in kinase phosphorylation was examined in trametinib-sensitive versus trametinib-resistant melanoma cells (false discovery corrected-t-test $q<0.05$; Figure 4.4). Change in pERK levels (i.e. pERK in trametinib-treated cells/pERK in DMSO-treated cells) produced a q-value of 0.12 and was the best at discriminating the trametinib-sensitive versus resistant melanoma cells (Figure 4.4, Table S4.3).

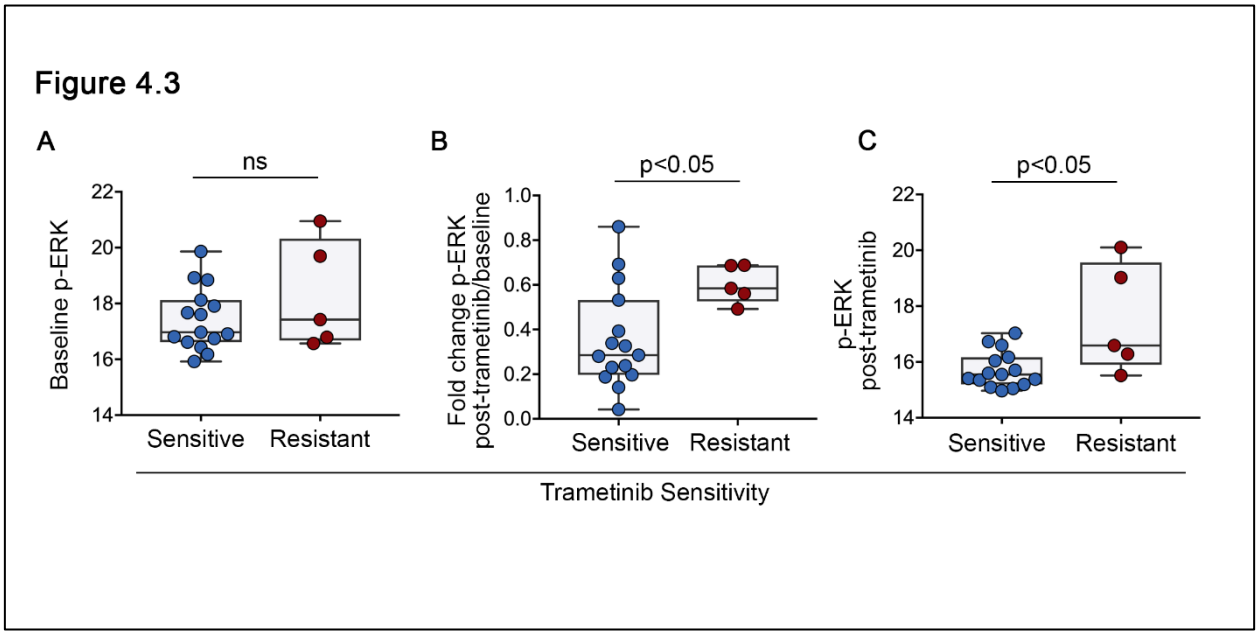

Figure 4.3: ERK phosphorylation in response to MEK inhibition reflects melanoma cell response to trametinib

The expression data for p-ERK were calculated as the mean of duplicated densitometry values from the Human Phospho-Kinase Array, median normalised as defined in Section 4.2.4. Box plots showing (A) baseline expression levels of p-ERK, (B) change in p-ERK (trametinib-treated/DMSO-treated cells) and (C) p p-ERK levels post-trametinib treatment across the panel of 20 melanoma cell lines. The individual points represent data of each cell line from one experiment. Cells showing high and intermediate sensitivity to trametinib have been grouped as sensitive cells. Median and interquartile ranges are shown on the box plots. Statistical comparison between two groups performed using Mann-Whitney test. ns, not significant.

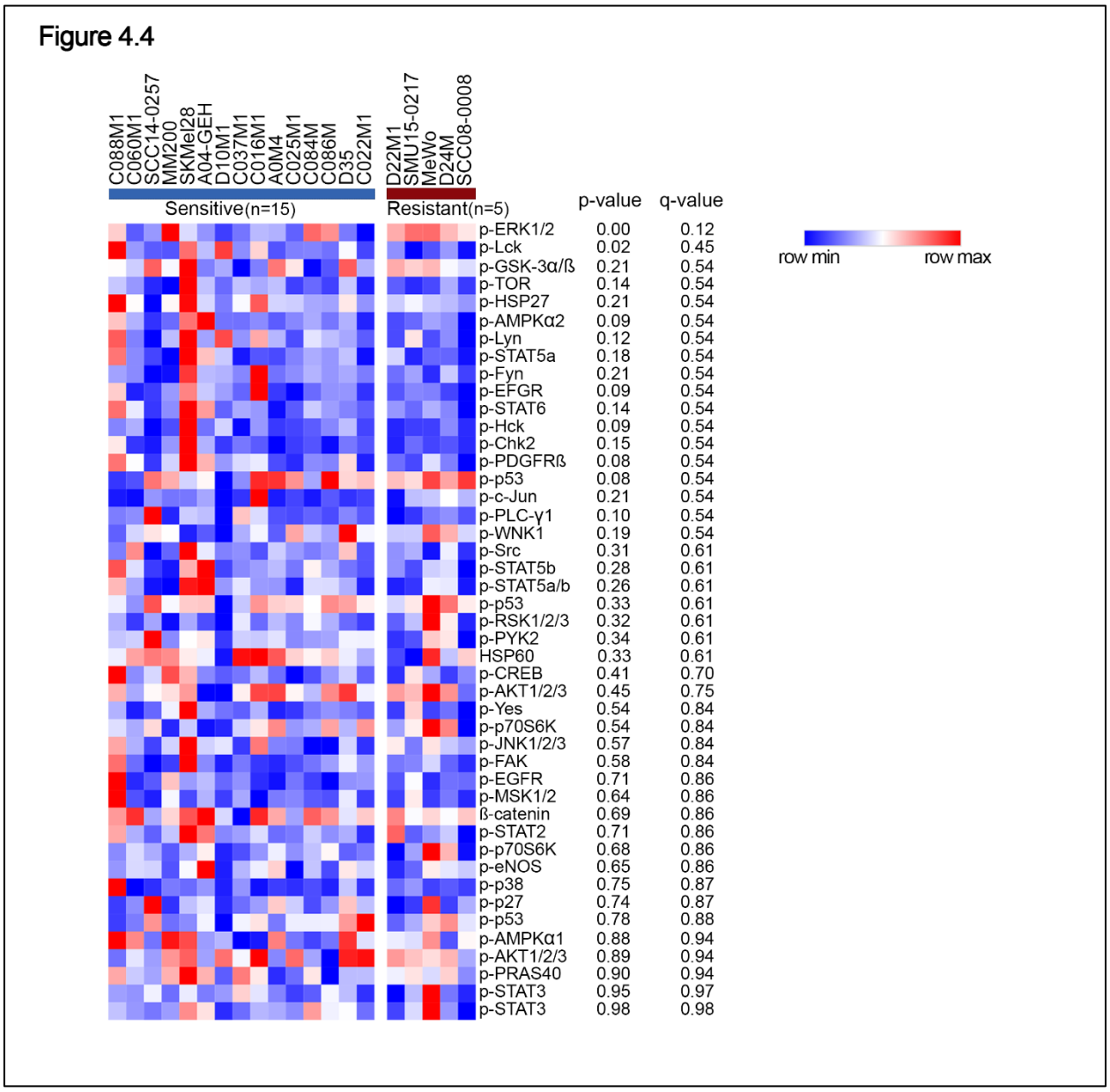

Figure 4.4: Heterogeneity in the phosphorylation of kinases and proteins in response to trametinib in a panel of 20 melanoma cell lines

Heat map showing fold change in phosphorylation of indicated kinases and proteins (post-trametinib/baseline levels) in melanoma cell lines. Melanoma cell lines displaying sensitivity (highly sensitive and intermediate sensitive, n=15) to trametinib were compared to trametinib-resistant (n=5) melanoma cell lines using a moderated t-test (https://software.broadinstitute.org/morpheus) with Benjamini and Hochberg false discovery rate (FDR) correction applied. Returned raw p-values and FDR-adjusted p-values (q-values) are shown (Table S4.3).

Melanoma genotype and kinase phosphorylation

We also compared kinase activation at baseline in *BRAF*^{V600}-mutant (n=7) versus *BRAF*/*RAS* WT (n=13) melanomas. The phosphorylation level of eight detected kinases including p-JNK, p-FAK, p-EGFR, p-p38, p-HSP27, ß-catenin, p-Lyn, p-Lck were significantly higher (q-value<0.05) in *BRAF*/*RAS* WT melanomas, while levels of two phosphorylated kinases including p-p70S6K, p-STAT3 were higher in *BRAF*^{V600}-mutant melanomas (Figure 4.5; Table S4.4).

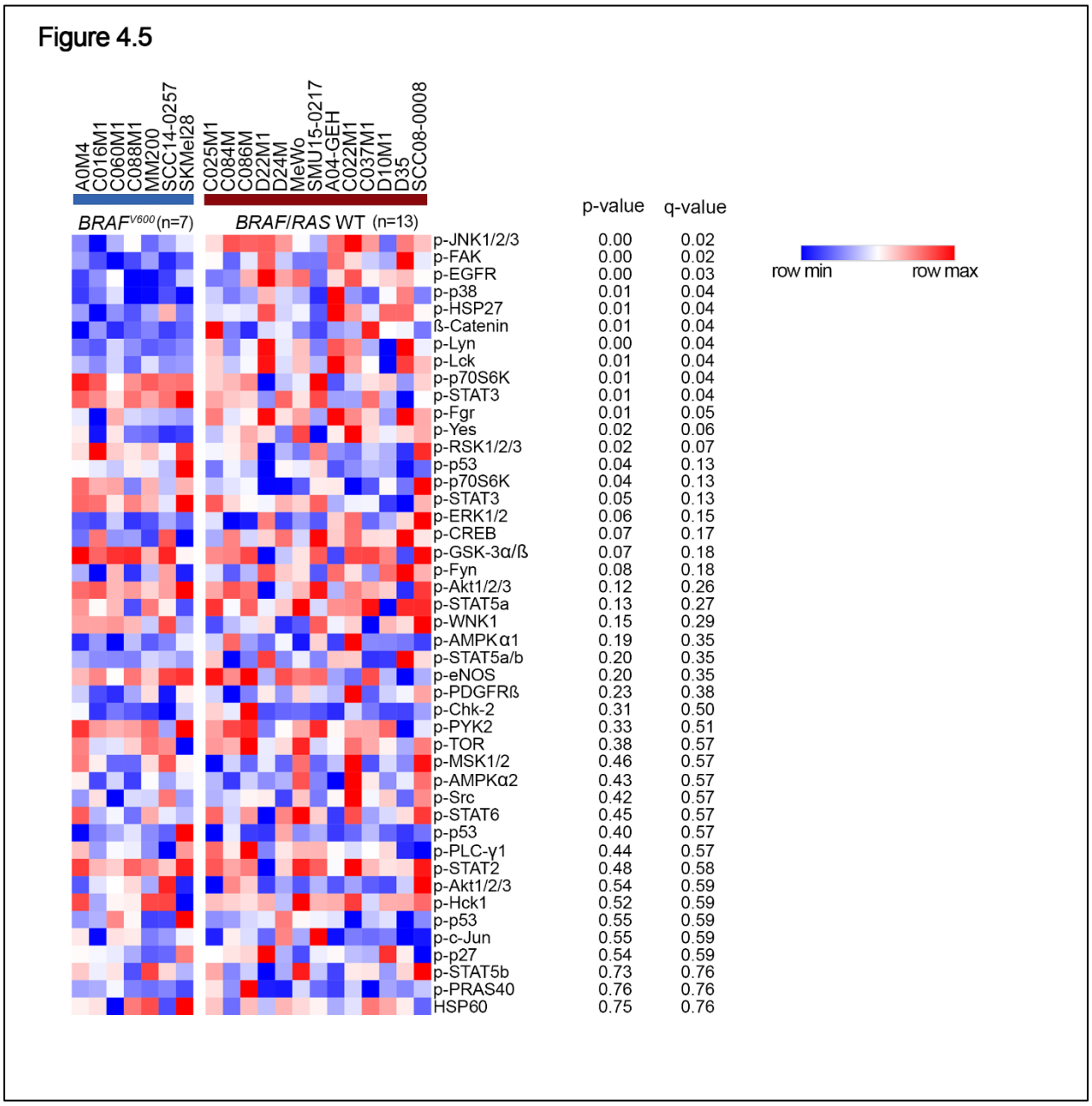

Figure 4.5: Heatmap showing baseline expression levels of phosphorylated kinases and proteins in *BRAF*^{V600}-mutant (n=7) compared to *BRAF*/*RAS* WT (n=13) cell lines

Heatmap was generated from the median normalised densitometry values for each protein across our panel of 20 melanoma cell lines. Comparison of phosphorylated kinases and proteins between *BRAF*^{V600} and *BRAF*/*RAS* WT melanoma cell lines was performed using a moderated t-test (https://software.broadinstitute.org/morpheus) with Benjamini and Hochberg FDR correction applied. Returned raw p-values and FDR-adjusted p-values (q-values) are shown (Table S4.4)

4.3.2 Heterogenous signalling associated with melanoma genotype and response to trametinib

To investigate the influence of differentially phosphorylated kinases in melanoma genotypes and trametinib response, we derived signalling pathway scores from the kinase phosphorylation data. A total of 10 pathway activity scores were calculated using the mean of z-scores of the relevant kinases, as described previously in Section 4.2.4 (Table 4.2). To examine whether response to MEK inhibitor is associated with distinct signalling cascades, baseline signalling activity in trametinib-sensitive (highly sensitive and intermediate sensitive) melanoma cell lines was compared to trametinib-resistant cells. Analysis of differentially expressed pathway scores at baseline and post-trametinib exposure produced no significantly enriched pathways ($q<0.05$) (Table S4.5, S4.6). We did note however an upregulation of AMPK and RTK signalling ($q<0.2$) at baseline, but not post-trametinib, when highly sensitive melanoma cells ($n=8$) were compared with five resistant melanoma cells (Figure 4.6, Tables S4.7 and S4.8).

We also explored differences in pathway activity between melanoma cells of specific genotypes. Compared to *BRAF*^{V600}-mutant melanomas, four signalling pathways showed significant upregulation in the *BRAF*/*RAS* WT melanomas ($p<0.05$), including SRC, RTK, WNT and AMPK pathways (Figure 4.7, Table S4.9).

Despite trametinib treatment, the WNT and SRC pathways remained high in many of the *BRAF*/*RAS* WT melanomas ($p<0.05$, $q<0.2$). Interestingly, the AMPK and RTK pathways did not show any significance between these two genotypes post-trametinib, and this was due to the upregulation of both pathways in many of the *BRAF*^{V600}-mutant melanomas post trametinib treatment (Figure 4.7, Table S4.10).

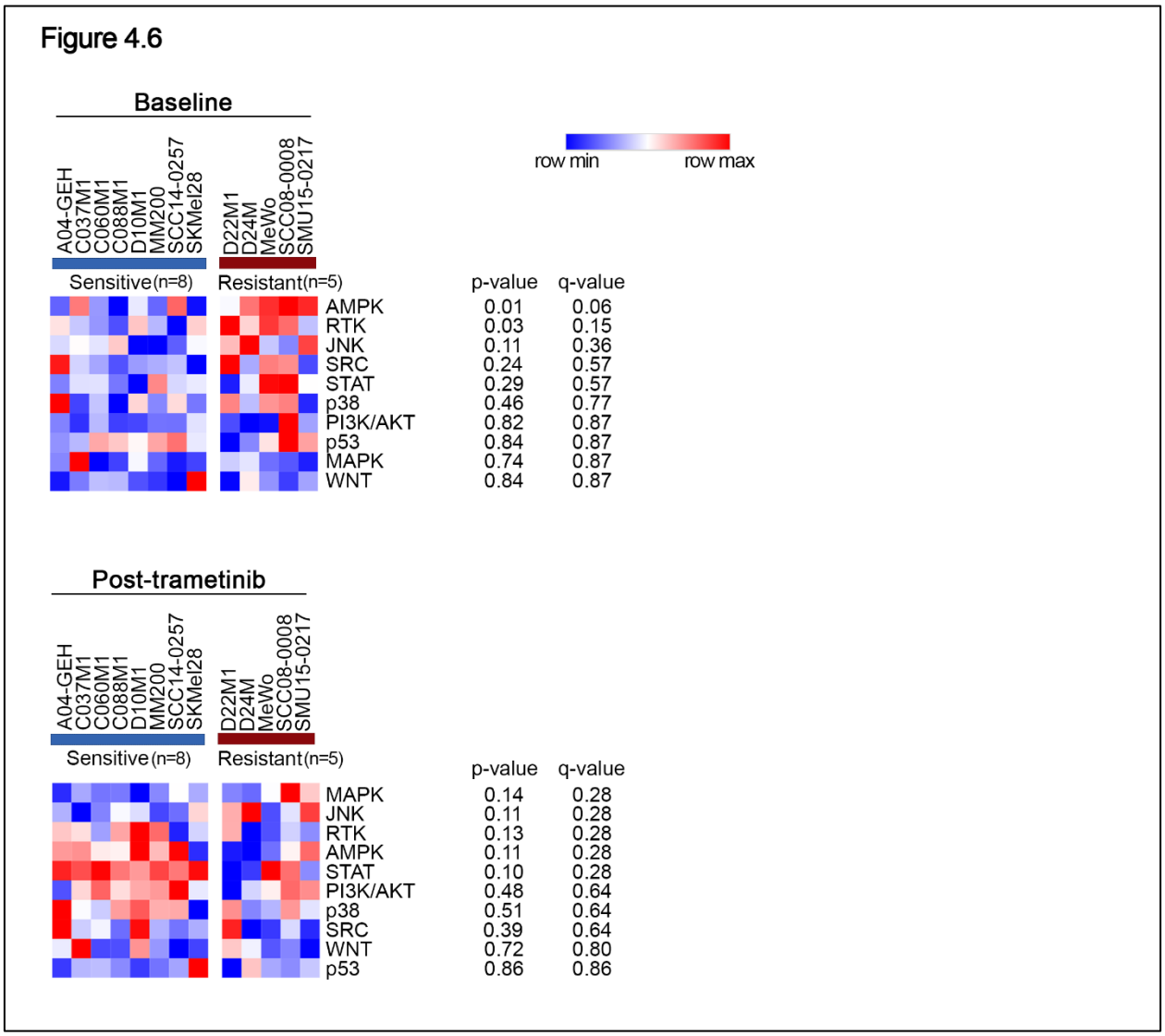

Figure 4.6: Heatmap showing pathway scores related to trametinib response

Heatmap was generated from the pathway scores (mean of z-scores of relevant kinases; see Table 4.2) in trametinib-sensitive (n=8) and -resistant (n=5) melanoma cell lines. Comparison of pathway scores at baseline (top panel) and post-trametinib (bottom panel) was performed using a moderated t-test (https://software.broadinstitute.org/morpheus) with Benjamini and Hochberg FDR correction applied. Returned raw p-values and FDR-adjusted p-values (q-values) are shown (Table S4.7, S4.8).

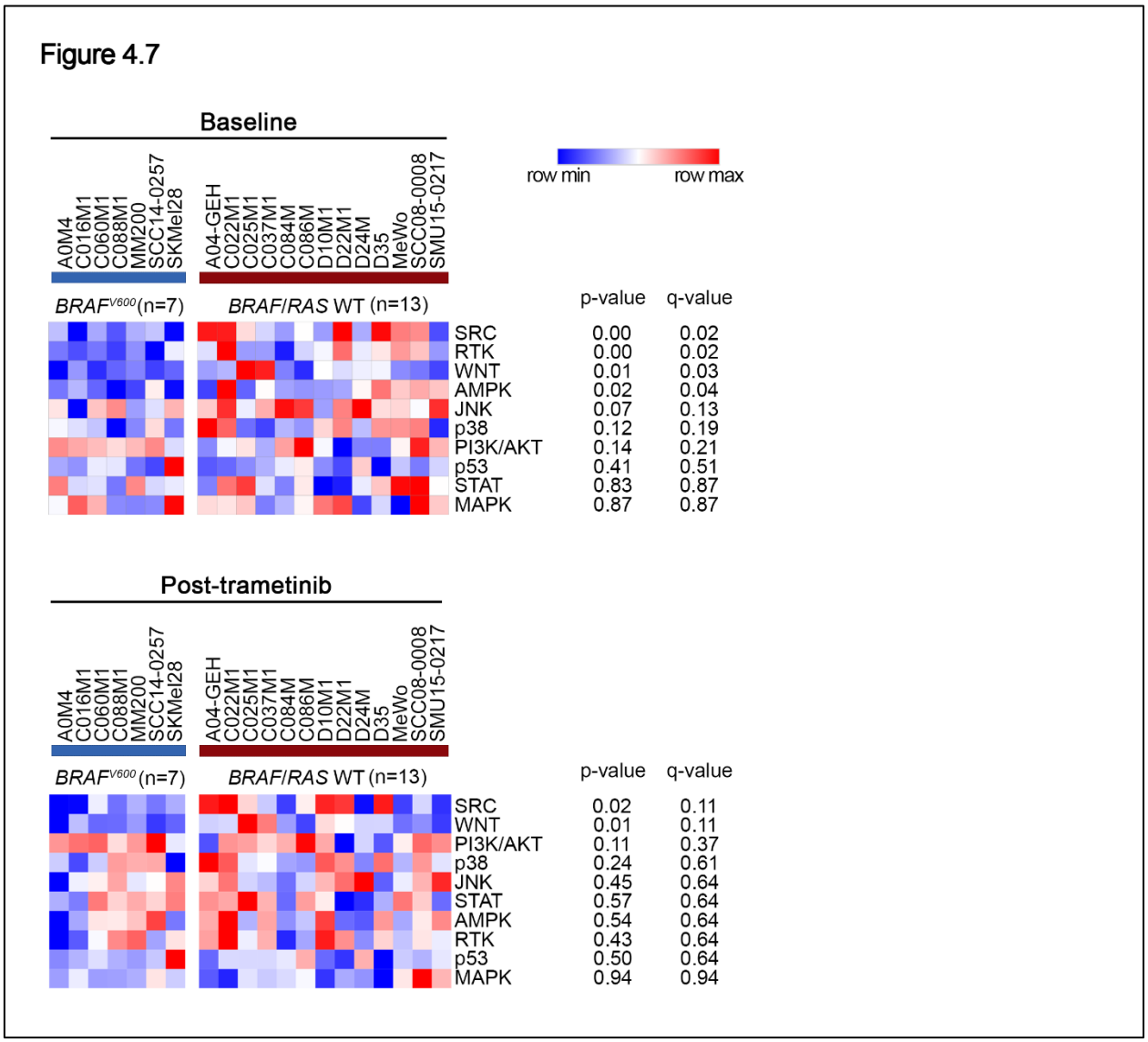

Figure 4.7: Heatmap comparing signalling pathway activity between *BRAF*^{V600} (n=7) and *BRAF*/*RAS* WT (n=13) melanoma cell lines

Heatmap was generated from the pathway scores (mean of z-scores of relevant kinases; see Table 4.2) in *BRAF*^{V600E} and *BRAF*/*RAS* WT cell lines. Comparison of pathway scores at baseline (top panel) and post-trametinib (bottom panel) was performed using a moderated t-test (https://software.broadinstitute.org/morpheus) with Benjamini and Hochberg FDR correction applied. Returned raw p-values and FDR-adjusted p-values (q-values) are shown (Table S4.9, S4.10).

4.3.3 Combination inhibition of RTKs and MAPK signalling are not sufficient to overcome trametinib resistance in *BRAF*/*RAS* WT melanomas

The frequent co-activation of RTKs and SRC pathways in *BRAF*/*RAS* WT cell lines (Figure 4.8), and the fact that only one cell line (A04-GEH) displayed high sensitivity to trametinib (Table 2.1), suggested that combination of RTK or SRC with MEK inhibitors may prove effective in suppressing melanoma cell proliferation and survival. To test this hypothesis, four *BRAF*/*RAS* WT melanoma cell lines, including three trametinib resistant cells (MeWo, D24M, D22M1) and one with intermediate sensitivity (C022M1), were selected; cell cycle responses were examined after treatment with the MEK inhibitor trametinib (10 nM), the EGFR inhibitor erlotinib (2 µM), the kinase inhibitor imatinib (10 nM) (a multi-target inhibitor of v-Abl, c-Kit and PDGFR), and the SRC inhibitor dasatinib (1 µM), either alone or in combination.

Figure 4.8

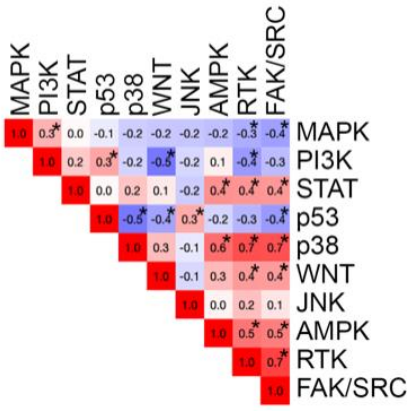

Figure 4.8: RTK, p38 and SRC signalling activity were highly correlated in *BRAF*/*RAS* WT melanoma cell lines (n=13)

Correlation matrix showing Spearman correlation analysis between signalling pathway scores in *BRAF*/*RAS* WT melanoma cells. Spearman correlation values are shown within the similarity matrix. *adjusted p-value<0.05.

To examine the impact of these kinase inhibitors on the EGFR, SRC, and MAPK signalling pathways, we also analysed the expression of downstream effector proteins (phosphorylated EGFR, phosphorylated SRC, phosphorylated ERK) of each pathway at baseline and after drug treatment using immunoblotting. Treatment of the four melanoma cell lines with kinase inhibitors showed varied pathway inhibition (Figure 4.9). For instance, the C022M1 cell line showing intermediate sensitivity to trametinib displayed the most substantial reduction in p-ERK levels (i.e. p-ERK/ERK) (Figure 4.10). Monotherapy of erlotinib, imatinib or dasatinib had very limited impact on ERK phosphorylation in all four cell lines (Figure 4.9). Dasatinib effectively decreased the phosphorylation of SRC in all cell lines without impacting the other signalling pathways, whereas erlotinib only consistently inhibited p-EGFR in the intermediate sensitive C022M1 cells (Figure 4.9). Treatment of the melanoma cell lines with imatinib had no obvious impact in down-regulating phosphorylation of any of these effectors, but did promote phosphorylation of SRC in the D22M1 and D24M cells (Figure 4.9).

Selected RTK and SRC kinase inhibitors, either alone or in combination, induced minimal cell death (change in subG1) or S phase inhibition in these *BRAF*/*RAS* WT melanoma cell lines. Though a slightly increased S phase inhibition was observed in three resistant cell lines (MeWo, D24M and D22M1) treated with multiple inhibitors compared to a single treatment, no potent cell cycle arrest was detected (Table 4.3). Therefore, we conclude that addition of RTK and SRC inhibitors were not sufficient to enhance trametinib-induced cell cycle arrest and/or melanoma cell death in *BRAF*/*RAS* WT melanoma models (Table 4.3), and this presumably reflects the inability of these inhibitors to suppress MAPK signalling beyond post-trametinib levels (Figure 4.9).

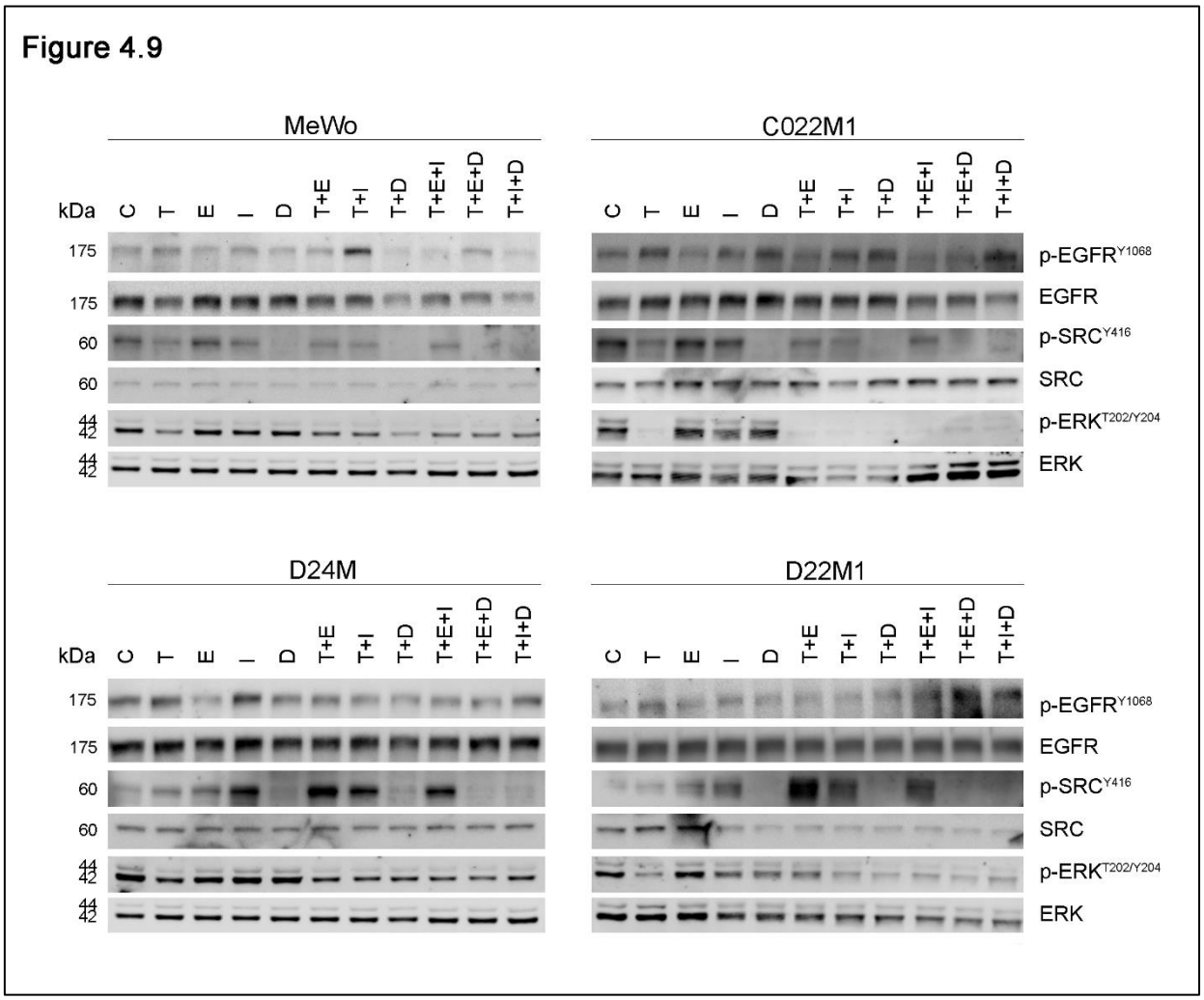

Figure 4.9: Signaling pathway alterations in melanoma cells exposed to various kinase inhibitors

Indicated melanoma cell lines were treated with DMSO as control (C), and with trametinib (T) at 10 nM, erlotinib (E) at 2 µM, imatinib (I) at 10 nM, dasatinib (D) at 1 µM, either alone or in combination. Western immunoblotting of cell lysates showing protein markers of EGFR, SRC and MAPK pathway activity 24 h after treatment. The REVERT total protein stain was performed as loading control (Figure S4.1). Two biological replicates were performed, and the results showed derived from one representative experiment.

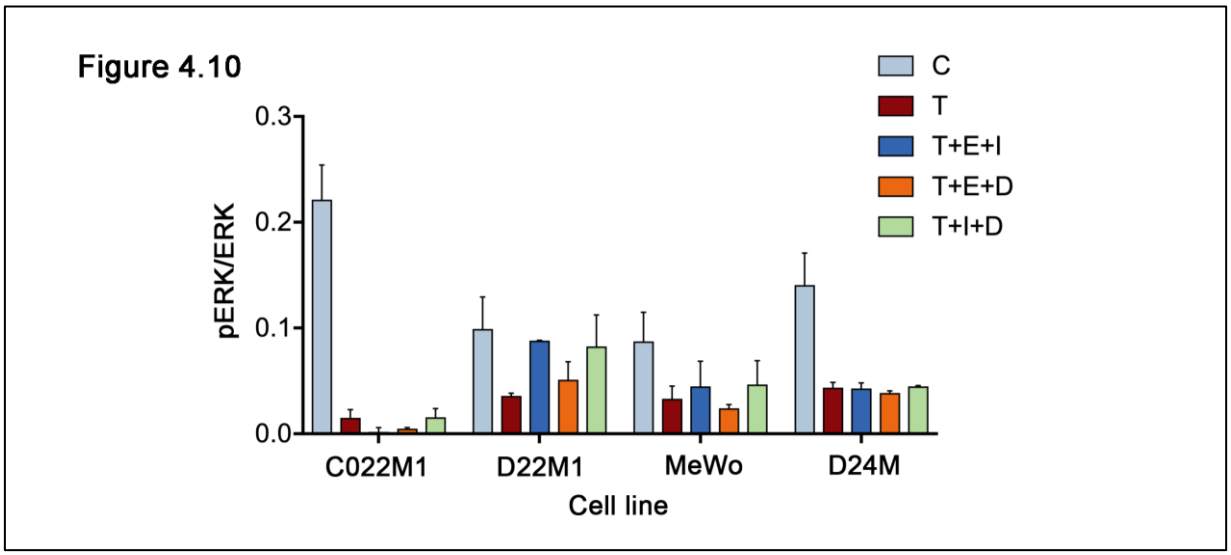

Figure 4.10: Effects of combination RTK, SRC and MEK inhibitors on ERK phosphorylation in *BRAF/RAS* WT melanoma

Densitometric analysis of pERK/ERK in indicated melanoma cells before (C) and 24 h after treatment with trametinib (T) at 10 nM, in combination with erlotinib (E) at 2 µM, dasatinib (D) at 1 µM and/or imatinib (I) at 10 nM. Data represent mean and standard error of the mean of two independent experiments.

Table 4.3: Cell cycle responses to kinase inhibitors

Cell line	MeWo		D24M		D22M1		C022M1	
Treatment	Change in sub G1	% S phase inhibition	Change in sub G1	% S phase inhibition	Change in sub G1	% S phase inhibition	Change in sub G1	% S phase inhibition
Trametinib	0±1	42±4	1±1	23±5	0±0	26±8	2±3	76±2
Erlotinib	0±0	3±0	1±0	0±0	0±0	17±10	0±0	0±0
Imatinib	1±0	2±0	0±0	0±0	0±0	0±0	0±0	0±0
Dasatinib	0±1	0±0	3±2	20±12	2±2	9±2	0±0	42±4
Trametinib + erlotinib	0±1	51±2	2±1	23±6	0±1	52±14	3±2	77±4
Trametinib + imatinib	0±1	41±4	1±1	27±5	0±0	34±10	2±2	74±1
Trametinib + dasatinib	0±1	53±1	8±5	40±8	3±3	36±4	1±1	78±3
Trametinib + erlotinib +imatinib	2±1	57±10	1±1	23±5	0±0	55±8	1±2	78±1
Trametinib + erlotinib + dasatinib	1±1	60±2	9±4	43±8	4±2	46±6	1±1	80±1
Trametinib + imatinib + dasatinib	0±1	55±3	8±5	42±10	4±2	37±8	1±1	78±1

Change in sub G1 calculated as (percentage of sub G1 in trametinib-treated cells - percentage of sub G1 in the DMSO-treated cells). Percentage of S phase inhibition calculated as [((percentage of DMSO-treated cells in S phase – percentage of trametinib-treated cells in S phase) / (percentage of DMSO-treated cells in S phase)) x100].

4.4 Discussion

Despite the clinical success of BRAF and MEK inhibitors in patients with *BRAF*^{V600}-mutant melanoma, options for *BRAF*/*RAS* WT melanoma patients remain limited. Although we have previously shown that a subset of *BRAF*/*RAS* WT melanoma cell lines (8/13) display sensitivity to MEK inhibition, many *BRAF*/*RAS* WT melanoma cell lines (5/13) remain resistant to trametinib (Chapter 2). Because of the high mutation load and concurrent mutations that may contribute to the development of *BRAF*/*RAS* WT melanoma, we hypothesized that activation of alternative survival signalling pathways may drive *BRAF*/*RAS* WT melanoma resistance to MEK inhibition, and combination therapies that inhibit these alternate pathways may improve anti-tumour activity in patients with *BRAF*/*RAS* WT melanoma.

We did not find enormous differences in signalling pathway activity between trametinib-sensitive and trametinib-resistant melanoma cell lines at baseline. Nevertheless, we noted upregulation of AMPK (p=0.01) and RTK (p=0.03) in resistant melanoma cells compared to sensitive cells. We also examined the association of signalling activity with melanoma genotype and noted that *BRAF*/*RAS* WT melanomas, most of which were resistant to trametinib, showed upregulation of SRC, RTK, WNT and AMPK pathways at baseline when compared to *BRAF*^{V600}-mutant melanomas. There was also a trend towards active WNT (p=0.02) and SRC (p=0.01) signalling in resistant *BRAF*/*RAS* WT melanoma cells after trametinib treatment (Figure 4.7), suggesting that these pathways may contribute to primary MEK inhibitor resistance in *BRAF*/*RAS* WT melanoma. Interestingly, *BRAF*^{V600}-mutant melanoma cells showed upregulation of RTK and AMPK signalling post-trametinib, and this is in line with trametinib-induced inhibition of negative feedback loops that suppress RTK

and AMPK activity (Figure 4.11). MAPK signalling was shown to inversely correlate with AMPK activity in *BRAF*^{V600}-mutant melanoma due to activation of ERK-induced phosphorylation and inactivation of LKB1 (liver kinase B1), an upstream activator of AMPK (395). In *BRAF* WT melanoma, AMPK activation has been shown to contribute to cell growth inhibition and apoptosis (396).

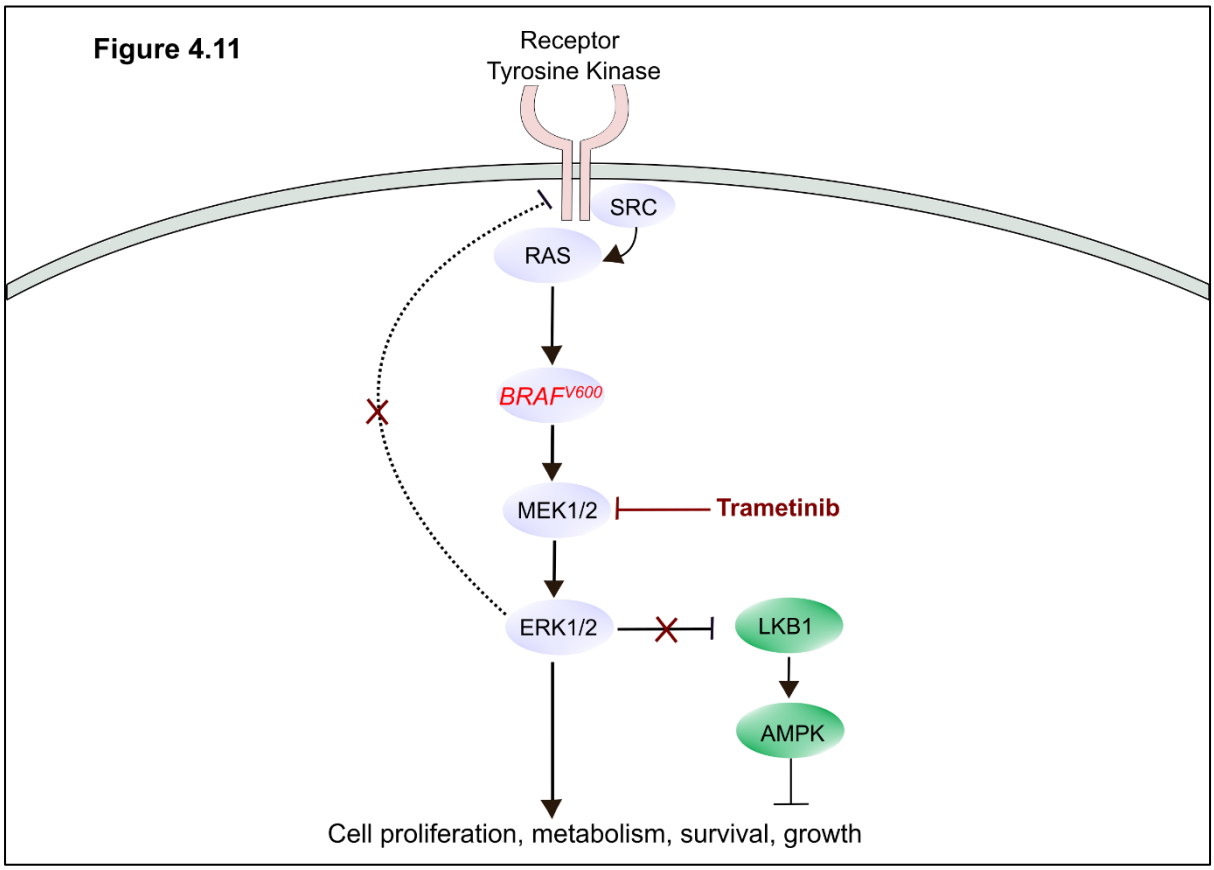

Figure 4.11: Trametinib enhances AMPK and RTK activity in *BRAF*^{V600}-mutant melanoma.

BRAF^{V600} mutation negatively regulates AMPK activation through MAPK activation and LKB1 inactivation. Activation of SRC is regulated by RTKs. MEK inhibition also leads to activation of RTKs in *BRAF*^{V600}-mutant melanoma via loss of negative feedback (395).

Constitutive activation of RTKs has been reported in many types of human cancers,

often as a result of gain-of-function mutations, genomic amplifications, chromosomal rearrangements, and autocrine activation (397). In melanoma, RTK pathway activation, and the downstream phosphorylation of effectors (i.e. PLCγ, PI3K, and MAPK) have been shown to promote tumour cell proliferation, differentiation, survival, and migration (398). Upregulation of PDGFRß, IGFR-1R and EGFR are associated with BRAF inhibitor resistance in melanoma (297, 300, 356, 399, 400), hence inhibiting RTK signalling may circumvent resistance. This is in line with a recent study demonstrating RTK and BRAF co-inhibition overcoming resistance to BRAF inhibition (401). Given that single-agent EGFR inhibitor has very limited impact in metastatic melanoma (402), it was not unexpected that erlotinib alone had minimal impact on the four tested *BRAF*/*RAS* WT cell lines. However, these cells also had minimal response to erlotinib in combination with imatinib and/or trametinib. These results suggest that beyond EGFR and PDGFRß, initial resistance to trametinib in *BRAF*/*RAS* WT melanoma may involve other RTKs or signalling pathways, and thus blocking EGFR and PDGFRß was not sufficient to cause cell cycle arrest or apoptosis.

Despite the disappointing efficacy of the EGFR inhibitor on our melanoma cell lines, several studies have shown moderate benefits in inhibiting RTK signalling pathways as potential treatment strategies for *BRAF*/*RAS* WT melanomas. For instance, given that the NRG1/ ERBB3 pathway is overactivated in *BRAF*/*RAS* WT melanoma cells, ERBB3 and/or ERBB2 were identified as potential targets (403), and the combination of the ERBB inhibitor afatinib with trametinib has been shown to reduce cell viability and inhibit proliferation in *BRAF*/*RAS* WT melanoma cell lines (404). The tyrosine kinase inhibitor nilotinib, which blocks Bcr-AbI, in combination with trametinib also showed potent anti-tumour effects *in vitro* in melanoma cell lines and *in vivo* in patient-derived xenografts (405). A recent study screened 240 different drugs for growth-

inhibitory and cytotoxic effects and identified the synergistic efficacy of the pan-RTK inhibitor ceritinib and trametinib in *BRAF*/*RAS* WT melanomas (406).

The SRC-family tyrosine kinases lie downstream of RTK signalling, and SRC activity is regulated, in part, by EGFR (407, 408). SRC is frequently expressed in melanoma, phosphorylated in around 61-75% of cutaneous melanoma, and 31% of mucosal melanoma (409). The level of SRC expression predicted survival in melanoma patients, with stronger SRC staining correlating with worse median survival (410, 411). Inhibition of SRC activity using dasatinib in melanoma has been shown to suppress melanoma cell growth and invasion (409, 410). The combined inhibition of SRC and MEK, using saracatinib and selumetinib, also had potent anti-proliferative and anti-invasive effects on melanoma cells (412). Moreover, activation of SRC and MET activity was detected in $BRAF^{V600}$-mutant melanoma cell lines resistant to vemurafenib, and combination inhibition of MAPK signalling with SRC or MET inhibitors effectively suppressed cell proliferation and reduced cell invasion and migration (413). Similarly, in BRAF inhibitor-resistant melanoma cell lines, the combination of BRAF inhibitor with a SRC inhibitor or EGFR inhibitor suppressed growth and invasion of melanoma cells (414). Several clinical trials have been established to examine the activity of dasatinib in patients with advanced melanoma, and although partial responses were detected in *BRAF*/*RAS* WT melanoma patients, the clinical outcome was not significant (415). In the present study, treatment of melanoma cell lines with dasatinib, alone or combined with trametinib showed minimal effects, with no increase in cell death, and only additive effects for S-phase inhibition in one cell line (D24M; S phase inhibition: trametinib=23%, dasatinib=20%, dasatinib plus trametinib = 40%). The minimal activity of dasatinib may reflect the fact that p-ERK remained unchanged in the *BRAF*/*RAS* WT cells, even though p-SRC levels

were decreased (Figure 4.9). These data indicate that ERK activity in *BRAF*/*RAS* WT melanoma does not depend on SRC signalling.

The limited efficacy of targeting multiple signalling pathways in our panel of melanoma cells strongly suggest that molecular targeted therapies may need to be combined with immunotherapies in these highly mutated melanomas. In a preclinical study, the combination of MEK inhibitor with immune checkpoint inhibitors targeting PD-1 and CTLA-4 produced more potent anti-tumour activity compared to the single agents in *BRAF*^{V600}-melanoma cells (416). In a phase I study, *BRAF* WT melanoma patients receiving combination PD-1 inhibitor (i.e. MEDI4736) and trametinib showed an objective response rate of 21% and disease control rate of 79% at 16 weeks (310). Another phase Ib study that included *BRAF* WT melanoma patients treated with the MEK inhibitor cobimetinib and the PD-L1 inhibitor atezolizumab showed an objective response rate of 45% and disease control rate of 75% (417). Ongoing clinical studies (i.e. NCT02130466) are currently exploring the efficacy of combination targeted therapies and immunotherapies in *BRAF* WT melanoma patients, though dose-limiting hepatotoxicity remains a major issue for these combinations (283-285).

Supplementary Tables

Table S4.1: Comparison of phosphorylated kinases and proteins expressed at baseline in trametinib-sensitive (n=15) versus trametinib-resistant (n=5) melanoma cell lines

Kinase	T-Test	p-value	q-value
Akt1/2/3^{S473}	-0.13	0.9	0.97
Akt1/2/3^{T308}	0.42	0.69	0.92
AMPKα1^{T183}	0.39	0.71	0.92
AMPKα2^{T172}	-0.88	0.41	0.92
ß-Catenin	0.32	0.75	0.92
c-Jun^{S63}	-0.9	0.41	0.92
Chk-2^{T68}	1.3	0.21	0.92
CREB^{S133}	-1.29	0.23	0.92
EGFR^{Y1086}	-1.7	0.14	0.92
eNOS^{S1177}	0.1	0.93	0.97
ERK1/2$^{T202/Y204,T185/Y187}$	-0.93	0.39	0.92
FAK^{Y397}	-0.51	0.62	0.92
Fgr^{Y412}	-0.91	0.39	0.92
Fyn^{Y420}	-0.93	0.38	0.92
GSK-3α/ß$^{S21/S9}$	0.91	0.4	0.92
Hck^{Y411}	-0.77	0.47	0.92
HSP27$^{S78/S82}$	-0.1	0.93	0.97
HSP60	0.69	0.5	0.92
JNK1/2/3$^{T183/Y185,T221/Y223}$	-0.71	0.49	0.92
Lck^{Y394}	-1.19	0.27	0.92
Lyn^{Y397}	-1.1	0.31	0.92
MSK1/2$^{S376/S360}$	-0.54	0.61	0.92
p27^{T198}	0.5	0.64	0.92
p38α$^{T180/Y182}$	-0.34	0.74	0.92
p53^{S15}	-1.29	0.22	0.92
p53^{S392}	-0.45	0.67	0.92
p53^{S46}	0.37	0.72	0.92
p70S6Kinase^{T389}	0.55	0.61	0.92
p70S6Kinase$^{T421/S424}$	0.8	0.46	0.92
PDGFRß^{Y751}	-1.73	0.11	0.92
PLC-γ1^{Y783}	0.48	0.65	0.92
PRAS40^{T246}	1.06	0.32	0.92
PYK2^{Y402}	0.9	0.4	0.92
RSK1/2/3$^{S380/S386/S377}$	0.35	0.74	0.92
Src^{Y419}	0.06	0.95	0.97
STAT2^{Y689}	0.3	0.77	0.92
STAT3^{S727}	-0.97	0.34	0.92
STAT3^{Y705}	0	1	1
STAT5a^{Y694}	-0.61	0.56	0.92
STAT5a/b$^{Y694/Y699}$	-0.92	0.39	0.92
STAT5b^{Y699}	-0.33	0.76	0.92
STAT6^{Y641}	-0.77	0.48	0.92
TOR^{S2448}	-0.32	0.75	0.92
WNK1^{T60}	-0.15	0.89	0.97
Yes^{Y426}	-0.19	0.85	0.97

Melanoma cell lines displaying sensitivity (highly sensitive and intermediate sensitive) to trametinib were compared to trametinib-resistant melanoma cell lines using a moderated t-test (https://software.broadinstitute.org/morpheus) with Benjamini and Hochberg false discovery rate (FDR) correction applied. Returned raw p-values and FDR-adjusted p-values (q-values) are shown.

Table S4.2: Comparison of phosphorylated kinases and proteins post trametinib treatment in trametinib-sensitive (n=15) versus trametinib-resistant (n=5) melanoma cell lines

Kinase	T-Test	p-value	q-value
Akt1/2/3^{S473}	-0.06	0.95	0.95
Akt1/2/3^{T308}	0.31	0.77	0.94
AMPKα1^{T183}	0.78	0.46	0.93
AMPKα2^{T172}	1.95	0.09	0.57
ß-Catenin	0.56	0.59	0.94
c-Jun^{S63}	-1.25	0.27	0.74
Chk-2^{T68}	2.4	0.03	0.57
CREB^{S133}	-0.09	0.93	0.95
EGFR^{Y1086}	-0.74	0.47	0.93
eNOS^{S1177}	0.54	0.61	0.94
ERK1/2$^{T202/Y204,T185/Y187}$	-1.99	0.11	0.57
FAK^{Y397}	0.28	0.79	0.94
Fgr^{Y412}	0.19	0.85	0.94
Fyn^{Y420}	0.08	0.94	0.95
GSK-3α/ß$^{S21/S9}$	0.81	0.45	0.93
Hck^{Y411}	1.32	0.21	0.69
HSP27$^{S78/S82}$	0.68	0.52	0.94
HSP60	1.7	0.11	0.57
JNK1/2/3$^{T183/Y185,T221/Y223}$	-0.41	0.7	0.94
Lck^{Y394}	0.35	0.74	0.94
Lyn^{Y397}	0.26	0.8	0.94
MSK1/2$^{S376/S360}$	0.46	0.66	0.94
p27^{T198}	1.94	0.09	0.57
p38α$^{T180/Y182}$	-0.14	0.89	0.95
p53^{S15}	-1.13	0.3	0.74
p53^{S392}	-0.92	0.39	0.91
p53^{S46}	0.26	0.8	0.94
p70S6Kinase^{T389}	0.72	0.5	0.93
p70S6Kinase$^{T421/S424}$	0.79	0.47	0.93
PDGFRß^{Y751}	1.45	0.18	0.61
PLC-γ1^{Y783}	1.9	0.1	0.57
PRAS40^{T246}	1.51	0.15	0.57
PYK2^{Y402}	1.89	0.11	0.57
RSK1/2/3$^{S380/S386/S377}$	-0.21	0.84	0.94
Src^{Y419}	1.75	0.13	0.57
STAT2^{Y689}	2.39	0.05	0.57
STAT3^{S727}	0.2	0.85	0.94
STAT3^{Y705}	0.45	0.67	0.94
STAT5a^{Y694}	1.14	0.29	0.74
STAT5a/b$^{Y694/Y699}$	0.59	0.57	0.94
STAT5b^{Y699}	0.58	0.59	0.94
STAT6^{Y641}	1.29	0.24	0.72
TOR^{S2448}	1.67	0.14	0.57
WNK1^{T60}	-0.33	0.75	0.94
Yes^{Y426}	1.68	0.12	0.57

Melanoma cell lines displaying sensitivity (highly sensitive and intermediate sensitive) to trametinib were compared to trametinib-resistant melanoma cell lines using a moderated t-test (https://software.broadinstitute.org/morpheus) with Benjamini and Hochberg false discovery rate (FDR) correction applied. Returned raw p-values and FDR-adjusted p-values (q-values) are shown.

Table S4.3: Comparison of kinase and protein phosphorylation changes (post-trametinib/baseline kinase expression) in trametinib-sensitive (n=15) versus trametinib-resistant (n=5) melanoma cell lines

Kinase	T-Test	p-value	q-value
Akt1/2/3^{S473}	-0.15	0.89	0.94
Akt1/2/3^{T308}	-0.8	0.45	0.75
AMPKα1^{T183}	0.15	0.88	0.94
AMPKα2^{T172}	1.8	0.09	0.54
ß-Catenin	0.4	0.69	0.86
c-Jun^{S63}	-1.35	0.21	0.54
Chk-2^{T68}	1.5	0.15	0.54
CREB^{S133}	0.87	0.41	0.7
EGFR^{Y1086}	0.39	0.71	0.86
eNOS^{S1177}	0.47	0.65	0.86
ERK1/2$^{T202/Y204,T185/Y187}$	-3.51	0	0.12
FAK^{Y397}	0.57	0.58	0.84
Fgr^{Y412}	1.78	0.09	0.54
Fyn^{Y420}	1.31	0.21	0.54
GSK-3α/ß$^{S21/S9}$	-1.32	0.21	0.54
Hck^{Y411}	1.76	0.09	0.54
HSP27$^{S78/S82}$	1.29	0.21	0.54
HSP60	1.08	0.33	0.61
JNK1/2/3$^{T183/Y185,T221/Y223}$	-0.58	0.57	0.84
Lck^{Y394}	2.61	0.02	0.45
Lyn^{Y397}	1.7	0.12	0.54
MSK1/2$^{S376/S360}$	0.49	0.64	0.86
p27^{T198}	0.35	0.74	0.87
p38α$^{T180/Y182}$	0.32	0.75	0.87
p53^{S15}	-0.28	0.78	0.88
p53^{S392}	-1.91	0.08	0.54
p53^{S46}	-1.05	0.33	0.61
p70S6Kinase^{T389}	-0.66	0.54	0.84
p70S6Kinase$^{T421/S424}$	-0.44	0.68	0.86
PDGFRß^{Y751}	1.93	0.08	0.54
PLC-γ1^{Y783}	1.75	0.1	0.54
PRAS40^{T246}	-0.13	0.9	0.94
PYK2^{Y402}	1.04	0.34	0.61
RSK1/2/3$^{S380/S386/S377}$	-1.11	0.32	0.61
Src^{Y419}	1.07	0.31	0.61
STAT2^{Y689}	0.4	0.71	0.86
STAT3^{S727}	-0.07	0.95	0.97
STAT3^{Y705}	0.03	0.98	0.98
STAT5a^{Y694}	1.4	0.18	0.54
STAT5a/b$^{Y694/Y699}$	1.2	0.26	0.61
STAT5b^{Y699}	1.14	0.28	0.61
STAT6^{Y641}	1.57	0.14	0.54
TOR^{S2448}	1.53	0.14	0.54
WNK1^{T60}	-1.41	0.19	0.54
Yes^{Y426}	0.65	0.54	0.84

Melanoma cell lines displaying sensitivity (highly sensitive and intermediate sensitive) to trametinib were compared to trametinib-resistant melanoma cell lines using a moderated t-test (https://software.broadinstitute.org/morpheus) with Benjamini and Hochberg false discovery rate (FDR) correction applied. Returned raw p-values and FDR-adjusted p-values (q-values) are shown.

Table S4.4: Comparison of phosphorylated kinases and proteins expressed at baseline in *BRAF*^{V600}-mutant (n=7) versus *BRAF*/*RAS* WT (n=13) melanoma cell lines

Kinase	T-Test	p-value	q-value
Akt1/2/3^{S473}	0.64	0.54	0.59
Akt1/2/3^{T308}	1.64	0.12	0.26
AMPKα1^{T183}	-1.37	0.19	0.35
AMPKα2^{T172}	-0.81	0.43	0.57
ß-Catenin	-2.96	0.01	0.04
c-Jun^{S63}	0.62	0.55	0.59
Chk-2^{T68}	-1.05	0.31	0.5
CREB^{S133}	-2.09	0.07	0.17
EGFR^{Y1086}	-3.76	0.00	0.03
eNOS^{S1177}	1.32	0.20	0.35
ERK1/2$^{T202/Y204,T185/Y187}$	-2.06	0.06	0.15
FAK^{Y397}	-3.97	0.00	0.02
Fgr^{Y412}	-2.89	0.01	0.05
Fyn^{Y420}	-1.92	0.08	0.18
GSK-3α/ß$^{S21/S9}$	1.9	0.07	0.18
Hck^{Y411}	-0.68	0.52	0.59
HSP27$^{S78/S82}$	-3	0.01	0.04
HSP60	0.33	0.75	0.76
JNK1/2/3$^{T183/Y185,T221/Y223}$	-4.15	0.00	0.02
Lck^{Y394}	-3.09	0.01	0.04
Lyn^{Y397}	-3.31	0.00	0.04
MSK1/2$^{S376/S360}$	0.76	0.46	0.57
p27^{T198}	-0.62	0.54	0.59
p38α$^{T180/Y182}$	-3.05	0.01	0.04
p53^{S15}	0.63	0.55	0.59
p53^{S392}	0.88	0.40	0.57
p53^{S46}	2.32	0.04	0.13
p70S6Kinase^{T389}	2.19	0.04	0.13
p70S6Kinase$^{T421/S424}$	3.1	0.01	0.04
PDGFRß^{Y751}	-1.26	0.23	0.38
PLC-γ1^{Y783}	-0.79	0.44	0.57
PRAS40^{T246}	-0.31	0.76	0.76
PYK2^{Y402}	1.02	0.33	0.51
RSK1/2/3$^{S380/S386/S377}$	2.61	0.02	0.07
Src^{Y419}	-0.83	0.42	0.57
STAT2^{Y689}	0.73	0.48	0.58
STAT3^{S727}	2.17	0.05	0.13
STAT3^{Y705}	2.94	0.01	0.04
STAT5a^{Y694}	-1.59	0.13	0.27
STAT5a/b$^{Y694/Y699}$	-1.35	0.20	0.35
STAT5b^{Y699}	0.36	0.73	0.76
STAT6^{Y641}	-0.78	0.45	0.57
TOR^{S2448}	-0.92	0.38	0.57
WNK1^{T60}	1.52	0.15	0.29
Yes^{Y426}	-2.75	0.02	0.06

BRAF^{V600}-mutant cell lines were compared to *BRAF*/*RAS* WT melanoma cell lines using a moderated t-test (https://software.broadinstitute.org/morpheus) with Benjamini and Hochberg false discovery rate (FDR) correction applied. Returned raw p-values and FDR-adjusted p-values (q-values) are shown.

Table S4.5: Differentially expressed pathway scores at baseline in melanoma cells displaying high and intermediate sensitivity to trametinib (n=15) versus trametinib-resistant (n=5) melanoma cell lines

Pathways	T-Test	p-value	q-value
AMPK	-2.30	0.04	0.28
SRC	-0.89	0.40	0.84
JNK	-1.44	0.19	0.62
MAPK	-0.36	0.74	0.84
p38	-0.65	0.54	0.84
p53	-0.14	0.89	0.89
PI3K/AKT	0.55	0.61	0.84
RTK	-2.20	0.06	0.28
STAT	-0.63	0.56	0.84
WNT	0.31	0.76	0.84

Pathway scores were calculated using the mean of z-scores of the relevant kinases (Table 4.2). Comparison of pathway activity scores was performed using a moderated t-test (https://software.broadinstitute.org/morpheus) with Benjamini and Hochberg FDR correction applied. Returned t-test, raw p-values and FDR-adjusted p-values (q-value) are shown.

Table S4.6: Differentially expressed pathway scores post-trametinib treatment in melanoma cells displaying high and intermediate sensitivity to trametinib (n=15) versus trametinib-resistant (n=5) melanoma cell lines

Pathways	T-Test	p-value	q-value
AMPK	1.12	0.30	0.68
SRC	0.88	0.41	0.68
JNK	-2.71	0.03	0.31
MAPK	-1.81	0.13	0.58
p38	0.28	0.78	0.87
p53	0.02	0.99	0.99
PI3K/AKT	0.98	0.37	0.68
RTK	0.40	0.70	0.87
STAT	1.57	0.17	0.58
WNT	0.56	0.59	0.84

Pathway scores were calculated using the mean of z-scores of the relevant kinases (Table 4.2). Comparison of pathway activity scores was performed using a moderated t-test (https://software.broadinstitute.org/morpheus) with Benjamini and Hochberg FDR correction applied. Returned t-test, raw p-values and FDR-adjusted p-values (q-value) are shown.

Table S4.7: Differentially expressed pathway scores at baseline in melanoma cells displaying high sensitivity (n=8) to trametinib versus trametinib-resistant (n=5) melanoma cell lines

Pathways	T-Test	p-value	q-value
AMPK	-3.38	0.01	0.06
SRC	-1.27	0.24	0.57
JNK	-1.84	0.11	0.36
MAPK	-0.35	0.74	0.87
p38	-0.77	0.46	0.77
p53	0.21	0.84	0.87
PI3K/AKT	0.24	0.82	0.87
RTK	-2.65	0.03	0.15
STAT	-1.18	0.29	0.57
WNT	0.16	0.87	0.87

Pathway scores were calculated using the mean of z-scores of the relevant kinases (Table 4.2). Comparison of pathway activity scores was performed using a moderated t-test (https://software.broadinstitute.org/morpheus) with Benjamini and Hochberg FDR correction applied. Returned t-test, raw p-values and FDR-adjusted p-values (q-value) are shown.

Table S4.8: Differentially expressed pathway scores post-trametinib in melanoma cells displaying high sensitivity (n=8) to trametinib versus trametinib-resistant (n=5) melanoma cell lines

Pathways	T-Test	p-value	q-value
AMPK	1.82	0.11	0.28
SRC	0.92	0.39	0.64
JNK	-1.92	0.11	0.28
MAPK	-1.75	0.14	0.28
p38	0.67	0.51	0.64
p53	0.18	0.86	0.86
PI3K/AKT	0.75	0.48	0.64
RTK	1.67	0.13	0.28
STAT	2.13	0.10	0.28
WNT	0.36	0.72	0.80

Pathway scores were calculated using the mean of z-scores of the relevant kinases (Table 4.2). Comparison of pathway activity scores was performed using a moderated t-test (https://software.broadinstitute.org/morpheus) with Benjamini and Hochberg FDR correction applied. Returned t-test, raw p-values and FDR-adjusted p-values (q-value) are shown.

Table S4.9: Differentially expressed pathway scores at baseline in *BRAF*^{V600}-mutant (n=7) versus *BRAF*/*RAS* WT (n=13) melanoma cell lines

Pathways	T-Test	p-value	q-value
AMPK	-2.71	0.02	0.04
SRC	-3.64	0.00	0.02
JNK	-2.04	0.07	0.13
MAPK	0.77	0.45	0.50
p38	-1.65	0.12	0.19
p53	0.87	0.41	0.50
PI3K/AKT	1.53	0.14	0.21
RTK	-3.22	0.00	0.02
STAT	-0.22	0.83	0.83
WNT	-2.96	0.01	0.03

Comparisons performed using a moderated t-test (https://software.broadinstitute.org/morpheus) with Benjamini and Hochberg FDR correction applied. Returned t-test, raw p-values and FDR-adjusted p-values (q-value) are shown.

Table S4.10: Differentially expressed pathway scores post-trametinib in *BRAF*^{V600}-mutant (n=7) versus *BRAF*/*RAS* WT (n=13) melanoma cell lines

Pathway scores post-trametinib	T-Test	p-value	q-value
AMPK	-0.64	0.54	0.64
SRC	-2.51	0.02	0.11
JNK	-0.78	0.45	0.64
MAPK	0.07	0.94	0.94
p38	-1.23	0.24	0.61
p53	0.7	0.5	0.64
PI3K/AKT	1.67	0.11	0.37
RTK	-0.83	0.43	0.64
STAT	0.57	0.57	0.64
WNT	-2.77	0.01	0.11

Comparisons performed using a moderated t-test (https://software.broadinstitute.org/morpheus) with Benjamini and Hochberg FDR correction applied. Returned t-test, raw p-values and FDR-adjusted p-values (q-value) are shown.

Supplementary Figures

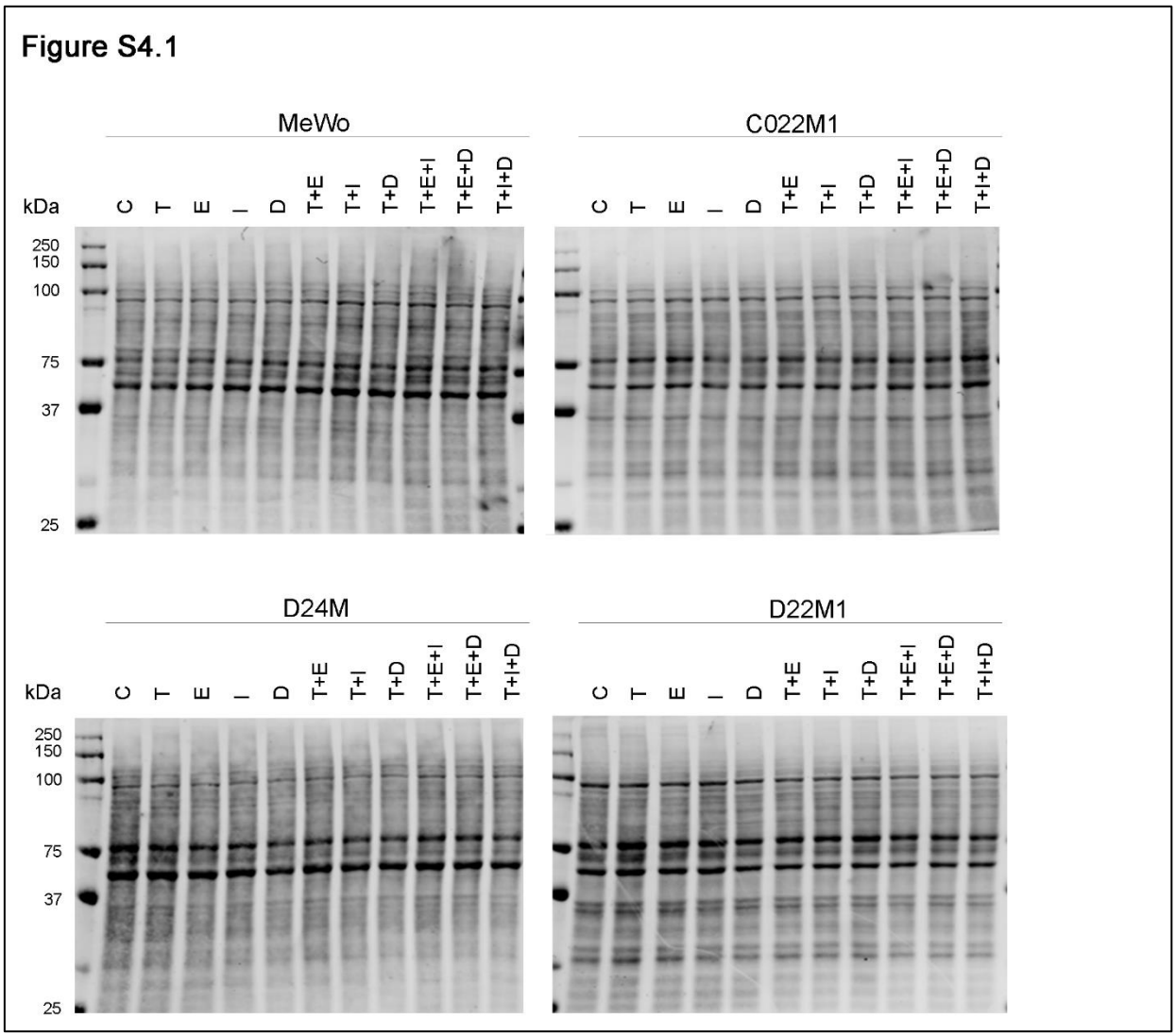

Figure S4.1: Detection of the REVERT total protein stain

The REVERT total protein stain was performed as loading control for Figure 4.9.

Chapter 5

Conclusion

The discovery of activating *BRAF* mutations in almost 50% of melanomas has led to the development and clinical application of selective BRAF and MEK inhibitors (339, 418, 419). Phase III clinical trial data have demonstrated unprecedented anti-tumour efficacy of these inhibitors compared to conventional chemotherapy (196, 420). Together with immune checkpoint inhibitors, the BRAF and MEK kinase inhibitors have revolutionized the treatment of patients with advanced *BRAF*^{V600}-mutant metastatic melanoma, tripling survival rates from 20% to 70% since 2010 (184, 191, 268, 299, 324, 421). BRAF and MEK inhibitors have now become the standard-of-care for patients with *BRAF*^{V600}-mutant melanoma in Australia (422).

The combination of BRAF and MEK inhibitors diminish some of the significant skin toxicities associated with BRAF inhibitor monotherapy and are more effective; overall response rates are approximately 70% with combination BRAF and MEK inhibitor versus 50% for BRAF inhibitor alone, and median overall survival rates are 25.1 versus 18.7 months for BRAF/MEK inhibitor combination compared to BRAF inhibitor monotherapy (HR 0.71; p=0.0107) (184, 185, 299). The combination of BRAF and MEK inhibitors also show activity in *BRAF*^{V600}-mutant brain metastases (423). Despite improvements in response rates and overall survival, melanoma patients treated with BRAF and MEK inhibitors rapidly acquire resistance, predominantly via MAPK pathway reactivation, and thus, salvage therapies are urgently needed (320, 356, 424, 425).

In contrast to *BRAF*^{V600}-mutant melanoma, there are currently no selective molecular therapies for *BRAF*/*RAS* WT melanoma. In the clinic, patients with *BRAF*/*RAS* WT melanoma are currently treated with inhibitors targeting the immune checkpoint receptors CTLA-4 and PD-1, and these can produce durable responses (275, 304) but are associated with low response rates; only 40-60% of patients will respond (250), and more than 40% will develop resistance and progress within two years, as reviewed in (426).

BRAF/*RAS* WT melanomas show hyperactivation of the MAPK pathway, as a consequence of frequent gene amplifications (*MEK1*, *ERK1*, *c-KIT*, *RAF1*), loss-of-function mutations (*NF1*, *RASA2*), and activating mutations (in RTKs) (59, 80, 305). Thus, there is interest in trialling MEK inhibitors for the treatment of *BRAF*/*RAS* WT melanoma, and preclinical studies have shown promising anti-tumour activity of MEK inhibitors (trametinib, PD0325901) in some *BRAF*/*RAS* WT melanoma models, indicating that this melanoma subtype may depend on MAPK signalling for survival (76, 204, 325).

In this PhD project, we sought to investigate MAPK dependency in 13 *BRAF*/*RAS* WT (*NF1*-mutant and triple WT) melanoma cell lines in comparison to 10 $BRAF^{V600}$-mutant melanoma cell lines. When treated with trametinib, $BRAF^{V600}$-mutant melanomas displayed high (6/10) or intermediate (4/10) sensitivity, whereas *BRAF*/*RAS* WT melanomas showed variable responses. The majority of *BRAF*/*RAS* WT melanoma cell lines (8/13, 62%) remained dependent on MAPK signalling for proliferation and/or survival, showing some degree of sensitivity to trametinib treatment. However, 5/13 *BRAF*/*RAS* WT melanoma cell lines were highly resistant to MEK inhibition, and notably, four of these were *NF1*-mutant, indicating that loss-of-function *NF1* mutation was strongly associated with MEK inhibitor resistance, and that *NF1* mutation status may predict response to MEK inhibitor monotherapy. These data contrast with previous reports showing MEK inhibitor sensitivity in *BRAF*/*RAS* WT melanomas was not associated with *NF1* mutation (76, 204, 325). It is worth noting, however, that sensitivity classifications in these earlier studies relied only on MTT metabolic assays, and we found that 4/7 (57%) *NF1*-mutant melanomas show IC_{50} values comparable to sensitive $BRAF^{V600}$-mutant melanoma cells. The inclusion of survival analysis, however, provides additional data and revealed that MEK inhibition was not sufficient to promote the death of *BRAF*/*RAS* WT melanomas with NF1 loss. Thus, our findings suggest that *NF1* gene status may be useful in guiding MEK inhibitor efficacy in *BRAF*/*RAS* WT melanoma and may help guide treatment selection.

NF1 mutation has been shown to confer BRAF or MEK inhibitor resistance in *BRAF*^{V600}-mutant melanomas (325), which was also confirmed in the present study. In contrast, we demonstrated that NF1 loss in *BRAF*/*RAS* WT melanomas did not affect response to MEK inhibition, suggesting that NF1 may not act as a dominant regulator of MAPK signalling in this melanoma subtype (Chapter 2). Mechanisms of MAPK activation and trametinib resistance appear to involve other oncogenic alterations in *BRAF*/*RAS* WT melanomas, and we confirmed that trametinib-resistant *BRAF*/*RAS* WT melanomas display a high mutation burden – including concurrent mutations affecting *TP53* and RASopathy genes. It has been previously reported that *BRAF*/*RAS* WT melanomas have a high mutational burden and a wide range of frequent gene mutations (305).

Alterations in RASopathy genes, including *RASA2*, *PTPN11*, *SOS1*, *RASSF2* and *RAF1* are associated with loss-of-function *NF1* mutation in *BRAF*/*RAS* WT melanoma (77). These mutations (*RASA2*, *SOS1* and *PTPN11*) were also enriched in our panel of *NF1*-mutant melanoma cells (Chapter 2). *PTPN11* was mutated in two *NF1*-mutant melanoma cell lines, and a recent study demonstrated that *PTPN11*^{E76K} mutation caused activation of MAPK signalling in *BRAF* WT melanomas. *PTPN11*^{E76K} -transgenic mouse model also had enhanced melanoma tumorigenesis (427). Dual MEK/PTPN11 inhibition potently induced *NRAS*-mutant melanoma cell death (427), and suppressed *RAS*-mutant tumour growth (428, 429). *RASA2* was mutated in two of the *NF1*-mutant melanoma cell lines used in our study and RASA2 loss has been associated with increased RAS activity, poor prognosis and enhanced melanoma proliferation and growth (391). Knockdown of both RASA2 and NF1 resulted in significant enhancement of MAPK activity (430) however, studies have yet to address whether concurrent mutations in *NF1* and *RASA2* contribute to MEK inhibitor resistance, and this is an area we are currently exploring.

Due to the importance of MAPK signalling, we attempted to block this pathway in *NF1*-mutant cells by co-targeting MEK and other protein kinases, including RAF and/or ERK.

Dual or triple inhibition of these kinases improved cell growth inhibition and/or apoptosis in the trametinib-resistant *NF1*-mutant cells (Chapter 2). These findings suggest that combination MEK with RAF or ERK may be effective in treating patients with *NF1*-mutant melanoma who have failed first-line immunotherapy. *NF1* loss also causes constitutively activation of the PI3K/AKT signalling pathway (431), and targeting MEK and mTOR has shown anti-tumour activity in xenograft models of *BRAF*^{V600}-mutant melanomas harbouring *NF1* mutation (75). As such, MEK inhibition in combination with PI3K/AKT inhibition may be another potential treatment strategy for patients with *NF1*-mutant melanoma. However, the high toxicity of PI3K inhibitors remains a hindrance to implementing these combinations in clinic, as reviewed in (432).

TP53 mutations were also found in seven melanoma cell lines, and four of these were *BRAF*/*RAS* WT melanoma cells. Importantly, *TP53* was also functionally impacted in an additional two *BRAF*/*RAS* WT cell lines confirming that mutation analysis is not sufficient to map the genomic/signalling profile of tumour cells. Not surprisingly, the majority of these *BRAF*/*RAS* WT cell lines (MeWo, SMU15-0217, D24M, D22M1, C077M1) were highly resistant to trametinib treatment, and thus p53 function was also associated with trametinib response. However, knockdown of p53 did not confer resistance to trametinib. Only one *BRAF*/*RAS* WT cell line, C037M1, showed decreased trametinib-induced cell death after p53 silencing, suggesting that p53 signalling may contribute to cell death induced by MEK inhibitor in this cell line. Thus, similar to NF1, loss of p53 function was significantly associated with, but did not contribute to trametinib resistance in *BRAF*/*RAS* WT cells (Chapter 3). Collectively, these results suggest that multiple, concurrent genetic mutations provide a complex network of signalling effectors that may be difficult to inhibit with single-agent targeted therapies.

In Chapter 4 we explored signalling pathway activity in 13 *BRAF*/*RAS* WT (6 triple WT and 7 *NF1*-mutant) and 7 *BRAF*^{V600}-mutant melanomas, using Human Phospho-Kinase

Antibody Arrays that measure the phosphorylation status of 43 kinases. We showed that four signalling pathways, FAK/SRC, RTK, WNT, and AMPK, were significantly upregulated in *BRAF*/*RAS* WT melanomas compared to *BRAF*^{V600}-mutant melanomas (Chapter 4). However, selective kinase inhibitors targeting RTK and SRC, alone or in combination with trametinib, did not inhibit cell proliferation or induce cell death in *BRAF*/*RAS* WT melanoma cells. This confirms the complex signalling activity in *BRAF*/*RAS* WT melanomas and suggests that alternate treatment strategies, possibly with a focus on immunotherapy and apoptotic regulators, should be prioritised (Chapter 2). For instance, Bcl-2 inhibition/knockout restored sensitivity of *NRAS*-mutant melanoma cells to MEK inhibition with marked apoptosis (433). Inhibition of anti-apoptotic Bcl-2 in combination with p53 activation effectively induced cell death in another tumour type (acute myeloid leukaemia) (434). Consequently, inhibition of anti-apoptotic proteins such as Bcl-2 in combination with MEK inhibitor and/or p53 activator may be worth exploring for the treatment of *BRAF*/*RAS* WT melanomas.

Immune checkpoint inhibitors are currently frontline therapies for *BRAF*/*RAS* WT melanoma patients in clinic. A phase III clinical trial comparing nivolumab with dacarbazine in patients with *BRAF* WT metastatic melanoma (n=418), showed improved objective response rate (40% vs 14%) and overall survival rate at one year (73% vs 42%, HR 0.42, $p<0.001$) (250). Furthermore, combination nivolumab plus ipilimumab in patients with *BRAF* WT melanoma demonstrated an improved response rate (61%) compared to ipilimumab monotherapy (11%) (277).

We also assessed trametinib response in six melanoma cell lines with *RAS*- and/or non-*BRAF*^{V600} mutations. Several studies have reported trametinib sensitivity in melanomas with rare *BRAF*^{L597} mutation or *NRAS* alterations (activating mutation or amplification) (435-437). In keeping with this, in our study, cell lines with *NRAS*^{Q61L}, *NRAS*^{Q61R}, *HRAS*^{Q61R}, or *BRAF*^{D594E}/*HRAS*^{G13R} mutations were sensitive to trametinib treatment.

However, two cell lines with *BRAF*^{G466R} or *BRAF*^{S457L} mutation were highly resistant to treatment (Chapter 3). Hence, melanomas with rare BRAF mutations may not be susceptible to treatment with MEK inhibitors, unlike *RAS*-mutant melanomas, as reviewed in (438). MEK inhibitors as combinatorial strategies in *RAS*-mutant melanoma have been described in several studies. For instance, dual treatment of MEK inhibitor with RAF inhibitor (439), ERK inhibitor (440), BET inhibitor (441), or CDK4/6 inhibitor (442) showed anti-tumour efficacy in preclinical *NRAS*-mutant melanoma models. Combination MEK (binimetinib) and CDK4 inhibitors (palbociclib) has also produced encouraging early clinical trial results in patients with *NRAS*-mutant melanoma (234). So far, *NRAS*-mutant melanomas are treated with first-line immunotherapy, though the response rates to ipilimumab plus PD-1 inhibitor are similar compared to *NRAS* WT melanomas (40% vs 39%), median OS is much lower of patients with *NRAS* mutation (21months versus 33 months, p=0.034) (202).

In summary, studies from this PhD project confirm that MAPK remains a major signalling pathway of *BRAF*/*RAS* WT melanoma and support the potential utility of including MEK inhibitors in the treatment of this melanoma subset. However, we also show that *BRAF*/*RAS* WT melanomas frequently display a high mutation burden and carry concurrent mutations in *TP53*, *NF1* and other RASopathy genes. This mutation profile is associated with activation of multiple pathways and resistance to MEK inhibition. Predictably, co-targeting alternative signalling pathways (i.e. SRC, MAPK, RTK) did not prove effective in these high mutation burden *BRAF*/*RAS* WT melanomas, but these tumours may be responsive to immunotherapies which are often more effective in controlling high mutation burden tumours. Thus, the genetic status of *NF1* may prove a useful surrogate marker for estimating the likelihood of response to targeted versus immune therapies. Recent studies have shown that patients with *NF1*-mutant melanoma significantly benefit from PD-1-based immune checkpoint blockade therapy (443).

Moreover, BRAF or MEK inhibition was shown to stimulate T-cell proliferation and activation (279) and BRAF inhibitors induced marked T-cell infiltration into melanoma tumours (280), supporting combination of molecular targeted and immune checkpoint inhibitor therapies. Several ongoing clinical trials are currently assessing efficacy of these combinations (NCT02130466, NCT02027961, NCT02967692, NCT02908672) (281, 282). Early clinical trial data have already shown that patients with *NRAS*-mutant or *NRAS* WT advanced melanoma treated with MEK inhibitor before or after immune checkpoint inhibitor therapy showed longer overall survival, compared to patients who did not receive a MEK inhibitor (202). However, dose-limiting hepatotoxicity remains a major issue for these combinations (283-285). It will be interesting to explore the efficacy of combination MEK inhibitor with PD-1 inhibitor or CTLA-4 inhibitor in our panel of *BRAF*/*RAS* WT melanoma cell lines.

References

1. Costin GE, Hearing VJ. Human skin pigmentation: melanocytes modulate skin color in response to stress. FASEB J. 2007;21(4):976-94.

2. Kaidbey KH, Agin PP, Sayre RM, Kligman AM. Photoprotection by melanin—a comparison of black and Caucasian skin. J Am Acad Dermatol. 1979;1(3):249-60.

3. Cichorek M, Wachulska M, Stasiewicz A, Tyminska A. Skin melanocytes: biology and development. Postepy dermatologii i alergologii. 2013;30(1):30-41.

4. Paluncic J, Kovacevic Z, Jansson PJ, Kalinowski D, Merlot AM, Huang ML, et al. Roads to melanoma: Key pathways and emerging players in melanoma progression and oncogenic signaling. Biochim Biophys Acta. 2016;1863(4):770-84.

5. Whiteman DC, Green AC, Olsen CM. The Growing Burden of Invasive Melanoma: Projections of Incidence Rates and Numbers of New Cases in Six Susceptible Populations through 2031. J Invest Dermatol. 2016;136(6):1161-71.

6. (AIHW). Australian Institute of Health and Welfare. Cancer in Australia 2017. CAN 100(204).

7. (AIHW). Australian Institute of Health and Welfare. Skin cancer in Australia 2016. CAN 96

8. Iannacone MR, Youlden DR, Baade PD, Aitken JF, Green AC. Melanoma incidence trends and survival in adolescents and young adults in Queensland, Australia. Int J Cancer. 2015;136(3):603-9.

9. Gandini S, Sera F, Cattaruzza MS, Pasquini P, Picconi O, Boyle P, et al. Meta-analysis of risk factors for cutaneous melanoma: II. Sun exposure. Eur J Cancer. 2005;41(1):45-60.

10. Wu S, Han J, Laden F, Qureshi AA. Long-term ultraviolet flux, other potential risk factors, and skin cancer risk: a cohort study. Cancer Epidemiol Biomarkers Prev. 2014;23(6):1080-9.

11. Miller AJ, Mihm Jr MC. Melanoma. N Engl J Med. 2006;355(1):51-65.

12. Kim SY, Yun SJ. Cutaneous Melanoma in Asians. Chonnam Med J. 2016;52(3):185-93.

13. Gandini S, Sera F, Cattaruzza MS, Pasquini P, Zanetti R, Masini C, et al. Meta-analysis of risk factors for cutaneous melanoma: III. Family history, actinic damage and phenotypic factors. Eur J Cancer. 2005;41(14):2040-59.

14. Miller SA, Hamilton SL, Wester UG, Cyr WH. An analysis of UVA emissions from sunlamps and the potential importance for melanoma. Photochem Photobiol. 1998;68(1):63-70.

15. Rastogi RP, Kumar A, Tyagi MB, Sinha RP. Molecular mechanisms of ultraviolet radiation-induced DNA damage and repair. Journal of nucleic acids. 2010;2010.

16. Sample A, He YY. Mechanisms and prevention of UV-induced melanoma. Photodermatol Photoimmunol Photomed. 2018;34(1):13-24.

17. Hodis E, Watson IR, Kryukov GV, Arold ST, Imielinski M, Theurillat JP, et al. A landscape of driver mutations in melanoma. Cell. 2012;150(2):251-63.

18. Melamed RD, Aydin IT, Rajan GS, Phelps R, Silvers DN, Emmett KJ, et al. Genomic Characterization of Dysplastic Nevi Unveils Implications for Diagnosis of Melanoma. J Invest Dermatol. 2017;137(4):905-9.

19. Geller AC, Miller DR, Annas G, Demierre M, Gilchrest BA, Koh HK. Melanoma incidence and mortality among us whites, 1969-1999. JAMA. 2002;288(14):1719-20.

20. Karagianni F, Njauw CN, Kypreou KP, Stergiopoulou A, Plaka M, Polydorou D, et al. CDKN2A/CDK4 Status in Greek Patients with Familial Melanoma and Association with Clinico-epidemiological Parameters. Acta Derm Venereol. 2018.

21. Yokoyama S, Woods SL, Boyle GM, Aoude LG, MacGregor S, Zismann V, et al. A novel recurrent mutation in MITF predisposes to familial and sporadic melanoma. Nature. 2011;480:99.

22. Garraway LA, Widlund HR, Rubin MA, Getz G, Berger AJ, Ramaswamy S, et al. Integrative genomic analyses identify MITF as a lineage survival oncogene amplified in malignant melanoma. Nature. 2005;436(7047):117-22.

23. Rafnar T, Sulem P, Stacey SN, Geller F, Gudmundsson J, Sigurdsson A, et al. Sequence variants at the TERT-CLPTM1L locus associate with many cancer types. Nat Genet. 2009;41(2):221-7.

24. Carbone M, Flores EG, Emi M, Johnson TA, Tsunoda T, Behner D, et al. Combined genetic and genealogic studies uncover a large BAP1 cancer syndrome kindred tracing back nine generations to a common ancestor from the 1700s. PLoS genetics. 2015;11(12):e1005633.

25. Demenais F, Mohamdi H, Chaudru V, Goldstein A, Newton Bishop J, Bishop D, et al. Association of MC1R variants and host phenotypes with melanoma risk in CDKN2A mutation carriers: a GenoMEL study. JNCI: Journal of the National Cancer Institute. 2010;102(20):1568-83.

26. Kazlow E, Ferguson R, Simpson D, Martinez CN, Vogelsang M, Moran U, et al. Novel germline risk loci in familial melanoma (FM). J Clin Oncol. 2017;35(15_suppl):1535-.

27. Scolyer RA, Long GV, Thompson JF. Evolving concepts in melanoma classification and their relevance to multidisciplinary melanoma patient care. Mol Oncol. 2011;5(2):124-36.

28. Naldi L, Altieri A, Imberti GL, Gallus S, Bosetti C, La Vecchia C, et al. Sun exposure, phenotypic characteristics, and cutaneous malignant melanoma. An analysis according to different clinico-pathological variants and anatomic locations (Italy). Cancer Causes Control. 2005;16(8):893-9.

29. Bastian BC. The molecular pathology of melanoma: an integrated taxonomy of melanocytic neoplasia. Annu Rev Pathol. 2014;9:239-71.

30. Cognetta Jr AB, Stolz W, Katz B, Tullos J, Gossain S. Dermatoscopy of lentigo maligna. Dermatol Clin. 2001;19(2):307-18.

31. Greveling K, Wakkee M, Nijsten T, van den Bos RR, Hollestein LM. Epidemiology of Lentigo Maligna and Lentigo Maligna Melanoma in the Netherlands, 1989-2013. J Invest Dermatol. 2016;136(10):1955-60.

32. Cohen LM. Lentigo maligna and lentigo maligna melanoma. J Am Acad Dermatol. 1995;33(6):923-36.

33. Menzies SW, Moloney FJ, Byth K, Avramidis M, Argenziano G, Zalaudek I, et al. Dermoscopic evaluation of nodular melanoma. JAMA Dermatol. 2013;149(6):699-709.

34. Rosendahl C, Hishon M, Cameron A, Barksdale S, Weedon D, Kittler H. Nodular melanoma: five consecutive cases in a general practice with polarized and non-polarized dermatoscopy and dermatopathology. Dermatol Pract Concept. 2014;4(2):69-75.

35. Volkovova K, Bilanicova D, Bartonova A, Letasiova S, Dusinska M. Associations between environmental factors and incidence of cutaneous melanoma. Review. Environ Health. 2012;11 Suppl 1:S12.

36. Duncan LM. The classification of cutaneous melanoma. Hematol Oncol Clin North Am. 2009;23(3):501-13, ix.

37. Liu W, Dowling JP, Murray WK, McArthur GA, Thompson JF, Wolfe R, et al. Rate of growth in melanomas: characteristics and associations of rapidly growing melanomas. Arch Dermatol. 2006;142(12):1551-8.

38. Edlundh-Rose E, Egyha S, Omholt K, Mansson-Brahme E, Platz A, Hansson J, et al. NRAS and BRAF mutations in melanoma tumours in relation to clinical characteristics: a study based on mutation screening by pyrosequencing. Melanoma Res. 2006;16(6):471-8.

39. Lee JH, Choi JW, Kim YS. Frequencies of BRAF and NRAS mutations are different in histological types and sites of origin of cutaneous melanoma: a meta-analysis. Br J Dermatol. 2011;164(4):776-84.

40. Reed RJ. New concepts in surgical pathology of the skin: John Wiley & Sons; 1976.

41. Lee HY, Chay WY, Tang MB, Chio MT, Tan SH. Melanoma: differences between Asian and Caucasian patients. Ann Acad Med Singapore. 2012;41(1):17-20.

42. Piliang MP. Acral lentiginous melanoma. Clin Lab Med. 2011;31(2):281-8.

43. Bradford PT, Goldstein AM, McMaster ML, Tucker MA. Acral lentiginous melanoma: incidence and survival patterns in the United States, 1986-2005. Arch Dermatol. 2009;145(4):427-34.

44. Zell JA, Cinar P, Mobasher M, Ziogas A, Meyskens FL, Jr., Anton-Culver H. Survival for patients with invasive cutaneous melanoma among ethnic groups: the effects of socioeconomic status and treatment. J Clin Oncol. 2008;26(1):66-75.

45. Hayward NK, Wilmott JS, Waddell N, Johansson PA, Field MA, Nones K, et al. Whole-genome landscapes of major melanoma subtypes. Nature. 2017;545(7653):175-80.

46. Quinn MJ, Crotty KA, Thompson JF, Coates AS, O'Brien CJ, McCarthy WH. Desmoplastic and desmoplastic neurotropic melanoma: experience with 280 patients. Cancer: Interdisciplinary International Journal of the American Cancer Society. 1998;83(6):1128-35.

47. Feng Z, Wu X, Chen V, Velie E, Zhang Z. Incidence and survival of desmoplastic melanoma in the United States, 1992–2007. J Cutan Pathol. 2011;38(8):616-24.

48. McLaughlin CC, Wu X-C, Jemal A, Martin HJ, Roche LM, Chen VW. Incidence of noncutaneous melanomas in the U.S. Cancer. 2005;103(5):1000-7.

49. McLean N, Tighiouart M, Muller S. Primary mucosal melanoma of the head and neck. Comparison of clinical presentation and histopathologic features of oral and sinonasal melanoma. Oral Oncol. 2008;44(11):1039-46.

50. Sheng X, Kong Y, Li Y, Zhang Q, Si L, Cui C, et al. GNAQ and GNA11 mutations occur in 9.5% of mucosal melanoma and are associated with poor prognosis. Eur J Cancer. 2016;65:156-63.

51. Singh AD, Turell ME, Topham AK. Uveal melanoma: trends in incidence, treatment, and survival. Ophthalmology. 2011;118(9):1881-5.

52. Damato B. Treatment of primary intraocular melanoma. Expert Rev Anticancer Ther. 2006;6(4):493-506.

53. Kaliki S, Shields CL, Shields JA. Uveal melanoma: Estimating prognosis. Indian J Ophthalmol. 2015;63(2):93-102.

54. Van Raamsdonk CD, Griewank KG, Crosby MB, Garrido MC, Vemula S, Wiesner T, et al. Mutations in GNA11 in uveal melanoma. N Engl J Med. 2010;363(23):2191-9.

55. Shoushtari AN, Carvajal RD. GNAQ and GNA11 mutations in uveal melanoma. Melanoma Res. 2014;24(6):525-34.

56. Park JJ, Diefenbach RJ, Joshua AM, Kefford RF, Carlino MS, Rizos H. Oncogenic signaling in uveal melanoma. Pigment cell & melanoma research. 2018.

57. Martin M, Masshofer L, Temming P, Rahmann S, Metz C, Bornfeld N, et al. Exome sequencing identifies recurrent somatic mutations in EIF1AX and SF3B1 in uveal melanoma with disomy 3. Nat Genet. 2013;45(8):933-6.

58. Berger MF, Hodis E, Heffernan TP, Deribe YL, Lawrence MS, Protopopov A, et al. Melanoma genome sequencing reveals frequent PREX2 mutations. Nature. 2012;485(7399):502-6.

59. Cancer Genome Atlas N. Genomic Classification of Cutaneous Melanoma. Cell. 2015;161(7):1681-96.

60. Krauthammer M, Kong Y, Ha BH, Evans P, Bacchiocchi A, McCusker JP, et al. Exome sequencing identifies recurrent somatic RAC1 mutations in melanoma. Nat Genet. 2012;44(9):1006-14.

61. Davies H. Mutations of the BRAF gene in human cancer. Nature. 9 June 2002.

62. Sclafani F, Gullo G, Sheahan K, Crown J. BRAF mutations in melanoma and colorectal cancer: a single oncogenic mutation with different tumour phenotypes and clinical implications. Crit Rev Oncol Hematol. 2013;87(1):55-68.

63. Cheng L, Lopez-Beltran A, Massari F, MacLennan GT, Montironi R. Molecular testing for BRAF mutations to inform melanoma treatment decisions: a move toward precision medicine. Mod Pathol. 2018;31(1):24.

64. Pollock PM, Harper UL, Hansen KS, Yudt LM, Stark M, Robbins CM, et al. High frequency of BRAF mutations in nevi. Nat Genet. 2002;33:19.

65. Corcoran RB, Dias-Santagata D, Bergethon K, Iafrate AJ, Settleman J, Engelman JA. BRAF gene amplification can promote acquired resistance to MEK inhibitors in cancer cells harboring the BRAF V600E mutation. Sci Signal. 2010;3(149):ra84-ra.

66. Horn S, Figl A, Rachakonda PS, Fischer C, Sucker A, Gast A, et al. TERT Promoter Mutations in Familial and Sporadic Melanoma. Science. 2013;339(6122):959.

67. Fredriksson NJ, Ny L, Nilsson JA, Larsson E. Systematic analysis of noncoding somatic mutations and gene expression alterations across 14 tumor types. Nat Genet. 2014;46:1258.

68. Maldonado JL, Fridlyand J, Patel H, Jain AN, Busam K, Kageshita T, et al. Determinants of BRAF Mutations in Primary Melanomas. JNCI Journal of the National Cancer Institute. 2003;95(24):1878-90.

69. Brash DE. UV signature mutations. Photochem Photobiol. 2015;91(1):15-26.

70. Jakob JA, Bassett RL, Jr., Ng CS, Curry JL, Joseph RW, Alvarado GC, et al. NRAS mutation status is an independent prognostic factor in metastatic melanoma. Cancer. 2012;118(16):4014-23.

71. Munoz-Couselo E, Adelantado EZ, Ortiz C, Garcia JS, Perez-Garcia J. NRAS-mutant melanoma: current challenges and future prospect. Onco Targets Ther. 2017;10:3941-7.

72. Bucheit AD, Syklawer E, Jakob JA, Bassett RL, Jr., Curry JL, Gershenwald JE, et al. Clinical characteristics and outcomes with specific BRAF and NRAS mutations in patients with metastatic melanoma. Cancer. 2013;119(21):3821-9.

73. Devitt B, Liu W, Salemi R, Wolfe R, Kelly J, Tzen CY, et al. Clinical outcome and pathological features associated with NRAS mutation in cutaneous melanoma. Pigment cell & melanoma research. 2011;24(4):666-72.

74. Platz A, Egyhazi S, Ringborg U, Hansson J. Human cutaneous melanoma; a review of NRAS and BRAF mutation frequencies in relation to histogenetic subclass and body site. Mol Oncol. 2008;1(4):395-405.

75. Maertens O, Johnson B, Hollstein P, Frederick DT, Cooper ZA, Messiaen L, et al. Elucidating distinct roles for NF1 in melanomagenesis. Cancer Discov. 2013;3(3):338-49.

76. Nissan MH, Pratilas CA, Jones AM, Ramirez R, Won H, Liu C, et al. Loss of NF1 in cutaneous melanoma is associated with RAS activation and MEK dependence. Cancer Res. 2014;74(8):2340-50.

77. Krauthammer M, Kong Y, Bacchiocchi A, Evans P, Pornputtapong N, Wu C, et al. Exome sequencing identifies recurrent mutations in NF1 and RASopathy genes in sun-exposed melanomas. Nat Genet. 2015;47(9):996-1002.

78. Cirenajwis H, Lauss M, Ekedahl H, Torngren T, Kvist A, Saal LH, et al. NF1-mutated melanoma tumors harbor distinct clinical and biological characteristics. Mol Oncol. 2017;11(4):438-51.

79. Goel VK, Lazar AJ, Warneke CL, Redston MS, Haluska FG. Examination of mutations in BRAF, NRAS, and PTEN in primary cutaneous melanoma. J Invest Dermatol. 2006;126(1):154-60.

80. Orouji E, Orouji A, Gaiser T, Larribere L, Gebhardt C, Utikal J. MAP kinase pathway gene copy alterations in NRAS/BRAF wild-type advanced melanoma. Int J Cancer. 2016;138(9):2257-62.

81. Nikolaev SI, Rimoldi D, Iseli C, Valsesia A, Robyr D, Gehrig C, et al. Exome sequencing identifies recurrent somatic MAP2K1 and MAP2K2 mutations in melanoma. Nat Genet. 2011;44(2):133-9.

82. Stark MS, Woods SL, Gartside MG, Bonazzi VF, Dutton-Regester K, Aoude LG, et al. Frequent somatic mutations in MAP3K5 and MAP3K9 in metastatic melanoma identified by exome sequencing. Nat Genet. 2011;44:165.

83. Wei X, Walia V, Lin JC, Teer JK, Prickett TD, Gartner J, et al. Exome sequencing identifies GRIN2A as frequently mutated in melanoma. Nat Genet. 2011;43:442.

84. Poulos RC, Thoms JAI, Shah A, Beck D, Pimanda JE, Wong JWH. Systematic Screening of Promoter Regions Pinpoints Functional Cis-Regulatory Mutations in a Cutaneous Melanoma Genome. Mol Cancer Res. 2015;13(8):1218.

85. Dutton-Regester K, Gartner JJ, Emmanuel R, Qutob N, Davies MA, Gershenwald JE, et al. A highly recurrent RPS27 5'UTR mutation in melanoma. Oncotarget. 2014;5(10):2912-7.

86. Guan J, Gupta R, Filipp FV. Cancer systems biology of TCGA SKCM: Efficient detection of genomic drivers in melanoma. Sci Rep. 2015;5:7857.

87. Gartner JJ, Parker SC, Prickett TD, Dutton-Regester K, Stitzel ML, Lin JC, et al. Whole-genome sequencing identifies a recurrent functional synonymous mutation in melanoma. Proceedings of the National Academy of Sciences. 2013;110(33):13481-6.

88. Fredriksson NJ, Elliott K, Filges S, Van den Eynden J, Ståhlberg A, Larsson E. Recurrent promoter mutations in melanoma are defined by an extended context-specific mutational signature. PLoS genetics. 2017;13(5):e1006773.

89. Gotea V, Gartner JJ, Qutob N, Elnitski L, Samuels Y. The functional relevance of somatic synonymous mutations in melanoma and other cancers. Pigment cell & melanoma research. 2015;28(6):673-84.

90. Aguissa-Toure AH, Li G. Genetic alterations of PTEN in human melanoma. Cell Mol Life Sci. 2012;69(9):1475-91.

91. Wu H, Goel V, Haluska FG. PTEN signaling pathways in melanoma. Oncogene. 2003;22:3113.

92. Jonsson G, Dahl C, Staaf J, Sandberg T, Bendahl PO, Ringner M, et al. Genomic profiling of malignant melanoma using tiling-resolution arrayCGH. Oncogene. 2007;26(32):4738-48.

93. Whiteman DC, Zhou XP, Cummings MC, Pavey S, Hayward NK, Eng C. Nuclear PTEN expression and clinicopathologic features in a population-based series of primary cutaneous melanoma. Int J Cancer. 2002;99(1):63-7.

94. Cerami E, Gao J, Dogrusoz U, Gross BE, Sumer SO, Aksoy BA, et al. The cBio cancer genomics portal: an open platform for exploring multidimensional cancer genomics data. AACR; 2012.

95. Gao J, Aksoy BA, Dogrusoz U, Dresdner G, Gross B, Sumer SO, et al. Integrative analysis of complex cancer genomics and clinical profiles using the cBioPortal. Sci Signal. 2013;6(269):pl1-pl.

96. Kandoth C, McLellan MD, Vandin F, Ye K, Niu B, Lu C, et al. Mutational landscape and significance across 12 major cancer types. Nature. 2013;502:333.

97. Box NF, Vukmer TO, Terzian T. Targeting p53 in melanoma. Pigment cell & melanoma research. 2014;27(1):8-10.

98. Hocker T, Tsao H. Ultraviolet radiation and melanoma: a systematic review and analysis of reported sequence variants. Hum Mutat. 2007;28(6):578-88.

99. Lee B, Sandhu S, McArthur G. Cell cycle control as a promising target in melanoma. Curr Opin Oncol. 2015;27(2):141-50.

100. Ji Z, Kumar R, Taylor M, Rajadurai A, Marzuka-Alcalá A, Chen YE, et al. Vemurafenib Synergizes with Nutlin-3 to Deplete Survivin and Suppress Melanoma Viability and Tumor Growth. Clinical cancer research : an official journal of the American Association for Cancer Research. 2013;19(16):4383-91.

101. Sun D, Li Z, Rew Y, Gribble M, Bartberger MD, Beck HP, et al. Discovery of AMG 232, a Potent, Selective, and Orally Bioavailable MDM2–p53 Inhibitor in Clinical Development. J Med Chem. 2014;57(4):1454-72.

102. Gil J, Peters G. Regulation of the INK4b–ARF–INK4a tumour suppressor locus: all for one or one for all. Nature Reviews Molecular Cell Biology. 2006;7:667.

103. Zhao R, Choi BY, Lee M-H, Bode AM, Dong Z. Implications of Genetic and Epigenetic Alterations of CDKN2A (p16(INK4a)) in Cancer. EBioMedicine. 2016;8:30-9.

104. Serrano M, Hannon GJ, Beach D. A new regulatory motif in cell-cycle control causing specific inhibition of cyclin D/CDK4. Nature. 1993;366:704.

105. Pomerantz J, Schreiber-Agus N, Liégeois NJ, Silverman A, Alland L, Chin L, et al. The Ink4a Tumor Suppressor Gene Product, p19Arf, Interacts with MDM2 and Neutralizes MDM2's Inhibition of p53. Cell. 1998;92(6):713-23.

106. Chin L, Garraway LA, Fisher DE. Malignant melanoma: genetics and therapeutics in the genomic era. Genes Dev. 2006;20(16):2149-82.

107. Potrony M, Puig-Butillé JA, Aguilera P, Badenas C, Carrera C, Malvehy J, et al. Increased prevalence of lung, breast and pancreatic cancers in addition to melanoma risk in families bearing the CDKN2A mutation: Implications for genetic counseling. J Am Acad Dermatol. 2014;71(5):888-95.

108. Mountzios G, Rampias T, Psyrri A. The mutational spectrum of squamous-cell carcinoma of the head and neck: targetable genetic events and clinical impact. Ann Oncol. 2014;25(10):1889-900.

109. Ullrich A, Schlessinger J. Signal transduction by receptors with tyrosine kinase activity. Cell. 1990;61(2):203-12.

110. Cheng Y, Zhang G, Li G. Targeting MAPK pathway in melanoma therapy. Cancer Metastasis Rev. 2013;32(3-4):567-84.

111. Low HB, Zhang Y. Regulatory Roles of MAPK Phosphatases in Cancer. Immune Netw. 2016;16(2):85-98.

112. Yoon S, Seger R. The extracellular signal-regulated kinase: multiple substrates regulate diverse cellular functions. Growth Factors. 2006;24(1):21-44.

113. Cargnello M, Roux PP. Activation and function of the MAPKs and their substrates, the MAPK-activated protein kinases. Microbiol Mol Biol Rev. 2011;75(1):50-83.

114. Roux PP, Blenis J. ERK and p38 MAPK-Activated Protein Kinases: a Family of Protein Kinases with Diverse Biological Functions. Microbiol Mol Biol Rev. 2004;68(2):320-44.

115. Gille H, Strahl T, Shaw PE. Activation of ternary complex factor Elk-1 by stress-activated protein kinases. Curr Biol. 1995;5(10):1191-200.

116. Cohen C, Zavala-Pompa A, Sequeira JH, Shoji M, Sexton DG, Cotsonis G, et al. Mitogen-actived protein kinase activation is an early event in melanoma progression. Clin Cancer Res. 2002;8(12):3728-33.

117. Vallarelli AF, Rachakonda PS, André J, Heidenreich B, Riffaud L, Bensussan A, et al. TERT promoter mutations in melanoma render TERT expression dependent on MAPK pathway activation. Oncotarget. 2016;7(33):53127.

118. McCubrey JA, Steelman LS, Chappell WH, Abrams SL, Montalto G, Cervello M, et al. Mutations and deregulation of Ras/Raf/MEK/ERK and PI3K/PTEN/Akt/mTOR cascades which alter therapy response. Oncotarget. 2012;3(9):954.

119. Li E, Hristova K. ROLE OF RECEPTOR TYROSINE KINASE TRANSMEMBRANE DOMAINS IN CELL SIGNALING AND HUMAN PATHOLOGIES. Biochemistry. 2006;45(20):6241-51.

120. Hubbard SR, Miller WT. Receptor tyrosine kinases: mechanisms of activation and signaling. Curr Opin Cell Biol. 2007;19(2):117-23.

121. Lau C, Killian KJ, Samuels Y, Rudloff U. ERBB4 mutation analysis: emerging molecular target for melanoma treatment. Methods in molecular biology (Clifton, NJ). 2014;1102:461-80.

122. Curtin JA, Busam K, Pinkel D, Bastian BC. Somatic activation of KIT in distinct subtypes of melanoma. J Clin Oncol. 2006;24(26):4340-6.

123. Dai J, Kong Y, Si L, Chi Z, Cui C, Sheng X, et al. Large-scale analysis of PDGFRA mutations in melanomas and evaluation of their sensitivity to tyrosine kinase inhibitors imatinib and crenolanib. Clin Cancer Res. 2013.

124. Satyamoorthy K, Li G, Gerrero MR, Brose MS, Volpe P, Weber BL, et al. Constitutive mitogen-activated protein kinase activation in melanoma is mediated by both BRAF mutations and autocrine growth factor stimulation. Cancer Res. 2003;63(4):756-9.

125. Tsavachidou D, Coleman ML, Athanasiadis G, Li S, Licht JD, Olson MF, et al. SPRY2 is an inhibitor of the ras/extracellular signal-regulated kinase pathway in melanocytes and melanoma cells with wild-type BRAF but not with the V599E mutant. Cancer Res. 2004;64(16):5556-9.

126. Garnett MJ, Rana S, Paterson H, Barford D, Marais R. Wild-Type and Mutant B-RAF Activate C-RAF through Distinct Mechanisms Involving Heterodimerization. Mol Cell. 2005;20(6):963-9.

127. Eblen ST, Slack JK, Weber MJ, Catling AD. Rac-PAK Signaling Stimulates Extracellular Signal-Regulated Kinase (ERK) Activation by Regulating Formation of MEK1-ERK Complexes. Mol Cell Biol. 2002;22(17):6023-33.

128. Atefi M, Titz B, Tsoi J, Avramis E, Le A, Ng C, et al. CRAF R391W is a melanoma driver oncogene. Sci Rep. 2016;6:27454.

129. Dumaz N, Hayward R, Martin J, Ogilvie L, Hedley D, Curtin JA, et al. In melanoma, RAS mutations are accompanied by switching signaling from BRAF to CRAF and disrupted cyclic AMP signaling. Cancer Res. 2006;66(19):9483-91.

130. Cohen Y, Goldenberg-Cohen N, Parrella P, Chowers I, Merbs SL, Pe'er J, et al. Lack of BRAF Mutation in Primary Uveal Melanoma. Investigative Opthalmology & Visual Science. 2003;44(7):2876.

131. Cuadrado A, Nebreda Angel R. Mechanisms and functions of p38 MAPK signalling. Biochem J. 2010;429(3):403-17.

132. Cuenda A, Rousseau S. p38 MAP-Kinases pathway regulation, function and role in human diseases. Biochimica et Biophysica Acta (BBA) - Molecular Cell Research. 2007;1773(8):1358-75.

133. Grossi V, Peserico A, Tezil T, Simone C. p38α MAPK pathway: A key factor in colorectal cancer therapy and chemoresistance. World Journal of Gastroenterology : WJG. 2014;20(29):9744-58.

134. Lopez‐Bergami P. The role of mitogen‐and stress‐activated protein kinase pathways in melanoma. Pigment cell & melanoma research. 2011;24(5):902-21.

135. Bulavin DV, Fornace AJ. p38 MAP Kinase's Emerging Role as a Tumor Suppressor. Adv Cancer Res. 92: Academic Press; 2004. p. 95-118.

136. Wagner EF, Nebreda ÁR. Signal integration by JNK and p38 MAPK pathways in cancer development. Nature Reviews Cancer. 2009;9:537.

137. Timofeev O, Lee TY, Bulavin DV. A subtle change in p38 MAPK activity is sufficient to suppress in vivo tumorigenesis. Cell Cycle. 2005;4(1):118-20.

138. Bulavin DV, Phillips C, Nannenga B, Timofeev O, Donehower LA, Anderson CW, et al. Inactivation of the Wip1 phosphatase inhibits mammary tumorigenesis through p38 MAPK–mediated activation of the p16Ink4a-p19Arf pathway. Nat Genet. 2004;36:343.

139. Ashwell JD. The many paths to p38 mitogen-activated protein kinase activation in the immune system. Nature Reviews Immunology. 2006;6:532.

140. Wilson KP, Fitzgibbon MJ, Caron PR, Griffith JP, Chen W, McCaffrey PG, et al. Crystal structure of p38 mitogen-activated protein kinase. J Biol Chem. 1996;271(44):27696-700.

141. Jørgensen K, Davidson B, Flørenes VA. Activation of c-jun N-terminal kinase is associated with cell proliferation and shorter relapse-free period in superficial spreading malignant melanoma. Mod Pathol. 2006;19:1446.

142. Estrada Y, Dong J, Ossowski L. Positive crosstalk between ERK and p38 in melanoma stimulates migration and in vivo proliferation. Pigment cell & melanoma research. 2009;22(1):66-76.

143. HuangFu W-C, Qian J, Liu C, Liu J, Lokshin AE, Baker DP, et al. Inflammatory signaling compromises cell responses to interferon alpha. Oncogene. 2012;31(2):161-72.

144. Smalley K, Eisen T. Differentiation of human melanoma cells through p38 MAP kinase is associated with decreased retinoblastoma protein phosphorylation and cell cycle arrest2002. 187-92 p.

145. Saha B, Singh SK, Sarkar C, Bera R, Ratha J, Tobin DJ, et al. Activation of the Mitf promoter by lipid-stimulated activation of p38-stress signalling to CREB. Pigment Cell Res. 2006;19(6):595-605.

146. Khanna P, Yunkunis T, Muddana HS, Peng HH, August A, Dong C. p38 MAP kinase is necessary for melanoma-mediated regulation of VE-cadherin disassembly. American Journal of Physiology - Cell Physiology. 2010;298(5):C1140-C50.

147. Neuder LE, Keener JM, Eckert RE, Trujillo JC, Jones SL. Role of p38 MAPK in LPS induced pro-inflammatory cytokine and chemokine gene expression in equine leukocytes. Vet Immunol Immunopathol. 2009;129(3-4):192-9.

148. Gollob JA, Sciambi CJ, Huang Z, Dressman HK. Gene expression changes and signaling events associated with the direct antimelanoma effect of IFN-γ. Cancer Res. 2005;65(19):8869-77.

149. Corre S, Primot A, Sviderskaya E, Bennett DC, Vaulont S, Goding CR, et al. UV-induced expression of key component of the tanning process, the POMC and MC1R genes, is dependent on the p-38-activated upstream stimulating factor-1 (USF-1). J Biol Chem. 2004;279(49):51226-33.

150. Davis RJ. Signal Transduction by the JNK Group of MAP Kinases. Cell. 2000;103(2):239-52.

151. Gupta S, Barrett T, Whitmarsh AJ, Cavanagh J, Sluss HK, Dérijard B, et al. Selective interaction of JNK protein kinase isoforms with transcription factors. The EMBO Journal. 1996;15(11):2760-70.

152. Karin M. The regulation of AP-1 activity by mitogen-activated protein kinases. J Biol Chem. 1995;270(28):16483-6.

153. Weston CR, Davis RJ. The JNK signal transduction pathway. Curr Opin Genet Dev. 2002;12(1):14-21.

154. Weston CR, Davis RJ. The JNK signal transduction pathway. Curr Opin Cell Biol. 2007;19(2):142-9.

155. López-Bergami P, Habelhah H, Bhoumik A, Zhang W, Wang L-H, Ronai Ze. Receptor for RACK1 mediates activation of JNK by protein kinase C. Mol Cell. 2005;19(3):309-20.

156. Leppä S, Saffrich R, Ansorge W, Bohmann D. Differential regulation of c-Jun by ERK and JNK during PC12 cell differentiation. The EMBO Journal. 1998;17(15):4404-13.

157. Vogt PK. Jun, the oncoprotein. Oncogene. 2001;20:2365.

158. Hayakawa J, Mittal S, Wang Y, Korkmaz KS, Adamson E, English C, et al. Identification of Promoters Bound by c-Jun/ATF2 during Rapid Large-Scale Gene Activation following Genotoxic Stress. Mol Cell. 2004;16(4):521-35.

159. Yamanishi DT, Buckmeier JA, Meyskens FL. Expression of c-jun, jun-B, and c-fos Proto-Oncogenes in Human Primary Melanocytes and Metastatic Melanomas. J Invest Dermatol. 1991;97(2):349-53.

160. Pathria G, Garg B, Garg K, Wagner C, Wagner SN. Dual c-Jun N-terminal kinase-cyclin D1 and extracellular signal-related kinase-c-Jun disjunction in human melanoma. Br J Dermatol. 2016;175(6):1221-31.

161. Wang Y, Zhang G, Jin J, Degan S, Tameze Y, Zhang JY. MALT1 promotes melanoma progression through JNK/c-Jun signaling. Oncogenesis. 2017;6(7):e365.

162. Cheung M, Sharma A, Madhunapantula SV, Robertson GP. Akt3 and mutant V600EB-Raf cooperate to promote early melanoma development. Cancer Res. 2008;68(9):3429-39.

163. Hennessy BT, Smith DL, Ram PT, Lu Y, Mills GB. Exploiting the PI3K/AKT pathway for cancer drug discovery. Nature reviews Drug discovery. 2005;4(12):988.

164. Manning BD, Toker A. AKT/PKB signaling: navigating the network. Cell. 2017;169(3):381-405.

165. Cantley LC. The phosphoinositide 3-kinase pathway. Science. 2002;296(5573):1655-7.

166. Sauter G, Maeda T, Waldman FM, Davis RL, Feuerstein BG. Patterns of epidermal growth factor receptor amplification in malignant gliomas. The American journal of pathology. 1996;148(4):1047.

167. Bachman KE, Argani P, Samuels Y, Silliman N, Ptak J, Szabo S, et al. The PIK3CA gene is mutated with high frequency in human breast cancers. Cancer Biol Ther. 2004;3(8):772-5.

168. Salmena L, Carracedo A, Pandolfi PP. Tenets of PTEN tumor suppression. Cell. 2008;133(3):403-14.

169. Dibble CC, Asara JM, Manning BD. Characterization of Rictor phosphorylation sites reveals direct regulation of mTOR complex 2 by S6K1. Mol Cell Biol. 2009;29(21):5657-70.

170. Babchia N, Calipel A, Mouriaux F, Faussat AM, Mascarelli F. The PI3K/Akt and mTOR/P70S6K signaling pathways in human uveal melanoma cells: interaction with B-Raf/ERK. Invest Ophthalmol Vis Sci. 2010;51(1):421-9.

171. Anastas JN, Moon RT. WNT signalling pathways as therapeutic targets in cancer. Nature Reviews Cancer. 2013;13(1):11.

172. Sherwood V. WNT Signaling: an Emerging Mediator of Cancer Cell Metabolism? Mol Cell Biol. 2015;35(1):2-10.

173. Liu C, Li Y, Semenov M, Han C, Baeg G-H, Tan Y, et al. Control of β-catenin phosphorylation/degradation by a dual-kinase mechanism. Cell. 2002;108(6):837-47.

174. MacDonald BT, Tamai K, He X. Wnt/β-catenin signaling: components, mechanisms, and diseases. Dev Cell. 2009;17(1):9-26.

175. Worm J, Christensen C, Grønbæk K, Tulchinsky E, Guldberg P. Genetic and epigenetic alterations of the APC gene in malignant melanoma. Oncogene. 2004;23(30):5215.

176. Rubinfeld B, Robbins P, El-Gamil M, Albert I, Porfiri E, Polakis P. Stabilization of β-catenin by genetic defects in melanoma cell lines. Science. 1997;275(5307):1790-2.

177. Goodall J, Martinozzi S, Dexter TJ, Champeval D, Carreira S, Larue L, et al. Brn-2 expression controls melanoma proliferation and is directly regulated by β-catenin. Mol Cell Biol. 2004;24(7):2915-22.

178. Zhang X, Gaspard JP, Chung DC. Regulation of vascular endothelial growth factor by the Wnt and K-ras pathways in colonic neoplasia. Cancer Res. 2001;61(16):6050-4.

179. Spranger S, Bao R, Gajewski TF. Melanoma-intrinsic β-catenin signalling prevents anti-tumour immunity. Nature. 2015;523(7559):231.

180. Luke JJ, Schwartz GK. Chemotherapy in the management of advanced cutaneous malignant melanoma. Clin Dermatol. 2013;31(3):290-7.

181. Atkins MB, Lotze MT, Dutcher JP, Fisher RI, Weiss G, Margolin K, et al. High-dose recombinant interleukin 2 therapy for patients with metastatic melanoma: analysis of 270 patients treated between 1985 and 1993. J Clin Oncol. 1999;17(7):2105-.

182. Leach DR, Krummel MF, Allison JP. Enhancement of antitumor immunity by CTLA-4 blockade. Science. 1996;271(5256):1734-6.

183. Hauschild A, Grob J-J, Demidov LV, Jouary T, Gutzmer R, Millward M, et al. Dabrafenib in BRAF-mutated metastatic melanoma: a multicentre, open-label, phase 3 randomised controlled trial. The Lancet. 2012;380(9839):358-65.

184. Robert C, Karaszewska B, Schachter J, Rutkowski P, Mackiewicz A, Stroiakovski D, et al. Improved overall survival in melanoma with combined dabrafenib and trametinib. N Engl J Med. 2015;372(1):30-9.

185. Long GV, Stroyakovskiy D, Gogas H, Levchenko E, De Braud F, Larkin J, et al. Dabrafenib and trametinib versus dabrafenib and placebo for Val600 BRAF-mutant melanoma: a multicentre, double-blind, phase 3 randomised controlled trial. The Lancet. 2015;386(9992):444-51.

186. Ascierto PA, McArthur GA, Dréno B, Atkinson V, Liszkay G, Di Giacomo AM, et al. Cobimetinib combined with vemurafenib in advanced BRAFV600-mutant melanoma (coBRIM): updated efficacy results from a randomised, double-blind, phase 3 trial. The Lancet Oncology. 2016;17(9):1248-60.

187. Hodi FS, O'day SJ, McDermott DF, Weber RW, Sosman JA, Haanen JB, et al. Improved survival with ipilimumab in patients with metastatic melanoma. N Engl J Med. 2010;363(8):711-23.

188. Robert C, Ribas A, Wolchok JD, Hodi FS, Hamid O, Kefford R, et al. Anti-programmed-death-receptor-1 treatment with pembrolizumab in ipilimumab-refractory advanced melanoma: a randomised dose-comparison cohort of a phase 1 trial. The Lancet. 2014;384(9948):1109-17.

189. Weber JS, D'Angelo SP, Minor D, Hodi FS, Gutzmer R, Neyns B, et al. Nivolumab versus chemotherapy in patients with advanced melanoma who progressed after anti-CTLA-4 treatment

(CheckMate 037): a randomised, controlled, open-label, phase 3 trial. The lancet oncology. 2015;16(4):375-84.

190. McArthur GA, Chapman PB, Robert C, Larkin J, Haanen JB, Dummer R, et al. Safety and efficacy of vemurafenib in BRAF(V600E) and BRAF(V600K) mutation-positive melanoma (BRIM-3): extended follow-up of a phase 3, randomised, open-label study. The Lancet Oncology. 2014;15(3):323-32.

191. Dummer R, Ascierto PA, Gogas HJ, Arance A, Mandala M, Liszkay G, et al. Overall survival in patients with BRAF-mutant melanoma receiving encorafenib plus binimetinib versus vemurafenib or encorafenib (COLUMBUS): a multicentre, open-label, randomised, phase 3 trial. The Lancet Oncology. 2018;19(10):1315-27.

192. Long GV, Trefzer U, Davies MA, Kefford RF, Ascierto PA, Chapman PB, et al. Dabrafenib in patients with Val600Glu or Val600Lys BRAF-mutant melanoma metastatic to the brain (BREAK-MB): a multicentre, open-label, phase 2 trial. The lancet oncology. 2012;13(11):1087-95.

193. Flaherty KT, Puzanov I, Kim KB, Ribas A, McArthur GA, Sosman JA, et al. Inhibition of mutated, activated BRAF in metastatic melanoma. N Engl J Med. 2010;363(9):809-19.

194. Ascierto PA, Minor D, Ribas A, Lebbe C, O'Hagan A, Arya N, et al. Phase II trial (BREAK-2) of the BRAF inhibitor dabrafenib (GSK2118436) in patients with metastatic melanoma. J Clin Oncol. 2013;31(26):3205-11.

195. Carlos G, Anforth R, Clements A, et al. Cutaneous toxic effects of braf inhibitors alone and in combination with mek inhibitors for metastatic melanoma. JAMA Dermatology. 2015;151(10):1103-9.

196. Flaherty KT, Robert C, Hersey P, Nathan P, Garbe C, Milhem M, et al. Improved survival with MEK inhibition in BRAF-mutated melanoma. N Engl J Med. 2012;367(2):107-14.

197. Hassel JC, Menzer C, Menzies AM, Carlino MS, Long GV, Kefford R, et al. BRAF/MEK inhibition in melanoma patients with rare BRAF mutations. American Society of Clinical Oncology; 2018.

198. Falchook GS, Lewis KD, Infante JR, Gordon MS, Vogelzang NJ, DeMarini DJ, et al. Activity of the oral MEK inhibitor trametinib in patients with advanced melanoma: a phase 1 dose-escalation trial. The Lancet Oncology. 2012;13(8):782-9.

199. Ascierto PA, Schadendorf D, Berking C, Agarwala SS, van Herpen CML, Queirolo P, et al. MEK162 for patients with advanced melanoma harbouring NRAS or Val600 BRAF mutations: a non-randomised, open-label phase 2 study. The Lancet Oncology. 2013;14(3):249-56.

200. van Herpen C, Agarwala SS, Hauschild A, Dummer R, Berking C, Beck JT, et al. LBA35OVERALL SURVIVAL AND BIOMARKER RESULTS FROM A PHASE 2 STUDY OF MEK1/2 INHIBITOR BINIMETINIB (MEK162) IN PATIENTS WITH ADVANCED NRAS-MUTANT MELANOMA. Ann Oncol. 2014;25(suppl_4):mdu438.43-mdu.43.

201. Dummer R, Schadendorf D, Ascierto PA, Arance Fernández AM, Dutriaux C, Maio M, et al. Results of NEMO: A phase III trial of binimetinib (BINI) vs dacarbazine (DTIC) in NRAS-mutant cutaneous melanoma. American Society of Clinical Oncology; 2016.

202. Kirchberger MC, Ugurel S, Mangana J, Heppt MV, Eigentler TK, Berking C, et al. MEK inhibition may increase survival of NRAS-mutated melanoma patients treated with checkpoint blockade: Results of a retrospective multicentre analysis of 364 patients. Eur J Cancer. 2018;98:10-6.

203. Verduzco D, Kuenzi BM, Kinose F, Sondak VK, Eroglu Z, Rix U, et al. Ceritinib Enhances the Efficacy of Trametinib in BRAF/NRAS-Wild-Type Melanoma Cell Lines. Mol Cancer Ther. 2018;17(1):73-83.

204. Ranzani M, Alifrangis C, Perna D, Dutton-Regester K, Pritchard A, Wong K, et al. BRAF/NRAS wild-type melanoma, NF1 status and sensitivity to trametinib. Pigment cell & melanoma research. 2015;28(1):117-9.

205. Robert C, Karaszewska B, Schachter J, Rutkowski P, Mackiewicz A, Stroyakovskiy D, et al. 3301 Two year estimate of overall survival in COMBI-v, a randomized, open-label, phase III study comparing the combination of dabrafenib (D) and trametinib (T) with vemurafenib (Vem) as first-line therapy in patients (pts) with unresectable or metastatic BRAF V600E/K mutation-positive cutaneous melanoma. Eur J Cancer. 2015;51:S663.

206. Robert C, Karaszewska B, Schachter J, Rutkowski P, Mackiewicz A, Stroyakovskiy D, et al. Three-year estimate of overall survival in COMBI-v, a randomized phase 3 study evaluating first-line dabrafenib (D)+ trametinib (T) in patients (pts) with unresectable or metastatic BRAF V600E/K–mutant cutaneous melanoma. Ann Oncol. 2016;27(suppl_6).

207. Ribas A, Gonzalez R, Pavlick A, Hamid O, Gajewski TF, Daud A, et al. Combination of vemurafenib and cobimetinib in patients with advanced BRAFV600-mutated melanoma: a phase 1b study. The Lancet Oncology. 2014;15(9):954-65.

208. Larkin J, Ascierto PA, Dréno B, Atkinson V, Liszkay G, Maio M, et al. Combined vemurafenib and cobimetinib in BRAF-mutated melanoma. N Engl J Med. 2014;371(20):1867-76.

209. Mackiewicz J, Mackiewicz A. BRAF and MEK inhibitors in the era of immunotherapy in melanoma patients. Contemp Oncol. 2018;22(1A):68-72.

210. Kwong LN, Davies MA. Navigating the therapeutic complexity of PI3K pathway inhibition in melanoma. AACR; 2013.

211. Rodon J, Dienstmann R, Serra V, Tabernero J. Development of PI3K inhibitors: lessons learned from early clinical trials. Nature reviews Clinical oncology. 2013;10(3):143.

212. Niessner H, Schmitz J, Tabatabai G, Schmid AM, Calaminus C, Sinnberg T, et al. PI3K pathway inhibition achieves potent antitumor activity in melanoma brain metastases in vitro and in vivo. Clin Cancer Res. 2016.

213. Meier FE, Niessner H, Schmitz J, Schmid A, Calaminus C, Pichler B, et al. The PI3K inhibitor BKM120 has potent antitumor activity in melanoma brain metastases in vitro and in vivo. American Society of Clinical Oncology; 2013.

214. Meier FE, Forschner A, Garzarolli M, Rauschenberg R, Beissert S, Garbe C, et al. An open-label, uncontrolled, single arm phase II trial of the PI3K inhibitor buparlisib in patients with melanoma brain metastases. American Society of Clinical Oncology; 2017.

215. Schneider P, Schön M, Pletz N, Seitz CS, Liu N, Ziegelbauer K, et al. The novel PI3 kinase inhibitor, BAY 80-6946, impairs melanoma growth in vivo and in vitro. Exp Dermatol. 2014;23(8):579-84.

216. Davies BR, Greenwood H, Dudley P, Crafter C, Yu D-H, Zhang J, et al. Preclinical pharmacology of AZD5363, an orally bioavailable inhibitor of AKT: pharmacodynamics, antitumor activity and correlation of monotherapy activity with genetic background. Mol Cancer Ther. 2012:molcanther. 0824.2011.

217. Bendell JC, Rodon J, Burris HA, de Jonge M, Verweij J, Birle D, et al. Phase I, dose-escalation study of BKM120, an oral pan-Class I PI3K inhibitor, in patients with advanced solid tumors. J Clin Oncol. 2012;30(3):282-90.

218. Yap TA, Yan L, Patnaik A, Fearen I, Olmos D, Papadopoulos K, et al. First-in-man clinical trial of the oral pan-AKT inhibitor MK-2206 in patients with advanced solid tumors. 2011.

219. Margolin K, Longmate J, Baratta T, Synold T, Christensen S, Weber J, et al. CCI‐779 in metastatic melanoma: a phase II trial of the California Cancer Consortium. Cancer: Interdisciplinary International Journal of the American Cancer Society. 2005;104(5):1045-8.

220. Hoeflich KP, Merchant M, Orr C, Chan J, Den Otter D, Berry L, et al. Intermittent administration of MEK inhibitor GDC-0973 plus PI3K inhibitor GDC-0941 triggers robust apoptosis and tumor growth inhibition. Cancer Res. 2012;72(1):210-9.

221. Posch C, Moslehi H, Feeney L, Green GA, Ebaee A, Feichtenschlager V, et al. Combined targeting of MEK and PI3K/mTOR effector pathways is necessary to effectively inhibit NRAS mutant melanoma in vitro and in vivo. Proceedings of the National Academy of Sciences. 2013;110(10):4015-20.

222. Sweetlove M, Wrightson E, Kolekar S, Rewcastle GW, Baguley BC, Shepherd PR, et al. Inhibitors of pan-PI3K Signaling Synergize with BRAF or MEK Inhibitors to Prevent BRAF-Mutant Melanoma Cell Growth. Front Oncol. 2015;5(135).

223. Sánchez-Hernández I, Baquero P, Calleros L, Chiloeches A. Dual inhibition of V600EBRAF and the PI3K/AKT/mTOR pathway cooperates to induce apoptosis in melanoma cells through a MEK-independent mechanism. Cancer Lett. 2012;314(2):244-55.

224. Atefi M, von Euw E, Attar N, Ng C, Chu C, Guo D, et al. Reversing melanoma cross-resistance to BRAF and MEK inhibitors by co-targeting the AKT/mTOR pathway. PLoS One. 2011;6(12):e28973.

225. Yam C, Xu X, Davies MA, Gimotty PA, Morrissette JJ, Tetzlaff MT, et al. A Multicenter Phase I Study Evaluating Dual PI3K and BRAF Inhibition with PX-866 and Vemurafenib in Patients with Advanced BRAF V600–Mutant Solid Tumors. Clin Cancer Res. 2018;24(1):22-32.

226. Gelbert LM, Cai S, Lin X, Sanchez-Martinez C, Del Prado M, Lallena MJ, et al. Preclinical characterization of the CDK4/6 inhibitor LY2835219: in-vivo cell cycle-dependent/independent anti-tumor activities alone/in combination with gemcitabine. Invest New Drugs. 2014;32(5):825-37.

227. Tripathy D, Bardia A, Sellers WR. Ribociclib (LEE011): mechanism of action and clinical impact of this selective cyclin-dependent kinase 4/6 inhibitor in various solid tumors. Clin Cancer Res. 2017;23(13):3251-62.

228. Sheppard KE, McArthur GA. The cell-cycle regulator CDK4: an emerging therapeutic target in melanoma. AACR; 2013.

229. Young RJ, Waldeck K, Martin C, Foo JH, Cameron DP, Kirby L, et al. Loss of CDKN 2A expression is a frequent event in primary invasive melanoma and correlates with sensitivity to the CDK 4/6 inhibitor PD 0332991 in melanoma cell lines. Pigment cell & melanoma research. 2014;27(4):590-600.

230. Yadav V, Burke TF, Huber L, Van Horn RD, Zhang Y, Buchanan SG, et al. The CDK4/6 inhibitor LY2835219 overcomes vemurafenib resistance resulting from MAPK reactivation and cyclin D1 upregulation. Mol Cancer Ther. 2014:molcanther. 0257.2014.

231. Kong Y, Sheng X, Wu X, Yan J, Ma M, Yu J, et al. Frequent genetic aberrations in the CDK4 pathway in acral melanoma indicate the potential for CDK4/6 inhibitors in targeted therapy. Clin Cancer Res. 2017.

232. Tang B, Sheng X, Kong Y, Chi Z, Si L, Cui C, et al. Palbociclib for treatment of metastatic melanoma with copy number variations of CDK4 pathway: case report. Chinese clinical oncology. 2018;7(6).

233. Kwong LN, Costello JC, Liu H, Jiang S, Helms TL, Langsdorf AE, et al. Oncogenic NRAS signaling differentially regulates survival and proliferation in melanoma. Nat Med. 2012;18(10):1503.

234. Sosman JA, Kittaneh M, Lolkema MPJK, Postow MA, Schwartz G, Franklin C, et al. A phase 1b/2 study of LEE011 in combination with binimetinib (MEK162) in patients with NRAS-mutant melanoma: Early encouraging clinical activity. J Clin Oncol. 2014;32(15_suppl):9009-.

235. Van Herpen C, Postow M, Carlino M, Kalkavan H, Weise A, Amaria R, et al. 3300 A phase 1b/2 study of ribociclib (LEE011; CDK4/6 inhibitor) in combination with binimetinib (MEK162; MEK inhibitor) in patients with NRAS-mutant melanoma. Eur J Cancer. 2015;51:S663.

236. Carvajal RD, Antonescu CR, Wolchok JD, Chapman PB, Roman RA, Teitcher J, et al. KIT as a therapeutic target in metastatic melanoma. JAMA. 2011;305(22):2327-34.

237. Guo J, Si L, Kong Y, Flaherty KT, Xu X, Zhu Y, et al. Phase II, open-label, single-arm trial of imatinib mesylate in patients with metastatic melanoma harboring c-Kit mutation or amplification. J Clin Oncol. 2011;29(21):2904-9.

238. Hodi FS, Corless CL, Giobbie-Hurder A, Fletcher JA, Zhu M, Marino-Enriquez A, et al. Imatinib for melanomas harboring mutationally activated or amplified KIT arising on mucosal, acral, and chronically sun-damaged skin. J Clin Oncol. 2013;31(26):3182.

239. Carlino MS, Todd JR, Gowrishankar K, Mijatov B, Pupo GM, Fung C, et al. Differential activity of MEK and ERK inhibitors in BRAF inhibitor resistant melanoma. Mol Oncol. 2014;8(3):544-54.

240. Morris EJ, Jha S, Restaino CR, Dayananth P, Zhu H, Cooper A, et al. Discovery of a novel ERK inhibitor with activity in models of acquired resistance to BRAF and MEK inhibitors. Cancer Discov. 2013:CD-13-0070.

241. Wong DJL, Robert L, Atefi MS, Lassen A, Avarappatt G, Cerniglia M, et al. Antitumor activity of the ERK inhibitor SCH772984 [corrected] against BRAF mutant, NRAS mutant and wild-type melanoma. Mol Cancer. 2014;13:194-.

242. Ong CC, Jubb AM, Jakubiak D, Zhou W, Rudolph J, Haverty PM, et al. P21-activated kinase 1 (PAK1) as a therapeutic target in BRAF wild-type melanoma. J Natl Cancer Inst. 2013;105(9):606-7.

243. Woods DM, Woan K, Cheng F, Wang H, Perez-Villarroel P, Lee C, et al. The anti-melanoma activity of the histone deacetylase inhibitor panobinostat (LBH589) is mediated by direct tumor cytotoxicity and increased tumor immunogenicity. Melanoma Res. 2013;23(5):341.

244. Wang L, de Oliveira RL, Huijberts S, Bosdriesz E, Pencheva N, Brunen D, et al. An acquired vulnerability of drug-resistant melanoma with therapeutic potential. Cell. 2018;173(6):1413-25. e14.

245. Hauschild A, Trefzer U, Garbe C, Kaehler KC, Ugurel S, Kiecker F, et al. Multicenter phase II trial of the histone deacetylase inhibitor pyridylmethyl-N-{4-[(2-aminophenyl)-carbamoyl]-benzyl}-carbamate in pretreated metastatic melanoma. Melanoma Res. 2008;18(4):274-8.

246. Millward M, Price T, Townsend A, Sweeney C, Spencer A, Sukumaran S, et al. Phase 1 clinical trial of the novel proteasome inhibitor marizomib with the histone deacetylase inhibitor vorinostat in patients with melanoma, pancreatic and lung cancer based on in vitro assessments of the combination. Invest New Drugs. 2012;30(6):2303-17.

247. Booth L, Roberts JL, Poklepovic A, Kirkwood J, Dent P. HDAC inhibitors enhance the immunotherapy response of melanoma cells. Oncotarget. 2017;8(47):83155.

248. Janeway CA, Travers P, Walport M, Shlomchik MJ. Immunobiology: the immune system in health and disease. 2005.

249. Postow MA, Callahan MK, Wolchok JD. Immune checkpoint blockade in cancer therapy. J Clin Oncol. 2015;33(17):1974.

250. Robert C, Long GV, Brady B, Dutriaux C, Maio M, Mortier L, et al. Nivolumab in previously untreated melanoma without BRAF mutation. N Engl J Med. 2015;372(4):320-30.

251. Larkin J, Lao CD, Urba WJ, McDermott DF, Horak C, Jiang J, et al. Efficacy and Safety of Nivolumab in Patients With BRAF V600 Mutant and BRAF Wild-Type Advanced Melanoma: A Pooled Analysis of 4 Clinical Trials. JAMA Oncol. 2015;1(4):433-40.

252. Topalian SL, Sznol M, McDermott DF, Kluger HM, Carvajal RD, Sharfman WH, et al. Survival, durable tumor remission, and long-term safety in patients with advanced melanoma receiving nivolumab. J Clin Oncol. 2014;32(10):1020-30.

253. Salomon B, Bluestone JA. Complexities of CD28/B7: CTLA-4 costimulatory pathways in autoimmunity and transplantation. Annu Rev Immunol. 2001;19(1):225-52.

254. Vogel I, Kasran A, Cremer J, Kim YJ, Boon L, Van Gool SW, et al. CD28/CTLA‐4/B7 costimulatory pathway blockade affects regulatory T‐cell function in autoimmunity. Eur J Immunol. 2015;45(6):1832-41.

255. Krummel MF, Allison JP. CD28 and CTLA-4 have opposing effects on the response of T cells to stimulation. J Exp Med. 1995;182(2):459-65.

256. Qureshi OS, Zheng Y, Nakamura K, Attridge K, Manzotti C, Schmidt EM, et al. Trans-endocytosis of CD80 and CD86: a molecular basis for the cell-extrinsic function of CTLA-4. Science. 2011;332(6029):600-3.

257. Egen JG, Kuhns MS, Allison JP. CTLA-4: new insights into its biological function and use in tumor immunotherapy. Nat Immunol. 2002;3(7):611.

258. Fong L, Small EJ. Anti–cytotoxic T-lymphocyte antigen-4 antibody: the first in an emerging class of immunomodulatory antibodies for cancer treatment. J Clin Oncol. 2008;26(32):5275-83.

259. Robert C, Thomas L, Bondarenko I, O'day S, Weber J, Garbe C, et al. Ipilimumab plus dacarbazine for previously untreated metastatic melanoma. N Engl J Med. 2011;364(26):2517-26.

260. Schadendorf D, Hodi FS, Robert C, Weber JS, Margolin K, Hamid O, et al. Pooled analysis of long-term survival data from phase II and phase III trials of ipilimumab in unresectable or metastatic melanoma. J Clin Oncol. 2015;33(17):1889.

261. Weber JS, Kähler KC, Hauschild A. Management of immune-related adverse events and kinetics of response with ipilimumab. J Clin Oncol. 2012;30(21):2691-7.

262. Sharpe AH, Wherry EJ, Ahmed R, Freeman GJ. The function of programmed cell death 1 and its ligands in regulating autoimmunity and infection. Nat Immunol. 2007;8(3):239.

263. Ott PA, Hodi FS, Robert C. CTLA-4 and PD-1/PD-L1 blockade: new immunotherapeutic modalities with durable clinical benefit in melanoma patients. AACR; 2013.

264. Okazaki T, Honjo T. PD-1 and PD-1 ligands: from discovery to clinical application. Int Immunol. 2007;19(7):813-24.

265. Sznol M, Chen L. Antagonist antibodies to PD-1 and B7-H1 (PD-L1) in the treatment of advanced human cancer. AACR; 2013.

266. Taube JM, Anders RA, Young GD, Xu H, Sharma R, McMiller TL, et al. Colocalization of inflammatory response with B7-h1 expression in human melanocytic lesions supports an adaptive resistance mechanism of immune escape. Sci Transl Med. 2012;4(127):127ra37-ra37.

267. Hino R, Kabashima K, Kato Y, Yagi H, Nakamura M, Honjo T, et al. Tumor cell expression of programmed cell death ‐ 1 ligand 1 is a prognostic factor for malignant melanoma. Cancer: Interdisciplinary International Journal of the American Cancer Society. 2010;116(7):1757-66.

268. Hodi FS, Chiarion-Sileni V, Gonzalez R, Grob J-J, Rutkowski P, Cowey CL, et al. Nivolumab plus ipilimumab or nivolumab alone versus ipilimumab alone in advanced melanoma (CheckMate 067): 4-year outcomes of a multicentre, randomised, phase 3 trial. The Lancet Oncology. 2018;19(11):1480-92.

269. Robert C, Schachter J, Long GV, Arance A, Grob JJ, Mortier L, et al. Pembrolizumab versus ipilimumab in advanced melanoma. N Engl J Med. 2015;372(26):2521-32.

270. Topalian SL, Sznol M, McDermott DF, Kluger HM, Carvajal RD, Sharfman WH, et al. Survival, durable tumor remission, and long-term safety in patients with advanced melanoma receiving nivolumab. J Clin Oncol. 2014;32(10):1020.

271. Jenkins RW, Barbie DA, Flaherty KT. Mechanisms of resistance to immune checkpoint inhibitors. Br J Cancer. 2018;118(1):1.

272. Zaretsky JM, Garcia-Diaz A, Shin DS, Escuin-Ordinas H, Hugo W, Hu-Lieskovan S, et al. Mutations associated with acquired resistance to PD-1 blockade in melanoma. N Engl J Med. 2016;375(9):819-29.

273. Nomi T, Sho M, Akahori T, Hamada K, Kubo A, Kanehiro H, et al. Clinical significance and therapeutic potential of the programmed death-1 ligand/programmed death-1 pathway in human pancreatic cancer. Clin Cancer Res. 2007;13(7):2151-7.

274. Tawbi HA, Forsyth PA, Algazi A, Hamid O, Hodi FS, Moschos SJ, et al. Combined Nivolumab and Ipilimumab in Melanoma Metastatic to the Brain. N Engl J Med. 2018;379(8):722-30.

275. Wolchok JD, Chiarion-Sileni V, Gonzalez R, Rutkowski P, Grob JJ, Cowey CL, et al. Overall Survival with Combined Nivolumab and Ipilimumab in Advanced Melanoma. N Engl J Med. 2017;377(14):1345-56.

276. Larkin J, Chiarion-Sileni V, Gonzalez R, Grob JJ, Cowey CL, Lao CD, et al. Combined Nivolumab and Ipilimumab or Monotherapy in Untreated Melanoma. N Engl J Med. 2015;373(1):23-34.

277. Postow MA, Chesney J, Pavlick AC, Robert C, Grossmann K, McDermott D, et al. Nivolumab and ipilimumab versus ipilimumab in untreated melanoma. N Engl J Med. 2015;372(21):2006-17.

278. Schachter J, Ribas A, Long GV, Arance A, Grob J-J, Mortier L, et al. Pembrolizumab versus ipilimumab for advanced melanoma: final overall survival results of a multicentre, randomised, open-label phase 3 study (KEYNOTE-006). The Lancet. 2017;390(10105):1853-62.

279. Hu-Lieskovan S, Mok S, Moreno BH, Tsoi J, Faja LR, Goedert L, et al. Improved antitumor activity of immunotherapy with BRAF and MEK inhibitors in BRAF(V600E) melanoma. Sci Transl Med. 2015;7(279):279ra41-ra41.

280. Wilmott JS, Long GV, Howle JR, Haydu LE, Sharma RN, Thompson JF, et al. Selective BRAF Inhibitors Induce Marked T-cell Infiltration into Human Metastatic Melanoma. Clin Cancer Res. 2012;18(5):1386-94.

281. Hu-Lieskovan S, Robert L, Moreno BH, Ribas A. Combining targeted therapy with immunotherapy in BRAF-mutant melanoma: promise and challenges. J Clin Oncol. 2014;32(21):2248.

282. Luke JJ, Flaherty KT, Ribas A, Long GV. Targeted agents and immunotherapies: optimizing outcomes in melanoma. Nature reviews Clinical oncology. 2017;14(8):463.

283. Ribas A, Hodi FS, Callahan M, Konto C, Wolchok J. Hepatotoxicity with Combination of Vemurafenib and Ipilimumab. N Engl J Med. 2013;368(14):1365-6.

284. Harding JJ, Pulitzer M, Chapman PB. Vemurafenib sensitivity skin reaction after ipilimumab. N Engl J Med. 2012;366(9):866-8.

285. Minor DR, Puzanov I, Callahan MK, Hug BA, Hoos A. Severe gastrointestinal toxicity with administration of trametinib in combination with dabrafenib and ipilimumab. Pigment cell & melanoma research. 2015;28(5):611-2.

286. Kim K, Flaherty K, Chapman P, Sosman J, Ribas A, McArthur G, et al. Pattern and outcome of disease progression in phase I study of vemurafenib in patients with metastatic melanoma (MM). J Clin Oncol. 2011;29(15_suppl):8519-.

287. Chan M, Haydu L, Menzies AM, Azer MW, Klein O, Guminski A, et al. Clinical characteristics and survival of BRAF-mutant (BRAF+) metastatic melanoma patients (pts) treated with BRAF inhibitor (BRAFi) dabrafenib or vemurafenib beyond disease progression (PD). American Society of Clinical Oncology; 2013.

288. Wang J, Yao Z, Jonsson P, Allen AN, Qin ACR, Uddin S, et al. A secondary mutation in BRAF confers resistance to RAF inhibition in a BRAF V600E-mutant brain tumor. Cancer Discov. 2018:CD-17-1263.

289. Poulikakos PI, Persaud Y, Janakiraman M, Kong X, Ng C, Moriceau G, et al. RAF inhibitor resistance is mediated by dimerization of aberrantly spliced BRAF (V600E). Nature. 2011;480(7377):387.

290. Johnson DB, Menzies AM, Zimmer L, Eroglu Z, Ye F, Zhao S, et al. Acquired BRAF inhibitor resistance: a multicenter meta-analysis of the spectrum and frequencies, clinical behaviour, and phenotypic associations of resistance mechanisms. Eur J Cancer. 2015;51(18):2792-9.

291. Shi H, Moriceau G, Kong X, Lee M-K, Lee H, Koya RC, et al. Melanoma whole-exome sequencing identifies V600E B-RAF amplification-mediated acquired B-RAF inhibitor resistance. Nature communications. 2012;3:724.

292. Rizos H, Menzies AM, Pupo GM, Carlino MS, Fung C, Hyman J, et al. BRAF inhibitor resistance mechanisms in metastatic melanoma; spectrum and clinical impact. Clin Cancer Res. 2014:clincanres. 3122.2013.

293. Vido MJ, Le K, Hartsough EJ, Aplin AE. BRAF Splice Variant Resistance to RAF Inhibitor Requires Enhanced MEK Association. Cell reports. 2018;25(6):1501-10. e3.

294. Lim SY, Menzies AM, Rizos H. Mechanisms and strategies to overcome resistance to molecularly targeted therapy for melanoma. Cancer. 2017;123(S11):2118-29.

295. Hatzivassiliou G, Song K, Yen I, Brandhuber BJ, Anderson DJ, Alvarado R, et al. RAF inhibitors prime wild-type RAF to activate the MAPK pathway and enhance growth. Nature. 2010;464(7287):431-5.

296. Montagut C, Sharma SV, Shioda T, McDermott U, Ulman M, Ulkus LE, et al. Elevated CRAF as a potential mechanism of acquired resistance to BRAF inhibition in melanoma. Cancer Res. 2008;68(12):4853-61.

297. Villanueva J, Vultur A, Lee JT, Somasundaram R, Fukunaga-Kalabis M, Cipolla AK, et al. Acquired resistance to BRAF inhibitors mediated by a RAF kinase switch in melanoma can be overcome by cotargeting MEK and IGF-1R/PI3K. Cancer Cell. 2010;18(6):683-95.

298. Johannessen CM, Boehm JS, Kim SY, Thomas SR, Wardwell L, Johnson LA, et al. COT drives resistance to RAF inhibition through MAP kinase pathway reactivation. Nature. 2010;468(7326):968.

299. Long GV, Stroyakovskiy D, Gogas H, Levchenko E, de Braud F, Larkin J, et al. Combined BRAF and MEK inhibition versus BRAF inhibition alone in melanoma. N Engl J Med. 2014;371(20):1877-88.

300. Nazarian R, Shi H, Wang Q, Kong X, Koya RC, Lee H, et al. Melanomas acquire resistance to B-RAF (V600E) inhibition by RTK or N-RAS upregulation. Nature. 2010;468(7326):973.

301. Heidorn SJ, Milagre C, Whittaker S, Nourry A, Niculescu-Duvas I, Dhomen N, et al. Kinase-dead BRAF and oncogenic RAS cooperate to drive tumor progression through CRAF. Cell. 2010;140(2):209-21.

302. Deng W, Vashisht Gopal Y, Scott A, Chen G, Woodman S, Davies M. Role and therapeutic potential of PI3K‐mTOR signaling in de novo resistance to BRAF inhibition. Pigment cell & melanoma research. 2012;25(2):248-58.

303. Sun C, Wang L, Huang S, Heynen GJ, Prahallad A, Robert C, et al. Reversible and adaptive resistance to BRAF (V600E) inhibition in melanoma. Nature. 2014;508(7494):118.

304. Hodi FS, Chesney J, Pavlick AC, Robert C, Grossmann KF, McDermott DF, et al. Combined nivolumab and ipilimumab versus ipilimumab alone in patients with advanced

melanoma: 2-year overall survival outcomes in a multicentre, randomised, controlled, phase 2 trial. The Lancet Oncology. 2016;17(11):1558-68.

305. Mar VJ, Wong SQ, Li J, Scolyer RA, McLean C, Papenfuss AT, et al. BRAF/NRAS wild-type melanomas have a high mutation load correlating with histologic and molecular signatures of UV damage. Clin Cancer Res. 2013;19(17):4589-98.

306. Menzies AM, Long GV. Systemic treatment for BRAF-mutant melanoma: where do we go next? The Lancet Oncology. 2014;15(9):e371-e81.

307. Downward J. Targeting RAS signalling pathways in cancer therapy. Nature Reviews Cancer. 2003;3:11.

308. Algazi AP, Esteve-Puig R, Nosrati A, Hinds B, Hobbs-Muthukumar A, Nandoskar P, et al. Dual MEK/AKT inhibition with trametinib and GSK2141795 does not yield clinical benefit in metastatic NRAS-mutant and wild-type melanoma. Pigment cell & melanoma research. 2018;31(1):110-4.

309. Dummer R, Schadendorf D, Ascierto PA, Arance A, Dutriaux C, Di Giacomo AM, et al. Binimetinib versus dacarbazine in patients with advanced NRAS-mutant melanoma (NEMO): a multicentre, open-label, randomised, phase 3 trial. The Lancet Oncology. 2017;18(4):435-45.

310. Ribas A, Butler M, Lutzky J, Lawrence DP, Robert C, Miller W, et al. Phase I study combining anti-PD-L1 (MEDI4736) with BRAF (dabrafenib) and/or MEK (trametinib) inhibitors in advanced melanoma. American Society of Clinical Oncology; 2015.

311. Infante J, Kim T, Friedmann J, Miller W. Safety and clinical activity of atezolizumab combined with cobimetinib in metastatic melanoma. 13th International Congress of the Society for Melanoma Research 2016. November 6-9, 2016:6-9.

312. Liu L, Mayes PA, Eastman S, Shi H, Yadavilli S, Zhang T, et al. The BRAF and MEK Inhibitors Dabrafenib and Trametinib: Effects on Immune Function and in Combination with Immunomodulatory Antibodies Targeting PD-1, PD-L1, and CTLA-4. Clin Cancer Res. 2015;21(7):1639-51.

313. Kuske M, Westphal D, Wehner R, Schmitz M, Beissert S, Praetorius C, et al. Immunomodulatory effects of BRAF and MEK inhibitors: Implications for Melanoma therapy. Pharmacol Res. 2018;136:151-9.

314. Yoshida T, Kakegawa J, Yamaguchi T, Hantani Y, Okajima N, Sakai T, et al. Identification and characterization of a novel chemotype MEK inhibitor able to alter the phosphorylation state of MEK1/2. Oncotarget. 2012;3(12):1533.

315. Nissan MH, Rosen N, Solit DB. ERK pathway inhibitors: how low should we go? Cancer Discov. 2013;3(7):719-21.

316. Liu Y, Gray NS. Rational design of inhibitors that bind to inactive kinase conformations. Nat Chem Biol. 2006;2(7):358.

317. Girotti Maria R, Lopes F, Preece N, Niculescu-Duvaz D, Zambon A, Davies L, et al. Paradox-Breaking RAF Inhibitors that Also Target SRC Are Effective in Drug-Resistant BRAF Mutant Melanoma. Cancer Cell. 2015;27(1):85-96.

318. Molnár E, Rittler D, Baranyi M, Grusch M, Berger W, Döme B, et al. Pan-RAF and MEK vertical inhibition enhances therapeutic response in non-V600 BRAF mutant cells. BMC Cancer. 2018;18(1):542.

319. Alavi S, Stewart AJ, Kefford RF, Lim SY, Shklovskaya E, Rizos H. Interferon Signaling Is Frequently Downregulated in Melanoma. Front Immunol. 2018;9(1414).

320. Long GV, Fung C, Menzies AM, Pupo GM, Carlino MS, Hyman J, et al. Increased MAPK reactivation in early resistance to dabrafenib/trametinib combination therapy of BRAF-mutant metastatic melanoma. Nature communications. 2014;5:5694.

321. Gallagher S, Kefford RF, Rizos H. Enforced expression of p14ARF induces p53-dependent cell cycle arrest but not apoptosis. Cell Cycle. 2005;4(3):465-72.

322. Haferkamp S, Scurr LL, Becker TM, Frausto M, Kefford RF, Rizos H. Oncogene-Induced Senescence Does Not Require the p16INK4a or p14ARF Melanoma Tumor Suppressors. J Invest Dermatol. 2009;129(8):1983-91.

323. Long GV, Hauschild A, Santinami M, Atkinson V, Mandala M, Chiarion-Sileni V, et al. Adjuvant Dabrafenib plus Trametinib in Stage III BRAF-Mutated Melanoma. N Engl J Med. 2017;377(19):1813-23.

324. Flaherty KT, Infante JR, Daud A, Gonzalez R, Kefford RF, Sosman J, et al. Combined BRAF and MEK inhibition in melanoma with BRAF V600 mutations. N Engl J Med. 2012;367(18):1694-703.

325. Whittaker SR, Theurillat JP, Van Allen E, Wagle N, Hsiao J, Cowley GS, et al. A genome-scale RNA interference screen implicates NF1 loss in resistance to RAF inhibition. Cancer Discov. 2013;3(3):350-62.

326. Ribas A, Hodi F, Lawrence D, Atkinson V, Agarwal S, Carlino M, et al. 1216OKEYNOTE-022 update: phase 1 study of first-line pembrolizumab (pembro) plus dabrafenib (D) and trametinib (T) for BRAF-mutant advanced melanoma. Ann Oncol. 2017;28(suppl_5).

327. Ascierto P, Ferrucci P, Stephens R, Del Vecchio M, Atkinson V, Schmidt H, et al. 1244O KEYNOTE-022 Part 3: Phase II randomized study of 1L dabrafenib (D) and trametinib (T) plus pembrolizumab (Pembro) or placebo (PBO) for BRAF-mutant advanced melanoma. Ann Oncol. 2018;29(suppl_8):mdy289.

328. Johnson DB, Wallender EK, Cohen DN, Likhari SS, Zwerner JP, Powers JG, et al. Severe cutaneous and neurologic toxicity in melanoma patients during vemurafenib administration following anti-PD-1 therapy. Cancer immunology research. 2013;1(6):373-7.

329. Urosevic-Maiwald M, Mangana J, Dummer R. Systemic inflammatory reaction syndrome during combined kinase inhibitor therapy following anti-PD-1 therapy for melanoma. Ann Oncol. 2017;28(7):1673-5.

330. Sasaki K, Uehara J, Iinuma S, Doi H, Honma M, Toki Y, et al. Hemophagocytic lymphohistiocytosis associated with dabrafenib and trametinib combination therapy following pembrolizumab administration for advanced melanoma. Ann Oncol. 2018;29(7):1602-3.

331. Grogan N, Swami U, Bossler AD, Zakharia Y, Milhem M. Toxicities with targeted therapies after immunotherapy in metastatic melanoma. Melanoma Res. 2018;28(6):600-4.

332. Freed-Pastor WA, Prives C. Mutant p53: one name, many proteins. Genes Dev. 2012;26(12):1268-86.

333. Olivier M, Hollstein M, Hainaut P. TP53 mutations in human cancers: origins, consequences, and clinical use. Cold Spring Harb Perspect Biol. 2010;2(1):a001008-a.

334. Muller Patricia AJ, Vousden Karen H. Mutant p53 in Cancer: New Functions and Therapeutic Opportunities. Cancer Cell. 2014;25(3):304-17.

335. Fischer M. Census and evaluation of p53 target genes. Oncogene. 2017;36(28):3943-56.

336. Wade M, Li Y-C, Wahl GM. MDM2, MDMX and p53 in oncogenesis and cancer therapy. Nature Reviews Cancer. 2013;13(2):83.

337. Muthusamy V, Hobbs C, Nogueira C, Cordon‐Cardo C, McKee PH, Chin L, et al. Amplification of CDK4 and MDM2 in malignant melanoma. Genes Chromosomes Cancer. 2006;45(5):447-54.

338. Rajabi P, Karimian P, Heidarpour M. The relationship between MDM2 expression and tumor thickness and invasion in primary cutaneous malignant melanoma. Journal of research in medical sciences : the official journal of Isfahan University of Medical Sciences. 2012;17(5):452-5.

339. Curtin JA, Fridlyand J, Kageshita T, Patel HN, Busam KJ, Kutzner H, et al. Distinct sets of genetic alterations in melanoma. N Engl J Med. 2005;353(20):2135-47.

340. Gembarska A, Luciani F, Fedele C, Russell EA, Dewaele M, Villar S, et al. MDM4 is a key therapeutic target in cutaneous melanoma. Nat Med. 2012;18(8):1239-47.

341. Danovi D, Meulmeester E, Pasini D, Migliorini D, Capra M, Frenk R, et al. Amplification of Mdmx (or Mdm4) directly contributes to tumor formation by inhibiting p53 tumor suppressor activity. Mol Cell Biol. 2004;24(13):5835-43.

342. Lu M, Breyssens H, Salter V, Zhong S, Hu Y, Baer C, et al. Restoring p53 function in human melanoma cells by inhibiting MDM2 and cyclin B1/CDK1-phosphorylated nuclear iASPP. Cancer Cell. 2013;23(5):618-33.

343. Korabiowska M, Betke H, Kellner S, Stachura J, Schauer A. Differential expression of growth arrest, DNA damage genes and tumour suppressor gene p53 in naevi and malignant melanomas. Anticancer Res. 1997;17(5A):3697-700.

344. Webber BA, Lawson D, Cohen C. Maspin and Mutant p53 expression in malignant melanoma and carcinoma: use of tissue microarray. Appl Immunohistochem Mol Morphol. 2008;16(1):19-23.

345. Sparrow L, English D, Heenan P, Dawkins H, Taran J. Prognostic significance of p53 over-expression in thin melanomas. Melanoma Res. 1995;5(6):387-92.

346. Haferkamp S, Tran SL, Becker TM, Scurr LL, Kefford RF, Rizos H. The relative contributions of the p53 and pRb pathways in oncogene-induced melanocyte senescence. Aging (Milano). 2009;1(6):542.

347. Slováčkova J, Grochova D, Navratilova J, Smarda J, Smardova J. Transactivation by temperature-dependent p53 mutants in yeast and human cells. Cell Cycle. 2010;9(11):2141-8.

348. Bardeesy N, Bastian BC, Hezel A, Pinkel D, DePinho RA, Chin L. Dual inactivation of RB and p53 pathways in RAS-induced melanomas. Mol Cell Biol. 2001;21(6):2144-53.

349. Berglind H, Pawitan Y, Kato S, Ishioka C, Soussi T. Analysis of p53 mutation status in human cancer cell lines: a paradigm for cell line cross-contamination. Cancer Biol Ther. 2008;7(5):699-708.

350. Mhaidat N, Zhang X, Allen J, Avery-Kiejda K, Scott R, Hersey P. Temozolomide induces senescence but not apoptosis in human melanoma cells. Br J Cancer. 2007;97(9):1225.

351. Luebker SA, Zhang W, Koepsell SA. Comparing the genomes of cutaneous melanoma tumors to commercially available cell lines. Oncotarget. 2017;8(70):114877.

352. Yang G, Rajadurai A, Tsao H. Recurrent Patterns of Dual RB and p53 Pathway Inactivation in Melanoma. J Invest Dermatol. 2005;125(6):1242-51.

353. Ji Z, Njauw CN, Taylor M, Neel V, Flaherty KT, Tsao H. p53 Rescue through HDM2 Antagonism Suppresses Melanoma Growth and Potentiates MEK Inhibition. J Invest Dermatol. 2012;132(2):356-64.

354. Zölzer F, Hillebrandt S, Streffer C. Radiation induced G1-block and p53 status in six human cell lines. Radiother Oncol. 1995;37(1):20-8.

355. Shen H, G Maki C. Pharmacologic activation of p53 by small-molecule MDM2 antagonists. Curr Pharm Des. 2011;17(6):560-8.

356. Hugo W, Shi H, Sun L, Piva M, Song C, Kong X, et al. Non-genomic and immune evolution of melanoma acquiring MAPKi resistance. Cell. 2015;162(6):1271-85.

357. Momand J, Zambetti GP, Olson DC, George D, Levine AJ. The mdm-2 oncogene product forms a complex with the p53 protein and inhibits p53-mediated transactivation. Cell. 1992;69(7):1237-45.

358. Marine J-CW, Dyer MA, Jochemsen AG. MDMX: from bench to bedside. J Cell Sci. 2007;120(3):371-8.

359. Terzian T, Torchia EC, Dai D, Robinson SE, Murao K, Stiegmann RA, et al. p53 prevents progression of nevi to melanoma predominantly through cell cycle regulation. Pigment cell & melanoma research. 2010;23(6):781-94.

360. Goel V, Ibrahim N, Jiang G, Singhal M, Fee S, Flotte T, et al. Melanocytic nevus-like hyperplasia and melanoma in transgenic BRAFV600E mice. Oncogene. 2009;28(23):2289.

361. Dovey M, White RM, Zon LI. Oncogenic NRAS cooperates with p53 loss to generate melanoma in zebrafish. Zebrafish. 2009;6(4):397-404.

362. Patton EE, Widlund HR, Kutok JL, Kopani KR, Amatruda JF, Murphey RD, et al. BRAF Mutations Are Sufficient to Promote Nevi Formation and Cooperate with p53 in the Genesis of Melanoma. Curr Biol. 2005;15(3):249-54.

363. Wang YF, Jiang CC, Kiejda KA, Gillespie S, Zhang XD, Hersey P. Apoptosis Induction in Human Melanoma Cells by Inhibition of MEK Is Caspase-Independent and Mediated by the Bcl-2 Family Members PUMA, Bim, and Mcl-1. Clin Cancer Res. 2007;13(16):4934-42.

364. Yu J, Zhang L. The transcriptional targets of p53 in apoptosis control. Biochem Biophys Res Commun. 2005;331(3):851-8.

365. Verhaegen M, Bauer JA, Martín de la Vega C, Wang G, Wolter KG, Brenner JC, et al. A Novel BH3 Mimetic Reveals a Mitogen-Activated Protein Kinase–Dependent Mechanism of Melanoma Cell Death Controlled by p53 and Reactive Oxygen Species. Cancer Res. 2006;66(23):11348-59.

366. Lin L, Ding D, Jiang Y, Li Y, Li S. MEK inhibitors induce apoptosis via FoxO3a-dependent PUMA induction in colorectal cancer cells. Oncogenesis. 2018;7(9):67-.

367. Jochemsen AG. Reactivation of p53 as therapeutic intervention for malignant melanoma. Curr Opin Oncol. 2014;26(1):114-9.

368. Krayem M, Journe F, Wiedig M, Morandini R, Najem A, Salès F, et al. p53 Reactivation by PRIMA-1Met (APR-246) sensitises V600E/KBRAF melanoma to vemurafenib. Eur J Cancer. 2016;55:98-110.

369. Bao W, Chen M, Zhao X, Kumar R, Spinnler C, Thullberg M, et al. PRIMA-1Met/APR-246 induces wild-type p53-dependent suppression of malignant melanoma tumor growth in 3D culture and in vivo. Cell Cycle. 2011;10(2):301-7.

370. Najem A, Krayem M, Salès F, Hussein N, Badran B, Robert C, et al. P53 and MITF/Bcl-2 identified as key pathways in the acquired resistance of NRAS-mutant melanoma to MEK inhibition. Eur J Cancer. 2017;83:154-65.

371. Wu C, Koay T, Esfandiari A, Ho Y, Lovat P, Lunec J. PO-450 Mek inhibition synergizes with mdm2 inhibitors through dusp6 suppression. BMJ Publishing Group Limited; 2018.

372. Moschos SJ, Sandhu SK, Lewis KD, Sullivan RJ, Johnson DB, Zhang Y, et al. Phase 1 study of the p53-MDM2 inhibitor AMG 232 combined with trametinib plus dabrafenib or trametinib in patients (Pts) with TP53 wild type (TP53WT) metastatic cutaneous melanoma (MCM). J Clin Oncol. 2017;35(15_suppl):2575-.

373. Berberich A, Kessler T, Thomé CM, Pusch S, Hielscher T, Sahm F, et al. Targeting resistance against the MDM2 inhibitor RG7388 in glioblastoma cells by the MEK inhibitor trametinib. Clin Cancer Res. 2018.

374. Lawrence MS, Stojanov P, Polak P, Kryukov GV, Cibulskis K, Sivachenko A, et al. Mutational heterogeneity in cancer and the search for new cancer-associated genes. Nature. 2013;499:214.

375. Alexandrov LB, Nik-Zainal S, Wedge DC, Aparicio SAJR, Behjati S, Biankin AV, et al. Signatures of mutational processes in human cancer. Nature. 2013;500:415.

376. Colombino M, Capone M, Lissia A, Cossu A, Rubino C, De Giorgi V, et al. BRAF/NRAS mutation frequencies among primary tumors and metastases in patients with melanoma. J Clin Oncol. 2012;30(20):2522-9.

377. Dhillon AS, Hagan S, Rath O, Kolch W. MAP kinase signalling pathways in cancer. Oncogene. 2007;26(22):3279-90.

378. Burotto M, Chiou VL, Lee JM, Kohn EC. The MAPK pathway across different malignancies: a new perspective. Cancer. 2014;120(22):3446-56.

379. Pan D, Kobayashi A, Jiang P, de Andrade LF, Tay RE, Luoma AM, et al. A major chromatin regulator determines resistance of tumor cells to T cell–mediated killing. Science. 2018;359(6377):770-5.

380. Heppt MV, Siepmann T, Engel J, Schubert-Fritschle G, Eckel R, Mirlach L, et al. Prognostic significance of BRAF and NRAS mutations in melanoma: a German study from routine care. BMC Cancer. 2017;17(1):536.

381. Helgadottir H, Höiom V, Tuominen R, Nielsen K, Jönsson G, Olsson H, et al. Germline CDKN2A mutation status and survival in familial melanoma cases. JNCI: Journal of the National Cancer Institute. 2016;108(11).

382. Shi H, Hugo W, Kong X, Hong A, Koya RC, Moriceau G, et al. Acquired resistance and clonal evolution in melanoma during BRAF inhibitor therapy. Cancer Discov. 2014;4(1):80-93.

383. Betti M, Aspesi A, Biasi A, Casalone E, Ferrante D, Ogliara P, et al. CDKN2A and BAP1 germline mutations predispose to melanoma and mesothelioma. Cancer Lett. 2016;378(2):120-30.

384. Slipicevic A, Herlyn M. KIT in melanoma: many shades of gray. J Invest Dermatol. 2015;135(2):337-8.

385. Carlino MS, Fung C, Shahheydari H, Todd JR, Boyd SC, Irvine M, et al. Preexisting MEK1P124 mutations diminish response to BRAF inhibitors in metastatic melanoma patients. Clin Cancer Res. 2015;21(1):98-105.

386. Emery CM, Vijayendran KG, Zipser MC, Sawyer AM, Niu L, Kim JJ, et al. MEK1 mutations confer resistance to MEK and B-RAF inhibition. Proceedings of the National Academy of Sciences. 2009;106(48):20411-6.

387. Wagle N, Emery C, Berger MF, Davis MJ, Sawyer A, Pochanard P, et al. Dissecting therapeutic resistance to RAF inhibition in melanoma by tumor genomic profiling. J Clin Oncol. 2011;29(22):3085.

388. Gold HL, Wengrod J, Tian J, Vega-Saenz de Miera E, Nadeem Z, Fleming NH, et al. The clinical and biologic impact of PPP6C mutations in melanoma. American Society of Clinical Oncology; 2013.

389. Peng W, Chen JQ, Liu C, Malu S, Creasy C, Tetzlaff MT, et al. Loss of PTEN promotes resistance to T cell–mediated immunotherapy. Cancer Discov. 2016;6(2):202-16.

390. Paraiso KH, Xiang Y, Rebecca VW, Abel EV, Chen A, Munko AC, et al. PTEN loss confers BRAF inhibitor resistance to melanoma cells through the suppression of BIM expression. Cancer Res. 2011:canres. 2954.010.

391. Arafeh R, Qutob N, Emmanuel R, Keren-Paz A, Madore J, Elkahloun A, et al. Recurrent inactivating RASA2 mutations in melanoma. Nat Genet. 2015;47:1408.

392. Mar VJ, Wong SQ, Logan A, Nguyen T, Cebon J, Kelly JW, et al. Clinical and pathological associations of the activating RAC1 P29S mutation in primary cutaneous melanoma. Pigment cell & melanoma research. 2014;27(6):1117-25.

393. Xiao W, Du N, Huang T, Guo J, Mo X, Yuan T, et al. TP53 Mutation as Potential Negative Predictor for Response of Anti-CTLA-4 Therapy in Metastatic Melanoma. EBioMedicine. 2018;32:119-24.

394. Team RC. R: A language and environment for statistical computing. 2013.

395. Zheng B, Jeong JH, Asara JM, Yuan Y-Y, Granter SR, Chin L, et al. Oncogenic B-RAF negatively regulates the tumor suppressor LKB1 to promote melanoma cell proliferation. Mol Cell. 2009;33(2):237-47.

396. Woodard J, Platanias LC. AMP-activated kinase (AMPK)-generated signals in malignant melanoma cell growth and survival. Biochem Biophys Res Commun. 2010;398(1):135-9.

397. Lemmon MA, Schlessinger J. Cell signaling by receptor-tyrosine kinases. Cell. 2010;141(7):1117-34.

398. Easty DJ, Gray SG, O'Byrne KJ, O'Donnell D, Bennett DC. Receptor tyrosine kinases and their activation in melanoma. Pigment cell & melanoma research. 2011;24(3):446-61.

399. Sun C, Wang L, Huang S, Heynen GJJE, Prahallad A, Robert C, et al. Reversible and adaptive resistance to BRAF(V600E) inhibition in melanoma. Nature. 2014;508:118.

400. Sabbatino F, Wang Y, Wang X, Flaherty KT, Yu L, Pepin D. PDGFRα up-regulation mediated by sonic hedgehog pathway activation leads to BRAF inhibitor resistance in melanoma cells with BRAF mutation. Oncotarget. 2014;5(7):1926.

401. Ryabaya O, Malysheva A, Khochenkova YA, Solomko ES, Khochenkov D. Inactivation of Receptor Tyrosine Kinases Overcomes Resistance to Targeted B-RAF Inhibitors in Melanoma Cell Lines. Mol Biol. 2018;52(3):398-405.

402. Patel SP, Kim KB, Papadopoulos NE, Hwu W-J, Hwu P, Prieto VG, et al. A phase II study of gefitinib in patients with metastatic melanoma. Melanoma Res. 2011;21(4):357.

403. Capparelli C, Rosenbaum S, Berman-Booty LD, Salhi A, Gaborit N, Zhan T, et al. ErbB3-ErbB2 Complexes as a Therapeutic Target in a Subset of Wild-type BRAF/NRAS Cutaneous Melanomas. Cancer Res. 2015;75(17):3554-67.

404. Hutchinson KE, Johnson DB, Johnson AS, Sanchez V, Kuba M, Lu P, et al. ERBB activation modulates sensitivity to MEK1/2 inhibition in a subset of driver-negative melanoma. Oncotarget. 2015;6(26):22348-60.

405. Ranzani M, Kemper K, Michaut M, Krijgsman O, Aben N, Iyer V, et al. 2017.

406. Verduzco D, Kuenzi BM, Kinose F, Sondak VK, Eroglu Z, Rix U, et al. Ceritinib Enhances the Efficacy of Trametinib in BRAF/NRAS-Wild-Type Melanoma Cell Lines. Mol Cancer Ther. 2018;17(1):73-83.

407. Mirmohammadsadegh A, Hassan M, Bardenheuer W, Marini A, Gustrau A, Nambiar S, et al. STAT5 phosphorylation in malignant melanoma is important for survival and is mediated through SRC and JAK1 kinases. J Invest Dermatol. 2006;126(10):2272-80.

408. Niu G, Bowman T, Huang M, Shivers S, Reintgen D, Daud A, et al. Roles of activated Src and Stat3 signaling in melanoma tumor cell growth. Oncogene. 2002;21(46):7001.

409. Homsi J, Cubitt CL, Zhang S, Munster PN, Yu H, Sullivan DM, et al. Src activation in melanoma and Src inhibitors as therapeutic agents in melanoma. Melanoma Res. 2009;19(3):167-75.

410. Eustace AJ, Mahgoub T, Kennedy S, Crown J, Larkin A, Tryfonopoulos D, et al. Targeting SRC kinase (SRC) in melanoma cells. J Clin Oncol. 2010;28(15_suppl):8584-.

411. Homsi J, Messina J, Cubutt C, Maunglay S, Scalf L, Komarla A, et al. Targeting Src/Stat3 pathway in malignant melanoma. J Clin Oncol. 2006;24(18_suppl):8025-.

412. Ferguson J, Arozarena I, Ehrhardt M, Wellbrock C. Combination of MEK and SRC inhibition suppresses melanoma cell growth and invasion. Oncogene. 2012;32:86.

413. Vergani E, Vallacchi V, Frigerio S, Deho P, Mondellini P, Perego P, et al. Identification of MET and SRC Activation in Melanoma Cell Lines Showing Primary Resistance to PLX4032. Neoplasia. 2011;13(12):1132-IN17.

414. Girotti MR, Pedersen M, Sanchez-Laorden B, Viros A, Turajlic S, Niculescu-Duvaz D, et al. Inhibiting EGF receptor or SRC family kinase signaling overcomes BRAF inhibitor resistance in melanoma. Cancer Discov. 2013;3(2):158-67.

415. Algazi A, Weber J, Andrews S, Urbas P, Munster P, DeConti R, et al. Phase I clinical trial of the Src inhibitor dasatinib with dacarbazine in metastatic melanoma. Br J Cancer. 2012;106(1):85.

416. Liu L, Mayes PA, Eastman S, Shi H, Yadavilli S, Zhang T, et al. The BRAF and MEK inhibitors dabrafenib and trametinib: effects on immune function and in combination with immunomodulatory antibodies targeting PD-1, PD-L1, and CTLA-4. Clin Cancer Res. 2015.

417. Infante J, Kim T, Friedmann J, Miller W, editors. Safety and clinical activity of atezolizumab combined with cobimetinib in metastatic melanoma. 13th International Congress of the Society for Melanoma Research; 2016.

418. Ribas A, Flaherty KT. BRAF targeted therapy changes the treatment paradigm in melanoma. Nature reviews Clinical oncology. 2011;8(7):426.

419. Long GV, Menzies AM, Nagrial AM, Haydu LE, Hamilton AL, Mann GJ, et al. Prognostic and clinicopathologic associations of oncogenic BRAF in metastatic melanoma. J Clin Oncol. 2011;29(10):1239-46.

420. Chapman PB, Hauschild A, Robert C, Haanen JB, Ascierto P, Larkin J, et al. Improved survival with vemurafenib in melanoma with BRAF V600E mutation. N Engl J Med. 2011;364(26):2507-16.

421. Callahan MK, Kluger H, Postow MA, Segal NH, Lesokhin A, Atkins MB, et al. Nivolumab Plus Ipilimumab in Patients With Advanced Melanoma: Updated Survival, Response, and Safety Data in a Phase I Dose-Escalation Study. Journal of clinical oncology: official journal of the American Society of Clinical Oncology. 2018;36(4):391-8.

422. Atkinson V, Long GV, Menzies AM, McArthur G, Carlino MS, Millward M, et al. Optimizing combination dabrafenib and trametinib therapy in BRAF mutation‐positive advanced melanoma patients: Guidelines from Australian melanoma medical oncologists. Asia‐Pacific Journal of Clinical Oncology. 2016;12:5-12.

423. Davies MA, Saiag P, Robert C, Grob J-J, Flaherty KT, Arance A, et al. Dabrafenib plus trametinib in patients with BRAFV600-mutant melanoma brain metastases (COMBI-MB): a multicentre, multicohort, open-label, phase 2 trial. The Lancet Oncology. 2017;18(7):863-73.

424. Villanueva J, Infante JR, Krepler C, Reyes-Uribe P, Samanta M, Chen H-Y, et al. Concurrent MEK2 mutation and BRAF amplification confer resistance to BRAF and MEK inhibitors in melanoma. Cell reports. 2013;4(6):1090-9.

425. Wagle N, Van Allen EM, Treacy DJ, Frederick DT, Cooper ZA, Taylor-Weiner A, et al. MAP kinase pathway alterations in BRAF-mutant melanoma patients with acquired resistance to combined RAF/MEK inhibition. Cancer Discov. 2014;4(1):61-8.

426. Gide TN, Wilmott JS, Scolyer RA, Long GV. Primary and acquired resistance to immune checkpoint inhibitors in metastatic melanoma. Clin Cancer Res. 2018;24(6):1260-70.

427. Hill KS, Roberts ER, Wang X, Marin E, Park TD, Son S, et al. PTPN11 plays oncogenic roles and is a therapeutic target for BRAF wild-type melanomas. Mol Cancer Res. 2018.

428. Ruess DA, Heynen GJ, Ciecielski KJ, Ai J, Berninger A, Kabacaoglu D, et al. Mutant KRAS-driven cancers depend on PTPN11/SHP2 phosphatase. Nat Med https://doi org/101038/s41591-018-0024-8. 2018.

429. Wong GS, Zhou J, Liu JB, Wu Z, Xu X, Li T, et al. Targeting wild-type KRAS-amplified gastroesophageal cancer through combined MEK and SHP2 inhibition. Nat Med. 2018:1.

430. Arafeh R, Di Pizio A, Elkahloun AG, Dym O, Niv MY, Samuels Y. RASA2 and NF1; two-negative regulators of Ras with complementary functions in melanoma. Oncogene. 2018.

431. Johannessen CM, Reczek EE, James MF, Brems H, Legius E, Cichowski K. The NF1 tumor suppressor critically regulates TSC2 and mTOR. Proceedings of the National Academy of Sciences. 2005;102(24):8573-8.

432. LoPiccolo J, Blumenthal GM, Bernstein WB, Dennis PA. Targeting the PI3K/Akt/mTOR pathway: effective combinations and clinical considerations. Drug Resistance Updates. 2008;11(1-2):32-50.

433. Najem A, Krayem M, Sales F, Hussein N, Badran B, Robert C, et al. P53 and MITF/Bcl-2 identified as key pathways in the acquired resistance of NRAS-mutant melanoma to MEK inhibition. Eur J Cancer. 2017;83:154-65.

434. Pan R, Ruvolo V, Mu H, Leverson JD, Nichols G, Reed JC, et al. Synthetic lethality of combined Bcl-2 inhibition and p53 activation in AML: Mechanisms and superior antileukemic efficacy. Cancer Cell. 2017;32(6):748-60. e6.

435. Dahlman KB, Xia J, Hutchinson K, Ng C, Hucks D, Jia P, et al. BRAF L597 mutations in melanoma are associated with sensitivity to MEK inhibitors. Cancer Discov. 2012:CD-12-0097.

436. Winski S, Anderson D, Bouhana K, Rhodes S, Impastato R, Woessner R, et al. MEK162 (ARRY-162), a novel MEK 1/2 inhibitor, inhibits tumor growth regardless of KRas/Raf pathway mutations. Eur J Cancer Suppl. 2010;8:56.

437. Yan J, Wu X, Yu J, Yu H, Xu T, Brown KM, et al. Analysis of NRAS gain in 657 patients with melanoma and evaluation of its sensitivity to a MEK inhibitor. Eur J Cancer. 2018;89:90-101.

438. Sarkisian S, Davar D. MEK inhibitors for the treatment of NRAS mutant melanoma. Drug Des Devel Ther. 2018;12:2553-65.

439. Atefi M, Titz B, Avramis E, Ng C, Wong DJ, Lassen A, et al. Combination of pan-RAF and MEK inhibitors in NRAS mutant melanoma. Mol Cancer. 2015;14(1):27.

440. Rebecca VW, Alicea GM, Paraiso KH, Lawrence H, Gibney GT, Smalley KS. Vertical inhibition of the MAPK pathway enhances therapeutic responses in NRAS - mutant melanoma. Pigment cell & melanoma research. 2014;27(6):1154-8.

441. Yu Y. A novel combination treatment against melanoma with NRAS mutation and therapy resistance. EMBO Mol Med. 2018;10(5).

442. Posch C, Sanlorenzo M, Ma J, Kim ST, Zekhtser M, Ortiz-Urda S. MEK/CDK4, 6 co-targeting is effective in a subset of NRAS, BRAF and 'wild type'melanomas. Oncotarget. 2018;9(79):34990.

443. Eroglu Z, Zaretsky JM, Hu-Lieskovan S, Kim DW, Algazi A, Johnson DB, et al. High response rate to PD-1 blockade in desmoplastic melanomas. Nature. 2018;553(7688):347.